

INFLUENCE OF EUTROPHICATION ON THE CHARACTERIZATION AND
COAGULATION EFFICIENCY OF NATURAL ORGANIC MATTER

by

Hülya ÜNVER

BS. in Teaching in Science in Primary Education, Bogazici University, 2006

Submitted to the Institute of Environmental Sciences in partial fulfillment of

the requirements for the degree of

Master of Science

in

Environmental Sciences

Boğaziçi University

2010

ACKNOWLEDGMENTS

I would like to express my deeply grateful and sincere acknowledgments to my thesis supervisor Prof. Dr. Miray Bekbölet for giving me a great opportunity to study together. I am very thankful to her for her continuing support, perfect guidance, encouragement, contributions, and for devoting long hours throughout every step with her positiveness and kind-heartedness in all situations that gave rise to make this research achieved.

I gratefully acknowledge and thank the members of my thesis jury Assist. Prof. Başak Güven and Prof. Dr. İdil Arslan Alaton for all of their support and valuable contributions. I express my special thanks to Assist. Prof. Başak Güven for making the available time to provide me great contributions, help and suggestions for this study.

I wish to express my deep gratitude to Prof. Dr. Orhan Yenigün for his kindness and supporting me to start my thesis.

I am highly indebted to Dr. Ayşe Tomruk for her generous help and sharing invaluable knowledge during laboratory work. I am truly indebted to Gülhan Özkösem and all the staff in B.U. Environmental Sciences Laboratory for their help. I am very thankful to Sibel Şen-Kavurmacı and Dr. Ceyda Senem Uyguner for their invaluable help during my studies.

I am forever indebted to my parents Ayla and Mehmet Ünver for their irreplaceable love, endless support, and always being with me. I am very thankful to my grandparents, my brother Selçuk Ünver, Nesrin Özlen and all my family for giving me all their love and encouragement.

I wish to express my particular thanks to my friends Gökçe Egemen, Esra İlhan, Müge Paçal, Gülenay Hacıosmanoğlu, Sevinç İlgün, Derya Yenidünya, Hacer Cankurtaran for their friendship, love, encouragement, help, and sharing memorable days during laboratory works.

ABSTRACT

The aim of the present study was to investigate the influence of eutrophication on the coagulation efficiency of natural organic matter (NOM) with a specific focus on algal organic matter (AOM), and to find the effects of the anthropogenic sources of nutrients that lead to eutrophication by the algae growth on specific water quality parameters including nitrate, total phosphorous, and dissolved organic carbon (DOC).

The study involved preparation of synthetic freshwater samples by taking into account the quality of the natural waters using different combinations of nitrogen, phosphorous and other common inorganic ions and humic acid as culture media for freshwater algae. Water samples were spiked with algae inoculums resembling the consortium in natural water systems. Algae growth was daily followed by cell counting, reading the optical density at 600 nm, and chlorophyll a measurement until the optimum growth conditions were reached. Algal response to nutrient conditions of the simulated water samples were acquired from chromatographic and spectroscopic analysis of the water samples to assess the elements of eutrophication. Consumption of nitrate and phosphate by algae were attributed from the declining trend of both nutrients as the algae colonies propagated on the water media. The correlation between these factors provided the discussion of the relationship between algal growth and the effects of anthropogenic sources.

Optimized coagulation treatment method was performed for the assessment of the coagulation efficiency for removal of algae-laden natural organic matter found in natural waters. Optimum removal profiles of natural organic matter samples were determined by means of exploring the optimum coagulant doses and optimum pH of coagulation in water samples using alum and ferric chloride as coagulants. Removal efficiencies of coagulation tests were identified based on UV_{254} and similar results were reached when compared with

DOC removal profiles. According to UV_{254} measurements, using ferric chloride resulted in higher removal rates in comparison to using alum. Optimum pH values were found to be 5.5 for ferric chloride and 6.0 for alum. At high pH values such as pH 6.5 and pH 7.0, the optimum coagulant dose increased for alum and ferric chloride in comparison to the optimum dose values at pH 5.5 and pH 6.0.

The characterization of algal organic matter using a concentrated dissolved organic matter water sample was also assessed through the molecular size distribution profiles based on UV_{254} and DOC measurements that were determined by ultrafiltration using certain molecular size cutoffs before and after optimized coagulation treatment of the water samples. Optimum coagulant doses were found for alum and ferric chloride at the optimum pH values determined in the preliminary experiments using alum at pH 6.0 and ferric chloride at pH 5.5. The application of optimum coagulant conditions found resulted in an efficient removal of dissolved organic matter. The water samples passing through the filters indicated that the algal organic matter had both low and high molecular weight fractions and coagulation treatment shifted the molecular weight distribution of the dissolved organic matter sample to lower molecular weight ranges.

ÖZET

Bu çalışmanın amacı, ötrofikasyonun koagülasyonla doğal organik madde gideriminin özellikle alg kökenli organik maddenin gideriminin verimine etkisini araştırmak ve antropojenik besin kaynaklarının etkisiyle alg çoğalmasının neden olduğu ötrofikasyonun nitrat, toplam fosfor, çözünmüş organik karbon gibi belirli karakteristik su kalitesi özelliklerine etkilerini bulmaktır.

Çalışmada kullanılan tatlı su alg kültürünün çoğaltılması, alg yetiştirilmesi amacıyla hazırlanan yapay tatlı su örneklerinde, doğal sulardaki özellikler dikkate alınarak farklı kombinasyonlarda nitrojen, fosfor, diğer temel iyonlar ve hümik asit kullanılmasıyla gerçekleştirilmiştir. Alg çoğalması alg hücre sayımı, 600 nm’de optik yoğunluk ve klorofil a ölçümü parametreleriyle optimum çoğalma değerleri ulaşılan kadar günlük olarak izlenmiştir. Alg kültürünün sağlanan besin şartlarına çoğalmayla tepkisi kromatografik ve spektroskopik analizlerle incelenerek ötrofikasyonun boyutlarının ortaya konulmasında kullanılmıştır. Nitrat ve fosfat tüketimi alg kolonilerinin su kültüründe yayılmasıyla birlikte giderek azalan bir eğilim göstermesiyle ortaya çıkmıştır. Bu faktörler arasındaki korelasyon, alg çoğalımı ile antropojenik kaynakların etkileri arasındaki ilişkinin yorumlanmasını sağlamıştır.

Doğal sulardaki alg kökenli doğal organik maddenin gideriminde, koagülasyon yönteminin verimliliğinin değerlendirilmesi, optimize edilmiş koagülasyon metodlarının uygulanmasıyla gerçekleştirilmiştir. Optimum şartlarda organik madde giderimi profilleri, optimum koagülant ve optimum pH değerlerinin alum ve demir klorür koagülantları kullanılarak bulunmasıyla belirlenmiştir. Koagülasyon testlerinin organik madde giderim etkinlikleri UV_{254} ölçümlerine göre tanımlanmış ve sonuçlar çözünmüş organik karbon (DOC) giderim miktarlarıyla karşılaştırıldığında benzer sonuçlar elde edilmiştir. UV_{254} değerlerine göre ferrik klorür koagülantı alum koagülantına göre daha yüksek giderim sağlamıştır. Optimum pH değerleri ferrik klorür için 5.5, alum için 6.0 olarak saptanmıştır. pH 6.5 ve pH

7.0 gibi yüksek pH'larda optimum koagülant değerleri pH 5.5 ve 6.0 değerlerindeki sonuçlara göre yükselmiştir.

Alg organik maddesinin karakterizasyonu ayrıca, konsantre bir çözülmüş organik madde içeren su örneği kullanılarak, optimize edilmiş koagülasyonla giderim uygulanmadan önce ve uygulandıktan sonraki moleküler büyüklük dağılımının ultrafiltrasyon yöntemiyle belli moleküler büyüklük fraksiyonlarında elde edilen örneklerin UV_{254} ve DOC ölçümlerine göre değerlendirilmiştir. Konsantre çözülmüş organik madde örneğinin koagülasyonunda, alum ve ferrik klorür için optimum doz değerleri, çalışmanın ilk aşamadaki testlerinde belirlenen, alum için pH 6.0 ve ferrik klorür için pH 5.5 olarak bulunan optimum pH değerlerinde yapılmıştır. Belirlenen optimum şartlarda uygulanan koagülasyon yöntemiyle organik madde gideriminde etkili sonuçlar elde edilmiştir. Moleküler ağırlık dağılım değerleri, organik madde örneğinin ve bulunan optimum şartlarda alum ve ferrik klorürle giderim yapılan organik madde örneklerinin ultrafiltrasyon yöntemiyle azalan filtrasyon boyutlarından sırasıyla filtrelenmesiyle elde edilmiştir. Bulgular alg organik maddesinin moleküler dağılımının yüksek ve düşük ağırlıklı fraksiyonlar içerdiğini ve moleküler büyüklük dağılımının koagülasyonla organik madde gideriminden sonra değişim gösterdiğini ortaya koymuştur.

TABLE OF CONTENTS

ACKNOWLEDGEMENTS	iii
ABSTRACT	iv
ÖZET	vi
TABLE OF CONTENTS	viii
LIST OF FIGURES	xii
LIST OF TABLES	xxii
LIST OF SYMBOLS/ABBREVIATIONS	xxiii
1. INTRODUCTION	1
2. THEORETICAL BACKGROUND	3
2.1. Natural Organic Matter (NOM) in Freshwaters	3
2.1.1. The Relationship Between Dissolved Organic Carbon (DOC) and NOM	5
2.1.2. Characterization of Natural Organic Matter	6
2.1.3. Impact of Natural Organic Matter on Treatment of Drinking Water	7
2.2. Humic Substances	9
2.2.1. Isolation of Humic Substances	10
2.2.2. Composition and Structure of Humic Substances	11
2.3. Eutrophication in Freshwaters	14
2.3.1. Algae	15
2.3.2. Algae Growth Mechanism	17
2.3.3. Algal Blooms	22
2.3.4. Algal Organic Matter	23
2.3.5. Environmental Effects of Eutrophication	24
2.4. Coagulation	26
2.4.1. Colloids and Interfaces in Water	27
2.4.2. Particle Stability	29

2.4.3. Destabilization and Restabilization	31
2.4.4. Coagulants	32
2.4.5. Optimized Coagulation	33
2.4.6. Removal of NOM by Coagulation using Metal Salts in Natural Waters	34
2.5. Literature Review	36
3. MATERIALS AND METHODS	40
3.1. Materials	40
3.1.1. Synthetic Freshwater	40
3.1.2. Coagulants	40
3.1.3. Algae	40
3.1.4. Humic Acid	40
3.2. Methods	41
3.2.1. Cultivation of Algae	41
3.2.1.1. Preparation of Nutrients	41
3.2.1.2. Preparation of Synthetic Freshwater	43
3.2.1.3. Cultivating Algae Using Distilled Water	44
3.2.1.4. Cultivating Algae Using Synthetic Freshwater	44
3.2.2. Coagulation Experiments	45
3.2.3. Molecular Size Fractionation by Ultrafiltration	46
3.2.4. Analytical Methods	46
3.2.4.1. Optical Density Measurement	46
3.2.4.2. Dissolved Organic Carbon (DOC) Analysis	46
3.2.4.3. UV-vis Spectroscopy Measurements	47
3.2.4.4. Fluorescence Spectroscopy Measurements	47
3.2.5. Laboratory Instruments	48
3.2.5.1. Specific Instruments	48
3.2.5.2. General Laboratory Instruments and Materials	49
4. RESULTS AND DISCUSSION	50
4. 1. Natural Organic Matter Release Experiments	52

4.1.1. Algae Cultivation	52
4.1.1.1. Growth of Algae in Distilled Water	52
4.1.1.2. Growth of Algae in Synthetic Freshwater	54
4.1.2. Nutrient Consumption	56
4.1.3. Growth Kinetics in Algae Growth Mediums	59
4.2. Coagulation Experiments Using DOM Sample	65
4.2.1. Sample Specification for DOM Sample	67
4.2.2. Coagulation of DOM Sample with Alum	79
4.2.2.1. Optimum Dose of Alum with Respect to pH	79
4.2.2.2. Comparative Evaluation of pH Dependency for Coagulation with Alum	83
4.2.3. Coagulation of DOM Sample with Ferric Chloride	95
4.2.3.1. Optimum Dose of Ferric Chloride with Respect to pH	95
4.2.3.2. Comparative Evaluation of pH Dependency for Coagulation with Ferric Chloride	98
4.3. Coagulation Experiments Using Concentrated DOM (DOM _{conc}) Sample	110
4.3.1. Sample Specification for the DOM _{conc} Sample	111
4.3.2. Coagulation of the DOM _{conc} Sample with Alum	118
4.3.3. Coagulation of the DOM _{conc} Sample with Ferric Chloride	126
4.4. Molecular Size Distribution of Natural Organic Matter by Ultrafiltration	136
4.4.1. Preparation of the DOM _{conc} Sample for Ultrafiltration	138
4.4.2. Application of Ultrafiltration	139
5. CONCLUSIONS	147
REFERENCES	150
APPENDIX A: UV-VIS SPECTRA FOR COAGULATION WITH ALUM AT PH CONDITIONS OF 5.5, 6.5, 7.0	169
APPENDIX B: FLUORESCENCE SPECTRA FOR COAGULATION WITH ALUM AT PH CONDITIONS OF 5.5, 6.5, 7.0	171
APPENDIX C: UV-VIS SPECTRA FOR COAGULATION WITH FERRIC CHLORIDE AT PH CONDITIONS OF 6.0, 6.5, 7.0	176

APPENDIX D: FLUORESCENCE SPECTRA FOR COAGULATION WITH
FERRIC CHLORIDE AT PH CONDITIONS OF 6.0, 6.5, 7.0

178

LIST OF FIGURES

Figure 2.1. Model structure of a humic acid	13
Figure 2.2. Six phases of algae growth and variations in growth rate	17
Figure 2.3. Molecular size range of particles in natural waters	28
Figure 2.4. A model of electrical double layer	30
Figure 2.5. Destabilization and restabilization of colloids during coagulation	32
Figure 4.1. Algae propagation in distilled water mediums	52
Figure 4.2. Daily measurements of chlorophyll a ($\mu\text{g L}^{-1}$) in distilled water mediums	53
Figure 4.3. O.D.600 (m^{-1}) in distilled water mediums	54
Figure 4.4. Algae propagation in synthetic water mediums	55
Figure 4.5. O.D.600 (m^{-1}) in synthetic water mediums	55
Figure 4.6. Anions in distilled water medium $M_{1,1}$	56
Figure 4.7. Anions in distilled water medium $M_{5,2}$	57

Figure 4.8. Anions in synthetic freshwater medium SW ₁	58
Figure 4.9. Natural logarithm functions of the algae cell concentration in distilled water mediums	60
Figure 4.10. Growth rate values for distilled water mediums	61
Figure 4.11. Growth rate values (k_g) for the corresponding algae concentration in time for M _{1,2}	62
Figure 4.12. Limitation of k_g in M _{5,2} by N according to Michaelis-Menten model	64
Figure 4.13. Limitation of k_g in M _{5,2} by P according to Michaelis-Menten model	65
Figure 4.14. UV-vis spectra of the DOM sample, Aldrich Humic Acid (AHA), Fluka Humic Acid (FHA) and Nordic Humic Acid (NHA)	70
Figure 4.15. Fluorescence emission ₃₅₀ spectra of the DOM sample, Aldrich Humic Acid (AHA), Fluka Humic Acid (FHA) and Nordic Humic Acid (NHA)	72
Figure 4.16. Fluorescence emission ₃₇₀ spectra of the DOM sample, Aldrich Humic Acid (AHA), Fluka Humic Acid (FHA) and Nordic Humic Acid (NHA)	73

Figure 4.17. Fluorescence synchronous spectra of the DOM sample, Aldrich Humic Acid (AHA), Fluka Humic Acid (FHA) and Nordic Humic Acid (NHA)	75
Figure 4.18. DOM removal by coagulation with alum at pH 5.5 based on UV-vis parameters	79
Figure 4.19. DOM removal by coagulation with alum at pH 6.0 based on UV-vis parameters	81
Figure 4.20. DOM removal by coagulation with alum at pH 6.5 based on UV-vis parameters	82
Figure 4.21. DOM removal by coagulation with alum at pH 7.0 based on UV-vis parameters	83
Figure 4.22. Comparison of DOM removal by coagulation with alum under varying pH conditions with respect to UV_{254}	84
Figure 4.23. Comparison of DOM removal by coagulation with alum under varying pH conditions with respect to UV_{280}	85
Figure 4.24. Comparison of DOM removal by coagulation with alum under varying pH conditions with respect to UV_{365}	86
Figure 4.25. Comparison of DOM removal by coagulation with alum under varying pH conditions with respect to $Color_{436}$	87

Figure 4.26. Comparison of DOM removal by coagulation with alum under varying pH conditions with respect to DOC	88
Figure 4.27. UV-vis spectra of the DOM sample after coagulation with alum at pH 6.0	89
Figure 4.28. Fluorescence emission ₃₅₀ spectra of the DOM sample after coagulation with alum at pH 6.0	90
Figure 4.29. Fluorescence emission ₃₇₀ spectra of the DOM sample after coagulation with alum at pH 6.0	91
Figure 4.30. Fluorescence synchronous spectra of the DOM sample after coagulation with alum at pH 6.0	92
Figure 4.31. Comparison of the fluorescence intensities of the DOM sample after coagulation with alum at pH 6.0 in emission ₃₅₀ , emission ₃₇₀ and synchronous scan modes	93
Figure 4.32. DOM removal by coagulation with ferric chloride at pH 5.5 based on UV-vis parameters	95
Figure 4.33. DOM removal by coagulation with ferric chloride at pH 6.0 based on UV-vis parameters	96
Figure 4.34. DOM removal by coagulation with ferric chloride at pH 6.5 based on UV-vis parameters	97
Figure 4.35. DOM removal by coagulation with ferric chloride at pH 7.0 based on UV-vis parameters	98

Figure 4.36. Comparison of DOM removal by coagulation with ferric chloride under varying pH conditions with respect to UV ₂₅₄	99
Figure 4.37. Comparison of DOM removal by coagulation with ferric chloride under varying pH conditions with respect to UV ₂₈₀	100
Figure 4.38. Comparison of DOM removal by coagulation with ferric chloride under varying pH conditions with respect to UV ₃₆₅	101
Figure 4.39. Comparison of DOM removal by coagulation with ferric chloride under varying pH conditions with respect to Color ₄₃₆	102
Figure 4.40. Comparison of DOM removal by coagulation with ferric chloride under varying pH conditions with respect to DOC	103
Figure 4.41. UV-vis spectra of the DOM sample after coagulation with ferric chloride at pH 5.5	104
Figure 4.42. Fluorescence emission ₃₅₀ spectra of the DOM sample after coagulation with ferric chloride at pH 5.5	105
Figure 4.43. Fluorescence emission ₃₇₀ spectra of the DOM sample after coagulation with ferric chloride at pH 5.5	106
Figure 4.44. Fluorescence synchronous spectra of the DOM sample after coagulation with ferric chloride at pH 5.5	107

Figure 4.45. Comparison of the fluorescence intensities of the DOM sample after coagulation with ferric chloride at pH 5.5 in emission ₃₅₀ , emission ₃₇₀ and synchronous scan modes	108
Figure 4.46. UV-vis spectra of the DOM _{conc} sample, DOM sample, Aldrich Humic Acid (AHA), Fluka Humic Acid (FHA) and Nordic Humic Acid (NHA)	113
Figure 4.47. Fluorescence emission ₃₅₀ spectra of the DOM _{conc} sample, DOM sample, Fluka Humic Acid (FHA) and Nordic Humic Acid (NHA)	115
Figure 4.48. Fluorescence emission ₃₇₀ spectra of the DOM _{conc} sample, DOM sample, Aldrich Humic Acid (AHA), Fluka Humic Acid (FHA) and Nordic Humic Acid (NHA)	116
Figure 4.49. Fluorescence synchronous spectra of the DOM _{conc} sample, DOM sample, Aldrich Humic Acid (AHA), Fluka Humic Acid (FHA) and Nordic Humic Acid (NHA)	117
Figure 4.50. DOM _{conc} removal by coagulation with alum at pH 6.0 based on UV-vis parameters	119
Figure 4.51. DOM _{conc} removal by coagulation with alum at pH 6.0 based on DOC	120
Figure 4.52. UV-vis spectra of the DOM _{conc} sample after coagulation with alum at pH 6.0	122

Figure 4.53. Fluorescence emission ₃₅₀ spectra of the DOM _{conc} sample after coagulation with alum at pH 6.0	123
Figure 4.54. Fluorescence emission ₃₇₀ spectra of the DOM _{conc} sample after coagulation with alum at pH 6.0	124
Figure 4.55. Fluorescence synchronous spectra of the DOM _{conc} sample after coagulation with alum at pH 6.0	125
Figure 4.56. DOM _{conc} removal by coagulation with ferric chloride at pH 5.5 based on UV-vis parameters	127
Figure 4.57. DOM _{conc} removal by coagulation with ferric chloride at pH 5.5 based on DOC	128
Figure 4.58. UV-vis spectra of the DOM _{conc} sample after coagulation with ferric chloride at pH 5.5	130
Figure 4.59. Fluorescence emission ₃₅₀ spectra of the DOM _{conc} sample after coagulation with ferric chloride at pH 5.5	131
Figure 4.60. Fluorescence emission ₃₇₀ spectra of the DOM _{conc} sample after coagulation with ferric chloride at pH 5.5	133
Figure 4.61. Fluorescence synchronous spectra of the DOM _{conc} sample after coagulation with ferric chloride at pH 5.5	134
Figure 4.62. DOM _{conc} removal by jar tests using optimum coagulant doses of alum at pH 6.0 and ferric chloride at pH 5.5	138

Figure 4.63. Effect of molecular size distribution on UV-vis spectra of the untreated DOM _{conc} sample	140
Figure 4.64. Effect of molecular size distribution on UV-vis spectra of the DOM _{conc} sample after coagulation with alum	142
Figure 4.65. Effect of molecular size distribution on UV-vis spectra of the DOM _{conc} sample after cogulation with ferric chloride	143
Figure 4.66. Molecular size distribution of the DOM _{conc} sample before and after coagulation based on UV ₂₅₄	144
Figure 4.67. Molecular size distribution of the DOM _{conc} sample before and after coagulation based on DOC	145
Figure A.1. UV-vis spectra of the DOM sample after coagulation with alum at pH 5.5	169
Figure A.2. UV-vis spectra of the DOM sample after coagulation with alum at pH 6.5	170
Figure A.3. UV-vis spectra of the DOM sample after coagulation with alum at pH 7.0	170
Figure B.1. Fluorescence emission ₃₅₀ spectra of the DOM sample after coagulation with alum at pH 5.5	171
Figure B.2. Fluorescence emission ₃₇₀ spectra of the DOM sample after coagulation with alum at pH 5.5	172

Figure B.3. Fluorescence synchronous spectra of the DOM sample after coagulation with alum at pH 5.5	172
Figure B.4. Fluorescence emission ₃₅₀ spectra of the DOM sample after coagulation with alum at pH 6.5	173
Figure B.5. Fluorescence emission ₃₇₀ spectra of the DOM sample after coagulation with alum at pH 6.5	173
Figure B.6. Fluorescence synchronous spectra of the DOM sample after coagulation with alum at pH 6.5	174
Figure B.7. Fluorescence emission ₃₅₀ spectra of the DOM sample after coagulation with alum at pH 7.0	174
Figure B.8. Fluorescence emission ₃₇₀ spectra of the DOM sample after coagulation with alum at pH 7.0	175
Figure B.9. Fluorescence synchronous spectra of the DOM sample after coagulation with alum at pH 7.0	175
Figure C.1. UV-vis spectra of the DOM sample after coagulation with ferric chloride at pH 6.0	176
Figure C.2. UV-vis spectra of the DOM sample after coagulation with ferric chloride at pH 6.5	177
Figure C.3. UV-vis spectra of the DOM sample after coagulation with ferric chloride at pH 7.0	177

Figure D.1. Fluorescence emission ₃₅₀ spectra of the DOM sample after coagulation with ferric chloride at pH 6.0	178
Figure D.2. Fluorescence emission ₃₇₀ spectra of the DOM sample after coagulation with ferric chloride at pH 6.0	179
Figure D.3. Fluorescence synchronous spectra of the DOM sample after coagulation with ferric chloride at pH 6.0	179
Figure D.4. Fluorescence emission ₃₅₀ spectra of the DOM sample after coagulation with ferric chloride at pH 6.5	180
Figure D.5. Fluorescence emission ₃₇₀ spectra of the DOM sample after coagulation with ferric chloride at pH 6.5	180
Figure D.6. Fluorescence synchronous spectra of the DOM sample after coagulation with ferric chloride at pH 6.5	181
Figure D.7. Fluorescence emission ₃₅₀ spectra of the DOM sample after coagulation with ferric chloride at pH 7.0	181
Figure D.8. Fluorescence emission ₃₇₀ spectra of the DOM sample after coagulation with ferric chloride at pH 7.0	182
Figure D.9. Fluorescence synchronous spectra of the DOM sample after coagulation with ferric chloride at pH 7.0	181

LIST OF TABLES

Table 2.1. Elemental composition range and functional groups of humic and fulvic acids	12
Table 2.2. Parameter Estimations for Michalis-Menten (Monod) Equation	19
Table 3.1. Macronutrient stock solution list	42
Table 3.2. Micronutrient stock solution list	42
Table 3.3. Recipe for soft synthetic freshwater	43
Table 3.4. Dilution factors for making 5 L of soft synthetic freshwater	44
Table 4.1. Physico-chemical characteristics of the DOM sample	68
Table 4.2. Common cations and anions of the DOM sample	76
Table 4.3. Physico-chemical characteristics of the DOM _{conc} sample	111

LIST OF SYMBOLS/ABERREVIATIONS

Symbol	Explanation	Units used
AHA	Aldrich Humic Acid	mg L ⁻¹
AOC	Assimilable Organic Carbon	mg L ⁻¹
AOM	Algal Organic Matter	mg L ⁻¹
BDOC	Biodegradable Dissolved Organic Carbon	mg L ⁻¹
BOD	Biological Oxygen Demand	mg L ⁻¹
BOM	Biodegradable Organic Matter	mg L ⁻¹
chl _a	Chlorophyll a	
¹³ C-NMR	Carbon 13 Nuclear Magnetic Resonance	
COD	Chemical Oxygen Demand	mg L ⁻¹
Color ₄₃₆	Absorbance at 436 nm	cm ⁻¹
Da	Dalton	
DBPs	Disinfection by-products	
DOC	Dissolved Organic Carbon	mg L ⁻¹
DOM	Dissolved Organic Matter	mg L ⁻¹
DOM _{conc}	Concentrated Dissolved Organic Matter Sample	
EOC	Extracellular Organic Carbon	mg L ⁻¹
EOM	Extracellular Organic Matter	mg L ⁻¹
Emission ₃₅₀	Fluorescence Emission Scan with Excitation Wavelength of 350 nm	
Emission ₃₇₀	Fluorescence Emission Scan with Excitation Wavelength of 370 nm	
FA	Fulvic Acid	mg L ⁻¹
FHA	Fluka Humic Acid	mg L ⁻¹

FI	Maximum Fluorescence Intensity	
FS	Fluorescence Spectroscopy	
FTIR	Fourier Transform Infrared Spectroscopy	
GAC	Granular Activated Carbon	
GF/F	Fibre Glass Filter	
HA	Humic Acid	
HAAs	Haloacetic Acids	
HS	Humic Substance	
Hu	Humic	
IOM	Intracellular Organic Matter	mg L ⁻¹
Mm	Micrometer	
MSD	Molecular Size Distribution	
MWCO	Molecular Weight Cutoff	
MX	3-Chloro-4-(Dichloromethyl)-4-Oxobutenoic Acid	
NHA	Nordic Humic Acid	mg L ⁻¹
nm	Nanometer	
NOM	Natural Organic Matter	mg L ⁻¹
N:P	Nitrogen to Phosphorous Ratio	
OC	Optimized Coagulation	
O.D.600	Optical Density at 600 nm	m ⁻¹
OM	Organic Matter	
POC	Particulate Organic Carbon	mg L ⁻¹
POM	Particulate Organic Matter	mg L ⁻¹
Py-GC/MS	Pyrolysis-Gas Chromatography/Mass Spectrometry	
rpm	Revolutions per minute	
SCoA	Specific Color Absorbance	L mg ⁻¹ m ⁻¹
SUVA	Specific Ultraviolet Absorbance	L mg ⁻¹ m ⁻¹
SW	Synthetic Water	
T	Temperature	°C
THMs	Trihalomethanes	

TOC	Total Organic Carbon	mg L ⁻¹
UF	Ultrafiltration	
UV	Ultraviolet	
UV-A	UV Light between 320-400 nm	
UV-B	UV Light between 280-320 nm	
UV-vis	Ultraviolet-Visible	
UV ₂₅₄	Absorbance at 254 nm	cm ⁻¹
UV ₂₈₀	Absorbance at 280 nm	cm ⁻¹
UV ₃₆₅	Absorbance at 365 nm	cm ⁻¹
ΔUVA	Differential UV spectroscopy	
2-MIB	2-methyl isoborneol	

1. INTRODUCTION

Eutrophication is a common problem caused by over enrichment of nitrogen and phosphorous in rivers, lakes, estuaries, and coastal oceans. The increase of algae and vascular plants becomes harmful to aquatic ecosystem, terrestrial ecosystem, and other organisms. It creates a human health risk for drinking water quality standards and water used with other purposes such as industry, agriculture and recreation. To prevent the public health, limits are set in drinking water standards for nitrate and ammonium as nitrogenous species of concern. However no limit exist for phosphate, although it is the primary cause of eutrophication in some natural waters.

The major sources of N and P are agricultural and urban activities such as animal manures, fertilization, atmospheric deposition, human and animal waste, sedimentation, and sewage excess that moves to surface waters, ground waters, or enter the atmosphere via ammonia volatilization and nitrous oxide production (Smith, 1999). Increased N and P supplies can lead to diverse problems such as toxic algal blooms, loss of oxygen, fish kills, loss of biodiversity, loss of aquatic plant beds and coral reefs, and other problems (Carpenter et al., 1998). The abundance of N and P in water bodies sustains nutrient-enrichment for algae. Nitrogen and phosphorus are the primary controllable nutrients which have been the focus of most efforts to control eutrophication (Manahan, 2010).

The nutrient for cyanobacteria that potentially limits primary production can be predicted from total or dissolved nutrient concentrations of water (Lagus et al., 2004). Assessment of eutrophication has been based on concentrations of nitrogen, phosphorous and Chlorophyll a which is a photosynthetic pigment present in all species of algae. Advanced methods are based on monitoring both nitrogen and phosphorous such as N:P ratio (nitrogen-to phosphorous ratio) in aquatic ecosystems. Blue-green algae tended to be rare when N:P ratio is below 29:1 by weight (Smith, 1983). Indeed, water eutrophication is a function of multiple factors influencing its occurrence. Formation of algal blooms are not certainly understood yet and further investigation is needed.

Coagulation is one of the most used water treatment methods to remove natural organic matter (NOM) causing problems in natural waters. It is a mechanism that increases the tendency of small particles in aqueous suspension to attach one another. The attachment of the particles results in the formation of larger aggregates that are removed by sedimentation and/or filtration. Natural organic matter in raw waters is characterized by the parameters of total organic carbon (TOC), dissolved organic carbon (DOC), UV absorbance at 254 nm and specific UV absorbance (SUVA) (Barrett et al., 2000). The relationship between coagulation and eutrophication can be analyzed by DOC which is the fraction of TOC, ultra violet absorption, fluorescence and the fractionation of molecular weight (Cheng and Chi, 2003).

The objective of this study is to investigate the influence of eutrophication on the coagulation efficiency of natural organic matter, and to find the effects of the anthropogenic sources of nutrients that lead to eutrophication by the algal growth on specific water quality parameters including nitrate, phosphate, along with other inorganic ions and dissolved organic carbon. To achieve this goal, water samples were prepared by taking into account seasonal diversity in quality of the natural sources using different combinations of nitrate, phosphate and other common inorganic ions and humic acid. The correlation between these factors is the basis of the relationship between algal growth and the effects of anthropogenic sources. The data was acquired from spectroscopic analysis of the simulated water samples to assess the elements of eutrophication. The application of optimized coagulation (OC) method was performed for the assessment of the natural organic matter (NOM) removal efficiency of coagulation in natural waters with a specific focus on algae laden organic matter (AOM). The characterisation of the natural organic matter was assessed through the molecular size distribution profiles by ultrafiltration (UF) using appropriate filters with certain molecular size cutoffs.

2. THEORETICAL BACKGROUND

2.1. Natural Organic Matter (NOM) in Freshwaters

Organic matter (OM) is present in all water systems to varying degrees is derived primarily from plant and/or microbial residues. Even the clearest water bodies in a remote part of the world contain organic matter at least in a small concentration in the range of 1 to 3 mg L⁻¹. The presence of yellow-brown color is the evidence for organic content in lakes and rivers. Organic matter in water is mostly determined by its carbon content which is the essential element of organic compounds, is also present in the environment as a component of inorganic species in the carbonate family and the aquatic NOM is one of the largest carbon pool on the Earth (Thurman, 1986; Killops and Killops, 2005; vanLoon and Duffy, 2005). The content of natural organic material covers a wide range of organic matter that exist in soil and water environments that originated from decaying materials of plants and animals as well as their degradation products. Natural organic matter has a wide range in terms of acidity, molecular weight and molecular structure (Aiken et al., 1985).

Origin of organic matter in water is related to different sources thus allows to some extent the classification of the natural aquatic OM. The OM derived from natural sources through plant and/or microbial residues is usually referred to as natural organic matter, NOM. The terrestrial residues of OM can be transferred from the soil into the hydrosphere either in their original or chemically modified forms. The transport of OM occurs by rainfall or other surface waters by direct leaching or the NOM percolates through the soil column into streams, lakes, oceans or into groundwater. Organic matter originates mainly both from natural allochthonous and autochthonous sources and to some extent from anthropogenic sources. The allochthonous NOM originates from terrestrial sources usually making up the most important fraction of the total aquatic organic matter in freshwaters. The NOM is also produced in situ within a water body by the growth of aquatic vegetation and some aquatic organisms. Organic material produced by aquatic vegetation upon death is deposited in the water. macro- and microscopic animals, photosynthetic organisms like

algae and macrophytes, produce organic remains that become part of the total organic content of an aquatic system. Anthropogenic sources on the other hand, have an increasing impact on the OM in water by stimulating algae growth with the release of nutrient elements as well as large volumes of different wastes discharged directly or after treatment into surface waters. Besides the bulk effluents, anthropogenic sources also supply specific organic compounds such as agricultural chemicals, medicinals, and products or by-products of industrial processes in the range being as broad as that of organic chemistry itself. However, the distinction between the natural and anthropogenic sources is not always unambiguous because the anthropogenic source is not clearly defined in cases where organic material leached, e.g., from composts may sometimes be also assigned to this category (vanLoon and Duffy, 2005; Peuravuori and Pihlaja, 2006).

The NOM found in water supplies has been functionally defined as humic (nonpolar) and nonhumic (polar) based on adsorption results in XAD resins, though nonhumic fractions of NOM exhibit some of the properties typically observed for classic humic fractions. The NOM of most water sources is comprised of humic substances (humic and fulvic acids), hydrophilic acids, carboxylic acids, amino acids, carbohydrates, and hydrocarbons in the approximate portions of 50, 30, 6, 3, 10, and 1% respectively. In highly colored waters, the humic substance content may be as high as 50 to 90% (Collins and Vaughan, 1996; Barrett et al., 2000). Humic substances are organic compounds found in the environment that cannot be classified as any other chemical class of compounds. They arise from the decomposition of plant and animal tissues occurring in all soils, waters, and sediments of the ecosphere. Their size, molecular weight, elemental composition, structure, the number and position of functional groups vary depending on the origin and age of the material (Suffet and MacCarthy, 1989; Gaffney et al., 1996).

High concentrations of organic matter in natural freshwaters were reported to have an adverse effect on the fate and treatment of hazardous chemical pollutants thereby present a human health concern that must be managed in drinking water management. Evaluation of the influence of natural organic matter present in natural waters on the fate and treatment of pollutants is greatly related with the background organic matter and has not been totally understood. Understanding of pollutant impact and removal of organic matter generally

involves dealing with a trace concentration of a pollutant in solution such as microgram per liter ($\mu\text{g L}^{-1}$) concentrations or less within the background matrix of $\mu\text{g L}^{-1}$ concentrations of other natural organic materials (Suffet and MacCarthy, 1989).

2.1.1. The Relationship Between Dissolved Organic Carbon (DOC) and NOM

Traditionally NOM is quantified by measuring total organic carbon (TOC) or dissolved organic carbon (DOC). Organic carbon compounds in most natural freshwaters range in concentration between 0.5 to 50 mg L^{-1} C as TOC or DOC. With DOC concentrations in excess of 100 mg L^{-1} , Canadian prairies is known to have some of the highest DOC concentrations around the world (Waiser and Robarts, 2000; vanLoon and Duffy, 2005).

Generally, humic substances comprise up 60-80% of the total dissolved organic matter (DOM) of which 30-40% is aromatic carbon. Fulvic and humic acids represent a major fraction of DOC. In dystrophic waters, the humic material content can rise to 80-95% of the total DOC. Humic substances have a molecular weight of a few hundred to several thousand Daltons (Da). The latter exist as colloids with diameters of 1 nm to 1 micrometer (μm), and can pass through the pores of most membrane filters. Humic substances exist as particles if their diameter exceed 1 μm (Thurman, 1985; Steinberg, 2003; TOLONEN, 2004).

The separation of dissolved organic matter (DOM) and particulate organic matter (POM) is operationally defined through filtration of water with membrane filters of given pore-size. Usually, filters with pore size of 0.2-0.45 μm and occasionally finer or more rarely coarser pored filters are applied. The DOC fraction is determined as the concentration of the carbon in water passing through filters with 0.2 or 0.45 μm of pore size or through GF/F fibre glass filters. The carbon retained on the filter constitutes the fraction of particulate organic carbon (POC) which constitutes 10% of the TOC in most aquatic systems. Filters allow not only truly dissolved molecules to pass through, but also colloidal material. For instance, the filtrate contains a part of the humin fraction and various complexes with FA and particularly HA (Wetzel, 2001; Steinberg, 2003; TOLONEN, 2004).

2.1.2. Characterization of Natural Organic Matter

Characterization of NOM have been improved by using several elemental analysis. Ultraviolet absorption analysis at 254 nm and 285 nm, the ratio of UV absorbance to dissolved organic carbon (DOC) namely the specific UV absorbance (SUVA), differential UV spectroscopy (Δ UVA) at 272 nm are some of the commonly used indicators of NOM (Barrett et al., 2000). Since the aromatic content in natural organic matter absorbs the light always in the wavelength range between 240 and 260 nm, especially UV_{254} is widely used as a surrogate parameter of NOM and it correlated well with the concentration of TOC (Edzwald et al., 1985; Korshin and Li, 1996; Nissinen et al., 2001). In addition to 254 and 285 nm, a variety of absorption wavelengths have been used by researchers such as 250, 270, 280, 300, 365, 400, 436, 465 nm for the UV spectral differentiation of natural organic matter (Chin et al., 1994; Peuravuori and Pihlaja, 1997; Wilkinson et al., 1997; Frimmel, 1998b; Chen et al., 2002; Uyguner and Bekbolet, 2005a). Other techniques developed in NOM characterization include carbon 13 nuclear magnetic resonance (^{13}C -NMR), pyrolysis-gas chromatography/mass spectrometry (Py-GC/MS), fluorescence spectroscopy, size exclusion chromatography for molecular weight and molecular size determinations, and on-line TOC measurements (Bruchet et al., 1990; Chin et al., 1994; Harrington et al., 1996; Croué et al., 1999; Her et al., 2002; Baker et al., 2008).

Fractionation techniques traditionally used to separate humic and nonhumic NOM are XAD-8 resins that do not adsorb polar NOM, XAD-4 resins isolate some but not all the more polar portion of NOM from inorganic matter. In conjunction with the separation techniques, NOM detection methods were used including total organic carbon analysis, UV and fluorescence spectroscopy, elemental analysis, molecular size distributions, Py-GC/MS, fourier transform infrared spectroscopy (FTIR), and ^{13}C -NMR. Using more than one technique in combination with each other provides significantly more structural and functional group information than the result provided with a single method. (Barrett et al., 2000).

2.1.3. Impact of Natural Organic Matter on Treatment of Drinking Water

Organic matter can impact the quality of drinking water in the levels of nutrients (e.g., carbon) available for bacteria within distribution systems and disinfection by-products when chlorine or bromine react with NOM components such as humic and fulvic acids (Volk, 2000). NOM creates a disinfectant demand and forces the need to use higher disinfectant dosages to maintain an adequate residual in distribution systems. Organic matter in drinking water reservoirs can be sourced from both terrestrial and aquatic sources and its composition can vary with seasonal variation. Some NOM components may provide food for microorganisms in the water distribution systems. The portion of the organic matter called biodegradable organic matter (BOM) is utilized by bacteria as a source of energy and carbon. BOM in drinking water can promote bacterial regrowth and coliform occurrences within distribution systems. BOM also highly impacts the formation of disinfection by-products and the level of disinfectant demand (LeChevallier, 1990; LeChevallier et al., 1991; Van der Kooji, 1992; Volk, 2001).

Organic matter constituents from both natural and anthropogenic origins present in surface waters affect the drinking water supplies as they have a potential to form disinfection by-products when chlorinated during water treatment and play a key role in achieving drinking water quality standards. There is a substantial list of different chemicals, in addition to more than 1500 organochlorines with low-molecular masses, such as mono- and trichloromethane and 2,4,6-trichlorophenol, and with relatively high-molecular mass chlorinated organic complexes (Barrett et al., 2000; vanLoon and Duffy, 2005; Peuravuori and Pihlaja, 2006).

A number of molecules have been identified as final DBPs some of which are believed to be carcinogenic and the final concentrations are regulated in finished drinking water. The class of compounds known as trihalomethanes (THMs); the sum of chloroform, and bromodichloromethane, dibromochloromethane and bromoform are among the most frequently detected DBPs in tap water. In addition, more than 80 halogenated carboxylic acids have been identified of which haloacetic acids (HAAs) are known to induce live tumors in animals. Among others 3-chloro-4-(dichloromethyl)-4-oxobutenoic acid (MX) is

the most mutagenic by-product ever identified in drinking water and identified as an animal carcinogen. Humic substances are important precursors of halogenated compounds in drinking water therefore it is necessary to get more information on their behavior during water treatment and disinfection. Aromatic structures of the humic substances containing phenolic functional groups (hydroxyl-, carboxy-, and methoxy substituted aromatic units) have been reported to be responsible of the highly reactivity with chlorine in formation of DBPs (Reckhow et al., 1990; Bergamaschi et al., 2000; Frimmel et al., 2000). The presence of humic substances in the environment may have also a beneficial effect because they neutralize hazardous chemicals by complexation with toxic metals or by association with toxic organic chemicals. In water treatment, an evaluation of the impacts of humic substances in each situation must be carefully considered (Suffet and MacCarthy, 1989).

In drinking-water treatment NOM can be removed intact during coagulation, GAC adsorption, membrane filtration, or biological degradation, or it can be transformed through oxidation or advanced oxidation using oxidants such as ozone. NOM also competes with other organic compounds which are amenable to adsorption by powdered activated carbon (PAC) or granulated activated carbon (GAC) (EPA, 1999). In order to optimize water treatment processes for NOM removal, it is essential to understand the characterization of NOM, and NOM's reactivity with disinfectants i.e. identifying which fraction of the NOM is most important for minimizing the formation of DBPs. To control the bacteriological quality of drinking water some utilities use a minimal amount of disinfectant and most utilities improve the treatment for NOM removal before disinfection to reduce disinfection. Some utilities use alternative disinfectants i.e. chloramines, ozone, and chlorine dioxide, to minimize the DBPs formed. However these disinfectants, e.g. ozone, may also react with NOM. Conventional coagulation removes a portion of the NOM. Enhanced coagulation, GAC adsorption, membrane filtration can be used to improve the removal of NOM. Chlorination of water during treatment to reduce organic carbon content can create brominated THMs to form in water at the point of chlorination in waters containing bromide. However, using NOM removal technologies such as enhanced coagulation, GAC adsorption, membrane filtration still may achieve greater levels of risk reduction than considering THM risks only (Black et al., 1996; Barrett et al., 2000).

2.2. Humic Substances

The majority of the water-soluble NOM exists as aquatic humic substances in water supplies (Thurman, 1986; Killops and Killops, 2005). Humic substances are naturally found in soils, brown coals, freshwater, seawater, sediments. The soil humics are originally derived from plant material. They can be leached in time particularly from acidic soils and account for most of the organic carbon in freshwaters imparting the brown coloration to upland waters.

Humic substances in the environment result from the decomposition of plant and animal residues that does not fall into any of the discrete classes of compounds such as proteins, polysaccharides, and polynucleotides. Attempts have been done for many years to understand those pathways and define humic substances in specific chemical terms. Definitions succeeded in diminishing the degree of heterogeneity though none of them came close to refer a material as pure humic substance within a group of chemicals. In this essence, humic substances represent a unique category of material in nature which are unable to be defined in specific chemical terms by the analytical methods. Because of the vagueness of the definitions, when dealing with humic substances, researchers express the amount of material in terms of dissolved organic carbon (DOC). Much of the reactivity of humic substance class of organic matter in aqueous solution is attributed to functional groups such as carboxyl, carbonyl, phenolic, methoxyl, and carboxyl groups that provide most of the negative charge adding the mobility of humic substances in the environment (MacCarthy and Suffet, 1989; vanLoon and Duffy, 2005).

Humic substances influence the geochemical behavior of metals and radionuclides. Although there are a variety of functional groups in the humic and fulvic structures, the carboxylate groups are primarily responsible for binding metals and radionuclides under most natural conditions. Metal binding to DOC involves increased binding with a higher degree of ionization of the humic material. Binding of metal cations neutralizes the repulsive forces in water and promotes contraction of the polymer. At extensive metal loading, the humic molecule exists as a compact unit whose exterior is hydrophobic which

plays a role in coagulation and precipitation processes of water treatment and occurs at various ratios of bound cations to ionized carboxylates, depending on the cation charge. At low metal-to-carboxylate ratios, the metal-humic complexes are soluble in the aqueous systems (Gaffney et al., 1996).

In addition to complexing with metals in the aqueous phase, humic and fulvic materials are extremely important in the mobilization and concentration of toxic metals and radionuclides in the environment. Due to size changes induced by conformational rearrangement and aggregation/dissociation arising from intermolecular hydrogen bonding, humic and fulvic acids can form soluble complexes that can migrate long distances or precipitate carrying bound cations with them. This depends on the metallic ion, the cation charge, the degree of ionization of the organic molecule, the ionic strength of the media, and the metal loading (Chopin and Allard, 1985). The presence of humic materials can also promote the solubilization of nonpolar hydrophobic compounds. The ability of humic substances to bind hydrophobic organics can affect not only their mobility by decreasing the sorption to sediments, but also the rate of chemical degradation, photolysis, volatilization, and biological uptake of these organics. This interaction of humic acids with other materials can serve to lengthen the lifetimes and transport distances of these contaminants in the environment. The binding of organic and inorganic contaminants to humic substances was reported to alter their bioavailability (MacCarthy and Jimenez, 1985). Organic contaminants that are associated with humic substances are essentially unavailable for uptake by biota. In most studies, toxic metals associated with humic materials found to have also reduced uptake (Gaffney et al., 1996).

2.2.1. Isolation of Humic Substances

Humic substances occur in the environment mixed or in interaction with other classes of materials such as amino acids, sugars, aliphatic and aromatic acids and other organic compounds. In soils and sediments, and in suspension in aquatic systems, humic substances are generally bound to the mineral components. Some researchers isolated the humic substances from the nonhumic materials and evaluated the isolate part in the controlled conditions of laboratory. Over many years the investigations in subfractioning

of humic substances have resulted in operationally defined classification of the humic fractions according to their aqueous solubility, namely humic acid (HA), fulvic acid (FA), and humin (Hu). Fulvic acids (FA) are those organic materials that are soluble in water at all pH values. Humic acids (HA) are those materials that are insoluble at acidic pH values (pH<2) but are soluble at higher pH values. Humin is the fraction of natural organic materials that is insoluble in water at all pH values (Aiken et al., 1985; MacCarthy and Suffet, 1989; vanLoon and Duffy, 2005). These definitions indicate traditional methods for separating the different fractions from the original mixture. Humic materials have a wide range of molecular weights and sizes, ranging from a few hundred to as much as several hundred thousand atomic mass units and their composition varies depending on their source, location, and method of extraction. (Gaffney et al., 1996). Fulvic acids, being more soluble than humic acids, predominate in most waters and have lower molecular weight, typically in the range of 500–2000 Da. Humic acids are reported to have a wide range of molecular weights from a few thousand up to as high as 100, 000 although the high values may be a result of aggregation (Duan and Gregory, 2003).

2.2.2. Composition and Structure of Humic Substances

Humic substances vary in composition and structure depending on their source, methods of analysis and extraction, and other parameters (MacCarthy and Suffet, 1989). The structural features for various samples of fulvic and humic acid have been reported from around the world using the infrared spectra. The spectra band results revealed the features in the FA and HA samples suggesting that there are similar structural properties shared by all types of humic materials. The shared features of chemical units include functional groups of phenolic and aliphatic –OH groups, carboxyl and carbonyl groups, and aromaticity in double bonds in aliphatic units (Davies and Ghabbour, 1998; Steinberg, 2003). The accounting proportions of the elemental composition and functional groups of a wide variety of humic and fulvic acids has been approximated by Schnitzer (Schnitzer, 1972) as shown in Table 2.1 (Steinberg, 2003).

Table 2.1. Elemental composition range (weight %) and functional group (meq g⁻¹) of HA and FA, (Schnitzer, 1972).

Elements (%)	HA	FA
C	53.6-58.7	40.7-50.6
H	3.2-6.2	3.8-7.0
N	0.8-5.5	0.9-3.3
O	32.8-38.3	39.7-49.8
S	0.1-1.5	0.1-3.6
Functional Groups	HA	FA
acid groups	5.6-8.9	6.4-14.2
carboxylic acids	1.5-5.7	5.2-11.2
phenolic OH	2.1-5.7	0.3-5.7
alcoholic OH	0.2-4.9	2.6-9.5
quinoide/keto C=O	0.1-5.6	0.3-3.1
methoxy OCH ₃	0.3-0.8	0.3-1.2

The structures of fulvic acids were reported to be more aliphatic and less aromatic than humic acids and as being richer in carboxylic acid, phenolic, and ketonic groups which is responsible for their higher solubility in water at all pH values. Humic acids, being more highly aromatic, are insoluble when the carboxylate groups are protonated at low pHs. This structure of the humic materials provides them to function as surfactants, and the ability to bind both hydrophobic and hydrophilic materials. Together with their colloidal properties, this function makes humic and fulvic materials effective agents in transporting both organic and inorganic contaminants in the environment (Gaffney et al., 1996).

The carbon content changes in the order of FA<HA<Hu for a given source of humic substance, while the oxygen content follows the opposite trend for the same set of substance. The environment of the humic source also has an influence on the composition of the material. Carbon content is larger in soil humus than humate in lakes and oceans

while the oxygen and nitrogen contents change in reverse order. In sedimentary humic substance the relative proportion of Hu to HA and FA increases with depth (Steinberg, 2003). Terrestrial humic substances are larger than the aquatic humics (Killops and Killops, 2005).

A 2D hypothetical structure for humic acid was presented in Figure 2.1.

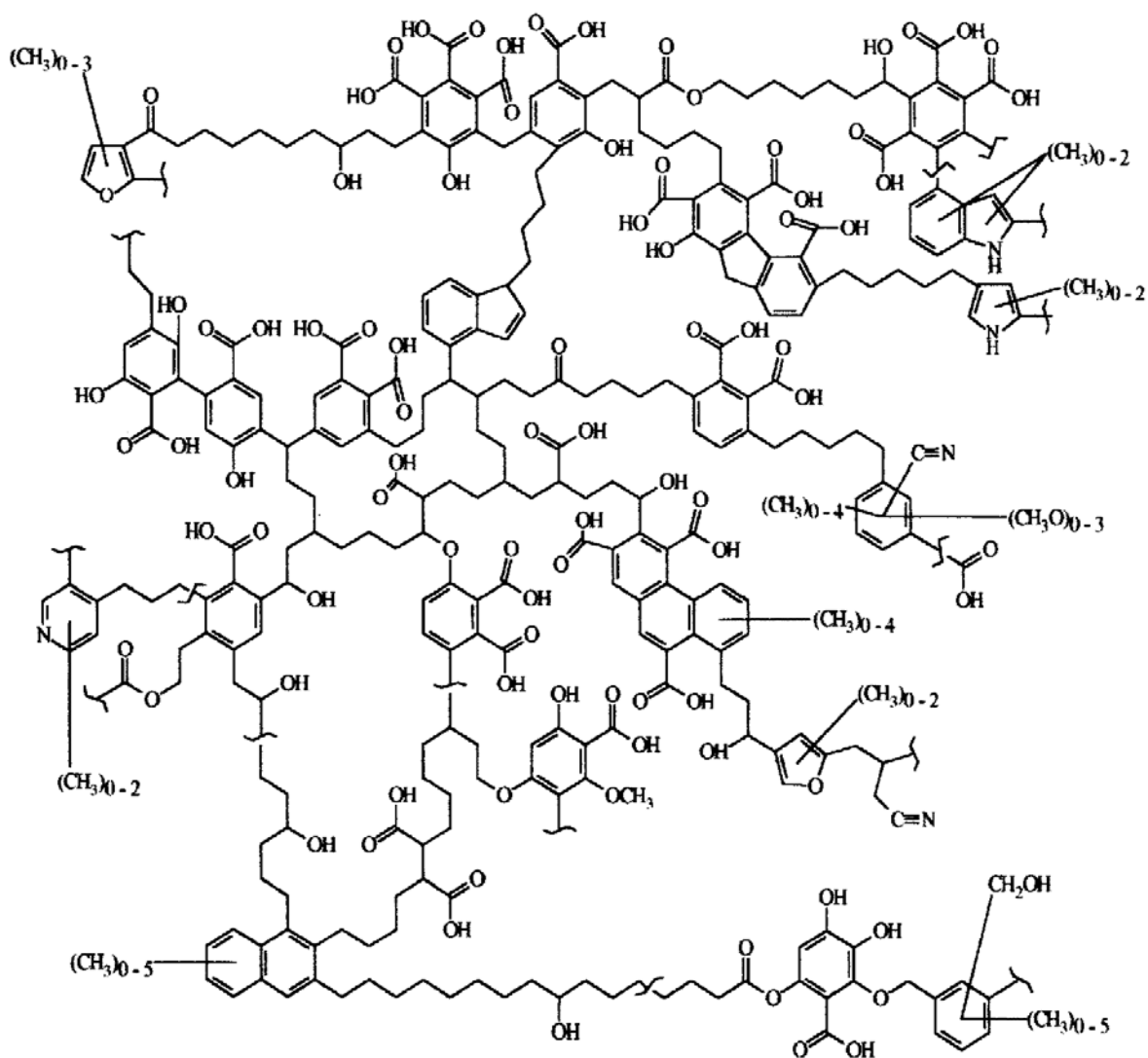


Figure 2.1. Model structure of a humic acid. Adapted from Schulten and Schnitzer, 1993 (Jones and Bryan, 1998).

The interest of scientists working in the environmental science in structural properties of humic substances was reflected by modern techniques of molecular modeling that were employed to propose two- (2D) and recently three-dimensional (3D) structural molecular-chemical models for humic substances (Schulten, 1996). The model structure given in Figure 2.1 has a molecular mass of 5539.7 and an empirical formula of $C_{308}H_{328}O_{90}N_5$ containing aromatic and aliphatic structures with a hydrophobic aromatic structure in the centers that are substituted by phenolic OH groups, nitrogen, oxygen as bridge units, and it has pyridine, pyrrole and furan residues as well as benzene moieties (Jones and Bryan, 1998). The humic models are important in that they enhance the explanations for the chemical reactions of natural organic matter based on the basis of humics from an analytical aspect (Schnitzer and Khan, 1972; Schulten, 1996).

2.3. Eutrophication in Freshwaters

Eutrophication literally means well-nourished though in fact it means an over-nourished condition in terms of certain nutritive components in a water body. The excess of organic carbon, inorganic nitrogen, phosphate and also other minerals causes algae, bacteria, and other flora and fauna to reproduce at very rapid rates. The natural aging process whereby a lake is transformed from a marsh into a meadow which can take thousands of years to occur naturally. However the process can be greatly accelerated by excess nutrients from human activities which is also called cultural eutrophication. The biosystem that can grow at the most rapid rate usually produces large quantities of slime and microbial tissue described as a bloom indicating an upset in the chemical composition of the stream or lake. Water bodies are generally classified according to their trophic status because it indicates productivity of organisms in the water environment. The poorly nourished waters are called oligotrophic, and moderately nourished ones as mesotrophic. Well-nourished and overnourished water bodies are classified respectively as eutrophic and hypereutrophic waters (Chapra, 1997; Manahan, 2010).

One of the chief indicators of river and lake eutrophication is the algae due to mainly their response to inorganic materials as well as light as their primary energy source. A

reduced number of algae is found in eutrophic lakes with the quantity of a few species greatly enriched (Wetzel, 2001).

Eutrophication is accompanied by an increase in both the population of Cyanophyceae and Diatomaceae species. Algae such as *Aphanizomenon*, *Anabaena*, *Microcystis*, and *Oscillatoria* aggregates into excessively large populations below the water surface. Blooms of the dinoflagellate *Ceratium* extend a reddish colour to the lake (Zajic, 1971a; Henderson-Sellers and Markland, 1987).

2.3.1. Algae

Algae group of organisms includes macroscopic and microscopic forms which are essentially plant-like. Macroscopic algal forms wash onto beaches or confine to shallow waters. The name of the group derived from the Latin word for sea-wrack. Most of the algae are aquatic organisms inhabit fresh or saline waters. They are usually free-living with some forms adopted symbiotic relationship with marine invertebrate forms like corals and sponges (Sigeo, 2005).

The phytoplankton, the algae of the open water of the lakes and large streams, consist of a diverse assemblage of major taxonomic groups. Many of these forms have different physiological needs and vary in response to physical and chemical factors such as light, temperature, and nutrient. The photosynthetic cyanobacteria, formerly called as the blue-green algae, is the major component of the phytoplankton (Wetzel, 2001).

Despite these taxonomic and physiological diversities, many algal and cyanobacterial species coexist in the same volume of water. Dominant genera in algal groupings change both spatially (horizontally and vertically) and seasonally as physical, chemical, and biological conditions change. The precise reasons for seasonal succession of phytoplankton are not well-known, yet these changes has been correlated with environmental factors of many lakes (Wetzel, 2001).

Overwhelming majority of algae are microscopic unicellular, floating forms which constitute the phytoplankton. The earth's surface is covered by water in a 70% and it is probable that algae fix more carbondioxide than all the land plants combined. Large volume of water which they occupy makes them the most abundant of all photosynthetic organisms. The classification of the algae is based on their cellular properties, the nature of the cell wall, photosynthetic pigments and the arrangement of the flagella motile cells (Sigeo, 2005).

The cyanobacteria (blue-green algae) is one of the most studied of all algal groups. They are true bacteria with a simple prokaryotic cell structure that lacks certain memberanous structures including nuclear membrane, mitochondria, and chloroplast. The majority of algal species have the ability to photosynthesize functionally like plants in aquatic systems. The cyanobacteria are distinguished from other bacteria by the presence of chlorophyll a. They are also able to use water as an electron donor in photosynthesis. They occur in unicellular filamentous and colonial forms mostly are enclosed in mucilaginous sheaths either individually and or in colonies (Wetzel, 2001).

A main algal characteristics is the presence of photosynthetic pigments which are chlorophylls, carotenoids, and proteins. Chlorophyll a is the primary photosynthetic pigment present in all oxygen-evolving photosynthetic organisms, including algae and cyanobacteria. Chlorophyll a has two in vitro adsorption bands, in the red-light at 660-665 nm and at lower wavelenghts near 430 nm. Chlorophyll b is found only in the green algae, euglenophytes, and some minor groups. Chlorophyll b is a light gathering pigment that transfers absorbed light energy to chlorophyll a in photochemical processes. Chlorophyll c is an accessory pigment to photosystem. Chlorophyll d is a minor pigment component found only in certain red algae (Wetzel, 2001).

The majority of algal species have the ability to photosynthesize. As a result they have very simple nutritional requirements and in the light may grow in a completely inorganic medium (Zajic, 1971a; Henderson-Sellers and Markland, 1987; Wetzel, 2001; Sigeo, 2005).

2.3.2. Algae Growth Mechanism

The growth rate varies between populations in an aquatic ecosystem. As an asexually producing microbial organism the algae has the capability to reproduce quickly into large populations and to optimize the beneficiary environmental changes which leads the blooming phenomena. This gives the algae the superiority in terms of reproducing rate and population size. However, when the conditions in the environment become adverse, the mortality in the algae bloom is high as they have weak competitive ability and ephemeral nature (Henderson-Sellers and Markland, 1987).

2.3.2.1. Modeling of Growth Kinetics. The growth of algae in a batch culture under sufficient initial nutrients and favorable conditions was based on the microbial kinetics of bacterial growth which typically includes six phases over time: lag phase, acceleration phase, exponential (growth) phase, retardation phase, stationary pahse, and death (decline) phase. Bacterial growth curve representing algae growth and changes in growth rate in each growth phase were demonstrated in Figure 2.2.

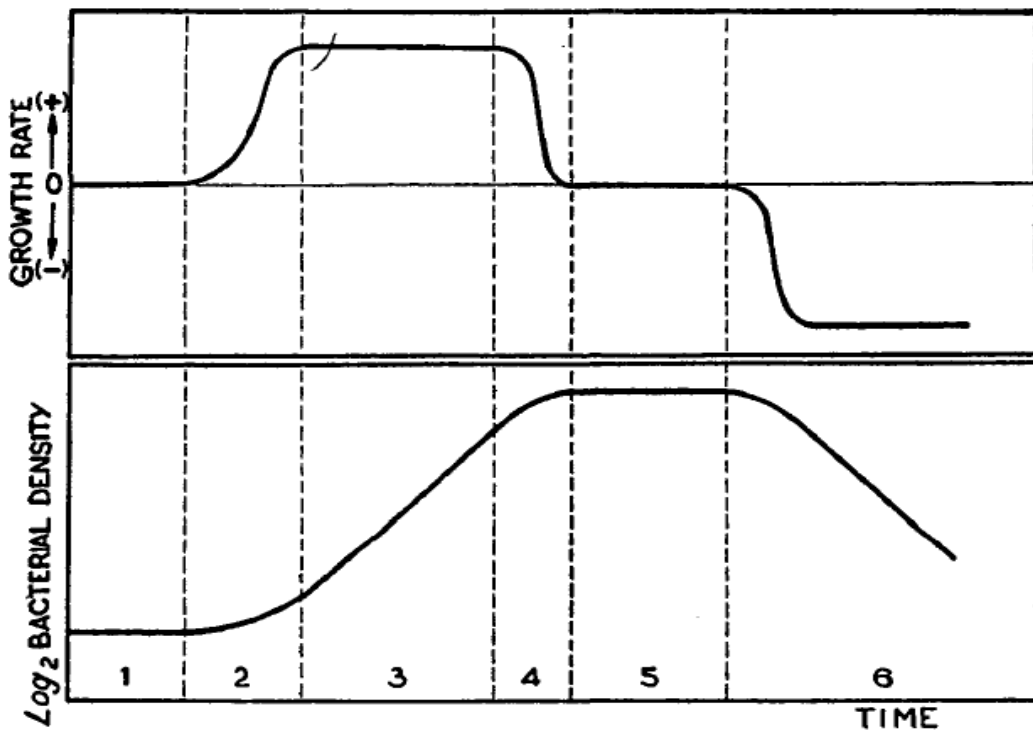


Figure 2.2. Six phases of algae growth and variations of growth rate (Monod, 1949).

Lag phase is described as a short period of inactivity after inoculation of the cells during which no growth occurs. The delay can be explained by the time taken for the cells to synthesize the enzymes necessary to metabolize the new substrate (Lester and Birkett, 1999). When the cells begin to grow they typically grow at a maximum rate because of the abundance of substrate (nutrients). The period of rapid increase by binary fission was called as exponential phase or growth phase that was limited to the substrate and the ability of the microorganisms to process the substrate. As the microorganism population exhausts the limiting substrate, the exponential growth enters the stationary phase in which the growth rate levels off and the new cells come into balance with the death of old cells hence net growth rate goes zero. The decline in growth rate may be hastened by environmental factors such as the generation of toxic metabolic by-products by the microorganisms. If incubation is continued, maintenance in stationary phase eventually outpaced by cell death and the population will decline in death phase. The cells will also lose their structural integrity and enter a process known as lysis as the cells start to break up (Chapra, 1997; Lester and Birkett, 1999).

The growth of algae population is balanced by the growth and death of cells in the population. Growth rate for algae could be represented by the balance between growth rate and death rate for the algae population as shown in equation 2.1 (Chapra, 1997):

$$dX/dt = (k_g - k_d) X \quad (2.1)$$

where X: cell concentration (cells mL⁻¹)

k_g: growth rate (per second: s⁻¹)

k_d: death rate (s⁻¹)

In addition to modeling algae growth by exponential growth substrate limited models have been developed. The relation between the algae growth rate and the concentration of substrate can be described by the model which is called as “Michaelis-Menten model” or

“Monod model”, after the Nobel Prize winning microbiologist Jacques Monod who was the first to apply it to model microbial growth, with the following empirical equation:

$$k_g = k_{g,max} S / k_s + S \quad (2.2)$$

where k_g : growth rate (s^{-1})

$k_{g,max}$: maximum growth rate in the abundance of substrate (s^{-1})

S : substrate concentration ($mg L^{-1}$)

k_s : half-saturation constant ($mg L^{-1}$)

At low food levels i.e. $S \ll k_s$, the growth rate becomes directly proportional to the supply of nutrients as given by equation 2.3.

$$k_g = k_{g,max} S / k_s \quad (2.3)$$

At high food levels i.e. $S \gg k_s$, the growth rate becomes constant and independent of the food supply as given by equation 2.4. Michaelis-Menten parameters can be evaluated by a variety of methods to estimate the growth rate parameters for simple reactions. Many approaches involved transforming the equation 2.2 so that a straight line could be plot. Some of the mostly known approaches were summarized in Table 2.2 (Chapra, 1997).

$$k_g = k_{g,max} \quad (2.4)$$

Table 2.2. Parameter Estimations for Michalis-Menten (Monod) Equation

Method	Equation
Lineweaver-Burk plot	$1/k_g = (k_s/k_{g,max} S) + (1/k_{g,max})$
Hanes equation	$S/k_g = (S/k_{g,max}) + (k_s/k_{g,max})$
Hofstee equation	$k_g = k_{g,max} - k_s (k_g/S)$

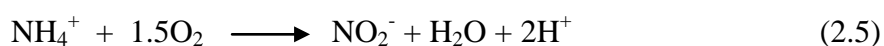
Michalis-Menten (Monod) equation allows the introduction of nutrient limits into the algae growth kinetics which is a characteristic of the eutrophication models. The approaches for parameter estimation have their own advantages and strictnesses so the best method for a good modeling of growth must be preferred according to the applied cases.

2.3.2.2. Factors Affecting Growth. Although one factor may limit growth, it would be quite unusual to find a system completely controlled by a single factor. The ecosystem normally responds to variations in temperature, pressure, pH, oxygen concentration, depth, nutrients such as nitrogen source, carbon source, phosphate source, etc. Performing a multivariate analysis of the simultaneous influence of these factors on growth and function is an ideal way of defining these variations (Zajic, 1971a).

Most natural waters are rich in nutrients but the quantities of various nutrients can vary considerably. In the abundance of some nutrients bloom formation of organisms occurs in a body of water. Water temperatures vary from 0 °C to 100 °C. Most microorganisms thrive in water at moderate temperature. The pH condition of freshwater varies from 2 to 9. Most microorganisms grow best in waters with a neutral pH. In aquatic environments, oxygen can be the limiting factor in the growth of microorganisms. Because of slow solubility of oxygen in water, its concentration never exceeds 0.007 g per 100 g of water. Oxygen is depleted by decomposers by oxidizing the organic matter, when water contains large quantities of organic matter which is more likely in lakes and ponds than in running water of rivers and streams that is continuously oxygenated by the running movement. The depth to which the sunlight penetrates the water is important for the algae receiving sunlight, especially in deep lakes. Photosynthetic organisms are limited to locations with adequate sunlight. Eucaryotic algae cyanobacteria only live in water that receives adequate sunlight (Csuros and Csuros, 1999).

2.3.2.3. Nitrate and Phosphate. Nitrate and phosphate are the two major nutrients for algae that were thought to primarily control excess growth of algae. Nitrate can be found in all natural waters in varying concentrations which may enhance the growth of algae when reached to high levels in water. Nitrate is produced by nitrification in a two step-reaction

by specialized bacteria. In the first step oxidation of ammonium (NH_4^+) to nitrite (NO_2^-) is catalyzed by bacteria species that were named beginning with nitroso- for e.g. nitrosomonas and nitrospira. In the second step nitrite is converted to nitrate (NO_3^-) by different bacteria that were called nitrobacter. The reactions were given in equations:



High levels of ammonium (NH_4) above 1 ppm in water are generally indicative of utilization by algae, bacteria and decomposition within the water system. Field measurements of nitrates (NO_3) and nitrites (NO_2) are good guides to the nutrient condition of lakes, streams and estuaries (Evangelou, 1998).

In soils the inorganic form of phosphate (orthophosphate) exist in various forms. Oxide-phosphate complexes are found as clay-mineral edge-phosphate complexes. Minerals of apatite (Ca-phosphates), Mn-phosphates, Fe(III)-phosphates, Al-phosphates, and to a lesser degree pyrophosphate (e.g., $\text{Ca}_2\text{P}_2\text{O}_7(\text{s})$). The concentration of P in soils from inorganic forms is very small (in the range of 0.03 mg L^{-1}). Therefore, the mobility of soluble inorganic phosphate in soil systems is insignificant for all practical purposes. However, most of the mobilized inorganic phosphate in soils is in the form of small mineral and/or colloidal particles. The mobility of large amounts of P can be accounted for by the mobility of organic waste during intense rainstorms. Such organic waste may be carried by runoff as suspended particles owing to this low density, and as colloidal particles owing to their high charge and/or soluble organic components. The mobility of phosphorous to streams, rivers and lakes is a major concern because of its contribution to eutrophication (Evangelou, 1998).

Nitrogen and phosphorous are the primarily controllable nutrients exporting to water systems from both point sources like for e.g. the use of phosphate detergents contributing to domestic sewage and from nonpoint sources such as forest, agricultural, urban and atmospheric sources. Since algae take up the nutrients from water in proportion to their cell

stoichiometry, it is important to identify which several nutrients control the level of algae in a water body. Generally these controlling nutrients are referred to as “limiting nutrient” by comparing the nutrient levels with cell stoichiometry and this is commonly concerned with assessing nitrogen and phosphorous levels in the water. Nitrogen-to-phosphorous ratio (N:P ratio) is a rough rule that is commonly used to identify the limiting nutrient. N:P ratio in biomass is approximately 7.2. An N:P ratio in the water below this level suggests that nitrogen is the limiting nutrient. Conversely, $N:P > 7.2$ imply that phosphorous will limit the algae growth (Chapra, 1997). Some researchers suggested estimations for formation of algal blooms based on the abundance of these elements. Smith reported that cyanobacteria tended to be rare when N:P ratio is below 29:1 by weight (Smith, 1983).

2.3.3. Algal Blooms

Algal blooms are dense populations of planktonic algae which develop in aquatic systems including lakes and rivers. Seasonal changes affect the characteristics of algal blooms. In many countries, the natural ecosystem has two algal blooms: a spring bloom and an autumn bloom. During the autumn overturn, blooms are partially associated with the nutrient releases from the hypolimnion to the epilimnion. The maximum chlorophyll a value of spring value is generally taken to be in the order of 20 mg m^{-3} which may be in the range of $2\text{-}200 \text{ mg m}^{-3}$ in different measurements (Henderson-Sellers and Markland, 1987; Sigeo, 2005).

In general, blooms of algae include spring diatom bloom, late-spring blooms of green algae, summer blooms of dinoflagellates and cyanobacteria. Common algal blooms in freshwater sources are the cyanobacteria. The origin of cyanobacterial blooms is due to the population increase as well as the ability to float to the water surface forming dense localized populations. The requirements for the sudden development of surface blooms include (Sigeo, 2005):

- High nutrient concentrations
- High light, temperature and high pH
- High proportion of cells with gas vacuoles

- Stable water column

The key factor in the success of the cyanobacteria in bloom formation is the ability of these organisms to out-compete other members of the phytoplankton at a time of year when certain environmental aspects are at an optimum.

2.3.4. Algal Organic Matter

Algal organic matter (AOM) formed by the metabolic processes of microorganisms of algae represents a significant proportion of the NOM in natural waters (Leenheer and Croué, 2003; Pivokonsky et al., 2006). AOM causes significant challenges in drinking water treatment is released by algae into water extracellularly and intracellularly. These organics were classified as extracellular organic matter (EOM) and intracellular organic matter (IOM) (Her et al., 2004; Tulong, 2004).

Intracellular organic matter (IOM) is the organic material due to cell lysis of the algae. Extracellular organic matter (EOM) released into water extracellularly consists of a large number of anabolic organics including glycolic acid, carbohydrates, polysaccharides, amino acids, peptides, organic phosphates, volatile substances, enzymes, vitamins, hormonal substances, inhibitors, and toxins (Wetzel, 2001; Her et al., 2004; Vasconcelos, 2006).

Two types of extracellular organics of algae are generally remarked which are metabolic intermediate compounds of low molecular weight and metabolic end products of usually higher molecular weight. The rates of extracellular release of these products are quite variable under in situ conditions (Wetzel, 2001; Her et al., 2004). In the epilimnion, the more productive lakes cause an increase in the amounts of released organic carbon. The reported rates changes on annual basis between of those equal to the rates of carbon fixation into cellular constituents < 1% of carbon fixation rate to the average value of 20% (Søndergaard and Schierup, 1982). High release rates of EOM have been a function of CO₂ limitation i.e. by high pH, high population densities, inhibiting light intensities, low light intensities, low cell densities and low growth rates (Wetzel, 2001; Karentz et al., 1994).

Particulate organic matter (POM) includes both living organisms (bacteria, phytoplankton, protozoa and metazoa) and particulate detritus (dead organic material). Transformation of POM to DOM is an essential factor determining the rates of microbial processes in aquatic systems. The POM and DOM fractions in aquatic systems can originate from two different sources of autochthonous and allochthonous organic matter. Autochthonous organic matter is produced in lakes by phytoplankton and other photosynthetic organisms including AOM. The autochthonous organics also comprises detritus and DOC excreted by photosynthetic organisms (EOC) or by heterotrophic organisms such as micro- and mesozooplankton. Secondly, terrestrial sources, since allochthonous organic matter leaches from the catchment area into rivers and lakes. Allochthonous carbon (C) also originates primarily from the photosynthetically produced C, mainly from vascular plants. However, allochthonous DOM usually passes through several degradation stages on its way to the lake and thus is comprised mostly of refractory, high-MW compounds i.e. humic substances (Steinberg, 2003; Tulong, 2004).

2.3.5. Environmental Effects of Eutrophication

Although most of the algal blooms have no adverse effects on the environment, the anthropogenic enrichment of the environment may cause to the formation of dense blooms of toxic dinoflagellates principally in marine and colonial cyanobacteria in freshwater which constitute the major problems of eutrophication. The major nuisance-algae of freshwater systems are colonial cyanobacteria. The cyanobacteria may cause deterioration in water quality and they have adverse environmental effects. In many eutrophic environments quite dense cyanobacterial blooms occur on annual basis when they totally out-compete other algae (Sigeo, 2005).

Primarily the cause of environmental pollution resulted by eutrophication is created by the existence of excessive nutrients in the environment such as nitrates and phosphates because they stimulate abundant growth of algal species leading to formation of plankton blooms in surface of the natural water sources effecting the physical and chemical quality of water and survival of other aquatic organisms. These nutrients increase the biological

oxygen demand (BOD) of the water and reduce the dissolved oxygen available for aquatic organisms. Dissolved organic matter is coupled with the nutritional requirements of algae for organic growth which depend upon the quantity and types of dissolved inorganic compounds in the water system. Organic compounds, in addition to being utilized as a carbon and energy sources by some organisms in water, can function as nonessential accessory substances that may stimulate the growth of algae. Growth substances include a large group of hormones produced by algae that are effective in growth regulation and cell development (Evangelou, 1998; Wetzel, 2001).

In the production of drinking water, eutrophication of surface water is the current and growing problem. Many water treatment plants have been troubled by excessive amount of algae in the raw water that leads to the treatment problems like risk of disinfection by-products (DBPs), shortened filtration cycle, taste and odor, and high organic content in raw water (Vlaski et al., 1996; Chen et al., 1998; Ma and Liu, 2002).

A number of hazardous effects have been exerted on water bodies by eutrophication. Growth of algae and respiration can affect the system's water chemistry such as oxygen and carbondioxide levels which are directly impacted by the activity of algae. Oxygen is crucial for the survival of aquatic organisms such as fish. Especially the bottom waters of thermally stratified water systems can become depleted of oxygen due to the decomposition of dead plants. Eutrophication can alter the species composition of an ecosystem as the environment becomes more productive. Certain species of algae cause taste and odor problems in drinking waters and some species can be toxic to animals feeding on them. Many of the problems become prominent as the eutrophic conditions progress in the water body (Chapra, 1997).

Some species of cyanobacteria are toxic and have been recognized as nuisance in the drinking water industry because they produce earthy and musty smelling compounds, notably geosmin and 2-methyl isoborneol (2-MIB), for which the odor detection thresholds of less than 10 ng L⁻¹ are remarkably low among sensitive individuals. Some genera of those were also known to include toxin-forming species and strains (Chorus and Bartram,

1999). 2-MIB is also controlled and reported in water quality parameters within secondary standards under “odor causing Geosmin” by the local authorities in Turkey (ISKI, 2010).

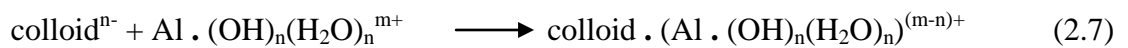
2.4. Coagulation

In drinking water treatment, coagulation is an essential process for the removal of various particulates and organic matter. It has been employed in the early years of water treatment practices primarily to decrease the levels of turbidity. Today it is the most important process in the drinking water treatment industry considering the mass of removed matter (Hendricks, 2006).

Coagulation means the process of inducing contacts between a chemical and colloidal particles to effect a reaction which results in the products called “micro-flocs”. The micro-flocs form larger aggregations by thermal motion i.e. Brownian motion, or by induced velocity gradients with paddle wheel or blade. The bonding together of micro-flocs is called “flocculation” and the large colloids are called “flocs”. The process involves choosing the proper chemicals that are called “coagulants” to destabilize particles, the proper dosages of the coagulants, providing contact between the coagulants and colloidal particles, and the proper pH to ensure micro-floc formation. The effectiveness of the coagulation method is important in water treatment by determining the effectiveness of the subsequent processes such as flocculation, floatation, sedimentation, settling, filtration (Tchobanoglous et al., 2003; Hendricks, 2006).

Coagulation reactions are complex and generally occur in two stages. The first stage is the reactions of metal ions like Al^{3+} , Fe^{3+} with water that result in various species dependent on the pH, dosage, ionic strength, alkalinity. The products are metal complexes with water in low pH range as $4 < \text{pH} < 6$, and at high pH levels like $6 < \text{pH} < 10$ and high coagulant dosages the products are metal hydroxides. The second stage of coagulation is that these metal complexes or metal hydroxydes react in turn with colloidal particles. The reactions vary according to the properties of reacting species and generally classified as “charge neutralization” and “sweep-floc” reactions (Tchobanoglous et al., 2003; Bratby, 2006; Hendricks, 2006).

Charge neutralization (also called adsorption) occurs when $\text{pH} < 6$ between metal complexes and colloids. The complexes incorporate into the diffused double layer of negatively charged colloids hence reduce the repulsive force and promote the Van der Waals forces of attraction to dominate. By means of the attractive forces the colloids come together and attach one another forming a precipitation as the final product. In the removal of organics, precipitation and adsorption are the two dominant mechanisms using hydrolyzing salts (Dempsey et al., 1984; Dempsey, 1989; O'Melia, 1987; Annadurai et al., 2003). An example of charge neutralization reaction for an alum complex was given as:



in which;

$\text{Al} \cdot (\text{OH})_n(\text{H}_2\text{O})_n^{m+}$: aluminum ion complex with water

colloid^{n-} : negatively charged colloid

$\text{colloid} \cdot (\text{Al} \cdot (\text{OH})_n(\text{H}_2\text{O})_n)^{(m-n)+}$: colloid-metal ion complex (micro-floc).

Other type of coagulation reaction is the sweep-floc described as the reaction between metal hydroxide precipitate and colloids when $\text{pH} > 6$. Because of the fractal nature and large surface area of the metal hydroxide precipitate, it provides enmeshment of the negatively charged colloids by a sweeping mechanism. Like in the charge neutralization process, again van der Waals are dominant causing a bonding between the colloidal particles and hydroxide flocs (Randtke, 1988; Hendricks, 2006).

Understanding coagulation requires a variety of knowledge from different fields. Because of this need, many terms have been assimilated from the fields such as colloid science, polymer science, aqueous chemistry as a part of coagulation practice (Hendricks, 2006).

2.4.1. Colloids and Interfaces in Water

The characteristics of colloidal particles which will be removed in water are important in the coagulation-flocculation process of water treatment. Size-range distributions of some components of natural aqueous systems are presented in Figure 2.3.

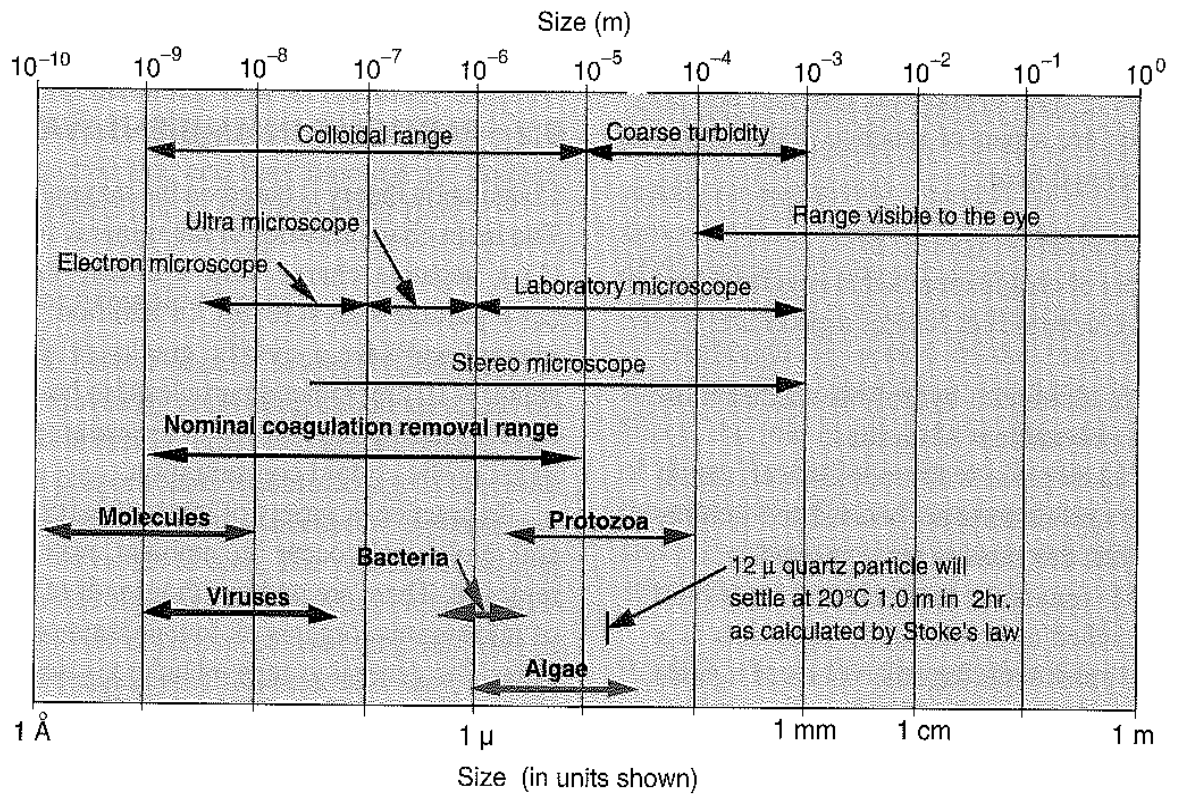


Figure 2.3. Molecular size range of particles in natural waters (Hendricks, 2006)

For practical purposes the dispersed particles in water may be classified as suspended and colloidal. Suspended particles are generally removable by gravity sedimentation. Materials between 0.01 μm and 100 μm are basically nonsettleable. Colloids are those which are nominally $<10 \mu\text{m}$. They are larger than atoms and small molecules and pass through ordinary filters. Bacteria are about 1 μm and algae are in the range of 1-50 μm . Viruses are smaller than bacteria and algae. Protozoa are in size of 5-100 μm . The coagulation is likely to be effective in a wide range from molecular sized viruses to macro particles. The existence and characteristics of the particles in a water body are dependent on the environmental conditions as well as human interventions (Zajic, 1971b; Tchobanoglous et al., 2003; vanLoon and Duffy, 2005; Hendricks, 2006).

Humic substances which are a major class of natural organic matter in the environment exhibit characteristic properties of colloidal particles in acid solution. They

display a range of important colloidal interactions in the presence of metal ions and some other substances. Humic colloids in the environment which are formed from plant and animal residues earn the colloidal property by microbial decay through undergoing several mechanisms of humification in soils, sediments and natural waters. At the end of their long time span of biodegradation and their exposure to water, oxygen, sunlight radiation in the environment, humics could be regarded as 'old molecules' after the biodegradative and oxidative route and possibly cannot be much further breakdown unless exposed to specific chemical agents which they have not previously encountered. The substantial aromatic and aliphatic content found in humics and the relatively small content of ionisable carboxylic groups comply with formation of colloidal aggregates of humics on charge neutralisation (Jones and Bryan, 1998).

2.4.2. Particle Stability

The chemical nature and structure of natural organic matter is an important factor in determining the stability of inorganic colloids. Research have been revealed that the presence of organic materials stabilized the inorganic colloids in water. The particles generally have negative charges in water (except some kinds such as chrysotile, asbestos fiber) causing a mutual repulsion coupled with their small size result in a suspension which makes them stable. The stability of inorganic colloids in water is brought by the formation of organic coating on the surface of inorganic particles causing the repulsive action and steric hindrance between the particles. Under environmental conditions, the fulvic acids are likely to be responsible for coating and imparting a negative charge to the colloids through a modification of their charge (Gibbs, 1983; Ma and Li, 1993; Wilkinson et al., 1997; Hendricks, 2006).

Surface charge of a particle may develop in a number of ways depending on the nature of the particle, composition and reactivity of the water medium. Isomorphous replacement is the charge development by replacement of the ions in a lattice structure e.g. Si^{4+} with ions from the solution e.g. Al^{3+} . Charge development can occur by structural imperfections such as brokening of the chemical bonds. When chemically inert substances are in water, they gain a negative charge through preferential adsorption of anions in particular hydroxyl

ions (Tchobanoglous et al., 2003). Particles like proteins or microorganisms acquire a surface charge by the ionization of carboxyl amino groups (Shaw, 1966).

Some researchers indicated that the chemical nature of the NOM has an important role in whether the colloids will be stabilized or destabilized. Fulvic substances are likely to stabilize the colloids by charge modification whereas aquagenic organic material appears to accelerate the coagulation process by bridging aggregation and both occurs simultaneously in a natural aquatic environment (Wilkinson et al., 1997).

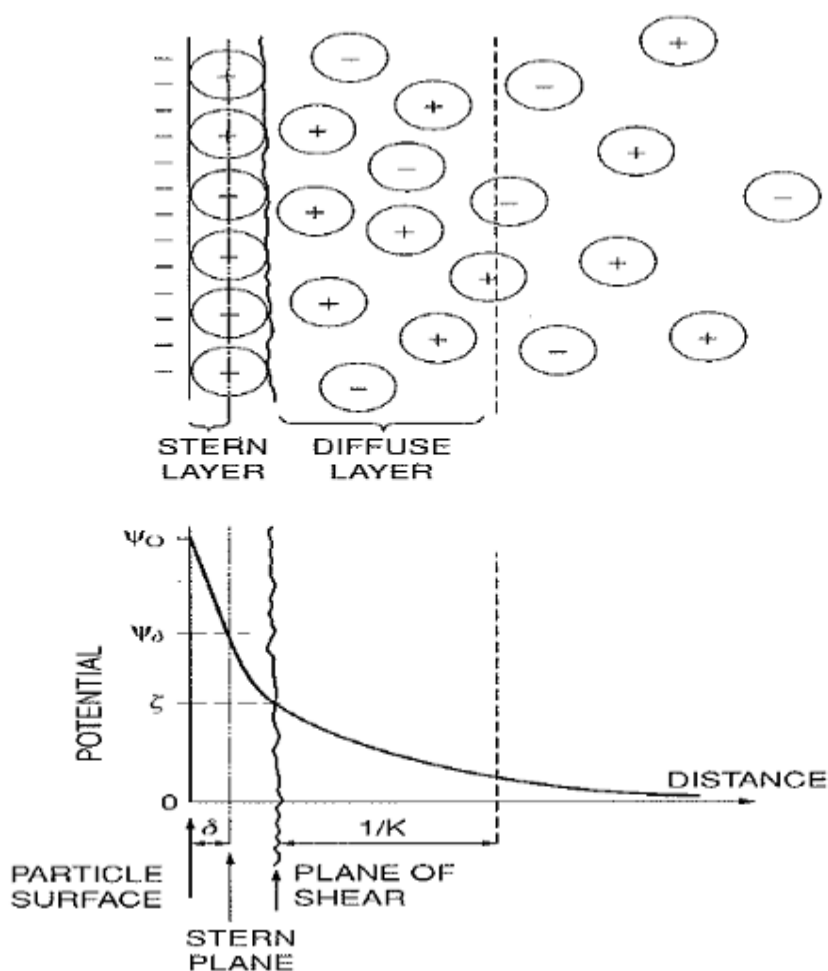


Figure 2.4. A model of electrical double layer (Bratby, 2006)

Once the colloid particle is charged, in the presence of opposite charges in a medium, an electric double layer forms at the interface of solid and aqueous phases. The electrical

double layer consists of the charged particle and an equivalent number of ions of the opposite charge that accumulate in the liquid near the surface of the particle. The particle charge causes an electrostatic potential that declines with distance from the interface. The counter ions form a “diffuse layer” in which the potential approaches to zero with distance. Another layer formed by electric double layer is the “Stern layer” formed between electrical double layer and diffuse layer as the potential drops with distance (Bratby, 2006). Figure 2.4 represents a model of electric double layer.

Repulsive forces are effective between colloidal particles because of the electrical double layer formed. The van der Waals forces of attractions complementarily exist to the repulsive forces i.e. when one is reduced the other force becomes dominant. Both forces have a different functional dependence to distance from the particle surface.

2.4.3. Destabilization and Restabilization

The aim in coagulation application is to reduce the repulsive forces between colloids to overcome the stability of the particles and thus providing the formation of particle aggregations. The charge forces can be overcome in a couple of ways. One of them is to add electrolytes that reduce the thickness of the diffuse layer and reduce the zeta potential. Another method is to use polyelectrolytes which are classified as anionic, cationic, nonionic. The action of the polyelectrolytes when placed in water is to ensure charge neutralization flocculation via polymer bridge formation that is formed when two or more particles adsorbed along the length of the polymer (Bratby, 2006; Hendricks, 2006).

Particle destabilization with metal salts are brought about by addition of metal salts such as alum or ferric salts that operates by two types depending on the pH which are formation of metal hydrolysis and metal complexes as explained in Section 2.4.

Another phenomenon in the concept of particle stability is the restabilization which is the reverse process of particle destabilization. When positively charged metal ions attach at discrete locations of the particle surface the suspension forces of particles is destabilized and precipitation occurs. The effect of metal hydroxide precipitation is not limited to

sweep floc and is preceded by charge neutralization as the positively charged metal hydroxide precipitation increases in solution. Eventually, charge reversal occurs in the medium which is called as restabilization (Bratby, 2006). Destabilization-restabilization phenomena is shown in Figure 2.5.

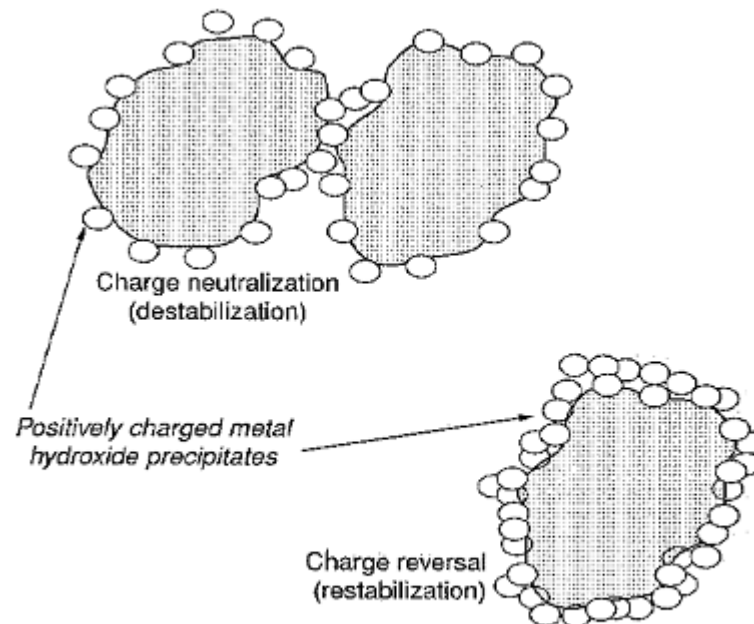


Figure 2.5. Destabilization and restabilization of colloids during coagulation (Bratby, 2006).

2.4.4. Coagulants

The commonly used conventional coagulants in water treatment include two categories: aluminum-based coagulants and iron-based coagulants. Aluminum-based coagulants are aluminum sulphate, aluminum chloride, sodium aluminate, aluminum chlorohydrate, polyaluminum chloride, polyaluminum sulphate chloride, polyaluminum silicate chloride and polyaluminum chlorides with other organic polymers. The iron coagulants are ferric sulphate, ferrous sulphate, ferric chloride, ferric chloride sulphate, poly-ferric sulphate, and ferric salts with organic polymers. There are also others used including hydrated lime and magnesium carbonate (Bratby, 2006; Shi et al., 2007).

Coagulant selection and dose when designing the water treatment conditions are governed by dissolved organic carbon (DOC), temperature, and turbidity of the raw water (Srinivasan and Viraraghavan, 2003). O'Melia and co-workers indicated the relative order of importance of these parameters as DOC > temperature > turbidity (O'Melia et al., 1987).

Coagulation with ferric or aluminium salt is very common in water treatment throughout the world. A number of related researches have been reported on the conventional coagulation with ferric and aluminium salts to reduce the turbidity, color and organic matter. Many authorities use alum as coagulant because of its proven performance in effective turbidity and pathogen removal (Srinivasan and Viraraghavan, 2003; Hendricks, 2006). The use of a coagulant containing aluminum may either increase or decrease the aluminum concentration in the finished water, depending on its speciation in the source water as well as species change during water treatment (van Benschoten and Edzwald, 1990). The relationship between NOM and alum is stoichiometric. An alum dosage in excess is needed for removal of that colloids like NOM which may be particularly achieved by excess alum adding process (Hendricks, 2006).

2.4.5. Optimized Coagulation

The coagulation performance may be enormously affected by many factors such as the type of coagulants, coagulation pH and the raw water quality (Yu et al., 2007). One of the most important factors in coagulation with hydrolyzing metal coagulants, is the effect of pH. The predominance of a particular hydrolysis species during destabilization is mostly dependent on the value of pH. For a particular colloidal suspension there is a particular hydrolysis species which is most effective for destabilization, either by virtue of the charge carried, or the adsorptivity of the species (Bratby, 2006).

It has been proved by many research that application of aluminum and iron salts cause reduction in color and removal of organic substances at the pH range of $5.0 < \text{pH} < 6.0$. Chow and colleagues reported the optimum pH for DOC removal with alum to be between

pH 5.0–6.0 and pH values lower than 5.0 coagulation as ineffective (Chow et al., 2009). An increase in pH above 7.0 enhances desorption of organic pollutants and promotes their reappearance in treated water. At pH 7.0, higher concentrations of residual DOC remain even at the higher dosing levels. For further reduction of the concentration of residual DOC in the water, treatment by using either higher alum doses or reduction to pH conditions between pH of 5.0–6.0 is necessary i.e., optimized coagulation conditions (Chow et al., 2009).

2.4.6. Removal of NOM by Coagulation using Metal Salts in Natural Waters

Coagulation using metal salts is one of the standard methods for removing natural organic matter (NOM) during drinking water treatment. A considerable effort has been focused toward optimizing the coagulation process for dissolved organic matter (DOM) removal. Parameters of DOM reduction have included dissolved organic carbon content, UV absorbance and color, trihalomethane formation potential and apparent molecular weight distribution (Croué et al., 1993).

The mechanisms of coagulation with regard to NOM removal are charge neutralization for colloidal organic material and charge complexation/precipitation of soluble compounds. Additional removal occurs due to adsorption of colloids onto precipitated flocs and metal hydroxides. The removal efficiency of organic matter by coagulation varies widely, generally between 10 and 90% (Randtke, 1988).

The elimination of organic materials by coagulation is impacted by many factors such as the conditions of the coagulation, the characteristics of natural organic matter, the nature and concentrations of inorganic compounds used as coagulant, and the design of the treatment processes (Volk et al., 2000). Studies have shown that the coagulant selection and dose are governed by raw water quality such as DOC, temperature and turbidity (O'Melia et al., 1987).

Many investigators have underlined the importance of DOC in the determination of effective coagulant dose (Croué et al., 1993). The effects of DOC characterization of the

organic matter have been investigated by several researchers according to hydrophobic/hydrophilic fractionation of DOC with the technique based on adsorption chromatography using XAD-8D resin (Semmens and Staples, 1986; Collins et al., 1986). The results have shown that hydrophobic compounds were slightly removed better than hydrophilic compounds with alum coagulation of the water samples.

In agreement with the fractionation findings, the change in the composition and characteristics of the organic matter creates a greater coagulant demand for the removal process. The hydrophobic (nonpolar) NOM fractions such as humic and fulvic acid fractions have a significantly higher charge density than the hydrophilic NOM fractions. The nonpolar NOM has been well characterized and removed by coagulation. In contrast the polar NOM have not been not well characterized and difficult to remove. Coagulation is an effective method for removing high molecular weight organic compounds which have a molecular size greater than 30 kDa. However, due to the heterogeneous mix of compounds it is still difficult to make conclusive statements with regards to the differences between these fractions (Dickenson and Amy, 2000; Nissinen et al., 2001; Sharp et al., 2006).

Coagulation of humic substances which plays a role in the formation of organic halide compounds such as THM in drinking water sources has been given attention in many studies. The stoichiometry of coagulation in the conducted studies has shown a relationship between initial concentration of humic substance and coagulation dose as well as pH, coagulant type, origin and nature of the humic substance (Kim et al., 1989). pH is one of the most significant variable affecting coagulants. An optimum pH range of 4.0 to 5.0 for iron and 5.0 to 6.0 for alum have been reported in the coagulation studies of humic substances. Aquatic fulvic acid showing hydrophilic acid characteristics which accounts for a significant percentage of the DOC in natural waters is observed to be less removable than aquatic humic acid of the same (Croué et al., 1993). In eutrophic water sources, the change of dissolved organic carbon (DOC) composition, i.e., the ratio of large molecules to small molecules declines as the algae propagate through the water system makes DOC removal difficult in the treatment processes of drinking water (Volk et al., 2000; Cheng and Chi, 2003; Hu et al., 2006).

2.5. Literature Review

Bekbölet and colleagues have been working on the characteristics of natural organic matter (NOM), removal of NOM, and molecular size distribution (MSD) of NOM and humic acids in their various studies. In one of their studies, coagulation characteristics of humic acids were evaluated using alum and ferric chloride coagulants (Uyguner et al., 2007). The optimum coagulant doses were found to be 30 mg L^{-1} and 60 mg L^{-1} for the alum and ferric chloride coagulants, respectively. By using the determined optimum doses for the two coagulants, the removal efficiency for UV_{254} was found to be 88 % for alum and 92% for ferric that came up with a higher removal efficiency than alum. When removal efficiency was monitored in terms of Color_{436} , alum coagulation was favored with an efficiency of 96 % while 86 % of removal efficiency was attained using ferric chloride.

Uyguner and Bekbölet found that during the degradation of humic substances, drastic changes were assessed in the absorption and fluorescence properties of humic acids relevant to the molecular size distribution profiles (Uyguner and Bekbolet, 2005b). According to the spectroscopic evaluation of the molecular size distribution, the degradation of humic acid reveals the formation of lower molecular size (small fractions) and higher UV absorbing compounds. Molecular size distribution data of the humic acid in terms of UV_{254} demonstrated a decreasing trend as the sizes of molecular weight cutoff were decreased. It was indicated that the decrease of the UV absorbing properties of each humic acid fraction could be a consequence of the decomposition of the humic material to smaller molecular size fractions. Using fluorescence spectroscopic analysis in synchronous scan they found a similar result that the spectra of each size fraction exhibited a decreasing trend in terms of fluorescence intensity. The evaluation made was significant in that the gradual decrease of fluorescence intensity in the 450–600 nm region in synchronous scan might indicate the degradation of the high molecular weight components of humic acid and formation of lower molecular size fractions of humic acid during photocatalysis.

Chow and colleagues studied on the optimized coagulation of natural organic matter with alum in Australian drinking water reservoirs (Chow et al., 2009). The removal of

NOM by alum treatment was found to be dependant on the molecular weight and composition of the organic matter. Following the treatment, the remaining DOC was found to have smaller molecular weight and lower SUVA value compared with the DOC of the raw water. They found maximum NOM removal occurred at pH 5.0 but the residual concentrations of aluminium exceeded the Australian Drinking Water Guideline with a value of 0.2 mg L^{-1} . Optimum coagulation was achieved at pH 6.0 with a removal of DOC rate about 50% whereby a concurrent lowering of the average molecular weights of the organic compounds detected.

Volk and co-workers assessed the impact of optimized coagulation on the removal of natural organic matter using alum and ferric salts (Volk et al., 2000). They found that the amount of NOM removal was strongly related to the pH of coagulation and the type of coagulant used. Using iron salt was reported to result in greater removal of DOC and BDOC mainly due to more favorable pH. Analysis of initial raw water characteristics was underlined in the effectiveness of both quantity and quality of NOM treatment efficiency with a ranging UV_{254} reduction between 8% and 96 % and ranging DOC removal between 4% and 76% between different samples tested.

Lorentsson and colleagues proposed a new approach to determine the optimal conditions such as pH, coagulant dose for the coagulation-based water purification for the elimination of the drawbacks inherent to the commonly adopted procedure (Lorentsson et al., 2002). Based on a modified coagulation test, they proposed the following stages for determining the optimum conditions of coagulation: 1. determination of the initial characteristics of the water such as pH, chemical oxygen demand (COD), color, turbidity; 2. determination of a tentative coagulant dose using, for example, empirical formulae; 3. determination of the dependence of the water purification efficiency on pH for a series of coagulant doses, including the tentative dose found in accordance with stage 2 and plotting the corresponding graphs; 4. selecting the optimal coagulant dose and conditions for the coagulation-based water purification based on of the data obtained.

Sen-Kavurmaci and Bekbolet worked on the reactivity of trivalent cations i.e. Al(III) and Fe(III) towards raw, ozonated, photocatalytically treated and sequentially oxidized

humic acids attained by the application of a combined system by performing jar tests using appropriate concentrations of trivalent cations that were added to raw and treated humic acid solutions at pH=5.5 (Kavurmacı and Bekbolet, 2010). The effective Fe(III) dosages were found to be higher than the effective Al(III) dosages as concluded by the removal efficiencies. For Al(III) application 95% UV₂₅₄ and 98% Color₄₃₆ removals and 94% removal for both of UV₂₅₄ and Color₄₃₆ was obtained for Fe(III) application.

In a study by Kerç, the removal of humic acids by ozonation revealed the effects of oxidation processes on the humic acid molecules that were assessed using molecular size distribution by ultrafiltration of the oxidized samples (Kerç, 2002). Molecular size distribution analysis applied was reported to indicate that changes in the structure of humic acids occurred due to oxidation. Molecular size range for the untreated humic acid was reported as 1,000 Da – 450, 000 Da. Preozonation after the photocatalysis were found to shift the molecular size to 500 – 100, 000 by the largest molecular size was 30,000 Da and 50 % of the molecules were less than 500 Da.

Alum and ferric chloride were found to be effective coagulants for removal of humic acids by coagulation in a study of Sen (Şen, 2004). Both coagulants were found to result in nearly same removal percentages of UV₂₅₄ and Color₄₃₆ by the application of their determined optimum dose at pH 5.5 but different optimum doses were determined which was higher for ferric than alum. In addition, with the application of each coagulant coagulation of humic acid was reported to lead more color removal than aromaticity removal in percentage base as the results of analysis indicate by Color₄₃₆ and UV₂₅₄ data.

Bekbolet addressed that the formation and speciation of disinfection by-products mostly depend on the source water characteristics both in terms of NOM and water matrix in a comparative study illustrating the effectiveness of various conventional and novel treatment schemes on the formation of DBPs (Bekbolet, 2009). It was reported that speciation and chemical properties of NOM could be changed resulting in diverse reactivities towards the applied treatment processes as significant variations in HAAs formation were observed both between the samples and treatment schemes. In case coagulation treatment, composition of NOM was designated as the major important

parameter in coagulation efficiency. It was found that application of Fe and Al based coagulants displayed quite similar reactivities towards the organic matter contents of water samples from Istanbul drinking water reservoirs. UV₂₅₄ removal efficiencies were found to be greater than DOC removal efficiencies irrespective of the coagulant type and source water.

3. MATERIALS AND METHODS

3.1. Materials

3.1.1. Synthetic Freshwater

Synthetic freshwater was used to cultivate algae. Detailed information on the preparation of synthetic freshwater is presented in Section 3.2.1.2.

3.1.2. Coagulants

Aluminum sulphate ($\text{Al}_2(\text{SO}_4)_3 \cdot 18\text{H}_2\text{O}$) and ferric chloride (FeCl_3) salts were used to prepare aluminum sulphate, ($\text{Al}_2(\text{SO}_4)_3$) and ferric chloride (FeCl_3) solutions to be used as coagulants in the coagulation experiments. Coagulant salts were supplied from Riedel-de Haen.

3.1.3. Algae

Freshwater algae inoculum was supplied from İSKİ Ömerli Drinking Water Purification Foundation.

3.1.4. Humic Acid

Humic acid was supplied from Aldrich (AHA) for the preparation of humic acid solutions. 1 L of stock solution was prepared in a concentration of 1000 mg L^{-1} by dissolving humic acid salt in distilled-deionized water and filtering through paper filter. 10 mg L^{-1} and 20 mg L^{-1} solutions of humic acid samples were prepared by diluting of the stock solution with distilled-deionized water. 10 mg L^{-1} humic acid solution was added into the synthetic freshwater algae cultivation media. 10 mg L^{-1} and 20 mg L^{-1} solutions of humic acid were used for comparing the spectral properties of dissolved organic matter

water samples to the humic acid. Stock humic acid solution was stored in a dark glass in dark to protect from light to prevent decomposition.

3.2. Methods

3.2.1. Cultivation of Algae

Algae cultivation was carried out in two kinds of medium namely distilled water medium and synthetic freshwater medium. Periodic sampling was provided to follow the algae growth and to attain the optimum growth conditions according to the basic algae growth curve profiles.

Considering the nutrient loading conditions, simulated water samples were prepared using different combination of nitrate, phosphate and other common inorganic anions, cations, and Aldrich humic acid to contribute as dissolved organic carbon (DOC, mg L⁻¹). The samples were spiked with algae representing the consortium in natural water systems.

Algae growth media were prepared using macronutrients and micronutrients (Table 3.1, Table 3.2) according to “Standard Methods for the Examination of Water and Wastewater” to cultivate the algae (APHA, 1998). Nutrients were added in the 0th day of the cultivation period as supply nutrients for algae and no other addition were done in the following days.

The cultures were maintained at room temperature between 18-25 °C where they received continuous light with a lamp of 80 Watt, and oxygen (O₂) aeration by bubbling air into the growth flasks twenty four hours a day. During the cultivation, to prevent the settlement of the algae cells the flasks were thoroughly hand shaken every day as the flask mouth kept closed.

3.2.1.1. Preparation of Nutrients. Nutrients of algae were added into the algae media using stock solutions of macronutrients and micronutrients in the amounts given in Table 3.1 and Table 3.2 in the nutrient lists (APHA, 1998).

Table 3.1. Macronutrient stock solution list (APHA, 1998)

Compound	Concentration mg L ⁻¹	Element	Resulting Concentration mg L ⁻¹
NaNO ₃	25.5	N	4.20
NaHCO ₃	15.0	Na/C	11.0/2.14
K ₂ HPO ₄	1.04	K/P	0.469/0.186
MgSO ₄ .H ₂ O	14.7	S	1.91
MgCl ₂	5.70	Mg	2.90
CaCl ₂ .2H ₂ O	4.41	Ca	1.20

Table 3.2. Micronutrient stock solution list (APHA, 1998)

Compound	Concentration µg L ⁻¹	Element	Resulting Concentration µg L ⁻¹
H ₃ BO ₃	186	B	32.5
MnCl ₂	264	Mn	115
ZnCl ₂	3.27	Zn	1.57
CoCl ₂	0.780	Co	0.354
CuCl ₂	0.009	Cu	0.004
Na ₂ .MoO ₄ .2H ₂ O	7.26	Mo	2.88
FeCl ₃	96.0	Fe	33.0
Na ₂ EDTA.2H ₂ O	300	---	---

3.2.1.2. Preparation of Synthetic Freshwater. Synthetic freshwater was prepared with the combination of three salts and high purity water. Prepared stock solutions of these salts were used to compose a final solution that is brought into equilibrium with the atmosphere according to the prescribed order of the given recipe for preparing soft synthetic freshwater in “Methods for Preparing Synthetic Freshwaters” (Smith et al., 2002). S_1 , S_2 , and S_3 denote the salts used in the recipe for soft freshwater. The compound ingredients and their substituent amounts are given in Table 3.3.

Table 3.3. Recipe for soft synthetic freshwater (Smith et al., 2002)

Stock solution	meq L ⁻¹	Final required concentration, mg L ⁻¹		Mass of salt per volume water, g L ⁻¹	Concentration factor
		C ^{Z+}	A ^{Z-}		
S_1					
MgCl ₂ .6H ₂ O	120	1458	4254	12.168	x 1000
CaCl ₂ . 6H ₂ O	160	3206	5672	17.500	
Ca(NO ₃) ₂ .4H ₂ O	30	0601	1860	3.542	
S_2					
CaCO ₃	340	6814	10201	0.0187	x 1.1
S_3					
Na ₂ SO ₄	230	5288	11046	16.334	x 1000
KHCO ₃	25	0977	1525	2.502	
NaHCO ₃	20	0458	1220	1.678	

(C: Cation A:Anion z: integer denoting charge of the ion)

Appropriate volumes of stock solutions S_1 and S_3 were added to the required volume of stock solution S_2 , while it was being vigorously stirred to avoid local super saturation. The volume made up to 5 L with high purity water to avoid introducing contamination and

organic substances into the water (Smith et al., 2002). Table 3.4 shows the required volumes of stock solutions S₁, S₂, and S₃ to make up the freshwater.

Table 3.4. Dilution factors for making 5 L of soft synthetic freshwater (Smith et al., 2002).

Stock solution	Volume, mL	Dilution factor
S ₁	5	1/1000
S ₂	4455	1/1.1
S ₃	5	1/1000
Distilled water	445	

3.2.1.3. Cultivating Algae Using Distilled Water. Cultivating algae using distilled water was achieved by inoculating mixed culture of unicellular green algae into 2 L distilled water in Erlenmeyer flask. Freshwater algae were supplied from İSKİ Ömerli Drinking Water Purification Foundation.

Four parallel sampling were used which were different in terms of phosphate nutrient amount included. Two of the mediums had the N:P ratio as 1x(N:P), and the other two mediums had 5 times the N and P amounts, (5xN:5xP). According to the nutrient amounts used, the N:P ratio of the mediums was 21 (4.20:0.186). Two of the mediums, namely M_{1,1} and M_{1,2}, had this ratio of 21 as 1x(N:P), while the other two mediums M_{5,1} and M_{5,2} had the same ratio by 5 times multiplied for each anions, (5xN:5xP).

3.2.1.4. Cultivating Algae Using Synthetic Freshwater. Synthetic freshwater algae growth media were prepared by using synthetic freshwater which was prepared as defined in materials and methods part. Parallel sampling was carried by using four identical samples in a size of 5 L.

Composition of nutrients, unlike distilled water algae media, consisted of only phosphate as a macronutrient (Table 3.1), and all the micronutrients (Table 3.2) in the

nutrient lists were added into the synthetic freshwater. The initial numbers of algae were selected as 1×10^4 - 2.5×10^4 for each synthetic water samples. The nitrogen to phosphorous ratio (N:P) was the same for all of the synthetic water samples by a value of 21 (4.20:0.186). The synthetic freshwater medium used in this study was denoted with capitals SW and samples were numbered as SW₁, SW₂, SW₃, SW₄.

3.2.2. Coagulation Experiments

Optimized coagulation method was applied for the removal of organic matter. Jar test experiments were conducted using alum and ferric chloride as coagulants to determine the optimum pH and optimum coagulant dose using 50 mL samples.

The specified pH values of coagulation were 5.5, 6.0, 6.5 and 7.0. Optimum removal profiles were identified for each pH of coagulation according to UV₂₅₄ removal. The optimum pH was determined as the pH at which maximum UV₂₅₄ and dissolved organic carbon (DOC, mg L⁻¹) removal were achieved. Other parameters such as UV-vis parameters of UV₂₈₀, UV₃₆₅, Color₄₃₆, and fluorescence spectra were also analyzed for each coagulation series.

The coagulants used were aluminum sulphate (Al₂(SO₄)₃) and ferric chloride (FeCl₃). 0.05% Al₂(SO₄)₃ stock solution was prepared using Al₂(SO₄)₃.18H₂O salt. FeCl₃ solution was freshly prepared before use in experiments as 0.05% of 50 mL solution using FeCl₃.6H₂O salt. The coagulant preparation was involved making the defined solutions by directly dissolving corresponding amount of alum and ferric salts into distilled-deionized water. The coagulant doses ranged from 5 mg L⁻¹ to 80 mg L⁻¹ for ferric chloride and from 5 mg L⁻¹ to 100 mg L⁻¹ for aluminum sulphate.

Samples were brought to room temperature (20-25 °C) before the jar test application. The standard jar test procedure consisted of 2 speeds of 200 revolutions per minute (rpm) and 30 rpm. The samples were initially mixed rapidly with a speed of 200 rpm for 1 minutes after the addition of chemical coagulant. Following rapid mixing, the sample was mixed at 30 rpm for a period of 20 minutes for the slow floc-growth. Then the sample was

allowed to settle for 60 minutes. The clear supernatant was collected by a syringe to analyze the removal efficiency in terms of UV absorbance, fluorescence intensity and dissolved organic carbon after filtering through 0.45 μm cellulose syringe filter.

3.2.3. Molecular Size Fractionation by Ultrafiltration

Molecular size distribution of the samples were determined by ultrafiltration experiments. The samples were ultrafiltered through molecular size cutoffs varying size to analyze the molecular weight composition of organic matter.

Amicon 8050 ultrafiltration stirred cell system was employed using Millipore YM series cellulose membrane filters. The samples were initially filtered through 0.45 μm Millipore cellulose filter. The filtered samples were then subjected to a sequential ultrafiltration with a decreasing filter size order of 100 kDa, 30 kDa 10 kDa, 3 kDa and 1 kDa to fractionate the molecules of different weight. The cell system worked using a magnetic stirrer. A nitrogen gas tube with a pressure control valve was attached to the stirrer to maintain the appropriate pressure inside the cell. Membrane filters were rinsed with deionized after each run. The filters were stored after washing with 0.1 M NaOH solution and kept in a 10 % ethanol water solution as stated in the manufacturer's guide. The retentate fractions were compared with each other and with 0.45 μm filtration of raw water sample according to UV-vis and fluorescence spectroscopy, and DOC (mg L^{-1}) characteristics of the samples.

3.2.4. Analytical Methods

3.2.4.1. Optical Density Measurement. Optical density was measured by reading absorbance at a wavelength of 600 nm by using a Hach DR/Portable Datalogging Spectrophotometer. A quartz cuvette of 2.5 cm in optical path length was employed.

3.2.4.2. Dissolved Organic Carbon (DOC) Analysis. Shimadzu TOC-V CSH Total Organic Carbon Analyzer was used for the DOC measurements of water samples. The

instrument was calibrated using potassium hydrogen phthalate in the concentration range of 2-25 mg L⁻¹.

3.2.4.3. UV-vis Spectroscopy Measurements. UV-vis spectroscopic analysis of the water samples were performed by using a Perkin Elmer λ 35 UV-vis Spectrophotometer employing quartz cells of 1.0 cm optical path length. UV-vis absorbance spectra between wavelengths 200-600 nm were measured to follow the changes in organic matter.

UV-vis parameters used in this study were UV₂₅₄, UV₂₈₀, UV₃₆₅ and Color₄₃₆. Absorbance at UV₂₅₄ was used to evaluate the organic matter removal efficiency of coagulation. UV₂₈₀, UV₃₆₅ were used in similar purpose as in UV₂₅₄ for detecting the organic carbon content of the water samples. SUVA₂₅₄ and SUVA₃₆₅ were calculated to analyze the TOC-normalized content of natural organic matter. Color₄₃₆ was measured to signify color forming species remaining after coagulation SCoA was calculated to analyze the TOC-normalized color forming content of natural organic matter.

3.2.4.4. Fluorescence Spectroscopy Measurements. Fluorescence spectra of the water samples were recorded on a Perkin Elmer LS 55 Luminescence Spectrometer in the emission and synchronous scan modes. A 150 W Xenon arc lamp and red sensitive photomultiplier was employed in the fluorescence spectrometer. A 1-cm pathlength Perkin Elmer quartz cells were used.

Synchronous scan spectra were recorded in excitation wavelength range of 200-600 nm with the bandwidth of 18 nm between the excitation and emission monochromators. The emission spectra were scanned through two excitation wavelengths of 350 nm (emission₃₅₀) and 370 nm (emission₃₇₀) separately. In the measurement of emission₃₅₀ spectra the wavelength range was 360-600 nm and in emission spectra of 370 nm the scanning range was 380-600 nm.

3.2.5. Laboratory Instruments

3.2.5.1. Specific Instruments. The specified measurements for analyzing DOM samples used in coagulation experiments and ultrafiltration studies such as common ion analysis, spectroscopic measurements in UV-vis and fluorescence spectroscopy, DOC measurements, and turbidity measurements of the water samples were done by using the following instruments:

Perkin Elmer λ 35 UV-vis Spectrophotometer. It was used to measure the UV-visible absorption spectra of the samples employing Perkin Elmer quartz cuvettes of 1.0 cm optical path length.

Perkin Elmer LS 55 Luminescence Spectrophotometer. It was used to measure fluorescence spectra of the samples employing Perkin Elmer quartz cuvettes of 1.0 cm optical path length.

Perkin Elmer, Optima 2100 DV Inductively Coupled Plasma Optical Emission Spectroscopy (ICP-OES). It was used for anion analysis.

Shimadzu TOC-V WP Total Organic Carbon Analyzer. It was used for analyzing TOC.

Dionex ICS-3000 Ion Chromatograph. It was used for cation analysis.

Hach 2100 Turbiditymeter. It was used to measure the turbidity of the water samples.

Hach DR/Portable Datalogging Spectrophotometer. It was used to record the UV-visible absorption data of the algae cultivation water samples at the wavelengths of 600 nm and 750 nm to follow the changes in optical density (O.D.600) and chlorophyll a ($\mu\text{g L}^{-1}$), employing a quartz cuvette of 2.5 cm in optical path length.

Amicon Model 8050 Ultrafiltration Stirred Cell System. It was used for molecular size fractionation. Nitrogen (N₂) gas tube was supplied from “BOS”. N₂ tube was attached to the cell system as pressure source for the application of molecular size fractionation.

3.2.5.2. General Laboratory Instruments and Materials. General laboratory instruments were employed for general laboratory applications and measurements by using the following instruments:

Memmert Oven. It was used to dry the glassware.

Scaltec SBA 31 Balance. The balance was used for weighing certain amounts of the coagulants, algae nutrient salts, humic acid, and other salts used.

Ultra Sonic Waterbath LC30. The homogenous suspensions of the aqueous solutions were provided by sonification of the slurry using an “Ultra Sonic Waterbath LC30”.

WTW pH Meter-pH 526. The pH values of the water samples were measured using a “WTW pH Meter-pH 526” to observe the pH changes in the samples during the coagulation experiments. The pH meter was calibrated with pH 4.0 and pH 10.0 buffer solutions.

Sterile Millex - HA Millipore Filter. Water samples from algae cultivation media and the supernatant of the coagulated samples were filtered through 0.45 µm Millipore syringe filter to remove turbidity for analytical measurements.

4. RESULTS AND DISCUSSION

In this study, the influence of eutrophication in natural waters on the coagulation efficiency of natural organic matter and the effects of the sources of nutrients for algae that lead to eutrophication on specific water quality parameters were investigated. To achieve this goal, synthetic freshwater samples were prepared by taking into account the quality of the natural water sources. Freshwater algae were cultivated in synthetic water samples to resemble the eutrophic conditions in natural waters. Algae growth was followed by cell counting until the optimum growth conditions were reached according to the basic algae growth curve profiles. Different combinations of nitrate, phosphate and other common inorganic ions were added into the water samples as supply nutrients for algae. Optimized coagulation treatment was performed using aluminum sulphate and ferric chloride coagulants for the purpose of natural organic matter removal. The optimum pH and optimum coagulant dose required were determined according to UV-vis and fluorescence spectroscopy and dissolved organic carbon (DOC, mg L⁻¹). The characterisation of the coagulated samples were assessed through the molecular size distribution profiles using certain molecular size cutoffs.

In the first stage, synthetic freshwater samples were prepared using different combinations of algal nutrients such as nitrate, phosphate and other common inorganic ions (APHA, 1998), and humic acid as a component of dissolved organic carbon (DOC, mg L⁻¹) to investigate the effect of water matrix mimicking eutrophication conditions. Resembling the consortium in natural water systems, the samples were spiked with algae inoculums. With the periodic sampling, the algae growth was followed until optimum growth conditions were reached according to the basic algae growth curve profiles. Algae growth was assessed by classical enumeration method and reading the optical density at a wavelength of 600 nm (O.D.600). Nutrient analysis were performed through measuring common anions such as nitrate (NO₃⁻, mg L⁻¹), nitrite (NO₂⁻, mg L⁻¹), chloride (Cl⁻, mg L⁻¹), sulphate (SO₄²⁻, mg L⁻¹) and phosphates (PO₄³⁻, mg L⁻¹), by using Dionex ICS-3000 Ion Chromatograph and counter cations (mg L⁻¹) such as Na⁺, K⁺, Mg²⁺, Ca²⁺, by Perkin Elmer, Optima 2100 DV Inductively Coupled Plasma Optical Emission

Spectroscopy (ICP-OES). Changes in the chlorophyll a (chl_a) content of the samples were measured daily by the method of extraction of photosynthetic pigments in methanol solution. Spectrophotometric measurements of chlorophyll a samples were recorded by reading the absorbance at the wavelengths of 665 nm and 750 nm.

In the second stage, optimized coagulation method was applied to find the optimum pH and optimum coagulant dose appropriate for the removal of natural organic matter content of the prepared mediums. Jar tests were performed by using alum and ferric chloride as coagulants at room temperature (20-25 °C) using 50 mL samples. pH was adjusted to the selected values of pH 5.5, pH 6.0, pH 6.5, and pH 7.0 for the coagulation of the water samples in which optimum coagulant doses were explored through serial coagulation experiments. Coagulant addition of either alum or ferric chloride was increased in each test until the optimum removal of natural organic matter was reached.

Evaluation of the experimental data was made by using the specified UV-vis parameters and DOC. The results were presented in terms of UV-vis spectroscopic analysis at UV₂₅₄, UV₂₈₀, UV₃₆₅, Color₄₃₆ and fluorescence spectroscopy in emission₃₅₀, emission₃₇₀ and synchronous scan modes between wavelengths of 200-600 nm, and remaining dissolved organic carbon (DOC, mg L⁻¹) content of the water samples for the removal characterization of natural organic matter.

In the final stage, coagulation tests were employed in samples under optimized conditions. Treated and untreated organic matter samples were then assessed through molecular weight fractionation. A series of ultrafiltration membranes with specified molecular weight cutoffs (100 kDa, 30 kDa, 10 kDa, 3 kDa and 1 kDa) were used to display the molecular weight distribution profiles of organic matter present in raw and treated samples by coagulation. Spectroscopic results of each fraction were compared by UV-vis results and dissolved organic carbon (DOC, mg L⁻¹) content of the samples.

4. 1. Natural Organic Matter Release Experiments

4.1.1. Algae Cultivation

Algae growth were followed using two kinds of media namely distilled water medium and sytnhetic freshwater medium. The results of algae cultivation for these media were presented in terms of chages in number of cells, optical density at 600 nm (O.D.600), and chlorophyll a.

4.1.1.1. Growth of Algae in Distilled Water. The medium compositions used were; $M_{1.1}$ and $M_{1.2}$ representing $1x(N:P = 21)$ and $M_{5.1}$ and $M_{5.2}$, representing $5xN:P$. The initial cell count was $1x10^4$ cells mL^{-1} for mediums $M_{1.1}$, $M_{5.1}$ and $M_{5.2}$ whereas $2x10^4$ cells mL^{-1} were inoculated in medium $M_{1.2}$. Changes in the number of algae and chlorophyll a content of the samples were daily measured. Algae growth curves of distilled water mediums were presented in Figures 4.1-4.3.

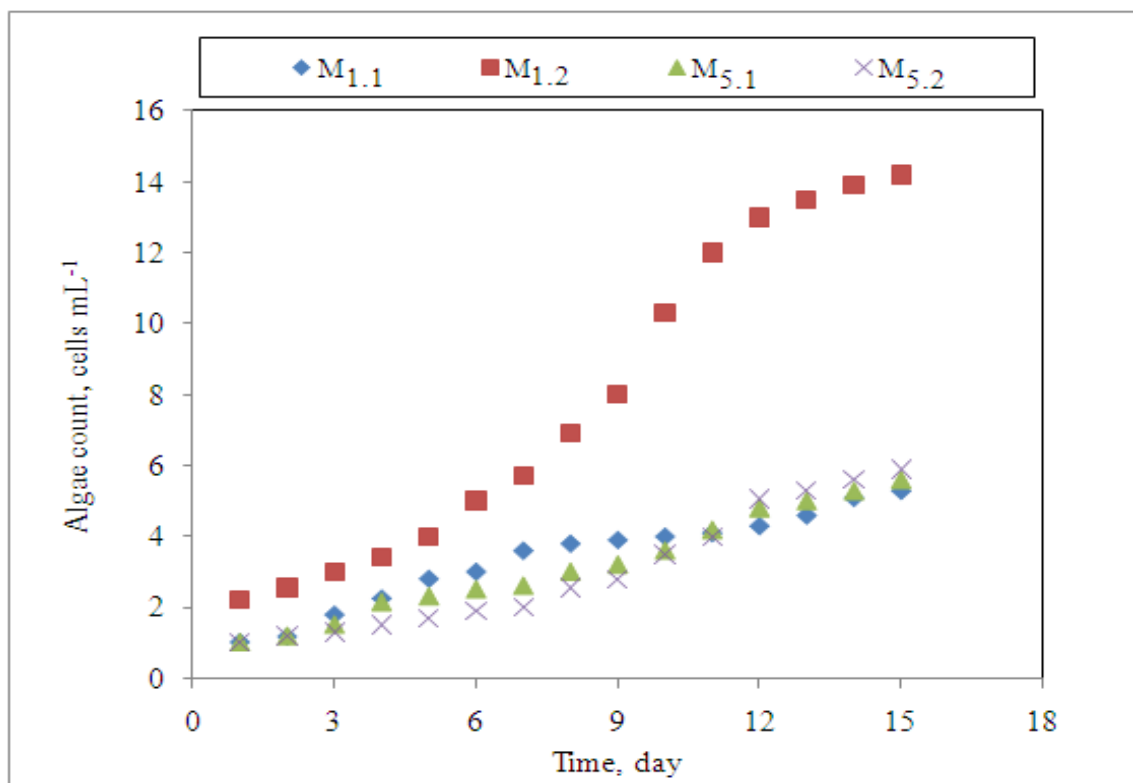


Figure 4.1. Algae propagation in distilled water mediums (cell number is shown in 10^4).

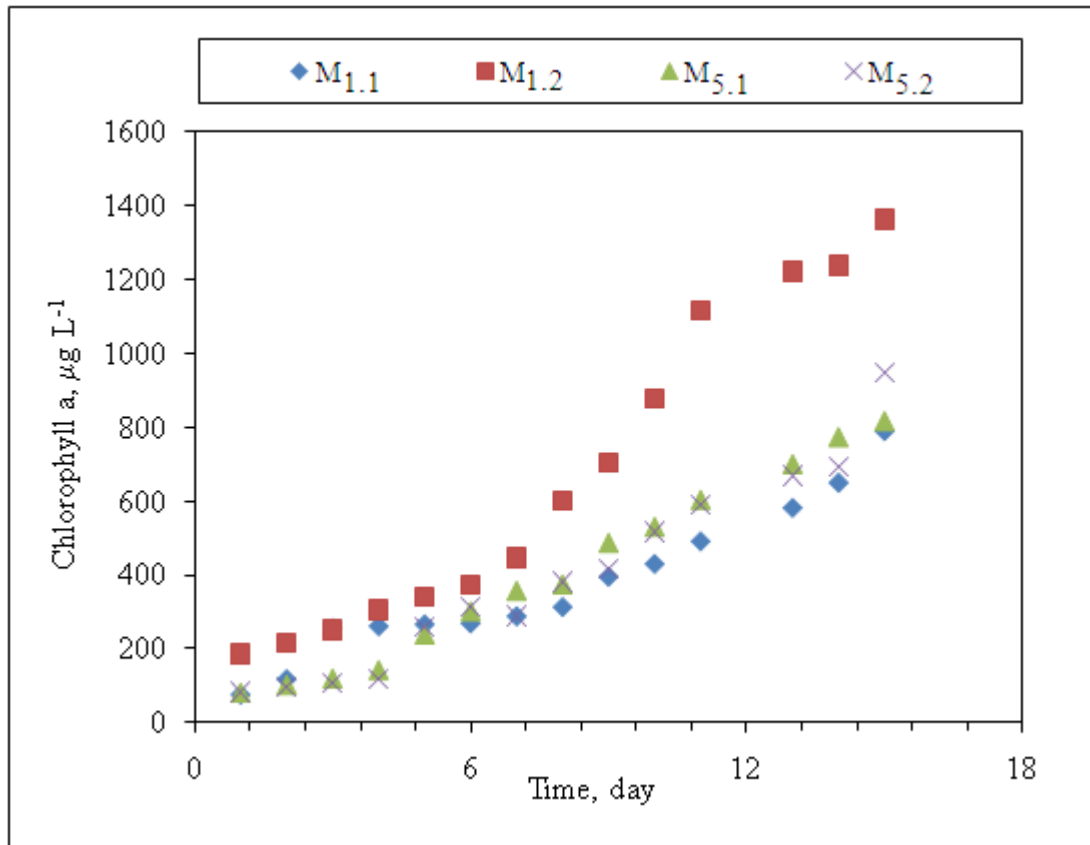


Figure 4.2. Daily measurements of chlorophyll a ($\mu\text{g L}^{-1}$) in distilled water mediums.

Daily measurements of cell number, chlorophyll a and O.D.600 results were matching with each other for all of the distilled water mediums. When the results were compared among all mediums the results of the three out of four distilled water mediums, which were M_{1.1}, M_{5.1}, and M_{5.2}, were found to be parallel in terms of the presented growth parameters in Figures 4.1-4.3. Algae growth profiles displayed a steady increase for six days. The initial slow growth phase was followed by an increasing trend irrespective of the medium properties for M_{1.1}, M_{5.1} and M_{5.2}. In M_{1.2}, the cell number, chlorophyll a and O.D.600 results were found to be nearly doubled which was in correlation with the higher initial cell number selected for this medium. Algae growth reached the exponential phase of growth curve in the 2nd week.

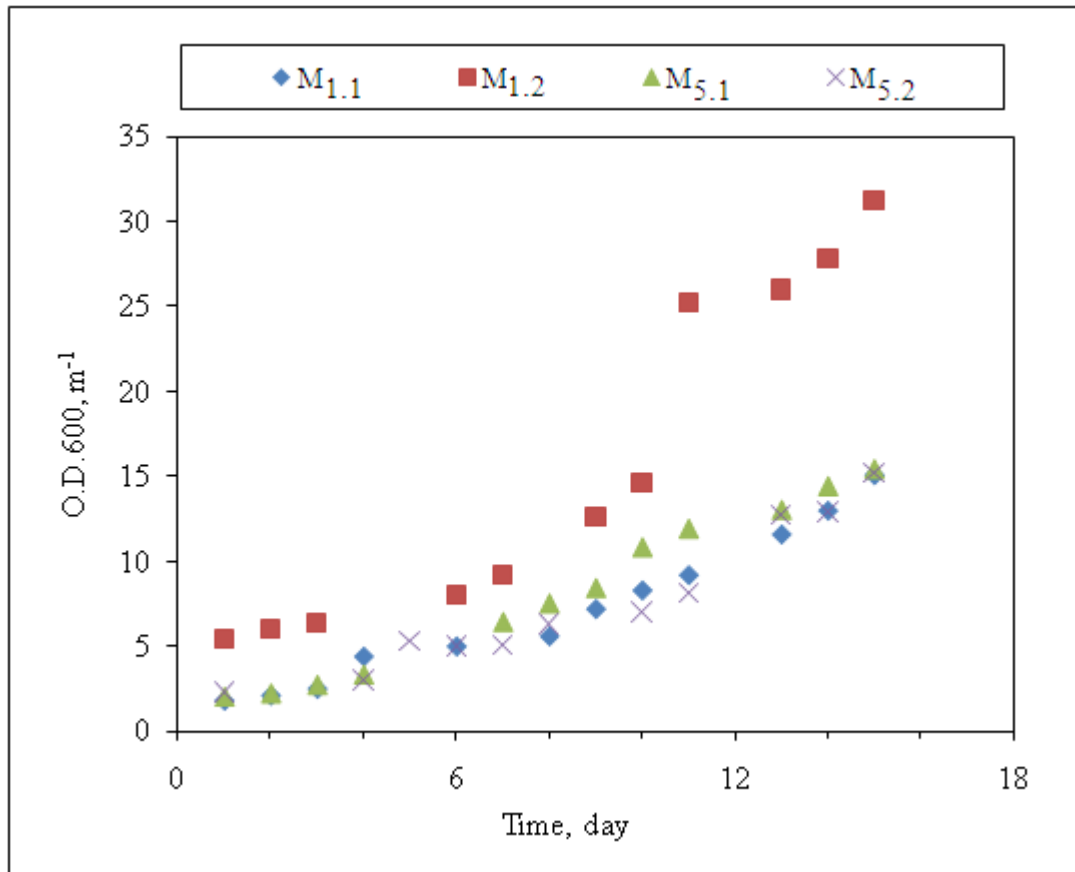


Figure 4.3. O.D.600 (m⁻¹) in distilled water mediums.

4.1.1.2. Growth of Algae in Synthetic Freshwater. For simplicity purposes algae growth was followed by cell count and O.D.600 measurements. The initial number of algae were 1×10^4 in synthetic freshwater mediums. All four of the synthetic water mediums had the same ratio 21 by 1x(N:P). Mediums were followed during two weeks by cell counting and reading the optical density.

Daily increases in the number of algae in synthetic water mediums were given in Figure 4.4. After two weeks the algae colonies reached the stationary level of the growth curve. The cell concentration in SW₂, SW₃ and SW₄ increased to similar values with a difference than the cell production in SW₁ that pursued lower concentrations than other mediums in the second week. Optical density measurements at 600 nm (O.D.600) were supporting algae counts following a parallel curve as shown in Figure 4.5.

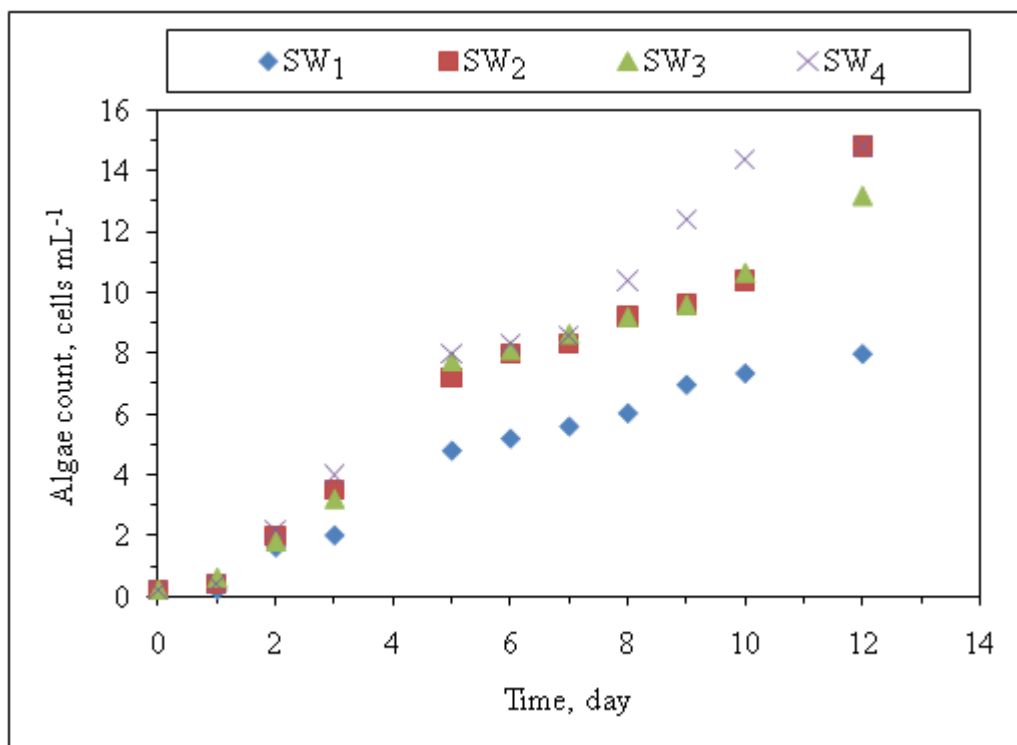


Figure 4.4. Algae propagation in synthetic water mediums (cell number is shown in 10^4).

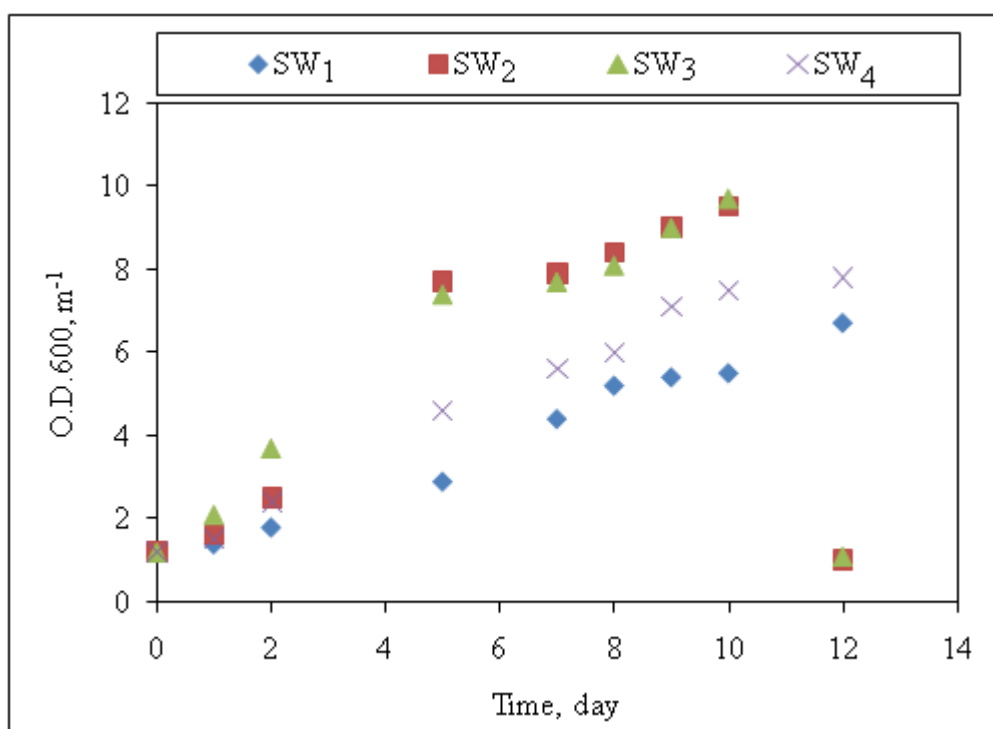


Figure 4.5. O.D.600 (m⁻¹) in synthetic water mediums.

4.1.2. Nutrient Consumption

The consumption of nutrients by the algae, and the changes in the concentrations of nutrients in the synthetic water algae mediums were presented based on the changes in the nitrate and phosphate concentrations which were the primary nutrient sources for algae. The anions nitrates (NO_3^-), and phosphates (PO_4^{3-}) were measured during two weeks as the algae propagated in the media in order to draw a conclusion about the dosages that the algae used these nutrients. Accordingly, phosphate concentration was decreased from 0.8 mg L^{-1} to under 0.2 mg L^{-1} at the end of two weeks in all of the synthetic freshwater samples. The nitrate concentration was reduced in a lesser rate in comparison to phosphate (Figures 4.6-4.8).

The results for changing anion concentration by day and nutrient consumption by algae were presented in Figure 4.6, Figure 4.7 and Figure 4.8.

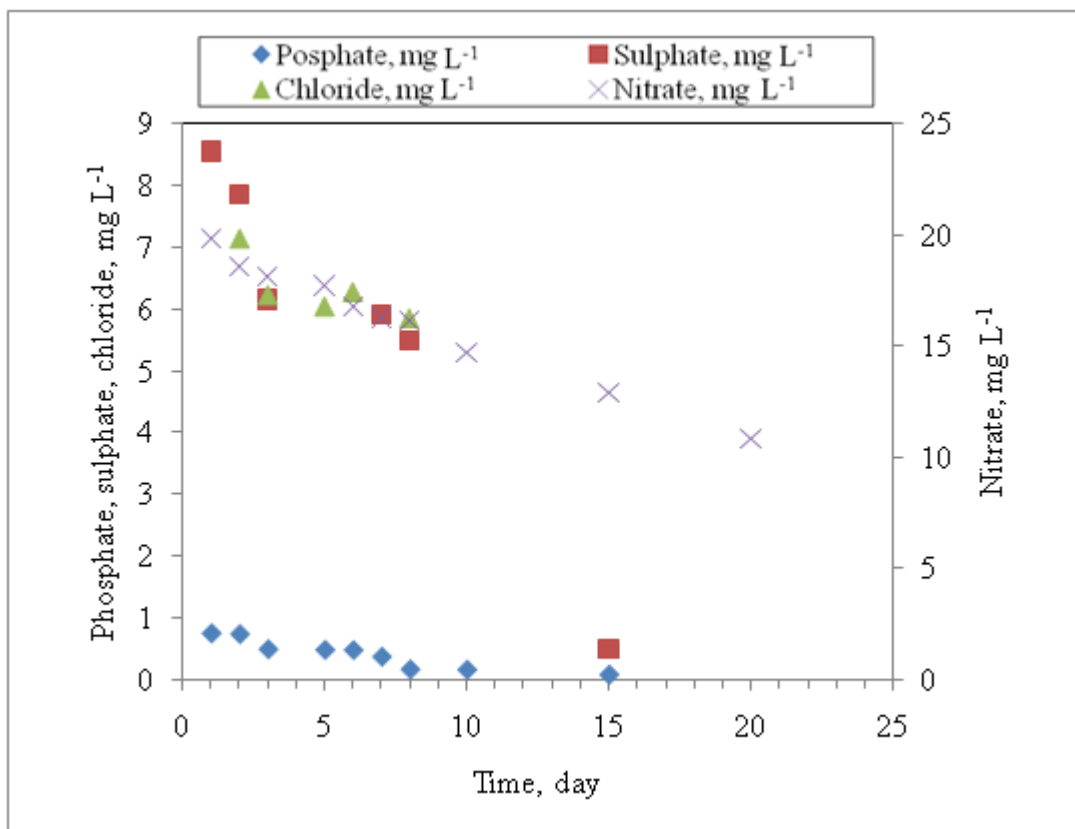


Figure 4.6. Anions in distilled water medium $M_{1.1}$.

Along with phosphate, nitrate, nitrite, ammonium, changes in the concentrations of other anions such as chloride, sulphate were also measured. As seen in Figure 4.6, Figure 4.7 and Figure 4.8, anion concentrations did not continuously decrease in the water mediums, except the anions phosphate and nitrate which are the basis nutrients for algae. Since the amounts of nitrate and phosphate were different in $M_{1,1}$ and $M_{5,2}$, the results of the two mediums can be compared in terms of nitrate and phosphate reduction. However, the difference was not observable from the cell counts in $M_{1,1}$, $M_{5,1}$, SW_1 , SW_2 , SW_3 , SW_4 (Figure 4.1, Figure 4.4). A higher consumption rate of phosphate than nitrate occurred in both medium $M_{5,1}$ and in $M_{1,1}$ which had similar initial number of algae cell. The reduction rates of phosphate and nitrate were also similar in the results of synthetic water cultures as shown in Figure 4.6, Figure 4.7, Figure 4.8.

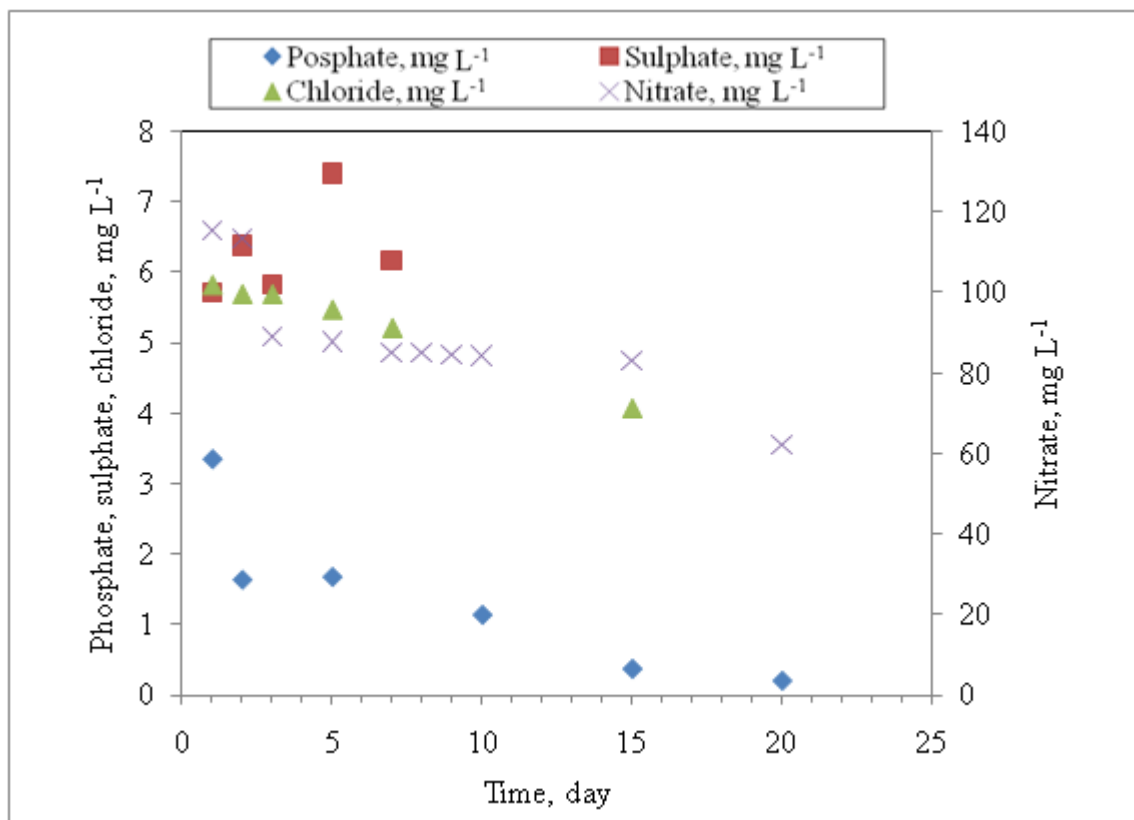


Figure 4.7. Anions in distilled water medium $M_{5,1}$.

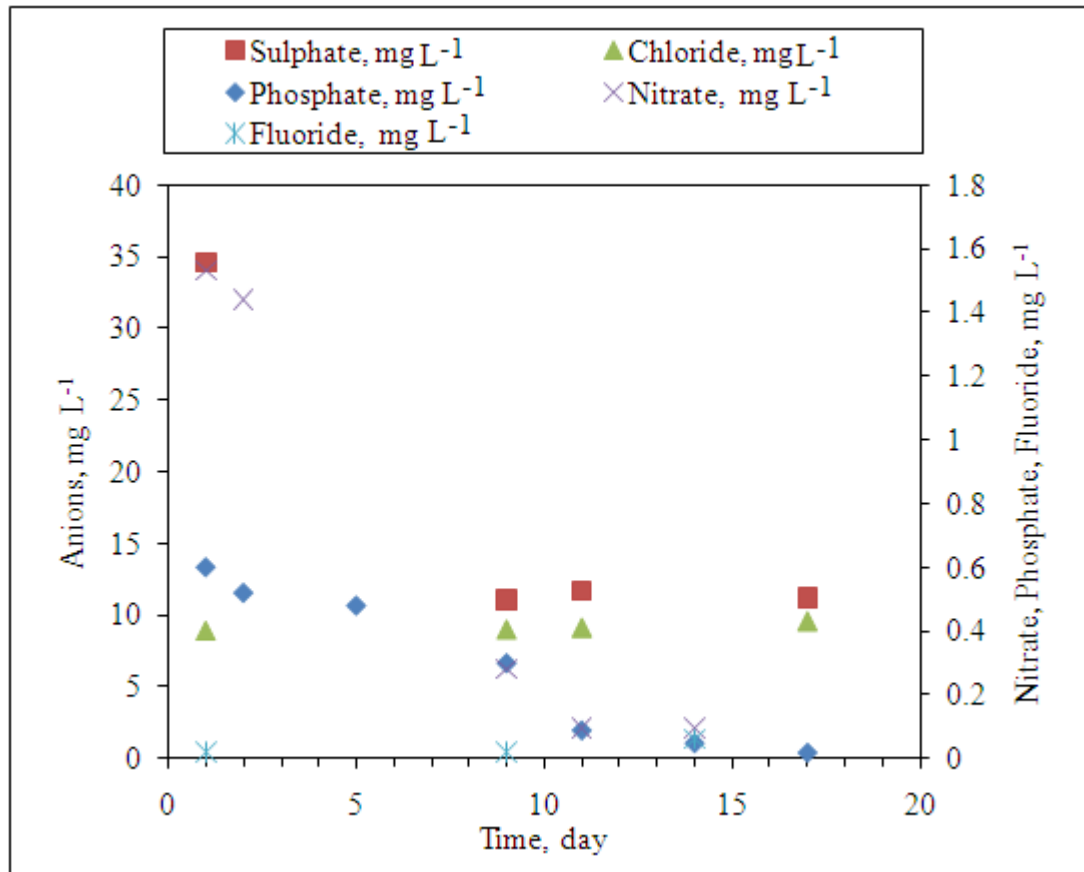


Figure 4.8. Anions in synthetic freshwater medium SW₁.

As indicated in materials and methods section, the N:P ratio of the media was 21 that was calculated according to the initial concentrations of these nutrients of N and P which were N = 4.20 mg L⁻¹ and P = 0.186 mg L⁻¹. The N:P ratio of 21 indicates very low concentration of P was supplied for algae relative to the supplied amount of N. The ratio of N:P = 21 in algae growth mediums of the present study suggests that growth was controlled by phosphorous rather than nitrogen since 21 < 7.2 which is the level for classifying the limiting nutrient as P since N:P < 7.2 was suggested for N-limited growth and N:P > 7.2 for P-limited growth (Chapra, 1997). It was suggested in previous research that in P-limited drinking waters very low amounts of P affect microbial growth. Miettinen and colleagues reported that low additions of phosphorous i.e. 1-5 mg L⁻¹ of P increased the concentration of microbial population (Miettinen et al., 1997).

4.1.3. Growth Kinetics in Algae Growth Mediums

As presented above, a two-weeks period of algae growth achieved in distilled and synthetic freshwater mediums resulted in an appropriate amount of algae population increase. In addition to cell growth measurements, by following the nitrate and phosphate levels nutrient consumption data was obtained. Using both cell growth and nutrient consumption data provides the calculation of growth rate of algal growth and nutrient consumption in algae growth mediums by using the growth kinetics suggested in previous research which were presented in section 2.3.2.

The mass balance for algal growth with time could be given as a function of growth rate with the equation 4.1. Solution of the equation 4.1 gives the algae concentration at a time “t”, depending on the initial concentration of algae (N_0) as shown by equation 4.2.

$$dN/dt = k_g N \quad (4.1)$$

$$N = N_0 e^{k_g t} \quad (4.2)$$

where N: concentration of algae (cells mL⁻¹)

dN/dt: rate of change in growth with respect to time

k_g : first order growth rate (per day: d⁻¹)

N_0 : initial concentration of algae (cells mL⁻¹)

From the equation 4.2, the growth rate for algae k_g could be calculated by substituting the initial concentration of algae N_0 (cells mL⁻¹) for algae mediums to find the growth rate values of algae cells that changed by day. The calculation of the growth rate involves the natural logarithm function of the concentration. A plot of natural logarithm of the algae cell concentration, $\ln N$, versus time shows the variation in growth rate of algae as shown in Figure 4.9. The values given in Figure 4.3 were used according to the cell growth in

distilled water mediums and the days that the measurements were taken in distilled water mediums to develop Figure 4.9.

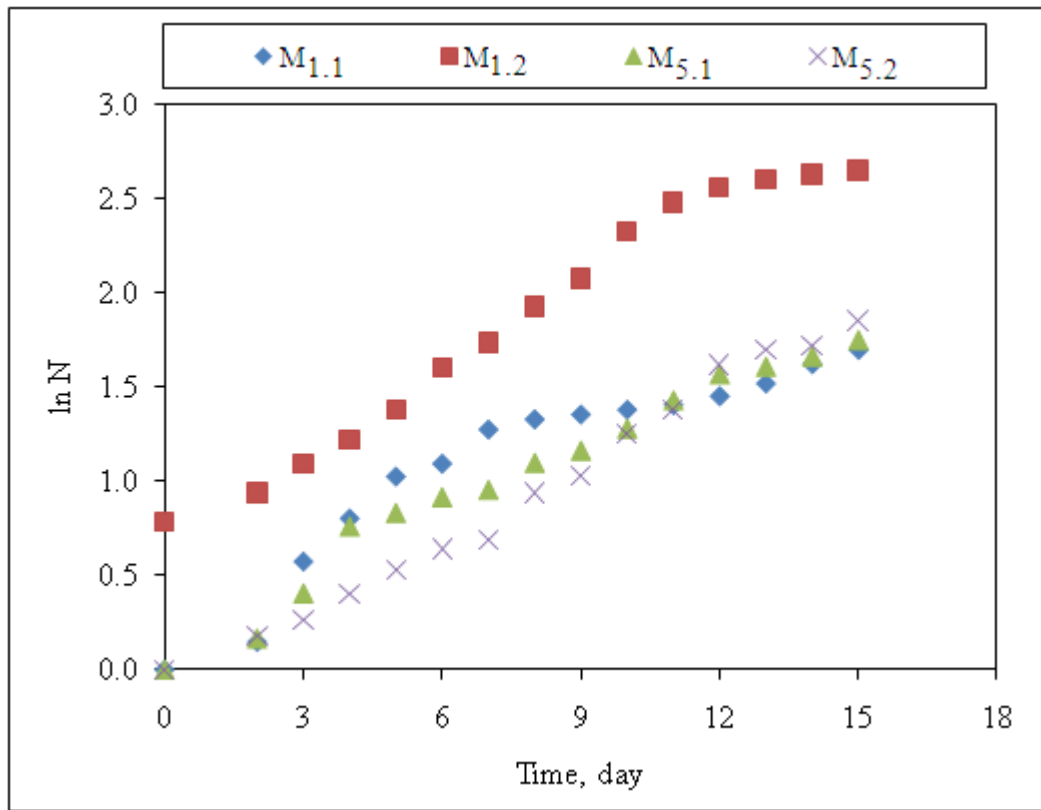


Figure 4.9. Natural logarithm functions of the algae cell concentration in distilled water mediums.

The values of growth rate (k_g) could be derived from the data presented by setting the equations to obtain k_g values for each day from the regression lines of algae concentration as given in Figure 4.9. The growth rate could be calculated as shown in equation 4.3.

$$k_g = \ln N_n - \ln N_{(n-1)} / t_n - t_{(n-1)} \quad (4.3)$$

Using equation 4.3, changing growth rate (k_g) values of algae could be calculated with respect to time in algae growth mediums. Growth rate values versus time (d^{-1}) were calculated for algae growth in distilled water mediums and presented in Figure 4.10.

According to the growth rate profile, it was observed that algae growth rate by day was increased in the first week reaching a highest value of $k_g = 0.25 \text{ d}^{-1}$ in the 8th day of growth for $M_{5.2}$. Then growth rate began to decrease in the second week in a similar rate to growth rate in the first week making up a triangular scheme in the whole Figure 4.10 with peak growth rate values of the mediums. The increase in growth rate started with an initial small rise very close to zero which was $k_g = 0.02 \text{ d}^{-1}$ obtained at the 2nd day of growth. A similar value was observed also in the 15th day of the growth period suggests that the growth rate increase-decrease happened with a similar kinetics.

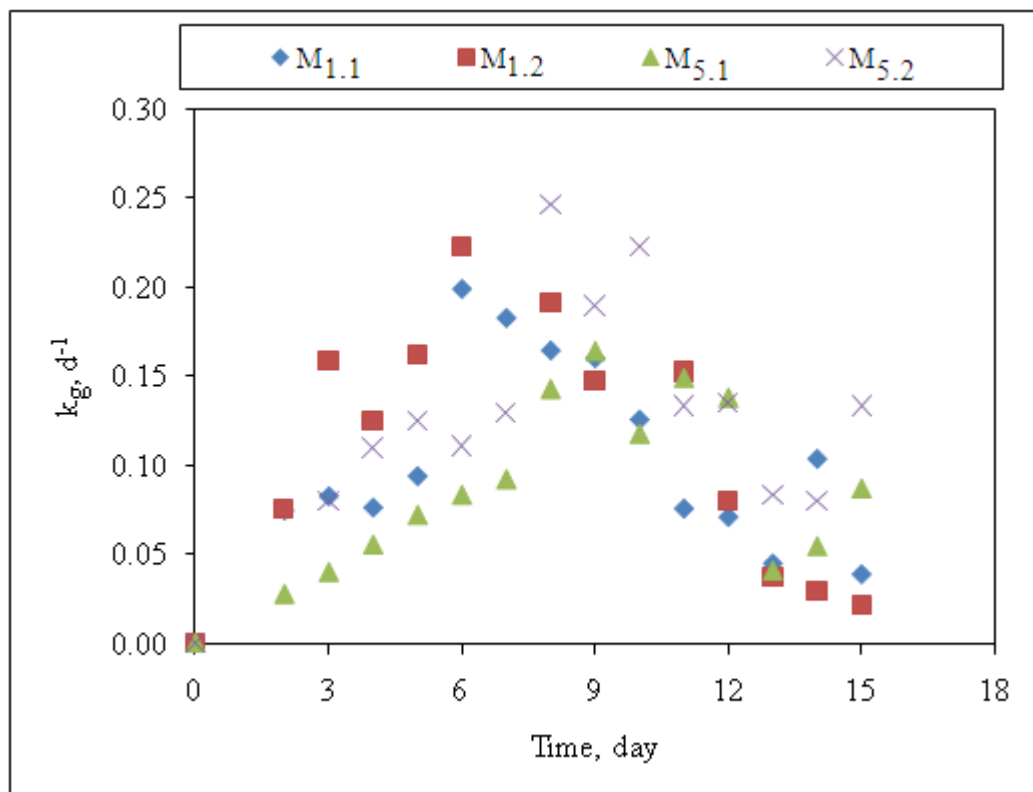


Figure 4.10. Growth rate values for distilled water mediums.

A graph of algae growth together with its corresponding algae growth rate provides the comparison and visualization of growth with growth rate in time. Algae growth results in distilled water medium $M_{1.2}$, as presented in Figure 4.3, was selected for this purposes to show how rate of growth was affected by algae growth in time in this medium as presented in Figure 4.11.

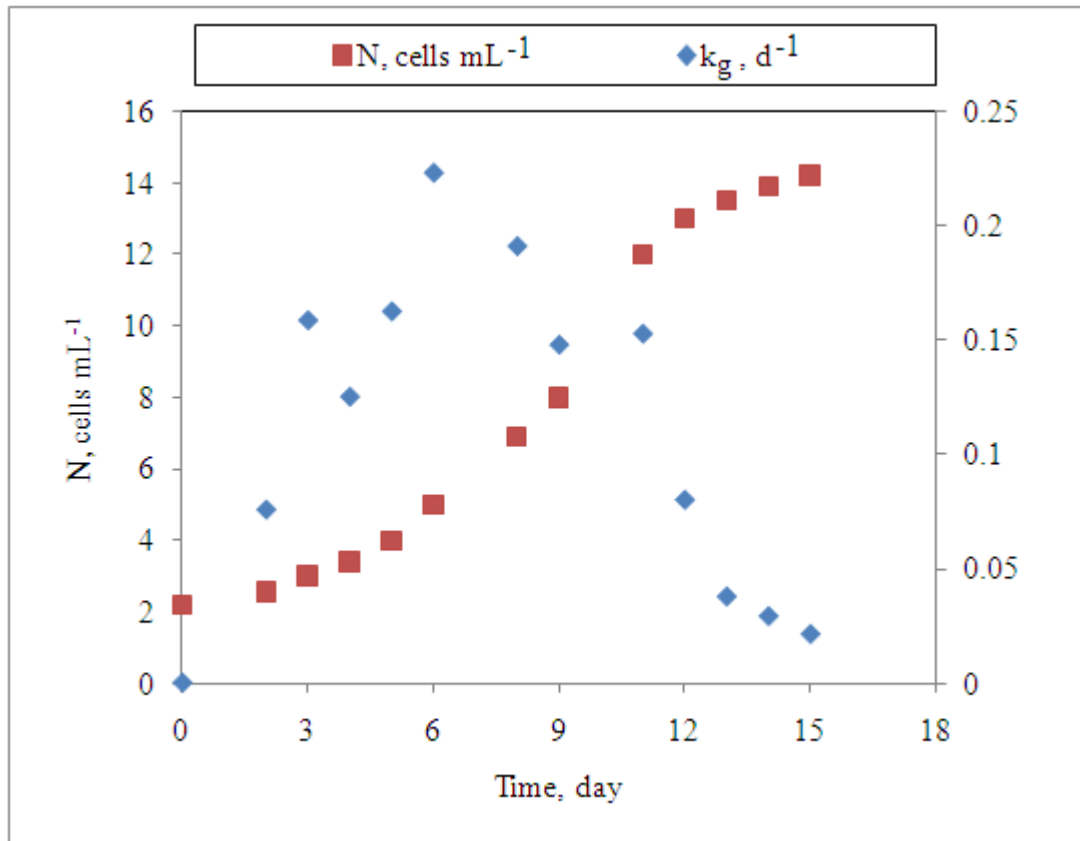


Figure 4.11. Growth rate values (k_g) for the corresponding algae concentration in time for $M_{1,2}$.

According to the general theoretical base, during the exponential phase the growth rate is constant. The growth rate values in Figure 4.10-4.11 would verify this information. If a mathematical fitting of the growth rate curve in Figure 4.11 between days 3-9 was set, it would be close to linear, steady-state. Monod suggested that exponential phase in fact the only phase of the growth cycle when the properties of the cells may be considered constant and can be described by a numeric value, the exponential growth rate, that corresponds to the over-all velocity of the steady-state system (Monod, 1949). It was suggested that it was reasonable to consider a steady state was established where the relative concentrations of all the metabolites and all the enzymes are constant.

Substrate limitation of algae growth could be explained by the Michaelis-Menten (Monod) model as given by the following equation:

$$k_g = k_{g,\max} S / k_s + S \quad (2.2)$$

where k_g : growth rate (s^{-1})

$k_{g,\max}$: maximum growth rate in the abundance of substrate (s^{-1})

S: substrate concentration ($\mu\text{g L}^{-1}$)

k_s : half-saturation constant ($\mu\text{g N L}^{-1}$ and $\mu\text{g P L}^{-1}$)

Algae growth rate could be characterized using the Michaelis-Menten (Monod) model as the function of substrate concentration which were N and P in the present case and growth rate (k_g, s^{-1}) in the algae growth mediums. Substrate concentration in medium M_{5.2} was utilized to estimate substrate limitation in this medium. $k_{g,\max}$ value to be used in Michaelis-Menten (Monod) model was selected as the $k_{g,\max}$ of algae growth in medium M_{5.2} ($k_{g,\max} = 2.89 \times 10^{-6} s^{-1}$) as presented in Figure 4.10. Because it was the highest $k_{g,\max}$ than the $k_{g,\max}$ obtained in other meidums, it could be a suitable value to use in estimation of substrate limitation of growth rate k_g in all mediums. Thebault and Qotbi reported half-saturation constants for N and P assimilation as $k_s = 25 \mu\text{g N L}^{-1}$ for N and $k_s = 3 \mu\text{g P L}^{-1}$ for P (Thebault and Qotbi, 1999).

Using $k_{g,\max} = 2.89 \times 10^{-6} s^{-1}$ and $k_s = 25 \mu\text{g N L}^{-1}$ for N and $k_s = 3 \mu\text{g P L}^{-1}$ for P, the limitaiton of growth rate k_g for algae growth medium M_{5.2} was calculated. M_{5.2} had a ratio of N:P = 21 nutrient condition such as (5xN):(5xP) = 21. M_{5.2} was selected whose $k_{g,\max}$ value was found to be $2.89 \times 10^{-6} s^{-1}$ to analyze substrate limitation of the growth rate of algae by N and P nutrients according to the Michaelis-Menten (Monod) model. In addition to the calculations for growth rate (k_g) values for medium M_{5.2}, k_g values were calculated

according to a $k_{g,max}$ value of $0.5 \times 10^{-6} \text{ s}^{-1}$ found by Thebault and Qotbi (Thebault and Qotbi, 1999) all of which were provided in the following Figures 4.12-4.13.

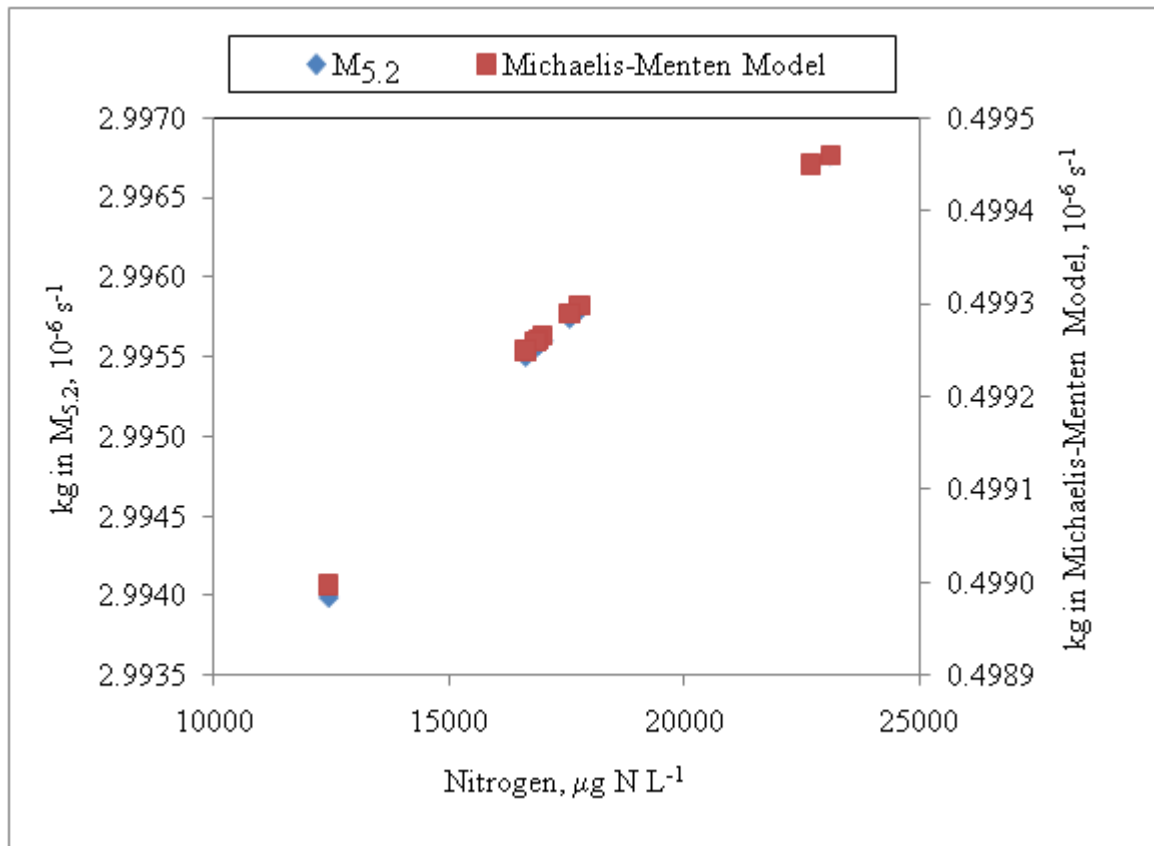


Figure 4.12. Limitation of k_g in $M_{5.2}$ by N according to Michaelis-Menten model.

It can be concluded that the nutrient effect on algae growth rate in growth mediums were limited by the concentrations of N and P as shown in figures above. Chen and colleagues studying on cyanobacteria population on a lake water suggested that if the two environment factors P and N are controlled considerably, the growth rate of a microbial population will decrease. They found that severe deficiency of P resulted in the decrease of microbial population, even extinction. They indicated that among controlling phosphate restriction for preventing eutrophication, N still has a definite meaning since the growth needs a high N concentration reaching to 5 mg L^{-1} of N which cannot be obtained only depending on the nitrogen fixation of cyanobacteria (Chen et al., 2009).

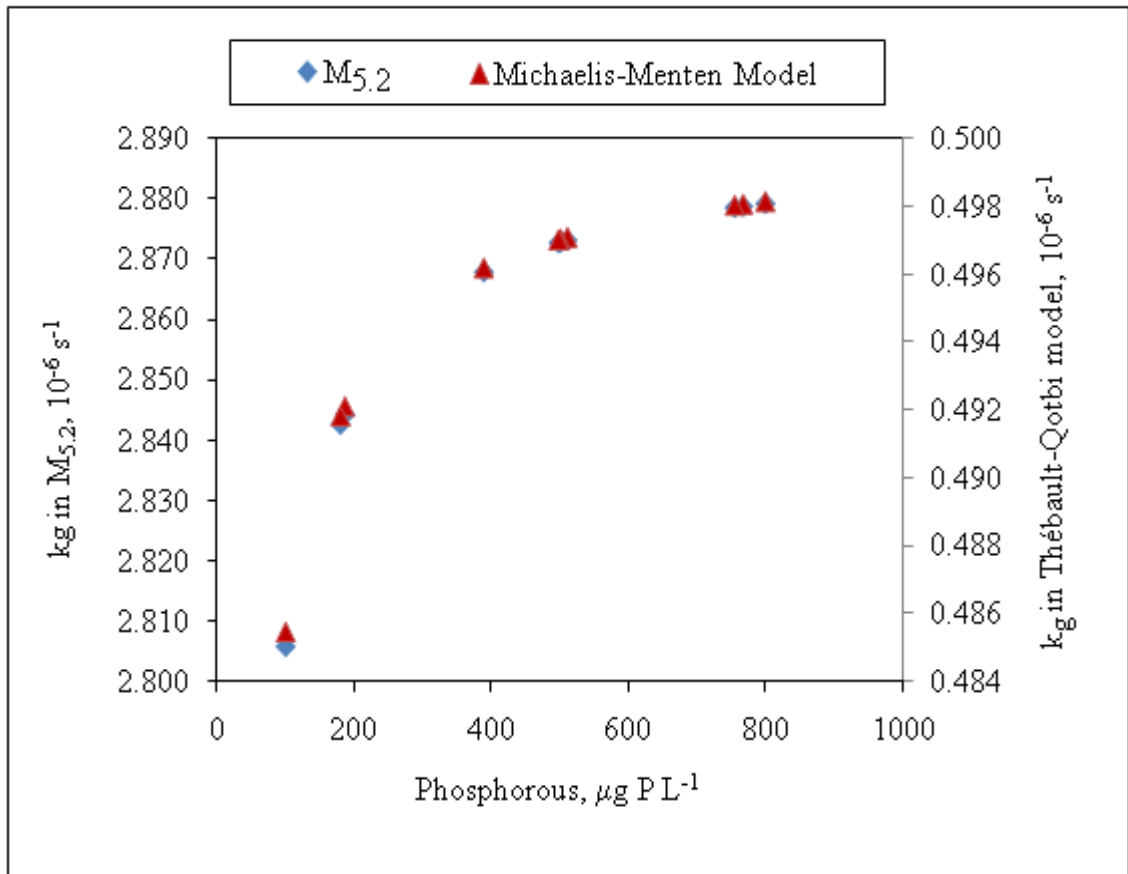


Figure 4.13. Limitation of k_g in $M_{5.2}$ by P according to Michaelis-Menten model

4.2. Coagulation Experiments Using DOM Sample

The removal of particles and organic matter from drinking water sources is often achieved by coagulation, usually performed by employing aluminum or iron salts. In the presence of organic matter in water, the required coagulant dosage generally increases. On addition to water, aluminum salts dissociate and the Al^{3+} ions undergo metal ion hydrolysis reactions such as the one exemplified in theoretical background part of this study. Many species have been proposed to form during hydrolysis including more commonly accepted species such as the monomers Al^{3+} , $\text{Al}(\text{OH})^{2+}$, $\text{Al}(\text{OH})_2^+$, $\text{Al}(\text{OH})_3(\text{am})$ and $\text{Al}(\text{OH})_4$, as well as a dimer ($\text{Al}_2(\text{OH})_2^{4+}$) a trimer ($\text{Al}_3(\text{OH})_4^{5+}$) and the tridecamer ($\text{Al}_{13}\text{O}_4(\text{OH})_{24}^{7+}$) in prehydrolyzed Al coagulants. Alum solutions consisted of only monomeric species

including the inner-sphere sulfate complex, AlSO_4^+ . The degree to which the reactions proceed and the nature of the resulting species depend on such variables as Al concentration, pH, temperature, and the presence of other ions. In addition to the proportions of Al species formed under various conditions, other interacting species in the water environment may also play a role in determining the efficiency of the coagulants. The speciation of aluminum may also be influenced by the presence of organic matter resulting in the formation of Al–organic complexes and the inhibition of formation of the tridecamer species. It has been suggested that Al hydrolysis products form insoluble aluminum-humates or -fulvates with humic substances, producing colloids that settle very slowly. At higher coagulant doses, the aluminum–organic complexes may be removed by incorporation into $\text{Al}(\text{OH})_3$ flocs. During coagulation, the effect of temperature may cause a reduction in the proportion of AlSO_4^+ by lowering the temperature from 25°C to 5°C (Exall and vanLoon, 2003).

Less is known about coagulation mechanism with ferric salts than those with aluminum salts in removal of natural organic matter. Lefebvre and Legube proposed two possible pathways for the coagulation of simple aromatic and aliphatic acids with ferric chloride (FeCl_3). The first one is the ligand exchange on to the FeOOH surface, and the second is a complexation or a ligand exchange between soluble Fe monomers or oligomers and the organic matter leading to a precipitate (Lefebvre and Legube, 1993). Vilg -Ritter and colleagues studied on the mechanisms of NOM removal by ferric salts. Their findings indicate that the large variety of organic ligands like chemical nature, molecular weight, etc., present in surface water sources explains the wide range of Fe–Fe single corner linkages. The complexation of Fe by NOM greatly hinders the formation of Fe–Fe double-corner bonds to the benefit of single-corner linkages. The geometry of this latter Fe–O–Fe bond depends on the type of complex (mono- or multinuclear, mono- or multidentate) and most of all on the nature of the organic ligand. Different organic ligands induce different Fe–O–Fe bond angles and consequently different subunit sizes (Vilg -Ritter et al., 1999b). Si li chi and colleagues, studying on coagulation of humic acid with ferric chloride, suggested that the aggregation of humic acid with hydrolyzed-Fe species can be ascribed to a competition between humic network reformation rate and collision rate of destabilized colloids. As their study results revealed that the iron coagulant species were

poorly hydrolyzed in the destabilization range, they proposed a neutralization/complexation destabilization mechanism accompanied by a restructuration of flexible humic network to occur in the pHs of 6 and 8 investigated rather than mechanisms such as sweep flocculation or adsorption onto a hydroxyde precipitate (Siéliéchi et al., 2008).

In this study coagulation experiments were performed by jar tests using alum and ferric chloride as coagulants for the assessment of the coagulation performance in the DOM sample. Optimized coagulation (OC) was applied to find the optimum coagulant dose for alum and ferric chloride at the selected pH conditions in the range of 5.5-7.0 which were then compared in terms of DOM removal efficiency to determine the optimum pH of coagulation for each of the coagulants used. The removal of DOM was followed by the specified UV-vis spectroscopic parameters (UV_{254} , UV_{280} , UV_{365} and $Color_{436}$), UV-vis spectra between 200-600 nm as well as DOC ($mg\ Org.\ C\ L^{-1}$) contents. Moreover, fluorescence spectroscopy measurements were applied both in emission and synchronous scan modes. Fluorescence measurements were presented in results for the optimum coagulation conditions for alum and ferric chloride coagulants. UV-vis and fluorescence spectra of other pH and coagulant dose conditions included in the experiments were given in Appendix A, Appendix B, Appendix C and Appendix D.

4.2.1. Sample Specification for DOM Sample

Following the attainment of the optimum growth conditions, algae growth media were collected to resemble a single water sample which was to be used in the proceeding experiments. The obtained solution was referred to as “the dissolved organic matter (DOM) sample”. For characterization of the aqueous medium, the DOM sample was subjected to analysis according to the methods outlined in the materials and methods section. The water quality data of the sample are summarized in Table 4.1. The dissolved organic carbon content of the obtained DOM sample was found to be $DOC = 20.5\ mg\ L^{-1}$, UV_{254} was measured as $0.1106\ cm^{-1}$ and $Color_{436}$ as $0.0112\ cm^{-1}$. The DOM sample displayed neutral pH conditions ($pH = 7.55$). Total bacteria count was found to be 6×10^8 cells mL^{-1} .

Table 4.1. Physico-chemical characteristics of the DOM sample

Parameter	
UV ₂₅₄ , cm ⁻¹	0.1106
DOC, mg L ⁻¹	20.5
SUVA ₂₅₄ L mg ⁻¹ m ⁻¹	0.5395
SUVA ₃₆₅ L mg ⁻¹ m ⁻¹	0.1434
SCoA L mg ⁻¹ m ⁻¹	0.0546
pH	7.55
Turbidity, NTU	15.5
Alkalinity, mg CaCO ₃ L ⁻¹	77.8
Hardness, mg CaCO ₃ L ⁻¹	37.34
Number of Bacteria, cells mL ⁻¹	6 x 10 ⁸

The dissolved organic carbon (DOC, mg L⁻¹) content of the sample is 20.5 mg L⁻¹ which is comparable to some natural freshwater conditions such as 26.6 mg L⁻¹ for a brown lake (Frimmel, 1998a), 21.2 mg L⁻¹ for a forest lake (Peuravuori et al., 2002). Upon application of physico-chemical treatment techniques, the removal of TOC and UV absorbing substances generally increases with increasing TOC concentration and decreasing alkalinity with a preferential removal of UV-absorbing constituents over TOC. Turbidity of the sample was 15.5 NTU in which the amount of colloids, particulates, algal particulates, and mineralization were moderately high compared to a surface water sample as reported to be highly mineralized (27 NTU) by Vilgé-Ritter and colleagues (Vilge-Ritter et al., 1999b). In natural waters such a level of turbidity signifies highly mineralized waters (Vilgé-Ritter et al., 1999b). The alkalinity of DOM sample was 77.8 mg L⁻¹ which was close to high alkalinity values reported in other studies as high alkalinity water samples i.e. sample alkalinity >120 mg CaCO₃ L⁻¹ by Iriarté-Velasco and colleagues (Iriarté-Velasco et

al., 2007). With reference to these examples, in this case DOC concentration was high and alkalinity was moderately high in this study. Alkalinity-hardness of a water sample might affect the coagulation performance. Iriarté-Velasco and colleagues suggested that alkalinity-hardness of the water quality is an effective factor in especially coagulation with alum that it shifts optimum pH value downwards in higher alkalinity-hardness conditions of water (Iriarté-Velasco et al., 2007).

The specific UV absorbance, $SUVA_{254}$ ($L\ mg^{-1}\ m^{-1}$) is defined as the DOC ($mg\ L^{-1}$) normalized UV_{254} (m^{-1}) of a water sample. $SUVA_{254}$ of the DOM sample was $0.5395\ L\ mg^{-1}\ m^{-1}$ which is very low when compared to water samples from three of the Istanbul drinking water reservoirs had reported $SUVA_{254}$ as $2.14\ L\ mg^{-1}\ m^{-1}$, $2.83\ L\ mg^{-1}\ m^{-1}$, $4.04\ L\ mg^{-1}\ m^{-1}$) (Bekbolet, 2009) and from natural water samples having $SUVA_{254}$ changing between 5.3 to $1.8\ L\ mg^{-1}\ m^{-1}$, recorded by Weishaar and colleagues who compared the river and lake samples from different sources (Weishaar et al., 2003). Reported experiments have shown that coagulation and softening are generally not effective methods for removing DOC with low $SUVA_{254}$ values less than $2.0\ L\ mg^{-1}\ m^{-1}$ (Weishaar et al., 2003). The SUVA of a water reflects the reactivity of the organics in the water toward removal by coagulation and their organic halide formation potential. High-SUVA waters have higher TOC concentrations and lower alkalinity and are more amenable to organics removal by coagulation than are low-SUVA waters (Archer and Singer, 2006). $SUVA_{365}$ and SCoA values of the DOM sample were $0.1434\ L\ mg^{-1}\ m^{-1}$ and $0.0546\ L\ mg^{-1}\ m^{-1}$ respectively. Although $SUVA_{254}$ was lower than the most natural water samples, $SUVA_{365}$ was higher than the reported value of the aquatic humic samples from Istanbul Omerli drinking water reservoir ($SUVA_{254}$: $4.0\ L\ mg^{-1}\ m^{-1}$ $SUVA_{365}$: $0.7\ L\ mg^{-1}\ m^{-1}$).

The correlation between DOC and UV absorbance is generally used as a predictor of the amount of the dissolved organic matter. The UV-A was defined as the wavelength range of 320-400 nm, and the UV-B range was defined as the wavelength range of 280-320 nm (Frimmel, 1998a). As Frimmel showed in his study, an increase of UV-A and UV-B radiation leads to changes in the chemical and biological properties of aquatic NOM (Frimmel, 1998a). In natural waters the concentration of DOC alone is not a consistent predictor of the depth to which UV light between 280-320 nm (UV-B) penetrates because

of the spatial and temporal variability in the fractions of DOC. Surface water DOC concentrations are moderated with changes in the concentration and composition of both terrestrial and aquatic origins of dissolved organic matter making up the hydrologic characteristics of the water as well as changing climate conditions affecting potential exposure to UV-B radiation. Fulvic acids are formed from both algal and terrestrial precursors. Algal fulvic acids tend to have much lower ability to attenuate UV-B light and are more readily degraded. Consequently they have a shorter residence time in the aquatic environment, suggesting that UV-B attenuation should be controlled primarily by the terrestrially derived fulvic acid content. Because the chemical structures responsible for UV-B attenuation are found primarily in the terrestrially derived fulvic acid fraction of dissolved organic matter, the hydrologic characteristics of individual sites that control the delivery and residence time of terrestrial DOC in surface water are likely to control the amount of photoreactive fulvic acid present in surface waters (Brooks et al., 2005).

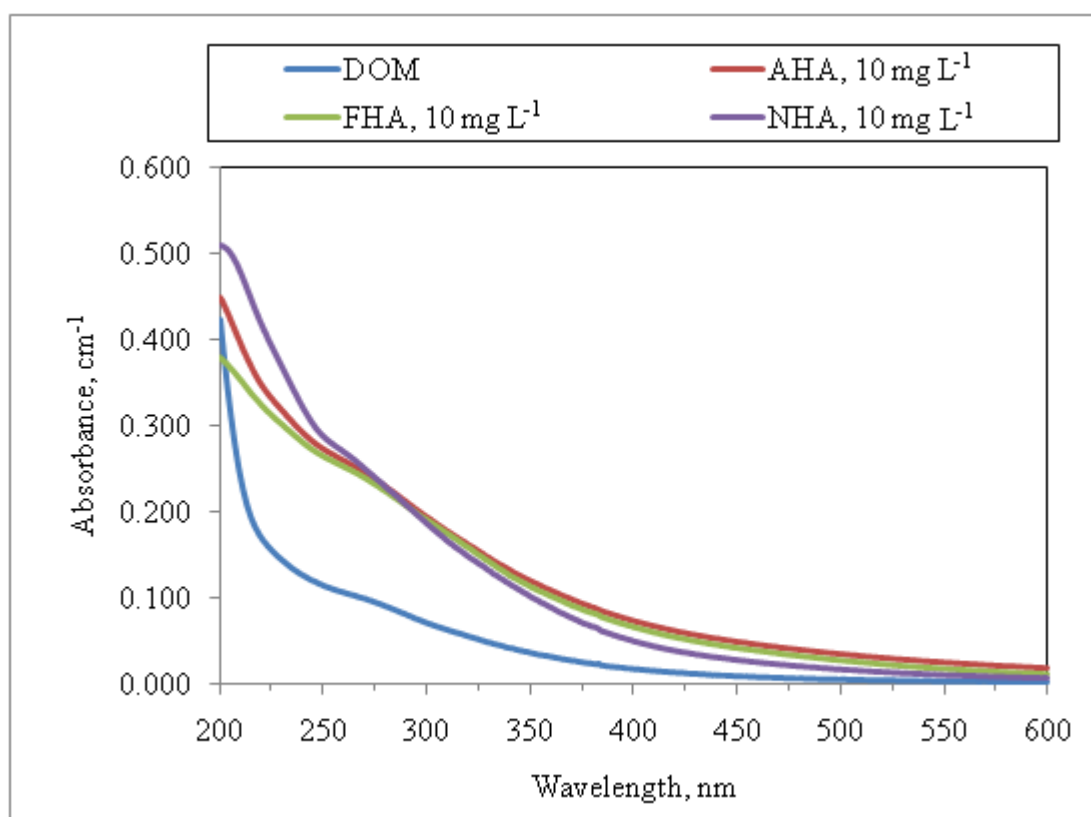


Figure 4.14. UV-vis spectra of the DOM sample, Aldrich Humic Acid (AHA), Fluka Humic Acid (FHA) and Nordic Humic Acid (NHA).

In Figure 4.14, DOM sample which was an algae laden dissolved organic matter sample, was compared with different types of organic matter such as humic acids from different sources such as Aldrich Humic Acid (AHA), Nordic Humic Acid (NHA), Fluka Humic Acid (FHA), Nordic Humic Acid (NHA) in terms of spectral properties in UV-vis spectroscopy. Spectral properties of Nordic Humic Acid (NHA), Fluka Humic Acid (FHA), Nordic Humic Acid (NHA) were taken from the study of Aktaş-İlgün (Aktaş-İlgün, 2010). The three of the given samples had different UV-vis absorption spectra and this property might be attributed to the fact that organic matter samples are assemblage of varying chemical structures of large polyfunctional molecules such as lipids, carbohydrates, aromatics, etc. Wershaw and colleagues studied the fractionation of the DOM of a natural water reservoir sample. Characterization by elemental, carbohydrate, and amino acid analyses showed that the fine-particulate organics and colloids are mainly composed of peptidoglycans, and lipopolysaccharides derived from algal, bacterial, and fungal cell walls (Wershaw et al., 2005).

UV-vis absorption spectra of 10 mg L⁻¹ of AHA, NHA and FHA displayed higher absorbance values than the absorption spectrum of DOM sample in 200-600 nm. Moreover, the spectral line of DOM sample followed an exponential trend from higher to lower wavelengths and much more lower than the humic samples compared, while the humic acid samples followed a comparatively more linear trend especially between 200-350 nm. Absorption at wavelengths higher than 400 nm was relatively low for all of the samples. Wang and Hsieh found by comparing UV-vis spectra of the NOM from different drinking water treatment plants and commercial humic acids a very similar profile to the DOM as displayed in Figure 4.14 (Wang and Hsieh, 2001). They observed that the wavelength dependent absorbance of the NOM increased as the concentrations increased. The absorbance determined at wavelength less than 250 nm was much higher than determined at longer wavelength and causing a sharp slope at the shorter wavelength i.e. less than 300nm, especially more apparent when the concentration of NOM was high. The absorbance at longer wavelength (> 400 nm) was relatively low. They also found a similar spectra for the commercial humic acids used to the presented humic acids in Figure 4.14. Although some minor differences were observed at shorter wavelengths (< 250 nm), the

absorbance for different humic acids were close to each other at wavelengths longer than 250 nm which is a good reference for the closeness of the spectra of humic acid samples in Figure 4.14 at higher wavelengths. At wavelengths between 200 and 270 nm, absorbance lines for AHA, NHA and FHA samples showed the presence of a diverse variety of UV₂₅₄ absorbing centers.

Humic acids are made up of heterogenous molecules of phenolic substances, aniline derivatives, benzoic acids, polyenes, and polycyclic aromatic hydrocarbons, which are main precursors or components of terrestrial HS, showing absorption in the region of 270–280 nm in UV-vis spectroscopy. Molar absorptivity at this wavelength yields estimation of the degree of aromaticity, extent of humification, and molecular weight. Oxygen-containing functional groups such as carboxylic, phenolic, and alcoholic groups are the most important groups that contribute to acidity of humic acid (Chin et al., 1994).

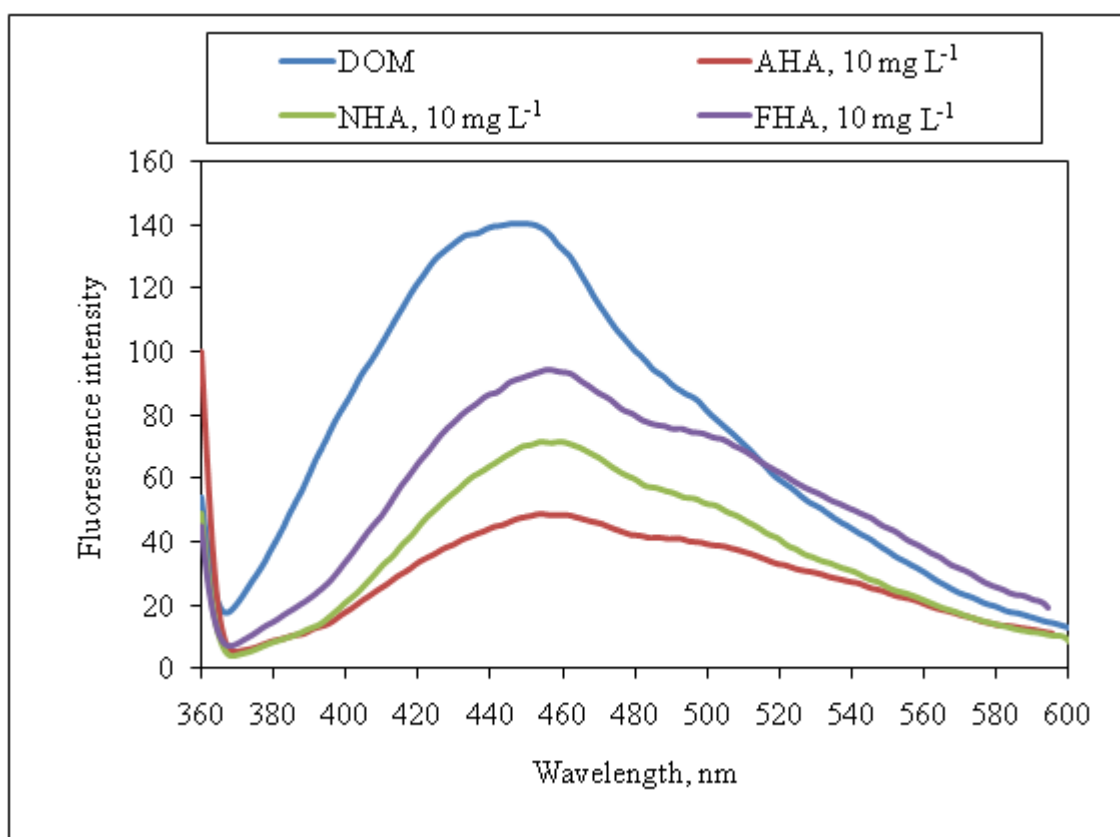


Figure 4.15. Fluorescence emission₃₅₀ spectra of the DOM sample, Aldrich Humic Acid (AHA), Fluka Humic Acid (FHA) and Nordic Humic Acid (NHA).

DOM sample with a peak in lower wavelength had its own effect on the fluorescence properties when compared to AHA, NHA and FHA humic acid samples. In emission₃₅₀ fluorescence scan, highest fluorescence intensity occurred for DOM sample, FHA, NHA, AHA at the wavelengths of 447 nm 456 nm, 454.5 nm, 454.0 nm respectively (Figure 4.15). DOM sample had the highest value but in the lowest wavelength of 447 nm when compared to all of the humic acid samples of AHA, NHA and FHA which might be because of its different chemical structure from the aforementioned commercially available humic acids. The highest peak intensity characteristic of DOM sample might have probably occurred because of overlapping contribution of fluorophores by humic acid and dissolved organic matter components of DOM sample. As the highest fluorescence intensity decreased among the compared humic acid samples, the wavelength at which maximum intensity occurred shifted to lower wavelengths, i.e. from 456 to 454 nm.

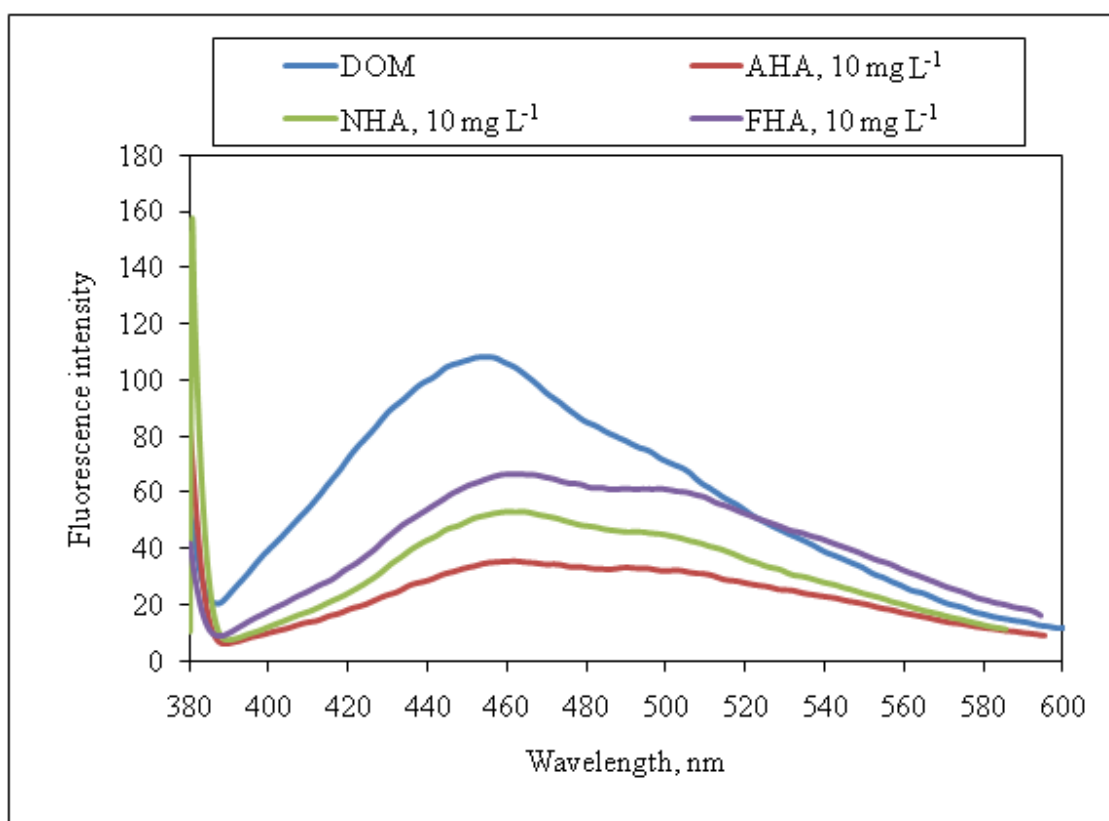


Figure 4.16. Fluorescence emission₃₇₀ spectra of the DOM sample, Aldrich Humic Acid (AHA), Fluka Humic Acid (FHA) and Nordic Humic Acid (NHA).

In emission₃₇₀ fluorescence scan, peak fluorescence intensity for DOM sample, FHA, NHA, AHA were observed at 455 nm, 463 nm, 460 nm, 461.5 respectively (Figure 4.16). Likewise in emission₃₅₀ results, highest intensity values of the presented samples followed a decreasing order such as DOM sample >FHA > NHA > AHA. DOM sample had a higher fluorescence intensity in lower wavelengths in emission₃₅₀, emission₃₇₀, synchronous scans than the humic samples of AHA, NHA and FHA. Sierra and co-workers found a similar result comparing humic and fulvic acids that the FA fluorescence intensities were higher than those of HA at identical concentrations indicating reasoning the possible explanations to the previous findings that high fluorescence intensity is, in general, associated with low molar mass components, low condensation and low aromatic degree (Sierra et al., 2005). Higher aromatic condensation in HA overlaps electronic transitions, producing an excitation spectrum less contrasted than that of fulvic acids. In addition, with respect to the acidic contents, the carboxylic group average concentration is, for these FA, higher than that of HA. Furthermore, it was also reported that in the HS plots, the emission maxima shifted to longer or shorter wavelengths according to the excitation wavelength employed (Sierra et al., 2005). A similar behavior to these results can also be reported for the comparative evaluation of the Figures 4.15 and 4.16 that the fluorescence maximum shifted to higher wavelengths in emission₃₇₀ than they were in the emission₃₅₀.

In synchronous scan mode, DOM sample had the highest fluorescence intensity of 31 at 279 nm while FHA had its the maximum intensity at 473.5 nm, NHA at 463 nm and AHA at 467 nm (Figure 4.17). Peuravuori and colleagues found a similar result comparing freshwater dissolved organic matter and isolated humic acid samples that the fluorescence properties of the humic solutes were quite close to those recorded for the dissolved organic matter. A further similarity was the case of minor intensities and most hydrophobic humic solutes than the freshwater sample similar to the case of the present study results in which the synchronous fluorescence maxima followed as the DOM sample > FHA > NHA > AHA (Peuravuori et al., 2002). However, the wavelength where the maximum intensity occurred was different when the DOM sample was compared to the maximum intensity wavelengths in fluorescence spectra of humic acids such that the DOM sample had the maximum intensity at much a lower wavelength of 279 nm than the humic acid samples

with a second peak around 469 nm which was irregular in shape. Maximum intensity was lower in humic acid samples presented and occurred at higher wavelengths of 460-470 nm.

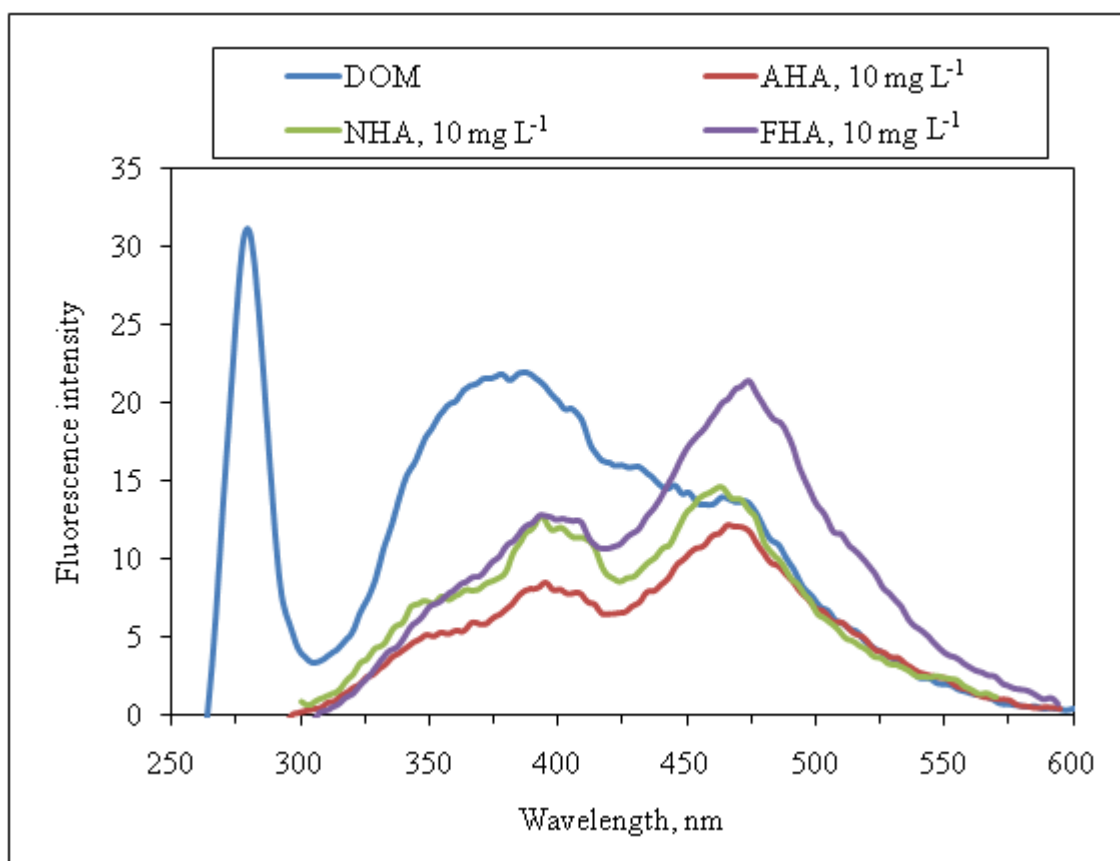


Figure 4.16. Fluorescence synchronous spectra of the DOM sample, Aldrich Humic Acid (AHA), Fluka Humic Acid (FHA) and Nordic Humic Acid (NHA).

Fluorescence measurements of the DOM sample, NHA and FHA in emission₃₅₀, emission₃₇₀ and synchronous scan modes were compared in Figures 4.15-4.17. Fluorescence emission spectra of NOM, as commonly observed for humic and fulvic substances subfractions, appear to be broad and featureless. Aquatic NOM or its subfractions showed an intense fluorescence as a result of its major fluorophore with its emission peak at 440–450 nm. The soil HA exhibited about a twofold lower peak fluorescence intensity than those of the aquatic humics. The maximum emission intensity of organic materials also depends on the excitation wavelength and varies among different natural organic matter components or subfractions. Chen and colleagues suggested that the

peak emission wavelength of NOM shifted from shorter to longer wavelengths with increased molecular size and aromatic content (Chen et al., 2003). Synchronous excitation spectra on the other hand were found to provide improved peak resolution and structural signatures. The peak intensity in synchronous in the region of about 450–480 nm could be used to differentiate the presence or absence of high molecular weight and polycondensed humic-like organic components or the multicomponent nature of NOM and its subfractions (Chen et al., 2003).

The DOM sample was also analyzed in terms of constituent chemical elements by anion and cation analysis. The results of analysisi showing common cations and anions present in the DOM sample were presented in Table 4.2.

Table 4.2. Common cations and anions of the DOM sample

Cations and Anions	Concentration, mg L ⁻¹
Na ⁺	18.075
K ⁺	2.550
Ca ²⁺	7.443
Mg ²⁺	1.970
Cl ⁻	14.048
NO ₃ ⁻	0.906
SO ₄ ²⁻	12.653
PO ₄ ³⁻	0.049

Since the algae cultivation samples were collected to constitute DOM sample after the optimum algae growth profiles were reached, nitrate and phosphate levels are very low in DOM sample because of consumption by algae. In comparison to the cation and anion contents that were introduced as the medium characteristics (Tables 4.1-4.2), the

concentrations of the nutrient elements were decreased. Moreover, Na^+ content could be considered as similar to the initial value.

Previous studies have shown that multivalent ions such as Ca^{2+} and Mg^{2+} interact strongly with the humic substances, leading to the formation of stable complexes or aggregation brought about by the chelating effect of the divalent cations. Consequently, there is an increase in both size and apparent molecular weight of the humic substances (Gjessing et al., 1999; Pinheiro et al., 2000). Xi and colleagues investigated the effects of Na^+ and Ca^{2+} interaction with NOM on the apparent molecular size distribution of the NOM samples derived from Singapore water reservoirs (Xi et al., 2004). They found that the effective size of the NOM was significantly reduced by adding Na^+ to the NOM solution due to the coil-to-globule conversion and polyelectrolyte interaction. In contrast, increasing Ca^{2+} showed two possible effects on the size of the NOM. At relatively low Ca^{2+} concentrations, NOM size was reduced presumably by the same mechanism as in the case of Na^+ . However, when the concentration of Ca^{2+} was increased, there was an increase in NOM size, possibly due to an aggregation or chelation between the humic acid in NOM and Ca^{2+} (Xi et al., 2004). In the present study the cation concentrations given in Table 4.2 are quite significant. Wall and Choppin studied the effects of the ionic strength (maintained by LiCl , NaCl or KCl) and Ca^{2+} and Mg^{2+} concentration on the coagulation of purified humic acids (HA) (Wall and Choppin, 2003). The study results showed an increase of coagulation with increasing cationic charge, increasing ionic strength, or decreasing size of the hydrated ions present in the double layer, in the case of alkali or divalent cations. The coagulation decreased for coagulation pH values of 4 to 7–8 in the absence of and presence of Mg^{2+} and Ca^{2+} . In the absence of the divalent cations, the coagulation had a constant value for $\text{pH} > 8$, but increased in the presence of Mg^{2+} and Ca^{2+} (Wall and Choppin, 2003). The significant concentrations of Mg^{2+} and Ca^{2+} in the present study (Table 4.2) might well have had an effect on the coagulation reactions of the DOM sample with alum and ferric chloride coagulants thus influencing the reactivity of the coagulation media studied at different pH values.

Andelković and colleagues reported the effect of anions on humic acid solution on turbidity increase (Andelković et al., 2004). They found the sequence of anions increased

turbidity formation in solution followed as chloride < nitrate < sulphate, but insignificant comparing the influence of cation creating turbidity upon the addition with a sequence of increasing effectiveness in turbidity increase as $\text{Na}^+ < \text{NH}_4^+ < \text{K}^+ < \text{Mg}^{2+} < \text{Ca}^{2+} < \text{Ce}^{3+}$ which is in agreement with that humic acid molecules are of negative charge. These previous findings presented could support the data of analyzed ions in DOM sample that the presence of given ions in Table 4.2 both anions and cations with detected concentrations would contribute to the chemical reactivity of the water samples including organic matter particles thus affect the coagulation performance on certain aspects such as the reactions between organic matter and coagulant particles i.e. floc-formation characteristics of the coagulants used for organic matter removal.

Another consideration about assessing the characteristics of the DOM sample that included both algal organic matter and humic acid could be based on the effect of humic acid in DOM sample to the production of organic matter by algae in this sample. Steinberg and colleagues indicated that the humic-rich lakes do not support the algal blooms characteristic of eutrophic but humic-poor lakes (Steinberg et al., 2006). It was also discussed that it was argued that humic substances (HS) were controlling factors in aquatic ecology as important, for instance, as nutrients, temperature or even light and the quality of HS plays a crucial role in the nutrition of planktonic microorganisms. Sustained growth of organisms requires the control parameters more than carbon and may be regulated by the presence of supply nutrients such as P and N. Since the DOC is contributed by both humic substances and algae to the water systems it shows differences according to natural water characteristics. Because of this source dependent property of DOC it had to be chemically characterized instead of simply measuring as bulk concentration. Using the C:N ratio was suggested as a parameter that may serve as a universal predictor of the microbial carrying capacity of a water body (Steinberg et al., 2006).

Considering the above presented properties, the derived DOM sample was accepted as a source of algal organic matter, and subjected to coagulation performance studies in the next section to find optimum coagulation performances of alum and ferric coagulants in DOM sample produced.

4.2.2. Coagulation of DOM Sample with Alum

4.2.2.1. Optimum Dose of Alum with Respect to pH. Optimum alum doses for an efficient removal of organic matter in DOM sample by coagulation were determined at the specified pH conditions that were pH 5.5, pH 6.0, pH 6.5, pH 7.0. the removal efficiency was based on UV-vis parameters which were UV_{254} , UV_{280} , UV_{365} , $Color_{436}$. Dissolved organic organic matter removal profiles based on these conditons were presented in the following Figures 4.18-4.21.

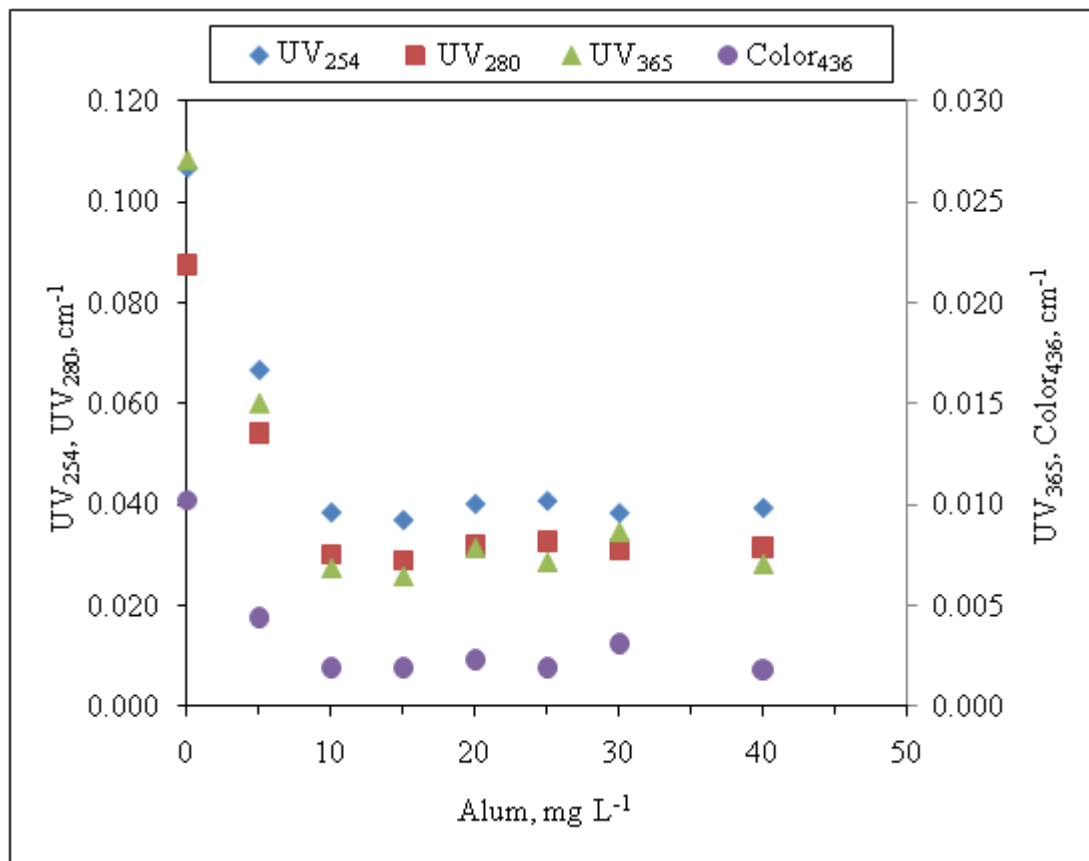


Figure 4.18. DOM removal by coagulation with alum at pH 5.5 based on UV-vis parameters.

Coagulation of the DOM sample at a low pH of 5.5 was performed by the application of various alum concentrations that were 5 mg L⁻¹, 10 mg L⁻¹, 15 mg L⁻¹, 20 mg L⁻¹, 25 mg L⁻¹, 30 mg L⁻¹, and 40 mg L⁻¹ which were applied in this increasing order to investigate the optimum dose of alum coagulant at this pH and to assess the effects of using higher doses of alum to the coagulation efficiency in the DOM sample (Figure 4.18). Through the application of 5 mg L⁻¹ alum, UV₂₅₄ decreased to nearly half of the initial value. There was a small difference between the removal rate of 10 mg L⁻¹ and 15 mg L⁻¹ alum doses applied. Best removal was approached by 15 mg L⁻¹ with a UV₂₅₄ decrease percent of 63.58. After using 15 mg L⁻¹ of alum, increasing the coagulant dose did not yield a better removal and a slight increase occurred in UV₂₅₄. UV₂₈₀ and UV₃₆₅ results followed a similar removal trend to UV₂₅₄ at the applied alum doses. Optimum doses for specified pH values were identified in this study according to the highest UV₂₅₄ removal efficiency. 15 mg L⁻¹ of alum dose at pH 5.5 was determined to be the optimum dose for coagulation of the DOM sample. Removal values according to Color₄₃₆ at the applied doses were similar to the removal values of other parameters with an exception of optimum removal reached by using 10 mg L⁻¹ alum rather than 15 mg L⁻¹ for Color₄₃₆ removal.

At pH 6.0, alum doses were applied in the order of 5 mg L⁻¹, 10 mg L⁻¹, 15 mg L⁻¹, 20 mg L⁻¹, 30 mg L⁻¹, 40 mg L⁻¹, 50 mg L⁻¹, 60 mg L⁻¹, 70 mg L⁻¹ of in coagulation of the DOM sample. The resultant removal profile was presented in Figure 4.19. using 5 mg L⁻¹ of alum removed 70 % of organic matter in terms of UV₂₅₄. Applying higher alum doses as 10 mg L⁻¹, 20 mg L⁻¹, 30 mg L⁻¹ and 40 mg L⁻¹ of alum improved the removal efficiency. Highest removal was found by using 40 mg L⁻¹ alum dose with a removal percent of 71.46 in terms of UV₂₅₄ removal. Other UV-vis parameters, UV₂₈₀, UV₃₆₅ and Color₄₃₆ resulted in similar efficiencies as obtained in UV₂₅₄ results. the Since the highest removal was achieved by an alum dose of 40 mg L⁻¹ at pH 6.0 this condition was determined as optimum dose of alum at this pH condition for optimum removal of dissolved organic matter in the DOM sample. Application of higher doses than 40 mg L⁻¹ of alum such as 50 mg L⁻¹, 60 mg L⁻¹ and 70 mg L⁻¹ did not improve efficiency, but instead a slight increase was observed according to UV-vis parameters which could be indicating a charge reversal and chemical restabilization of the particles occurred by using higher doses than the optimum dose.

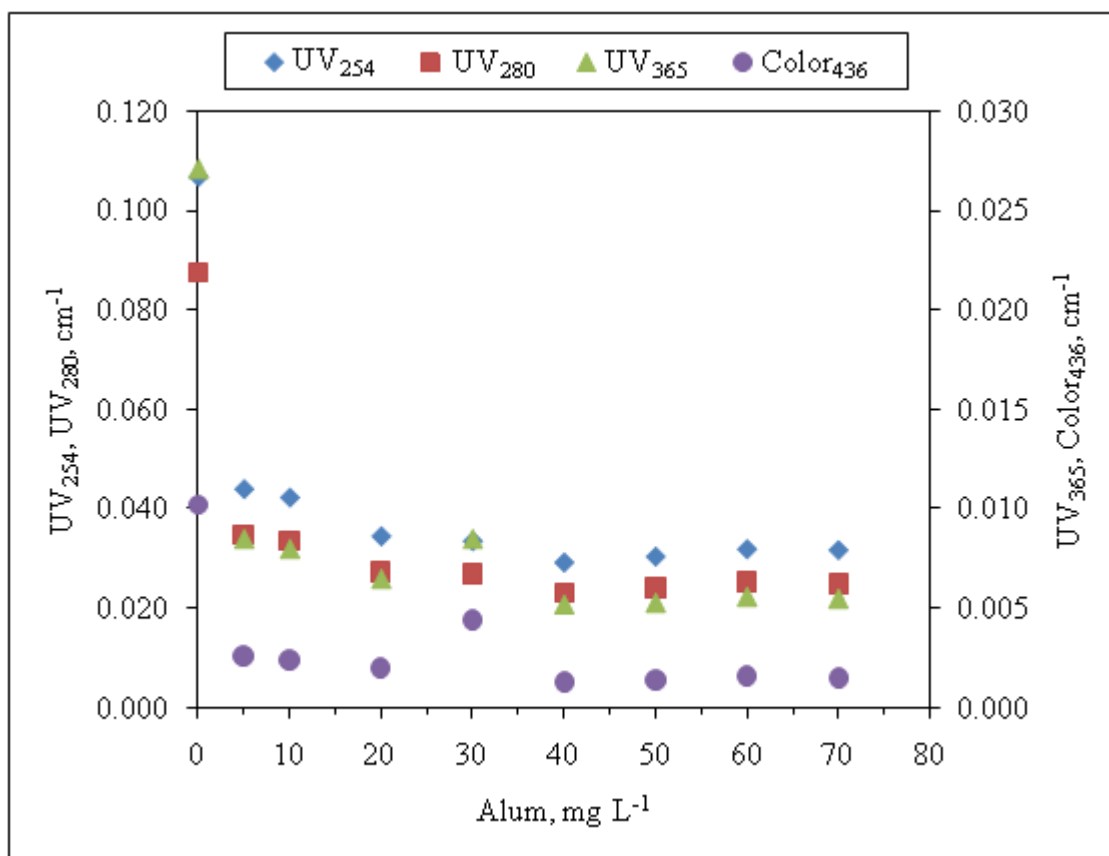


Figure 4.19. DOM removal by coagulation with alum at pH 6.0 based on UV-vis parameters.

Coagulation of the DOM sample with alum at pH 6.5 were performed by application of 10 mg L⁻¹, 20 mg L⁻¹, 30 mg L⁻¹, 40 mg L⁻¹, 50 mg L⁻¹, 60 mg L⁻¹ of alum doses (Figure 4.20). Using 10 mg L⁻¹ of alum reduced nearly 2/3 of the UV₂₅₄. Increasing the coagulant dose to 20 mg L⁻¹ and 30 mg L⁻¹ caused a further reduction in UV₂₅₄. Optimum alum dose of alum at pH 6.5 was identified as 30 mg L⁻¹ leading a UV₂₅₄ decrease in a percent of 66.83. UV₂₈₀, UV₃₆₅ and Color₄₃₆ results were in agreement with UV₂₅₄ findings with optimum removal values at the same dose as in UV₂₅₄ which was 30 mg L⁻¹ of alum. Increasing the coagulant dose did not yield to further removal of dissolved organic matter. In contrast, UV-vis spectroscopy results slightly increased when alum doses higher than 30

mg L⁻¹ were applied which could be because of restabilization of the suspension by addition of these amounts of alum doses at pH 6.5.

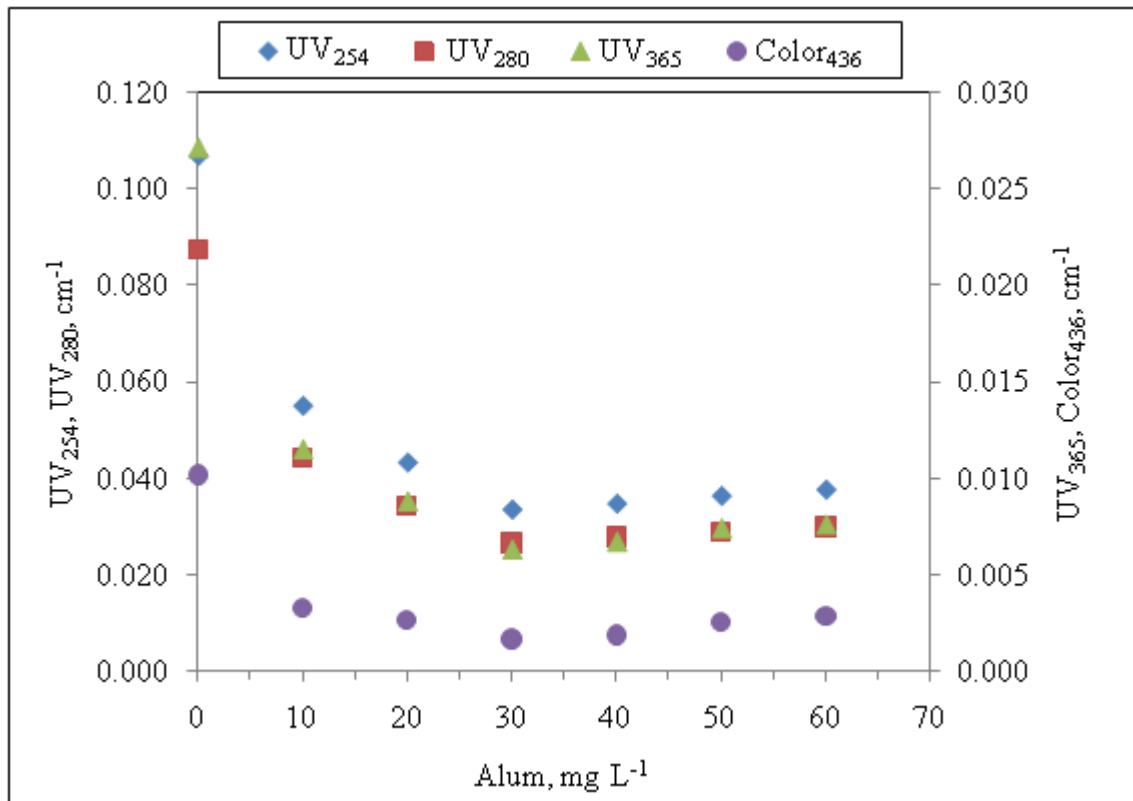


Figure 4.20. DOM removal by coagulation with alum at pH 6.5 based on UV-vis parameters.

At pH 7.0, 10 mg L⁻¹, 20 mg L⁻¹, 30 mg L⁻¹, 40 mg L⁻¹, 50 mg L⁻¹, 60 mg L⁻¹, 70 mg L⁻¹ of alum doses were applied in coagulation tests of DOM sample (Figure 4.21). Applying low doses of alum like 5 mg L⁻¹, 10 mg L⁻¹, 20 mg L⁻¹ leveled of the UV₂₅₄ values. Between 30-50 mg L⁻¹ of alum doses coagulation efficiency was improved. Best elimination of organics was obtained using 50 mg L⁻¹ of alum with a decrease percent of 67.42 in UV₂₅₄ was determined to be the optimum alum dose for coagulation of DOM sample at pH 7.0. Application of alum doses higher than 50 mg L⁻¹ such as 60 mg L⁻¹ and 70 mg L⁻¹ did not changed the removal efficiency of the specified UV-vis parameters. In fact a slight increase occurred in UV₂₅₄ while other parameters UV₂₈₀, UV₃₆₅, and Color₄₃₆ remained similar to the optimum removal values at alum dose of 50 mg L⁻¹ applied.

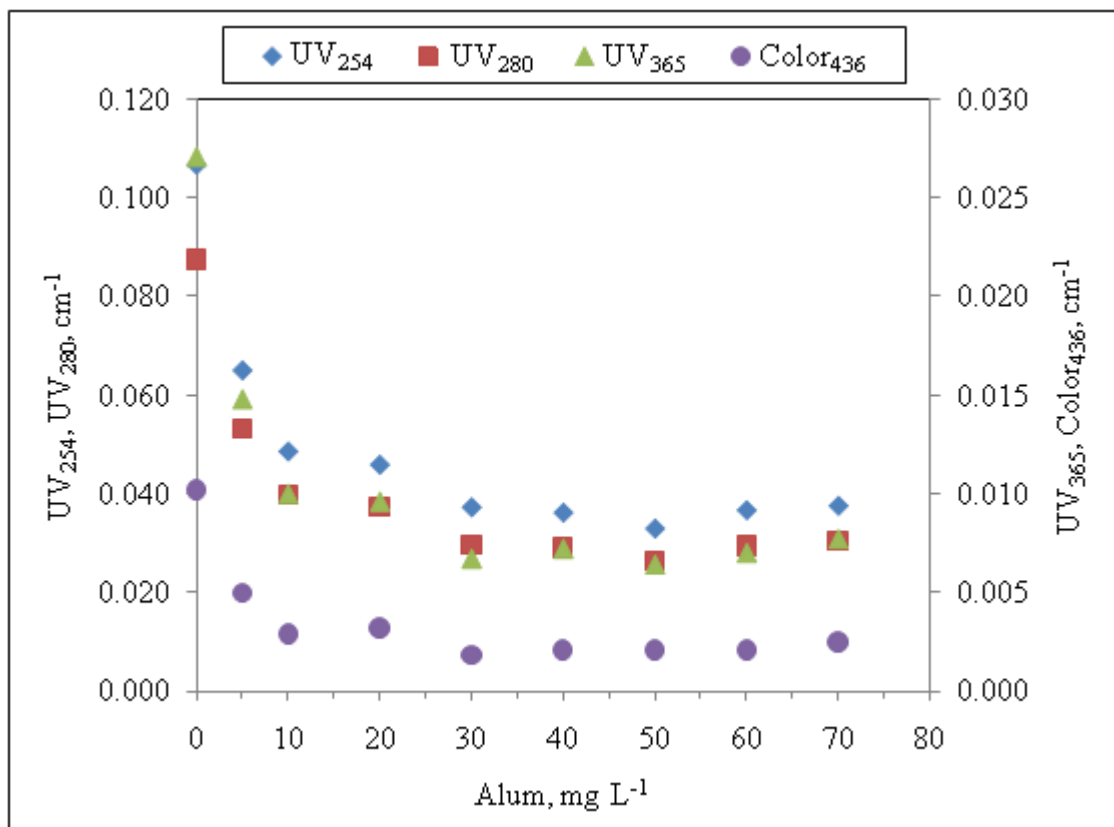


Figure 4.21. DOM removal by coagulation with alum at pH 7.0 based on UV-vis parameters.

4.2.2.2. Comparative Evaluation of pH Dependency for Coagulation with Alum. After determining the optimum dose conditions of alum in each pH value of coagulation, the optimum pH for an efficient removal of dissolved organic matter by coagulation using alum could be determined by comparing the removal profiles in the studied pH values. The effect of coagulation pH from as changed from low to high values between pH 5.5-7.0 to the coagulation efficiency of alum coagulant in treatment of the DOM sample was presented in terms of UV₂₅₄, UV₂₈₀, UV₃₆₅, and Color₄₃₆. For comparison purposes, the presented data on these UV-vis parameters in Figures 4.18-4.21 were selected and compiled in Figures 4.22-4.25 to show the pH dependency of the coagulation efficiency of alum coagulant for organic matter removal in the DOM sample.

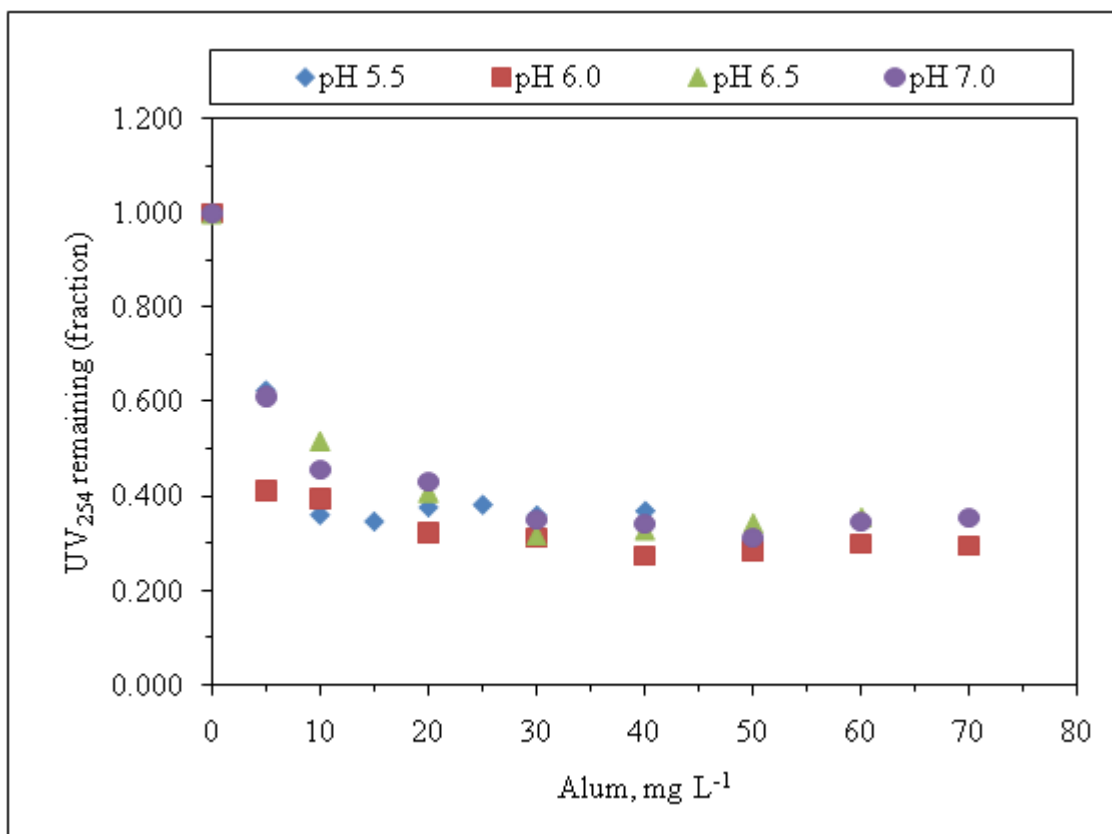


Figure 4.22. Comparison of DOM removal by coagulation with alum under varying pH conditions with respect to UV₂₅₄.

As could be seen from Figure 4.22, optimum coagulant doses increased in each series as the pH of the samples were increased. At pH 5.5 optimum coagulant dose was obtained using a minimum alum concentration of 15 mg L⁻¹ compared to the other coagulation tests performed at higher pH values: 6.0, 6.5, 7.0. However the highest organic matter removal efficiency based on UV₂₅₄ was achieved with a 71.46 % removal at pH 6.0 with an coagulant dose of 40 mg L⁻¹ of alum, which was determined as the optimum dose for coagulation of the DOM sample with alum. Coagulation profile at pH 6.0 using changing alum doses follows the most bottom path among other coagulation profiles of other pH conditions that were compared except a more efficient performance at pH 5.5 than 6.0 with a small difference using 10 mg L⁻¹ of alum. According to comparison of varying coagulation pH conditions of alum in Figure 4.22, the highest coagulation efficiency for removal of organic matter in the DOM sample according to UV₂₅₄ was achieved at a pH value of 6.0.

In addition to UV_{254} , comparison for UV_{280} , UV_{365} , $Color_{436}$ values according to varying pH for their removal results at the studied pH conditions of coagulation with alum between pH 5.5-7.0 were presented in Figures 4.23-4.25 to analyze the changes with pH also based on these UV-vis parameters.

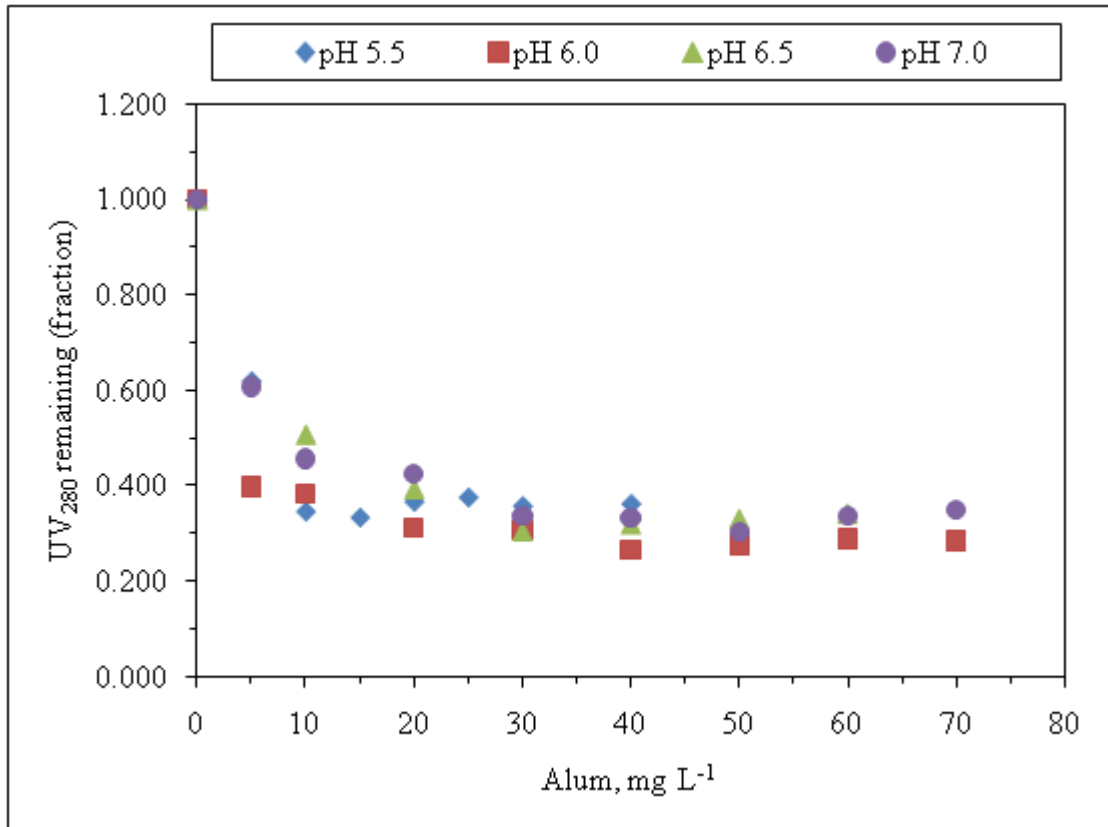


Figure 4.23. Comparison of DOM removal by coagulation with alum under varying pH conditions with respect to UV_{280} .

Comparison of pH dependent coagulation profiles between pH 5.5-7.0 in coagulation of DOM sample with alum in terms of UV_{280} was presented in Figure 4.23. The highest removal efficiency based on UV_{280} was achieved by a 73.49 % removal at pH 6.0 with a dose of 40 mg L^{-1} of alum. The change of UV_{280} by a dose of 40 mg L^{-1} of alum at different pH could be compared which represents how coagulation performance was affected by pH using this concentration of alum. At the determined optimum coagulant conditions for alum which is an optimum alum concentration of 40 mg L^{-1} at pH of 6.0,

UV₂₅₄ and UV₂₈₀ values followed the decreasing order according to the pH of the samples such that UV₂₈₀ at pH 5.5 was the highest, then UV₂₈₀ at pH 7.0 came below the UV₂₈₀ values of pH 5.5. UV₂₈₀ at pH 6.5 occurred in lower values than the UV₂₈₀ at pH 7.0. UV₂₈₀ values at pH 6.0 followed below the UV₂₈₀ at all other pH values. While it provided the best removal for a pH value of 6.0, it did not lead to a good result for pH 5.5 relative to its own optimum alum dose of 15 mg L⁻¹. At the higher pHs of 6.5 and 7.0, coagulation did not reach to the optimum removal condition as the values at these pHs were higher than pH 6.0 using 40 mg L⁻¹. The demonstrated comparison of UV₂₈₀ values in Figure 4.23 resulted in almost the same as the one in comparison of UV₂₅₄. The similarity between two comparisons shows that these two parameters of UV₂₅₄ and UV₂₈₀ might be interchangeably used to assess the DOM removal efficiency in the DOM sample in UV-vis spectroscopy.

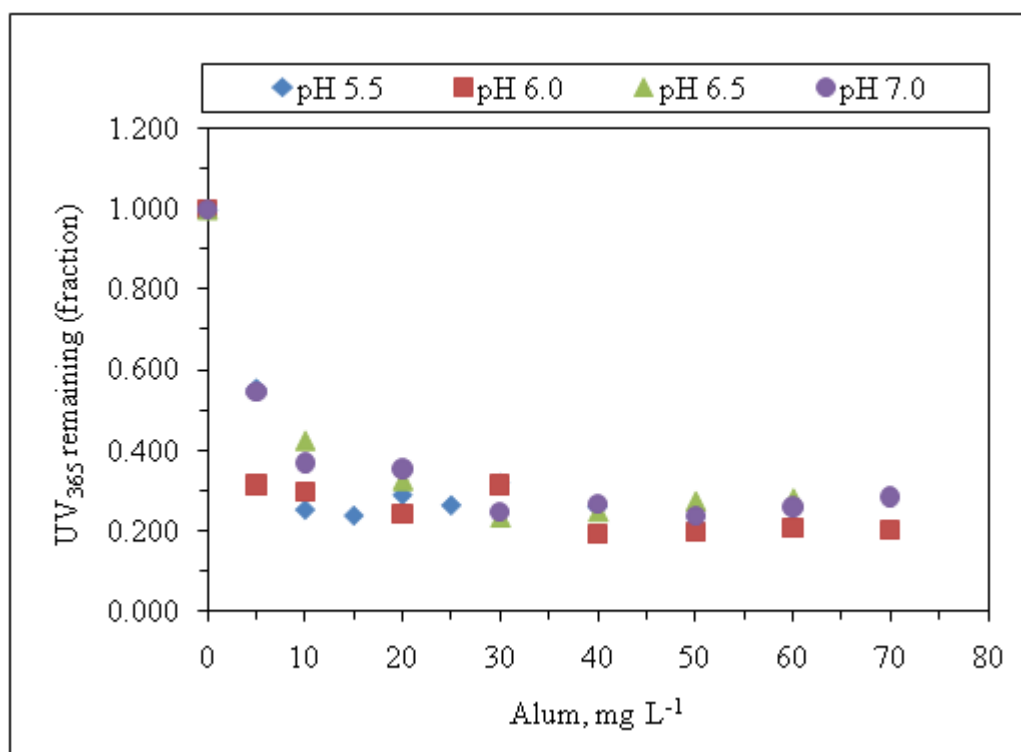


Figure 4.24. Comparison of DOM removal by coagulation with alum under varying pH conditions with respect to UV₃₆₅.

Comparison of UV₃₆₅ values and comparison of Color₄₃₆ values of pH dependent coagulation profiles with alum coagulation were given in Figure 4.24 and Figure 4.25

respectively. Likewise the similarity between the pH-dependent comparisons of UV₂₅₄ and UV₂₈₀ in Figure 4.22 and Figure 4.23, the comparison profiles of UV₃₆₅ and Color₄₃₆ at the given pH conditions displayed very similar trends. Using UV₃₆₅ and Color₄₃₆ parameters, 40 mg L⁻¹ of alum at pH 6.0 still could be referred as the optimum coagulation condition with alum for the DOM sample.

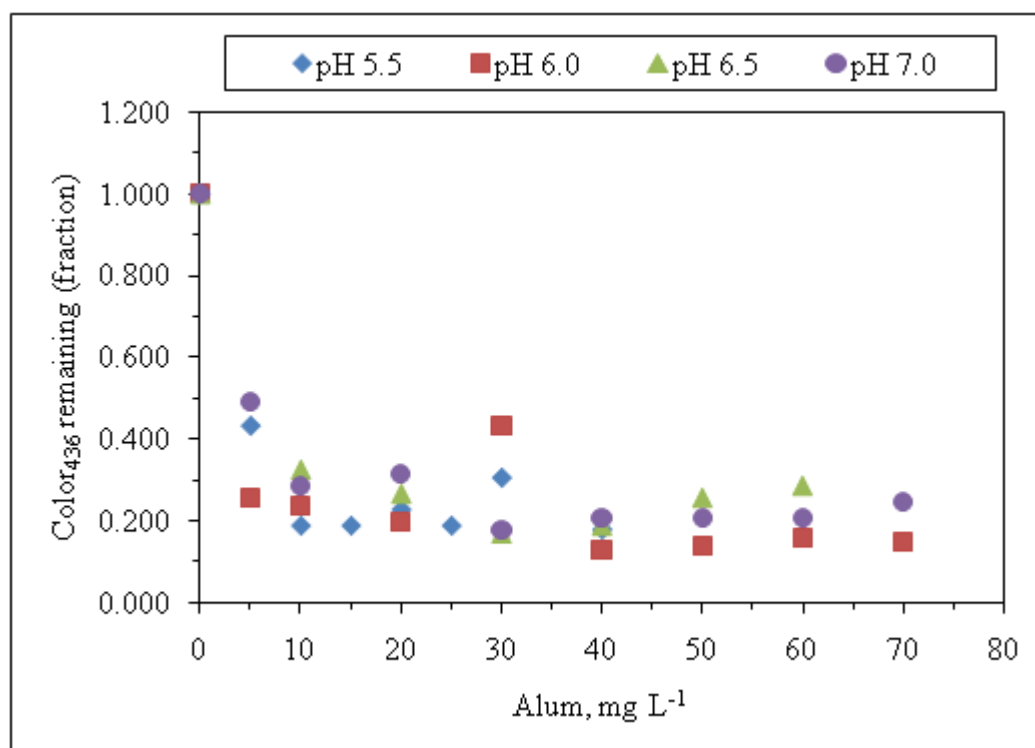


Figure 4.25. Comparison of DOM removal by coagulation with alum under varying pH conditions with respect to Color₄₃₆.

Comparison of dissolved organic carbon (DOC, mg L⁻¹) removal by coagulation with alum at different pH conditions in the DOM sample showed a significant difference at the lower pH values of 5.5, 6.0 in comparison to pH 6.5 and pH 7.0 that the coagulation was more efficient in removing DOC in lower pH conditions of 5.5 and 6.0 as shown in Figure 4.26. The comparison of DOC removals by pH change reveals that coagulation efficiency of DOM sample with alum was more dependent on suppressing pH for removing DOC than it is for removing UV₂₅₄ (Figure 4.22, Figure 4.26). Especially relatively low DOC removal at pH 7.0 more clearly shows how DOC removal efficiency decreased by increasing the

coagulation pH to this level. Best DOC removal was reached at pH 6.0 using 50 mg L⁻¹ alum with a rate of 89%. At pH 5.5, 87% DOC removal was achieved by 20 mg L⁻¹ alum. At pH 6.5, using 30 mg L⁻¹ alum led the lowest DOC with a removal percent of 79. At pH 7.0, 61% of the DOC was removed using 50 mg L⁻¹ alum.

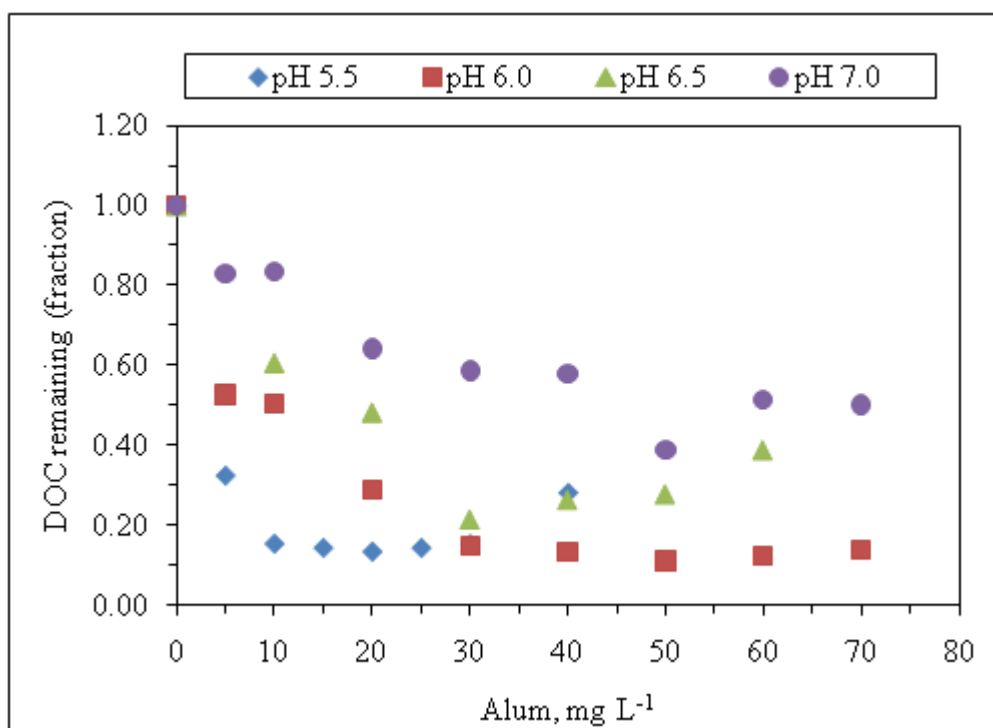


Figure 4.26. Comparison of DOM removal by coagulation with alum under varying pH conditions with respect to DOC.

According to UV₂₅₄ and DOC measurements, pH 6.0 was determined to be the optimum pH at which the highest removal rates of the dissolved organic matter were achieved in the DOM sample. To provide a deeper insight to the optimum pH conditions, comparative presentation of the results achieved for the specified UV-vis parameters as well as DOC and UV-vis spectra between 200-600 nm, and fluorescence spectra in emission₃₅₀, emission₃₇₀ and synchronous were introduced as given in Figures 4.27-4.30. UV-vis and fluorescence spectra in emission₃₅₀, emission₃₇₀ and synchronous measurements attained under other pH conditions of 5.5, 6.5 and 7.0 were given in Appendix A and Appendix B.

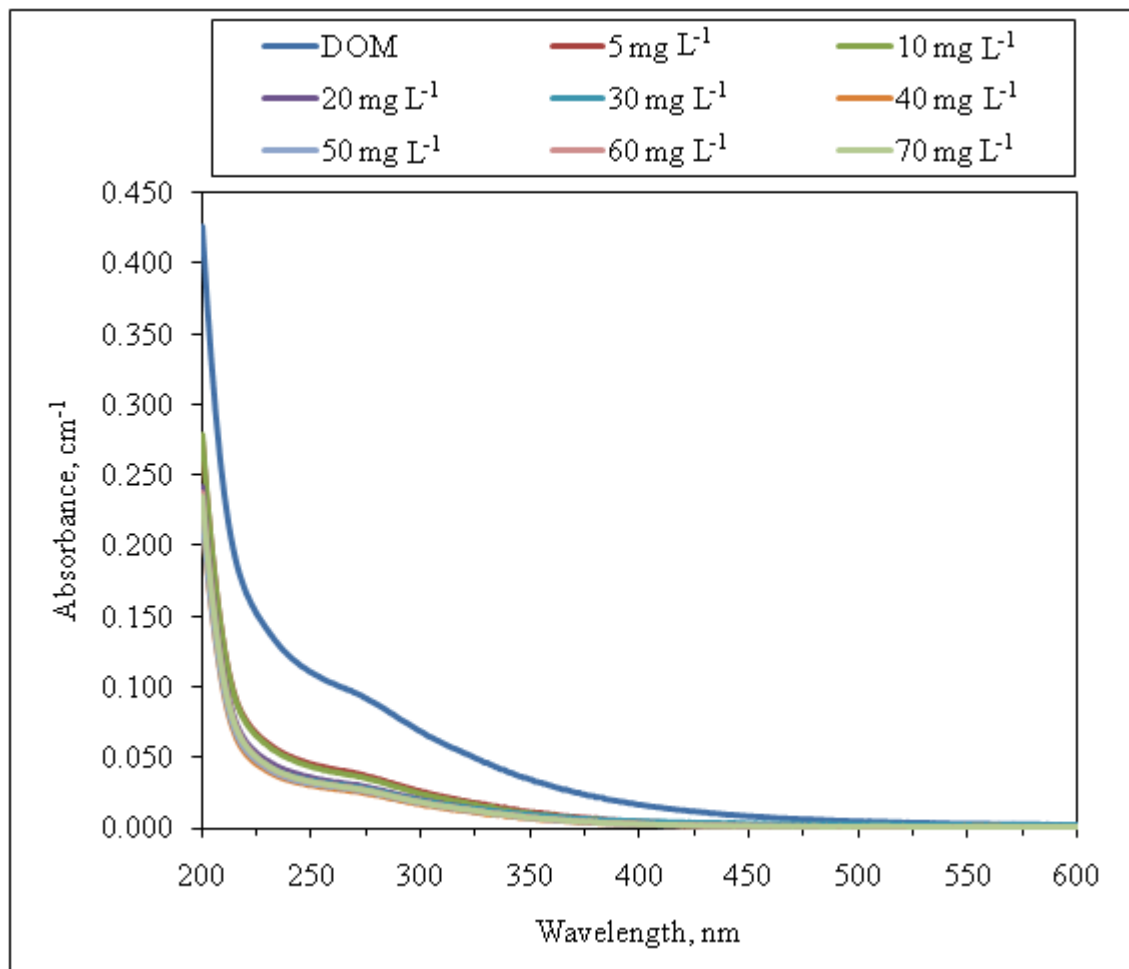


Figure 4.27. UV-vis spectra of the DOM sample after coagulation with alum at pH 6.0.

UV-vis spectra of the untreated and the coagulated DOM sample with alum were presented in Figure 4.27. Treated samples showed a similar decreasing trend as the spectrum of the untreated DOM sample after coagulation with alum at the optimum pH of 6.0. UV-vis spectra of the DOM sample in Figure 4.27 at pH 6.0 could be comparable with the results obtained according to the specified UV-vis parameters (UV_{254} , UV_{280} , UV_{365} , $Color_{436}$) at pH 6.0 presented in Figure 4.19. Such a comparison between Figure 4.19 and Figure 4.27 reveals that both of the methods based on UV-vis spectroscopy could be used to evaluate DOM removal efficiency of coagulation with alum in the DOM sample. Application of 5 mg L^{-1} and 10 mg L^{-1} of alum greatly reduced the UV-vis spectra line of the DOM sample in Figure 4.27. Application of alum doses higher than that resulted in an

overlapping view of all the spectra that were very close to each other which could be concluded that the organic matter removal efficiency was achieved by using low doses of alum at the optimum pH for coagulation of the DOM sample with alum which was 6.0.

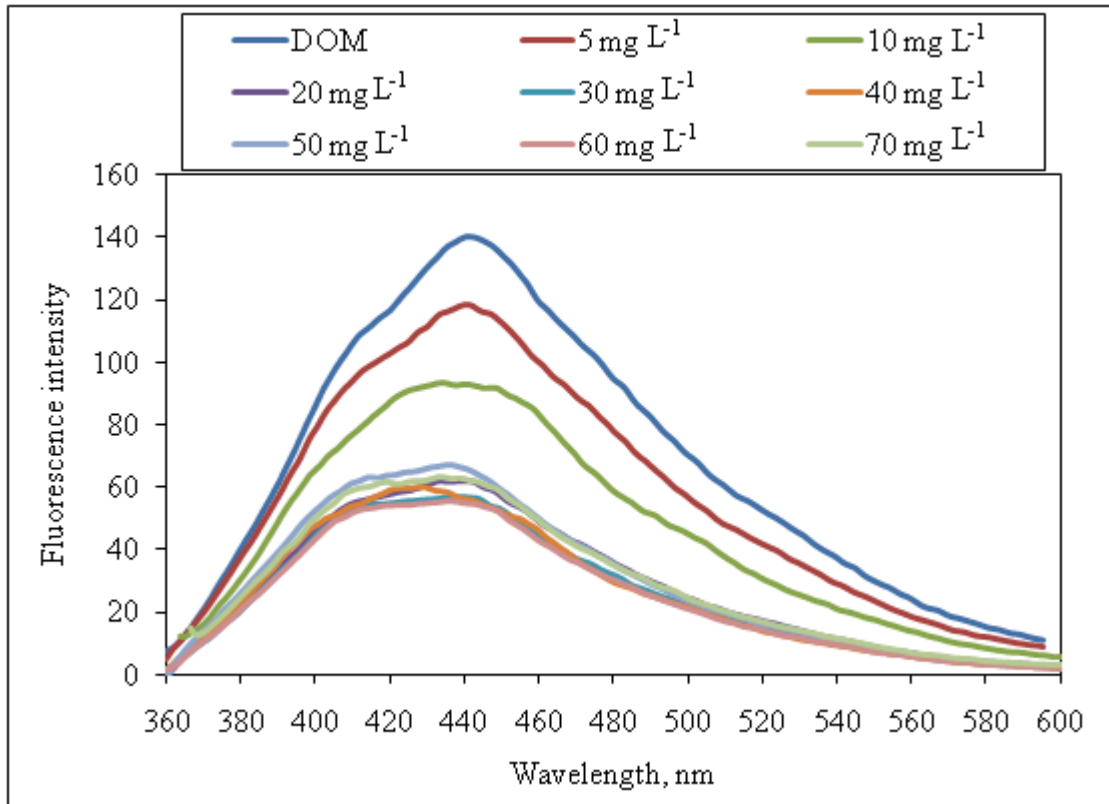


Figure 4.28. Fluorescence emission₃₅₀ spectra of the DOM sample after coagulation with alum at pH 6.0.

The fluorescence spectra taken in emission scan recorded in two different excitation wavelengths as 350 nm and 370 nm showed coagulation performance of alum in the DOM sample. Accordingly, these measurements of emission₃₅₀ and emission₃₇₀ did not express any significant difference when compared to each other (Figure 4.28, Figure 4.29). A homogeneous decay profile trended in fluorescence intensity of the treated samples and was obtained for all of the applied coagulant doses. However, a slight broadening in peak shape was observed for excitation at 350 nm wavelength when compared to the spectra recorded at excitation wavelength of 370 nm.

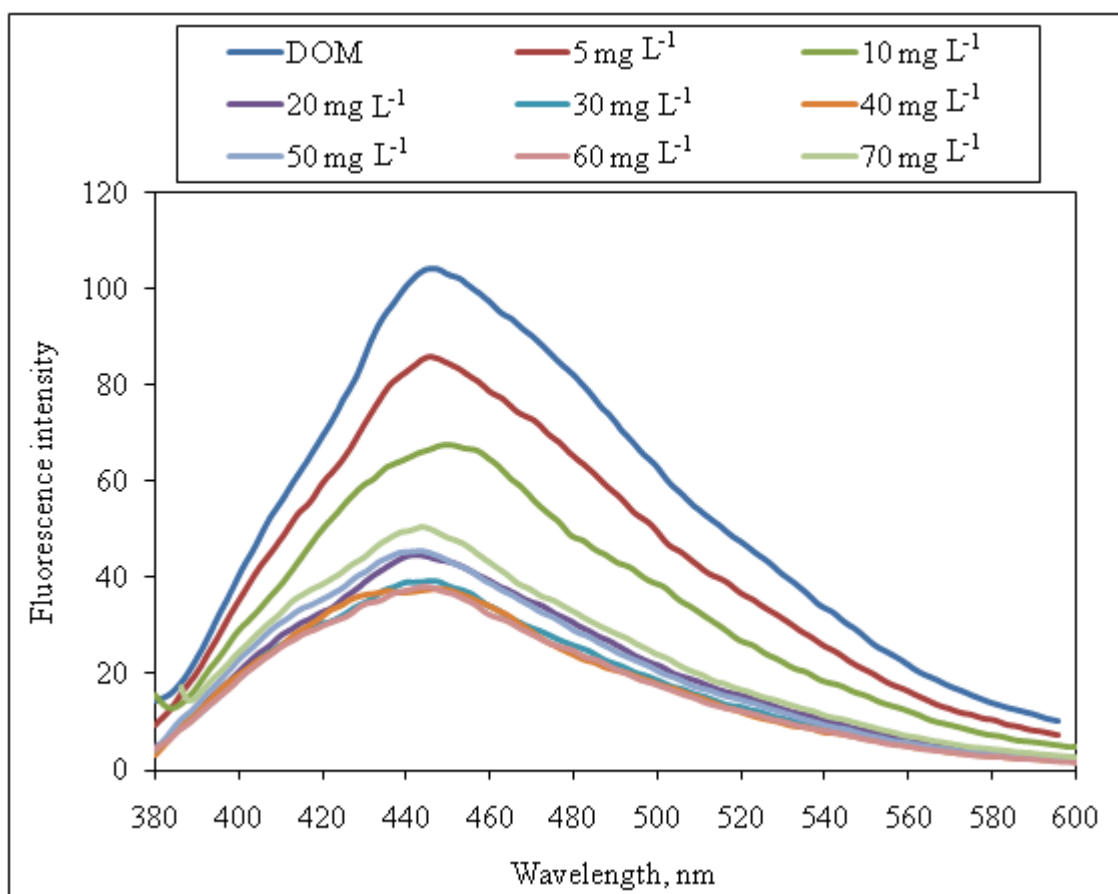


Figure 4.29. Fluorescence emission₃₇₀ spectra of the DOM sample after coagulation with alum at pH 6.0.

The fluorescence spectra of DOM samples after treatment with alum recorded by using synchronous scan mode displayed a regular peak at 280 nm as could be seen in Figure 4.30. The fluorescence intensity values obtained at wavelength region of 350 nm to 450 nm could be regarded as irregular in shape. By looking at the behavior of DOM sample at the peak wavelength of 280 nm it can be concluded that a homogeneous decay of treated samples according to coagulation performance with different doses also holds for synchronous scan as in the case of emission scan measurements. In all of the fluorescence measurements, it was observed that spectra of treated samples began to pass very close to each other as the optimum organic matter removal efficiency of coagulation was approached with an alum dose of 30 mg L⁻¹ and remained similar for the applications higher than this concentration.

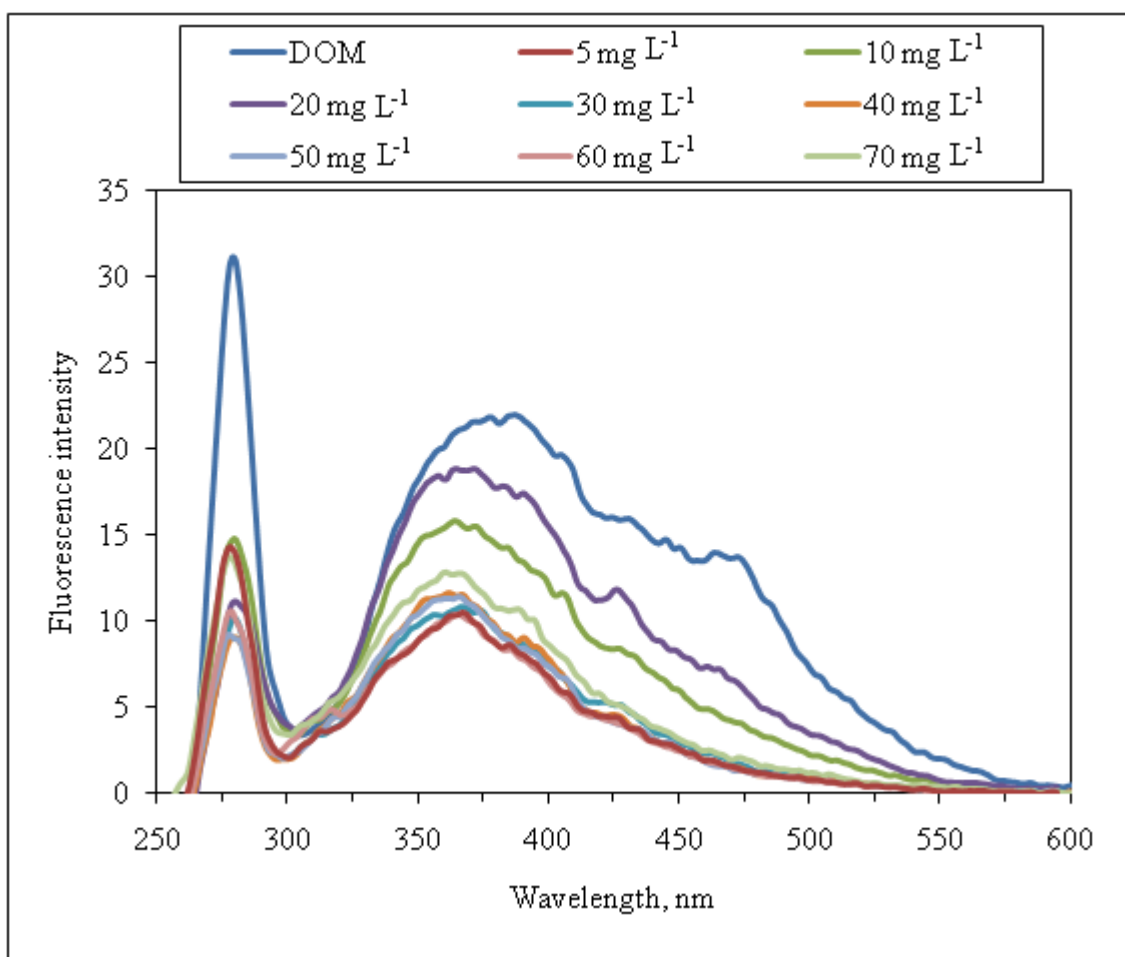


Figure 4.30. Fluorescence synchronous spectra of the DOM sample after coagulation with alum at pH 6.0.

Maximum fluorescence intensities of the DOM sample before and after coagulation with changing doses of alum varied between 5-70 mg L⁻¹ were compared as shown in Figure 4.31. The untreated DOM sample had the highest intensity in emission₃₅₀, emission₃₇₀ and synchronous scans than the coagulated samples. In general, maximum intensities were ordered as $FI_{\text{emission350}} < FI_{\text{emission370}} < FI_{\text{synchronous}}$ for all of the samples obtained by coagulation with reference to the DOM sample. Fluorescence intensities of the DOM sample was 140 in emission₃₅₀, 108 in emission₃₇₀ and 31 in synchronous scan. Intensities of the DOM sample were reduced significantly by treatment with 5 mg L⁻¹, 10 mg L⁻¹, 20 mg L⁻¹ and 30 mg L⁻¹ of alum. Coagulation with an optimum dose of alum which was determined to be 40 mg L⁻¹ in coagulation tests resulted in a decrease in the

fluorescence intensity of the DOM sample to 54 in emission₃₅₀, 37 in emission₃₇₀, and 9 in synchronous scan. Maximum fluorescence intensities for FI_{emission350}, FI_{emission350} and FI_{synchronous} remained similar by the application of a higher dose of 50 mg L⁻¹ but a minor increase occurred by 60 mg L⁻¹ and 70 mg L⁻¹ of alum which could be evaluated to have occurred as a result of an increase in the remaining amount of organic matter (decrease in removal efficiency of organic matter) because of a possible charge reversal and restabilization of the particles during the coagulation process of the DOM sample, and the final chemical species occurred in sample solution affected by using high doses of alum.

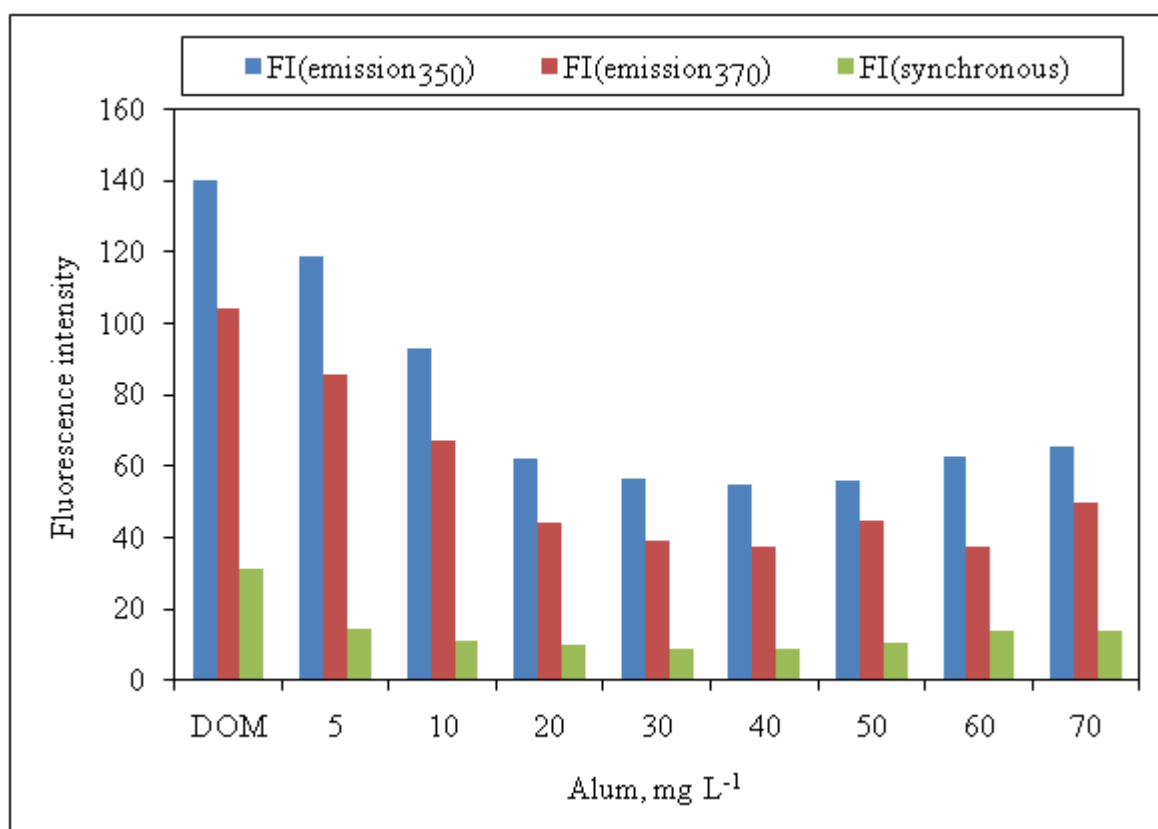


Figure 4.31. Comparison of the fluorescence intensities of the DOM sample after coagulation with alum at pH 6.0 in emission₃₅₀, emission₃₇₀ and synchronous scan modes.

Optimum pH for coagulation of the DOM sample with alum in this study was determined to be pH = 6.0. The result is in accordance with previous findings reported in the literature (Gregor et al., 1997; Iriarté-Velasco et al., 2007). To meet 35% DOC removal

as required by the USEPA, Iriarté-Velasco and colleagues reported that it was necessary to reduce pH to 6.0 units (Iriarté-Velasco et al., 2007). Working with water samples from a low DOC (2.1–2.4 mg L⁻¹) and low turbidity (<1 NTU) surface water, they obtained results suggesting that the optimum dose for alum was about 40 mg L⁻¹ corresponding to an aluminium dose of 3.24 mg Al³⁺ L⁻¹, and further coagulant addition did not result in any significant improvement in water quality (Iriarté-Velasco et al., 2007). An efficient removal of organic matter in the DOM sample could be achieved by using 40 mg L⁻¹ of alum at pH 6.0 though it was determined to be the optimum dose of alum at these conditions. Comparing these results to what Iriarte and co-workers found in coagulation of surface water sample, although the DOC content of DOM sample (20.5 mg L⁻¹) was higher than their surface water samples, using same amount of alum coagulant dose at the same pH of 6.0 as in their study was efficient in removing organics in the DOM sample. Relatively higher DOC in the DOM sample did not lead to higher coagulant demand which could be as a result of different water quality characteristics, and differences in the content of the organic matter. In a study by Gregor and colleagues on optimizing NOM removal by coagulation, the optimum coagulation pH for DOM removal and minimum soluble aluminium residual for three low turbidity drinking-water reservoir samples were explored. Similar to the findings of the present study on coagulation with alum, they found optimum pH for alum to be in the range of 6.0-7.0. It was indicated that relying on soluble NOM removal alone as the indicator would have resulted in an optimum pH range of at least 5.0-7.0, if the residual soluble aluminium concentrations did not narrow the acceptable range. Residual soluble aluminium is an important consideration in water treatment which is a measure of aluminium that is not incorporated into micro-floc (monomeric aluminium, soluble NOM-aluminium complexes, and/or soluble aluminium hydrolysis products), and therefore pass through the clarifiers and either precipitate during final pH correction or pass through the treatment plant and persist in the treated water (Gregor et al., 1997).

The dissolved organic matter sample used in this study which was named as DOM sample was derived from algal organic matter. The fraction of NOM in surface waters originates from algae and bacteria cell wall debris, bacterial metabolism (exopolymers) and plant residues, all of which being either cellulose or cellulose-type molecules are polysaccharide biopolymers (Biber et al., 1996). Vilg -Ritter and colleagues showed that

aluminum is preferentially bound to polysaccharides in coagulation of NOM water samples from Seine river with alum (Vilg -Ritter, 1999a). The previous studies have shown that coagulation mechanism of NOM with alum in relation to the binding between Al^{3+} and organic molecules were characterized by the existence of specific binding sites for Al in organic molecules that showed conformational changes with pH i.e. the deprotonation of the NOM at different pH conditions occurred on different sites (Masion et al., 2000).

4.2.3. Coagulation of DOM Sample with Ferric Chloride

4.2.3.1. Optimum Dose of Ferric Chloride with Respect to pH. Optimum dose of ferric chloride coagulant for coagulation of the DOM sample were determined by coagulation tests at pH values of 5.5, pH 6.0, pH 6.5, pH 7.0. The coagulation efficiency DOM removal using ferric chloride at the specified pH conditions were presented based on UV-vis parameters in Figures 4.32-4.35.

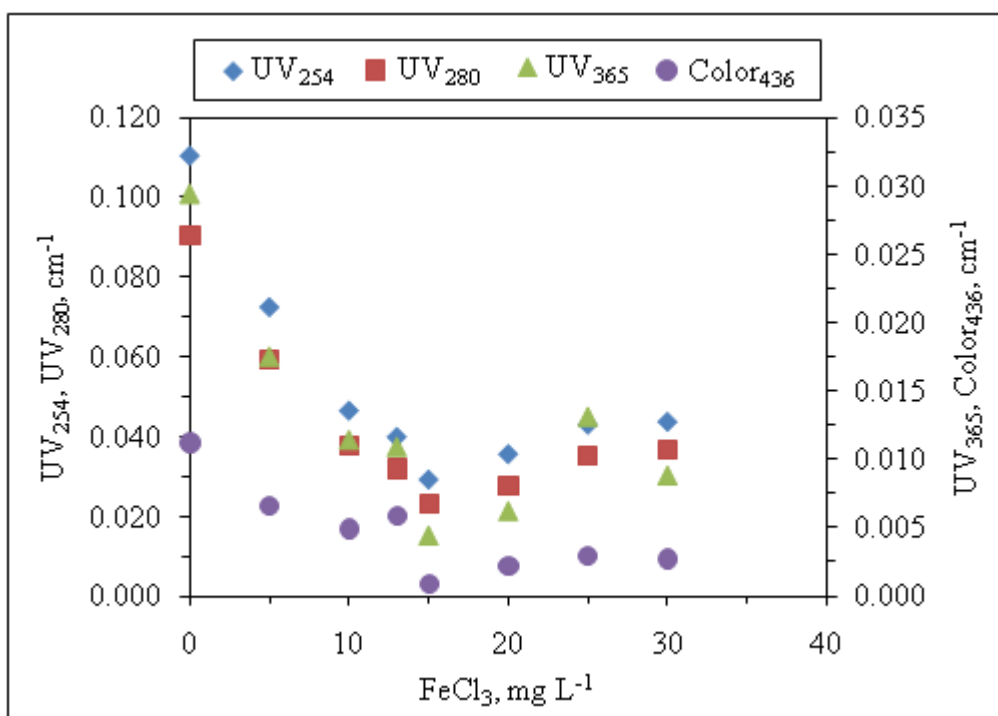


Figure 4.32. DOM removal by coagulation with ferric chloride at pH 5.5 based on UV-vis parameters.

At pH 5.5, ferric chloride doses of 5 mg L⁻¹, 10 mg L⁻¹, 13 mg L⁻¹, 15 mg L⁻¹, 20 mg L⁻¹, 25 mg L⁻¹, 30 mg L⁻¹ were applied in coagulation of DOM sample (Figure 4.32). Highest organic matter removal was found using 15 mg L⁻¹ with a UV₂₅₄ removal of 73.51%. Optimum removal dose was the same for different UV-vis parameters of UV₂₅₄, UV₂₈₀, UV₃₆₅ and Color₄₃₆ measurements. After the optimum dose of 15 mg L⁻¹, increasing the coagulant dose seemed to cause the restabilization of the suspensions as implied by the observed changes in UV₂₅₄, UV₂₈₀ and UV₃₆₅ in Figure 4.27. Optimum removal followed the same trend for the ferric doses applied higher than 15 mg L⁻¹ for UV₃₆₅ and Color₄₃₆.

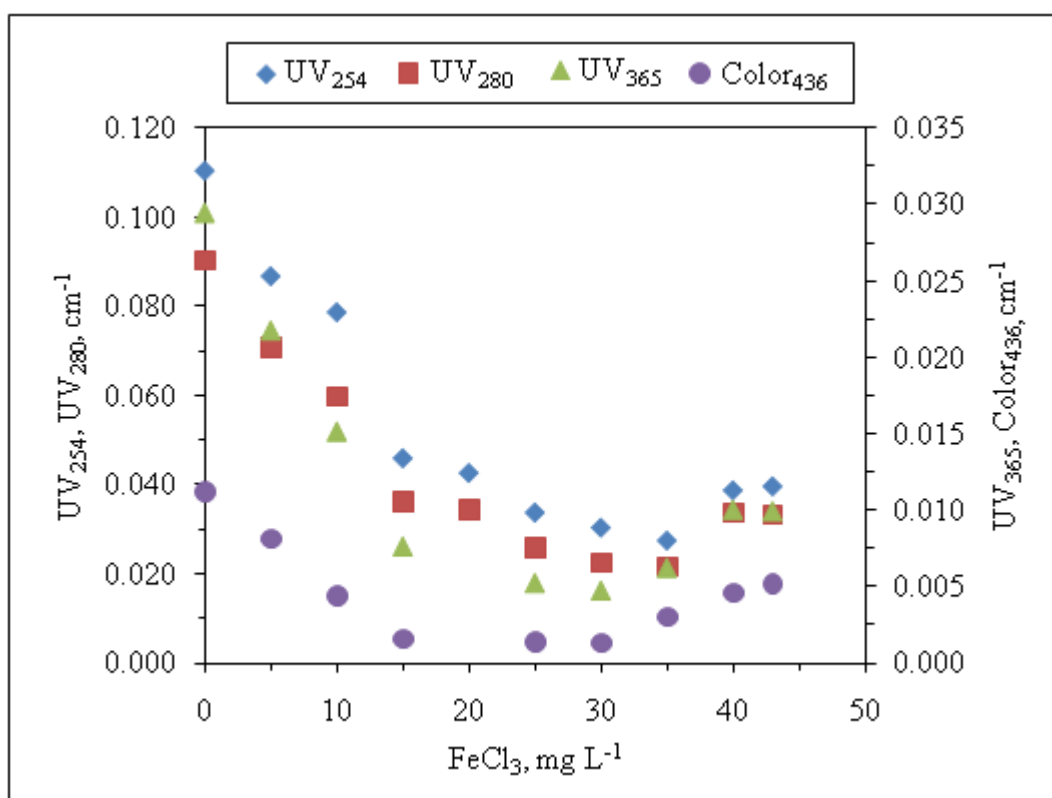


Figure 4.33. DOM removal by coagulation with ferric chloride at pH 6.0 based on UV-vis parameters.

At pH 6.0, ferric chloride concentrations of 5 mg L⁻¹, 10 mg L⁻¹, 15 mg L⁻¹, 20 mg L⁻¹, 25 mg L⁻¹, 30 mg L⁻¹, 35 mg L⁻¹, 40 mg L⁻¹, and 43 mg L⁻¹ were applied in coagulation of the DOM sample as shown in Figure 4.33. The most effective removal of organic matter was obtained using 35 mg L⁻¹ with a UV₂₅₄ removal efficiency of 75.14 %. According to

Figure 4.33, optimum doses of ferric chloride were found to be the same for UV₂₈₀, UV₃₆₅ and Color₄₃₆ as for UV₂₅₄. After reaching the optimum ferric dose of 35 mg L⁻¹, increasing the coagulant dose caused an increase in UV₂₅₄, UV₂₈₀, UV₃₆₅ and Color₄₃₆ measurements thus reduced the efficiency.

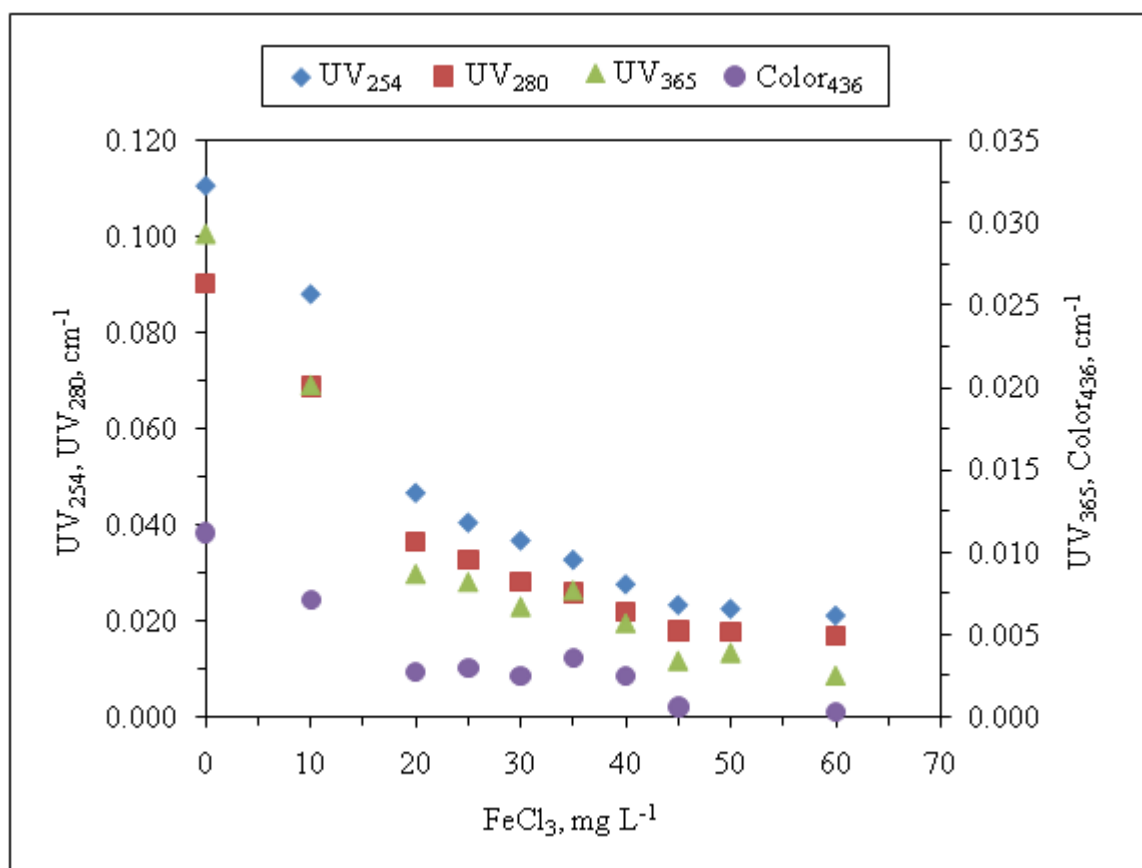


Figure 4.34. DOM removal by coagulation with ferric chloride at pH 6.5 based on UV-vis parameters.

At pH 6.5, 10 mg L⁻¹, 20 mg L⁻¹, 25 mg L⁻¹, 30 mg L⁻¹, 35 mg L⁻¹, 40 mg L⁻¹, 45 mg L⁻¹, 50 mg L⁻¹, 60 mg L⁻¹ ferric chloride doses were applied (Figure 4.34). The best removal of organic matter was obtained with 60 mg L⁻¹ with a UV₂₅₄ removal of 75.14 %. Optimum dose was determined to be 45 mg L⁻¹ of ferric chloride at pH 6.5 since increasing further the coagulant dose did not change the removal efficiency in a great proportion according to UV₂₅₄. The same trend was observed for UV₂₈₀. After the optimum dose of 45

mg L⁻¹ of ferric chloride, increasing the coagulant concentration dose did not change the removal rate for UV₃₆₅ and Color₄₃₆ measurements.

At pH 7.0, 10 mg L⁻¹, 20 mg L⁻¹, 25 mg L⁻¹, 30 mg L⁻¹, 35 mg L⁻¹, 40 mg L⁻¹, 45 mg L⁻¹, 50 mg L⁻¹, 60 mg L⁻¹, 70 mg L⁻¹, 80 mg L⁻¹ of ferric chloride doses were applied in coagulation tests (Figure 4.35). Optimum dose was obtained using 70 mg L⁻¹ of ferric chloride with an efficient DOM removal of 83% according to UV₂₅₄. Further increase in coagulant dose did not improved the removal rate in UV₂₅₄. UV₂₈₀, UV₃₆₅, and Color₄₃₆ results followed a similar line with optimum removal values of 70 mg L⁻¹ ferric chloride.

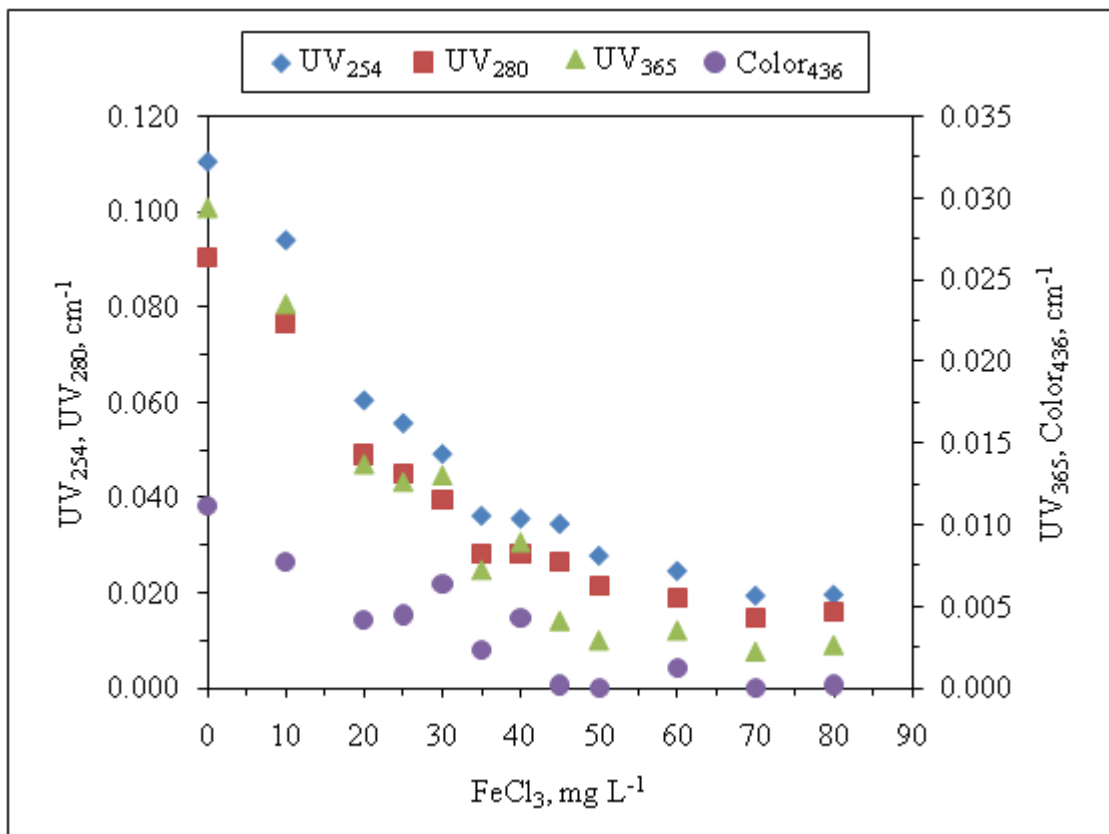


Figure 4.35. DOM removal by coagulation with ferric chloride at pH 7.0 based on UV-vis parameters.

4.2.3.2. Comparative Evaluation of pH Dependency for Coagulation with Ferric Chloride.

According to the determined optimum dose profiles at each pH between 5.5-7.0, the optimum pH for removal of organic matter in DOM sample with ferric coagulant could be

determined by comparing these profiles. For comparison purposes, the presented UV_{254} data at the studied pH values of coagulation (Figures 4.32-4.35) were selected and compiled in Figure 4.36. Optimum dose of ferric chloride for coagulation of the DOM sample decreased with decreasing pH similar to the removal characteristic revealed by coagulation of the DOM sample with alum. The smallest amount of optimum dose which is 15 mg L^{-1} of ferric chloride was obtained by coagulation of the DOM sample at pH 5.5 which is in agreement with the pH-dependent characteristics of ferric chloride reported in previous studies (Dempsey et al., 1984). The efficiency of organic matter removal in terms of UV_{254} using an optimum concentration of ferric chloride (15 mg L^{-1}) at pH 5.5 was 74 %.

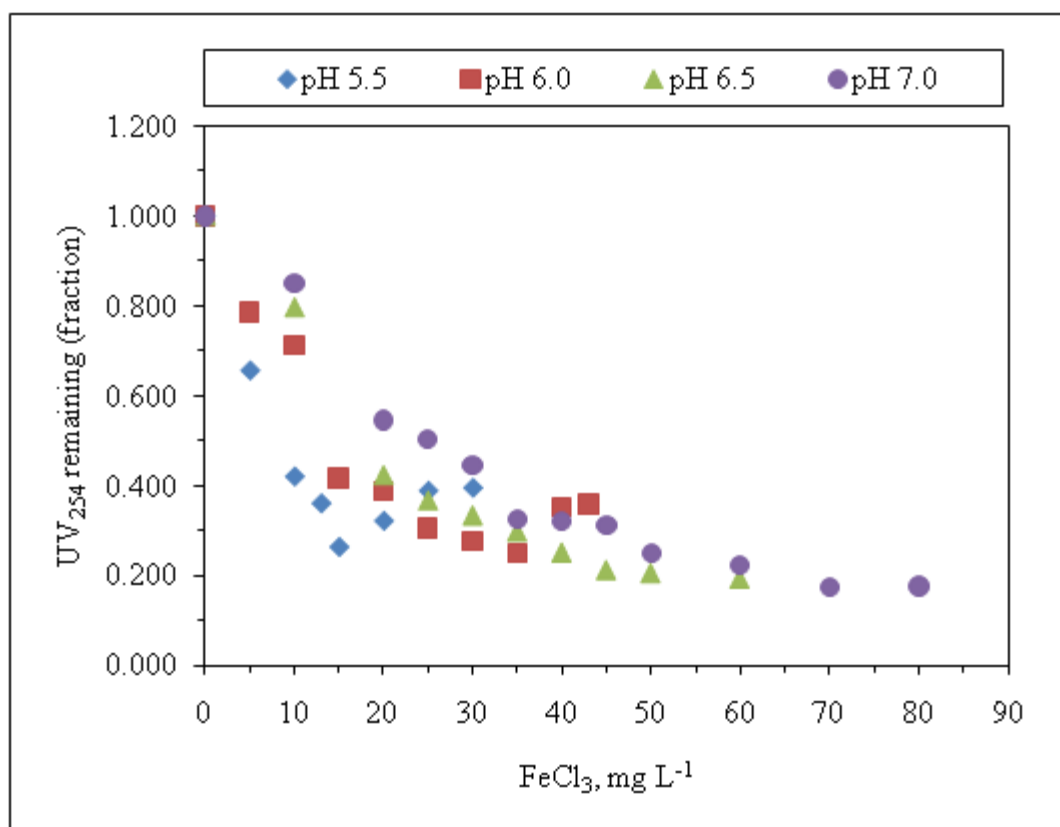


Figure 4.36. Comparison of DOM removal by coagulation with ferric chloride under varying pH conditions with respect to UV_{254} .

In addition to UV_{254} , comparison profiles of organic matter removal efficiency of ferric chloride in the DOM sample according to coagulation pH conditions were also

presented in terms of the other UV-vis parameters of UV_{280} , UV_{365} and $Color_{436}$ in Figures 4.37-4.39 to analyze the pH dependency of coagulation efficiency based on these parameters. UV_{280} comparison for coagulation with ferric in Figure 4.37 resembled to the comparison profile of UV_{254} in Figure 4.36 which was also true for comparisons given for coagulation with alum of these parameters. It could be concluded from these comparisons that coagulation efficiency with ferric chloride was more dependent on pH than it was with alum coagulant. It is obvious from the Figures 4.36-4.37 that at the highest pH, coagulation profile at pH of 7.0 the removal trends in UV_{254} and UV_{280} draw a top line above others between applied doses of 10-35 $mg L^{-1}$ of ferric chloride indicating that coagulation efficiency was lower in these doses at this pH (7.0) and it could only reach the optimum removal rates at higher coagulant doses of ferric chloride. However, an almost equal efficiency rate of organic matter removal could be gained by using lower doses of ferric chloride by adjusting the pH condition of coagulation to lower pH values i.e. 5.5 and 6.0 which provides averting from using excess doses of coagulant.

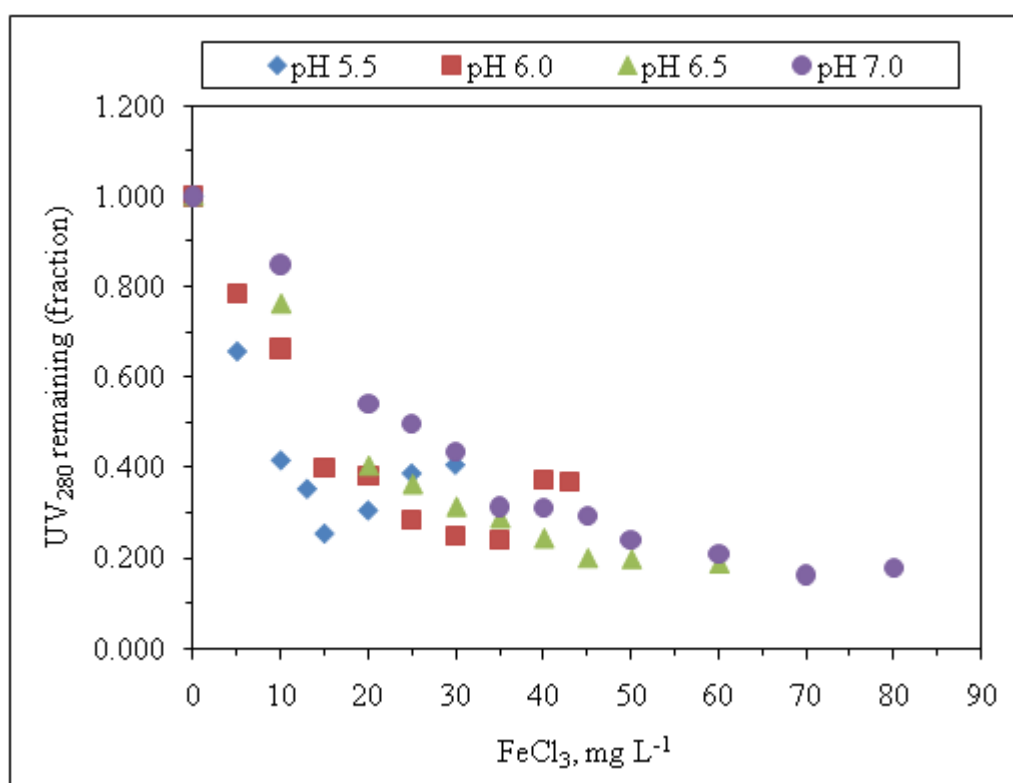


Figure 4.37. Comparison of DOM removal by coagulation with ferric chloride under varying pH conditions with respect to UV_{280} .

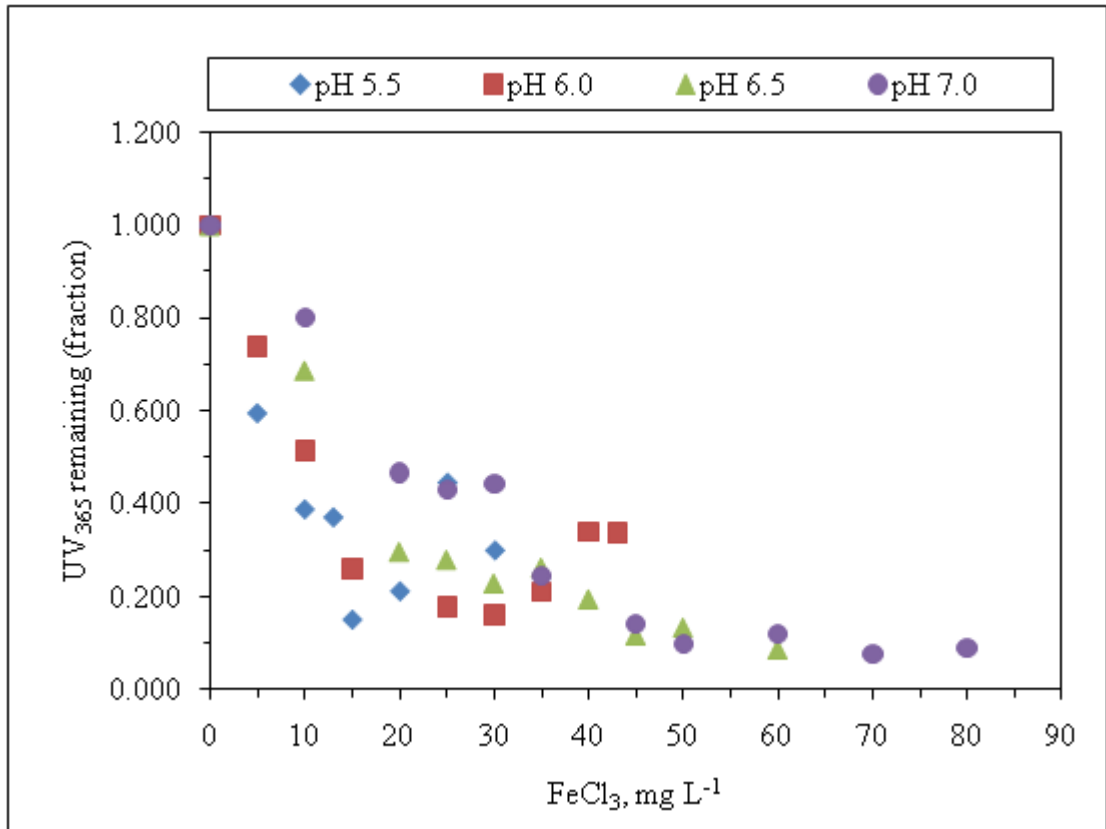


Figure 4.38. Comparison of DOM removal by coagulation with ferric chloride under varying pH conditions with respect to UV₃₆₅.

Comparisons for UV₃₆₅ and Color₄₃₆ measurements of pH-dependent coagulation profiles of the DOM_{conc} sample with ferric chloride were given in Figure 4.38 and Figure 4.39. At low pH conditions like 5.5 and 6.0, increasing the ferric dose in coagulation tests above the optimum dose at pH 5.5 and 6.0 caused a significant decrease in removal rates of UV₃₆₅ and Color₄₃₆ as well as UV₂₅₄ and UV₂₈₀ but with less amount of decreases. The same phenomenon was not observed for pH values of 6.5 and 7.0. In contrast, at high coagulant doses such as 70 mg L⁻¹ and 80 mg L⁻¹ at pH 7.0, further removal of organic matter was achieved based on all UV-vis parameters presented. At pH 6.5 the removal rates in these UV-vis parameters remained almost stable with an increase in ferric concentration used above the optimum dose as far as the range of the applied coagulant dose included in this study. In addition, the determined conditions for an optimum removal with ferric salt based on UV₂₅₄ was 15 mg L⁻¹ of ferric chloride applied at pH 5.5. This

determination holds true also with respect to the other UV-vis parameters of UV_{280} , UV_{365} , and $Color_{436}$ achieving a maximum removal on these conditions.

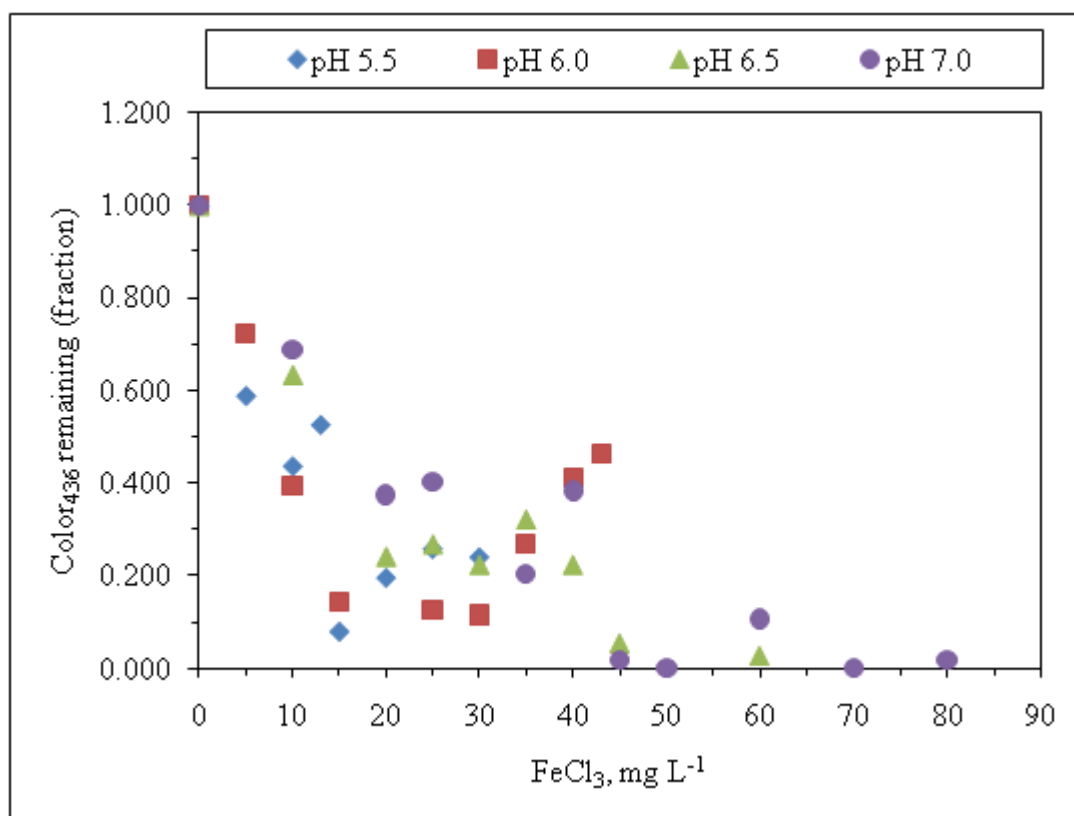


Figure 4.39. Comparison of DOM removal by coagulation with ferric chloride under varying pH conditions with respect to $Color_{436}$.

Comparison of dissolved organic carbon (DOC, $mg L^{-1}$) removal rates of coagulation with ferric chloride for all pHs of coagulation were presented in Figure 4.40. Taking into account DOC removal comparisons in Figure 4.40, DOC removal behaviour observed could be classified into two regions. At the top the removal data of pH 7.0 being far from the other pHs follows a linear decrease line in DOC by increasing ferric chloride concentration. Other points were clustered in the bottom indicating the high removal rates of DOC at 5.5, 6.0 and 6.5. An equal rate of DOC removal at pH 7.0 could be reached by using high doses of 70 and 80 $mg L^{-1}$. The data supported the effect of pH in using ferric chloride as reported in the literature by the differences in removal rates in lower pH values in comparison to removal efficiencies at higher pHs such that the DOC was mostly

removed in lower pH values by 91 %. The difference in DOC removal rate existed even between close pHs of 5.5 and 6.0 in the aspect that DOC removal efficiency achieved by 15 mg L^{-1} at pH 5.5 could only be reached in a higher dose such as 35 mg L^{-1} at pH 6.0. DOC removal efficiency was also better in using ferric chloride than the DOC removal using alum.

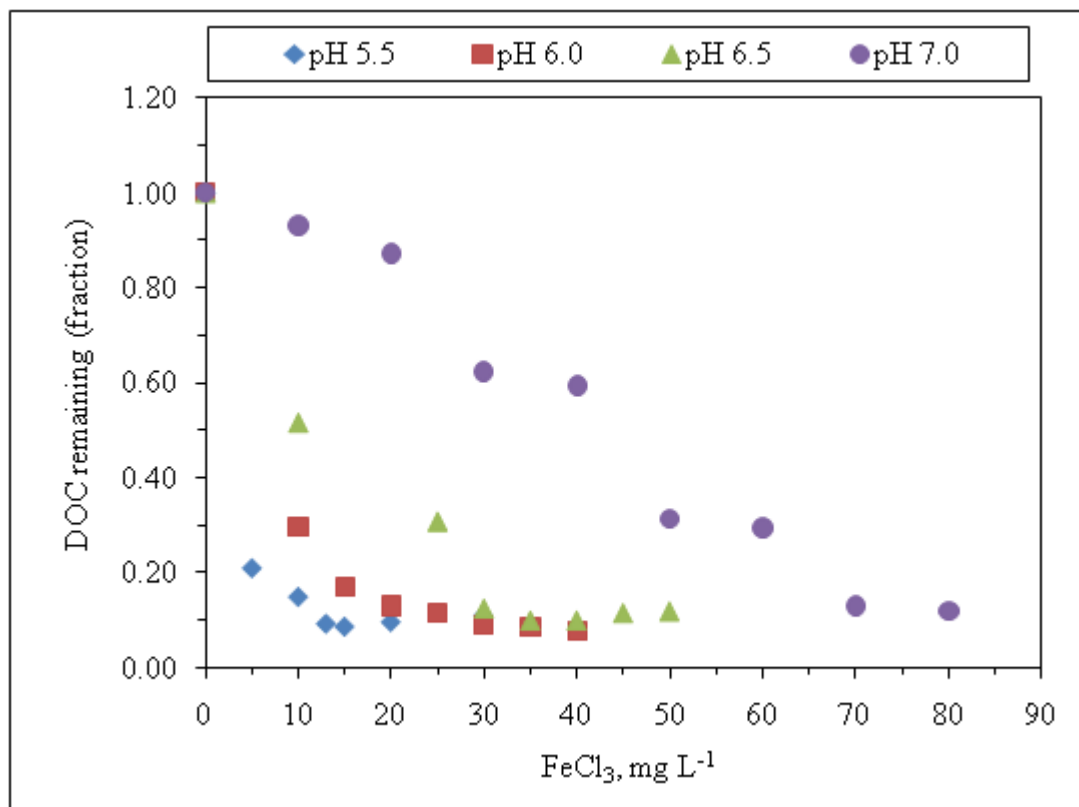


Figure 4.40. Comparison of DOM removal by coagulation with ferric chloride under varying pH conditions with respect to DOC.

Optimum coagulation with ferric chloride resulted in organic matter removal efficiency by 91 % of DOC removal and 74 % of reduction in UV_{254} . Based on the presented evaluations on the UV_{254} , UV_{280} , UV_{365} , $Color_{436}$ and DOC measurements, using 15 mg L^{-1} of ferric chloride at pH 5.5 is the optimum coagulation condition for the coagulation of the DOM sample with an high efficiency in removal of organic matter. For the optimum coagulation conditons with ferric chloride, dose dependent UV-vis spectra (Figure 4.41) between wavelengths 200-600 nm and fluorescence spectra of emission₃₅₀,

emission₃₇₀, synchronous measurements are given in the Figures 4.42-4.44. The related spectra at the other pH values of 6.0, 6.5, and 7.0 were given in Appendix D.

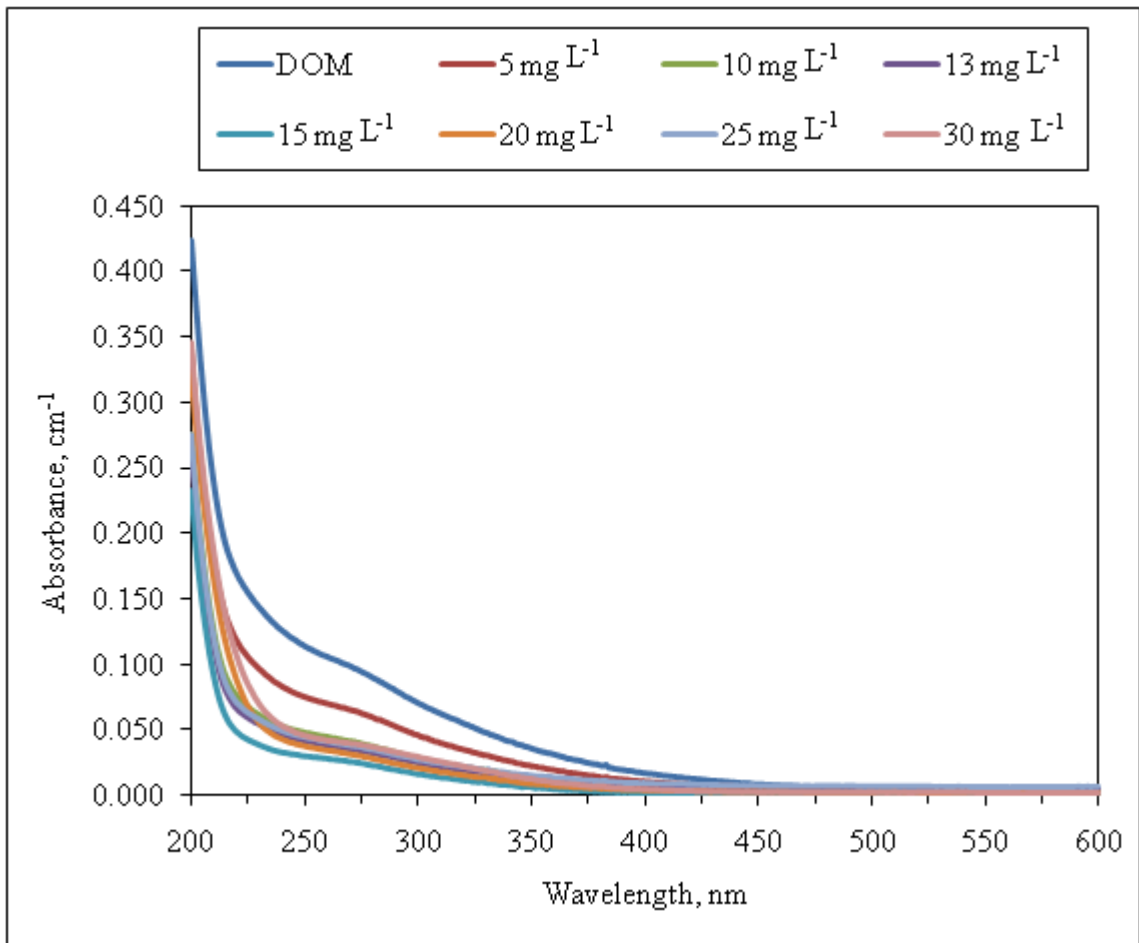


Figure 4.41. UV-vis spectra of the DOM sample after coagulation with ferric chloride at pH 5.5.

UV-vis spectra of all of the samples in Figure 4.41 showed a similar decreasing trend of the untreated DOM sample by means of coagulation with ferric chloride at pH 5.5. the UV-vis spectra at pH 5.5 revealed the information when compared with the pH 5.5 results of specified UV-vis parameters presented in Figure 4.32 (UV₂₅₄, UV₂₈₀, UV₃₆₅, Color₄₃₆) could all be used for the evaluation of the removal efficiency of coagulation with ferric chloride (Figure 4.41). It is clearly observed from the UV-vis spectra that after the optimum dose of 15 mg L⁻¹ ferric the spectra lines are very close to each other which could be concluded that the removal efficiency remained almost stable after the optimum dose.

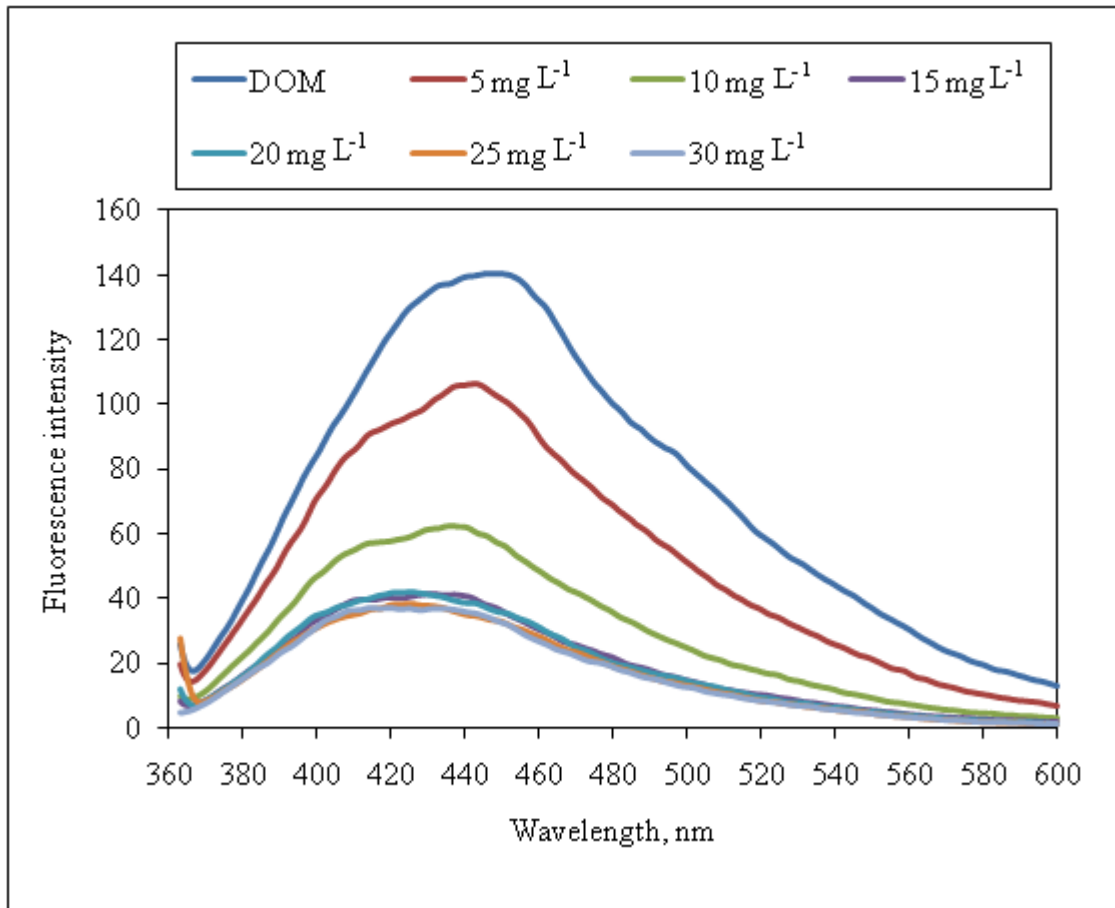


Figure 4.42. Fluorescence emission₃₅₀ spectra of the DOM sample after coagulation with ferric chloride at pH 5.5.

The fluorescence spectra in emission₃₅₀, emission₃₇₀, synchronous measurements supported the presented evaluations about the optimum conditions of ferric chloride determined (Figures 4.42-4.44). Emission₃₅₀, emission₃₇₀, synchronous spectra of untreated and coagulated DOM sample at pH 5.5 were in agreement with a remarkable decline in fluorescence intensity using 15 mg L⁻¹ ferric which is in accordance with the determination made to specify the optimum ferric dose for coagulation of the DOM sample. The spectra of the treated DOM sample with ferric concentrations higher than the optimum dose which are 20 mg L⁻¹, 25 mg L⁻¹, 30 mg L⁻¹ almost overlapped with the spectra of treatment with 15 mg L⁻¹ of ferric in emission₃₅₀ scan. In emission₃₇₀ the optimum and higher doses of ferric were similarly very close to each other except with a shift in maximum intensity of

coagulated DOM sample with the optimum dose (15 mg L⁻¹) to the lower wavelengths. The shift might have occurred because of the change in the structure of remaining functional groups leading a different fluorescence behavior in the coagulated sample after a high removal rate of organics was achieved by optimized coagulation. In synchronous, the spectra of the DOM sample increased at ferric doses higher than the optimum dose.

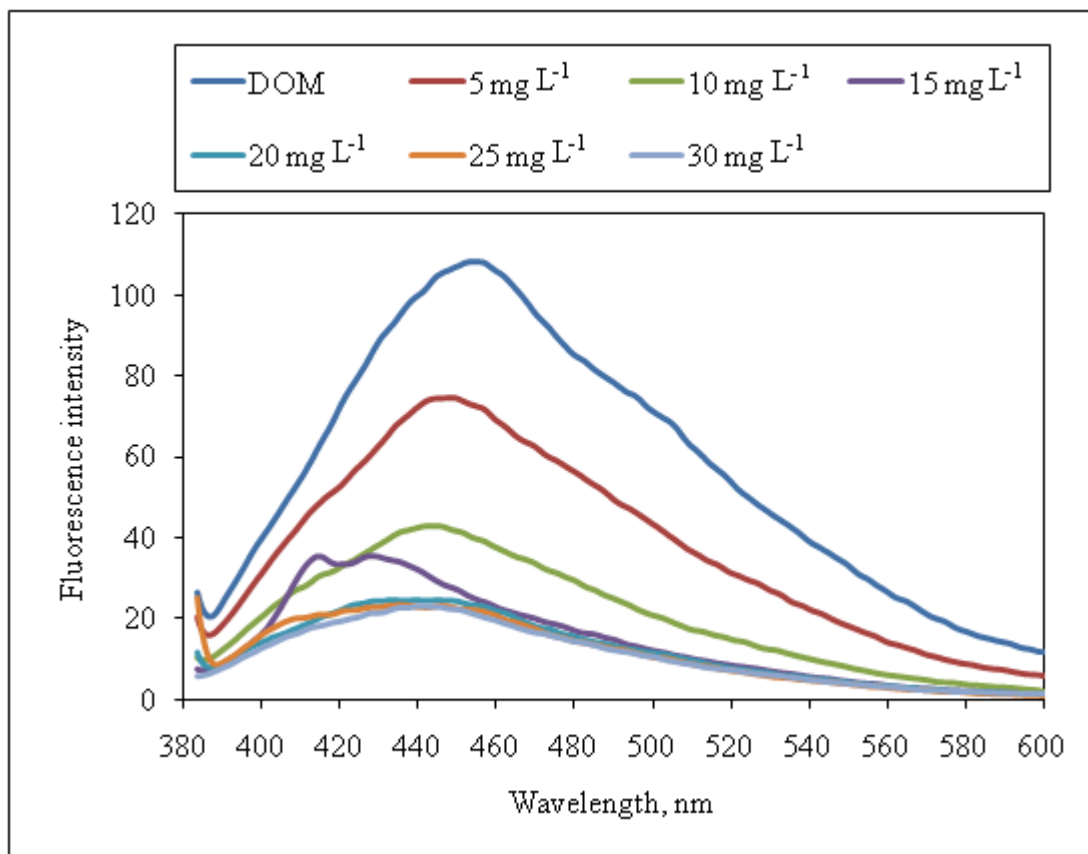


Figure 4.43. Fluorescence emission₃₇₀ spectra of the DOM sample after coagulation with ferric chloride at pH 5.5.

The characteristics of the DOM sample in fluorescence spectroscopy according to Emission₃₅₀, emission₃₇₀, synchronous were analyzed in detail in ‘Sample Specification’ part of the study. In addition, The wavelength ranges of peak intensity of coagulated DOM sample with ferric chloride in emission₃₅₀, emission₃₇₀, synchronous came out to be the same with those arrived by removal with alum. Coagulation of DOM sample with metal

salts of alum and ferric chloride seemed to result in similar results which could be concluded that an efficient removal of organics were achieved by using these coagulants.

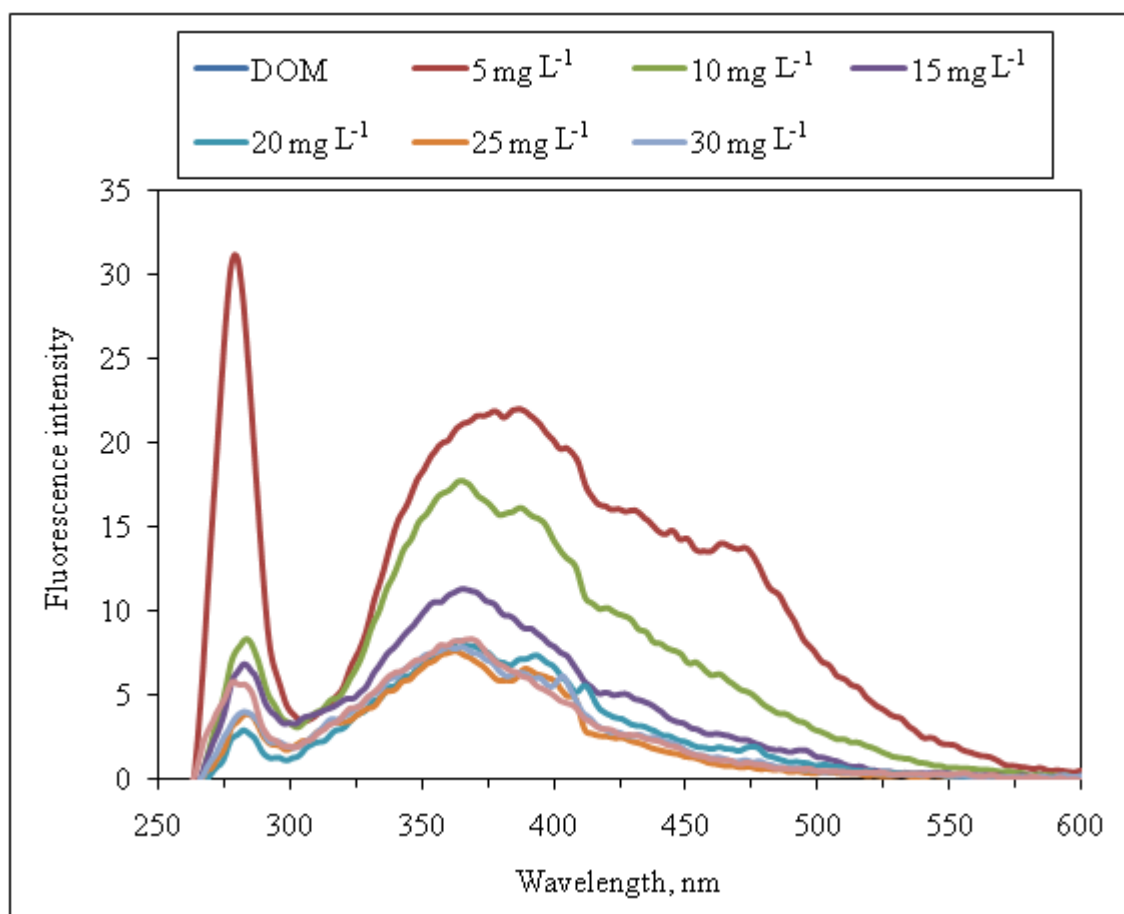


Figure 4.44. Fluorescence synchronous spectra of the DOM sample after coagulation with ferric chloride at pH 5.5.

Maximum fluorescence intensities of the DOM sample and coagulated DOM sample with the applied doses of ferric chloride varied between 5-30 mg L⁻¹ were compared in Figure 4.45. Untreated DOM sample had the highest intensity in emission₃₅₀, emission₃₇₀ and synchronous scans than the coagulated samples. In general, maximum intensities were ordered as $FI_{\text{emission350}} < FI_{\text{emission370}} < FI_{\text{synchronous}}$ for all of the samples. Fluorescence intensities for the DOM sample was 140 in emission₃₅₀, 108 in emission₃₇₀ and 31 in synchronous scan. Intensities were leveled off with treatment of 5 and 10 mg L⁻¹ of ferric chloride. Coagulation with an optimum dose of ferric chloride which was 15 mg L⁻¹

resulted in a decrease in the fluorescence intensity of the DOM sample to 41 in emission₃₅₀, 24 in emission₃₇₀, and 2 in synchronous scan. Maximum fluorescence intensities remained similar by the application of higher doses of ferric chloride.

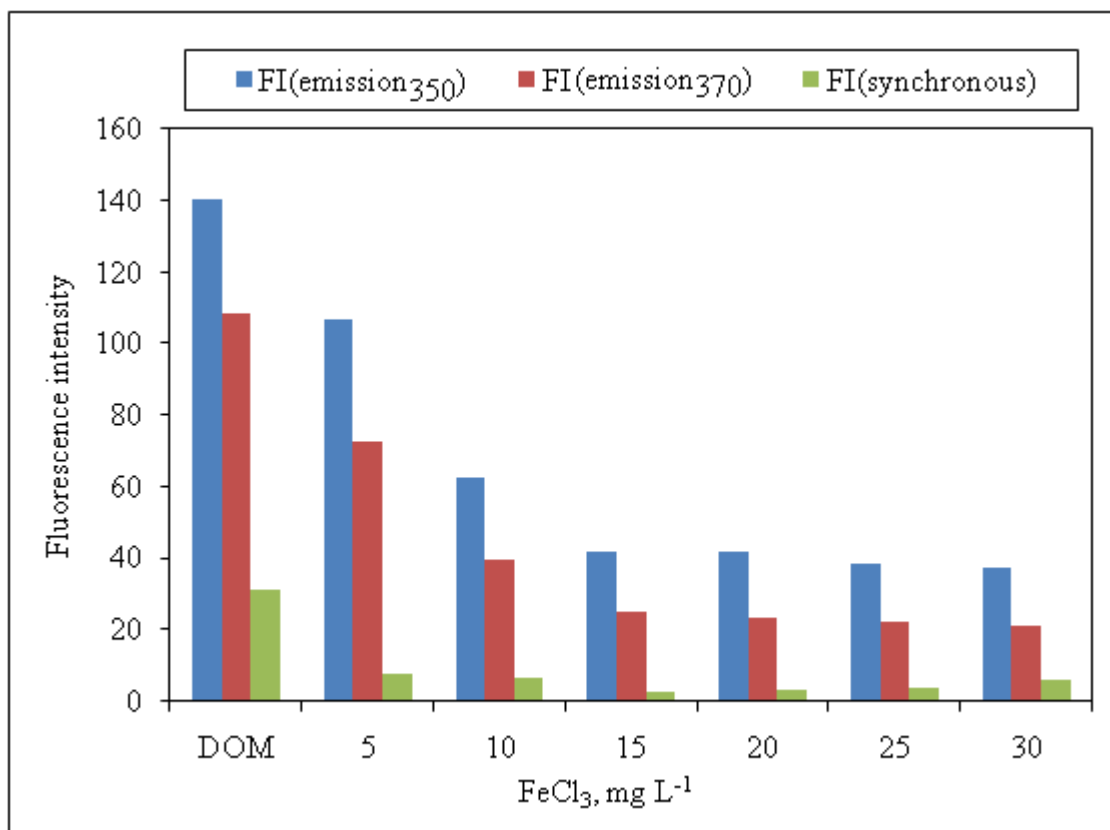


Figure 4.45. Comparison of the fluorescence intensities of the DOM sample after coagulation with ferric chloride at pH 5.5 in emission₃₅₀, emission₃₇₀ and synchronous scan modes.

The study of Jung and colleagues, providing useful findings on coagulation of NOM with ferric salt in surface waters at pH 8 and pH 6 using synthetic waters prepared with natural and synthetic humic acids was discussed herein to support the findings of the coagulation of the DOM sample with ferric chloride of the present study. The study also gave a useful insight into the destabilization mechanism of humic substances and NOM (Jung et al., 2005). They found at higher coagulant concentration the residual turbidity remained low but then increased strongly as the iron concentration was increased to higher doses than the optimum coagulant dose this is similar to the UV₂₅₄ results of this study

presented in Figures 4.32-4.35 in which UV_{254} increased after optimum coagulant dose when the pH was fixed. Especially at pH 5.5, a sudden increase was observed upon addition of more ferric salt could be because of the restabilization of the suspension. Dempsey and colleagues indicated the optimum pH falls within the 4.5–6.0 pH range for best removal of organic substances (Dempsey et al., 1984). Jung and colleagues found by coagulating a NOM sample from Moselle river water with iron at natural pH of 7.4 that the residual turbidity slightly reincreased above optimum coagulant concentration, and then decreased again at higher coagulant dosage. This phenomenon is similar to what observed at coagulation of the DOM sample at pH 7.0 and 6.5. Removal in UV_{254} were stabilized using higher doses of ferric chloride than the optimum dose and then using such high doses of 70 mg L^{-1} and 80 mg L^{-1} of ferric chloride led to an increase in UV_{254} removal at pH 7.0 (Figure 4.35). Evaluating the elemental ratio of N/C values it was suggested that NOM removal occurred in two main stages: up to optimum coagulant dose, a preferential coagulation of humic substances occurred, and above optimum coagulant dose the presence of proteinic matter in the coagulated sediment was indicated. Thus the restabilization above optimum dose was linked to the humic colloids in NOM sample of river water (Jung et al., 2005). Such a result is worthwhile to consider since more generally the hydrophobic fraction of NOM is reported to be more easily destabilized than hydrophilic compounds for e.g., proteinic matter in literature (Croué et al., 1993; Bose and Reckhow, 1998). The sample studied in this study namely the DOM sample contained also humic fractions in addition to algal organic matter. The determination of the optimum coagulant conditions could have resulted by the contribution of the reactivity properties of both humic acid and algal organic matter with ferric salt.

Different explanations were suggested for the relationship between the mechanism of NOM removal with iron salts and the effect of pH. It was often described as being complexation of Fe for pH values around 5 and adsorption of organic molecules on to Fe hydroxides at a pH of around 7 (Dempsey et al., 1984). Vilg -Ritter and colleagues suggested that pH and the nature of the NOM did not influence the Fe speciation or the level of complexation, but played a major role in the structuring of the flocs in the mechanism of NOM coagulation (Vilg -Ritter et al., 1999b). In the present study the removal of dissolved organic matter with ferric salt was based on the removal efficiency in

UV₂₅₄. There were distinct differences in the removal profiles between low pH values of 5.5, 6.0 and high pHs of 6.5, 7.0. Coagulation was more efficient in lower pH considering the less amount of dose of ferric coagulant used and high removal rate of organics. As a result, a pH dependent behavior was observed for the optimum coagulation conditions with FeCl₃ favored by low pH according to UV₂₅₄ in the removal of organics.

Coagulation of the DOM sample with ferric chloride resulted in a high removal efficiency of organic matter in terms of UV-vis parameters and DOC removal. Jarvis and colleagues studying on NOM removal in natural water samples by coagulation with ferric salt found similar results as high organic matter removal doses were obtained based on UV₂₅₄ and DOC by using similar ferric dose to the optimum ferric dose determined in the present study (Jarvis et al., 2006). Accordingly, UV₂₅₄ removal were found to be between 85 and 95% using coagulant dose of 8 mgL⁻¹ as Fe which was thus chosen to be the optimum coagulant dose in their study, while DOC removal efficiency was reported to be between 80 and 90% for ferric doses of 6 mg L⁻¹ Fe and above (Jarvis et al., 2006).

4.3. Coagulation Experiments Using Concentrated DOM (DOM_{conc}) Sample

In previous section, optimized coagulation profiles using alum and ferric chloride were assessed for dissolved organic matter removal in DOM sample. The optimum pH values determined for an optimized coagulation with alum and ferric chloride in coagulation of the DOM sample as pH:6.0 for alum and pH:5.5 for ferric chloride. In this part these formerly found optimum pH conditions specific to each coagulant used were employed such that coagulation with alum was performed only at the pH condition of 6.0, and coagulation with ferric chloride was performed only at the pH condition of 5.5 to investigate the optimum coagulant doses of these two coagulants for DOM removal in a concentrated dissolved organic matter sample that was called “the DOM_{conc} sample”.

Coagulation tests were firstly carried out to find the pH-dependent optimum coagulant dose profiles in batch of 50 mL sample size using alum and ferric chloride with the same jar test procedure used in the previous coagulation applications of the study. In this section, optimum coagulant doses were determined using the DOM_{conc} sample at previously

determined optimum pH values for each of the coagulant for dissolved organic matter removal namely coagulation with alum at pH 6.0, and coagulation with ferric chloride at pH 5.5.

4.3.1. Sample Specification for the DOM_{conc} Sample

The characteristics of the filtered DOM_{conc} water sample through 0.45 µm Millipore membrane filter was given in Table 4.3.

Table 4.3. Physico-chemical characteristics of the DOM_{conc} sample

Parameter	
UV ₂₅₄ , cm ⁻¹	0.5292
DOC, mg L ⁻¹	52.15
SUVA ₂₅₄ , L mg ⁻¹ m ⁻¹	1.0148
SUVA ₃₆₅ , L mg ⁻¹ m ⁻¹	0.1691
SCoA, L mg ⁻¹ m ⁻¹	0.0458
pH	8.7
Turbidity, NTU	10
Alkalinity, mg CaCO ₃ L ⁻¹	128.1
Hardness, mg CaCO ₃ L ⁻¹	58.07

The DOC content of the DOM_{conc} sample was found to be distinctly high when compared to the DOC concentration of the DOM sample (20.5 mg L⁻¹) and DOC found in natural waters. The UV₂₅₄ (0.5292 cm⁻¹) and SUVA₂₅₄ (1.0148 L mg⁻¹ m⁻¹), SUVA₃₆₅

(0.1691 L mg⁻¹ m⁻¹), SCoA₄₃₆, (0.0458 L mg⁻¹ m⁻¹) values were also considerably high relative to the DOM sample (UV₂₅₄: 0.1106 cm⁻¹, SUVA₂₅₄: 0.5395 L mg⁻¹ m⁻¹, SUVA₃₆₅: 0.1434 L mg⁻¹ m⁻¹ SCoA: 0.0546 L mg⁻¹ m⁻¹). The pH and alkalinity values were also higher than those of the DOM sample, hence represent how these parameters changed as the number of algae and thus organic content increased in an aged sample of algal organic matter. Under higher alkalinity–hardness conditions pH should be adjusted to slightly more acidic values independent from the utilised coagulant. These properties would certainly lead to a reliable assessment of the molecular size fractionation of the untreated and treated DOM_{conc} samples via coagulation with alum and ferric chloride by the application of the spectroscopic methods as well as DOC determination.

The DOM_{conc} sample was high in DOC (Table 4.3). Shin and colleagues found for waters high in turbidity and/or DOC, results for the removal of both settled and filtered turbidity were quite similar, so that conventional jar tests could be useful in determining the appropriate high coagulant doses for the conventional treatment plants needed for these waters (Shin et al., 2008). With a similar approach, all the tests were applied after filtering the sample through 0.45 µm Millipore membrane filter.

The values of UV₂₅₄ and DOC of the DOM_{conc} sample indicate a different water quality property because of its low UV₂₅₄ but high DOC content when compared to some natural waters for e.g., 7.6 mg L⁻¹ of DOC and 0.361 cm⁻¹ of UV₂₅₄ values given for a soft raw water collected from a surface water reservoir source (Jarvis et al., 2005). This characteristic of DOM_{conc} sample could be related to its chemical content and properties of algal organic matter having different absorption properties in UV-vis spectroscopy.

As NOM properties vary from source to source, characterization of the DOM_{conc} sample could be enhanced by assessing its optical properties in terms of UV-vis absorption and fluorescence intensity measurements as suggested in literature. Vecchio and Blough suggested that the absorption and emission spectra of natural organic matter could not result solely from a simple summation of the spectra of numerous electronically isolated chromophores (Vecchio and Blough, 2004). Supporting this suggestion, Boyle and colleagues found that the optical properties of humic substances were proposed to result in

part from intramolecular charge-transfer interactions between hydroxy-aromatic donors and quinoid or other acceptors formed by the partial oxidation of lignin precursors (Boyle et al., 2009).

Water quality of the DOM_{conc} sample were presented by UV-vis spectra between 200-600 nm and fluorescence spectroscopy measurements in emission₃₅₀, emission₃₇₀ and synchronous scan modes in Figures 4.46-4.49. Together with the DOM_{conc} sample, UV-vis spectra of the DOM sample which was used in optimized coagulation experiments Aldrich Humic Aldrich Humic Acid (AHA), Fluka Humic Acid (FHA) and Nordic Humic Acid (NHA) were presented for comparison purposes. Humic samples exhibited a featureless increase in absorbance with decreasing wavelength as expected (Chin et al., 1994).

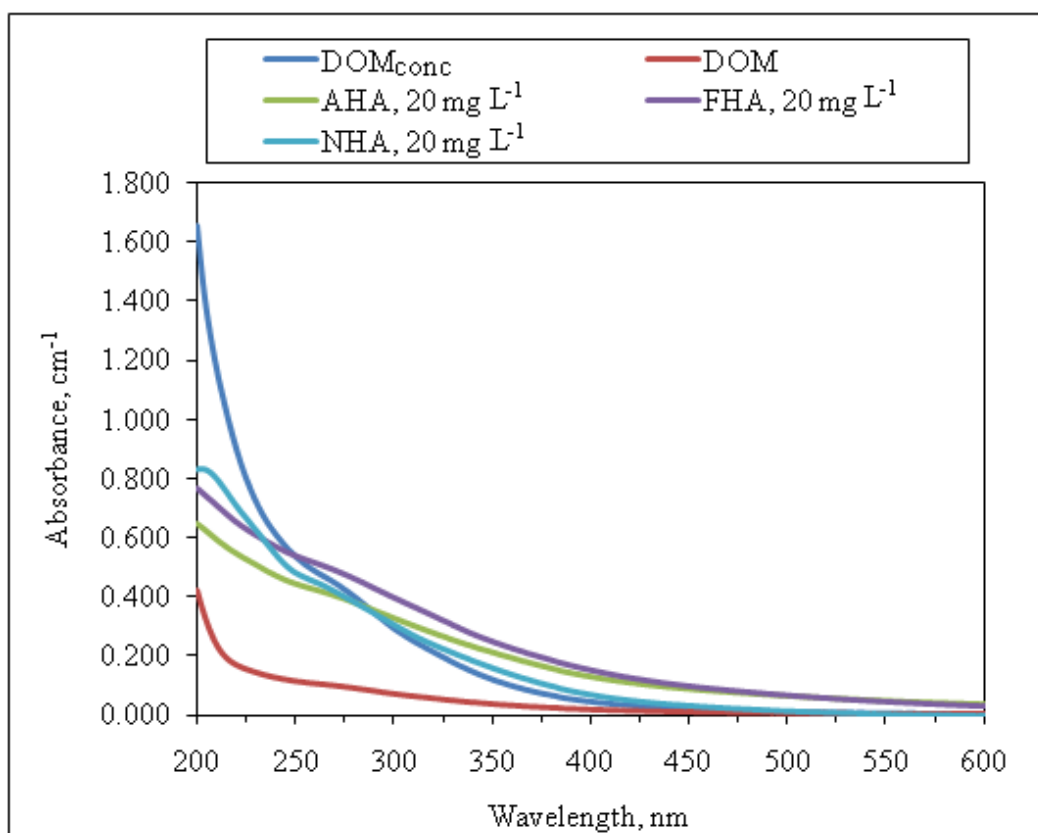


Figure 4.46. UV-vis spectra of the DOM_{conc} sample, DOM sample, Aldrich Humic Acid (AHA), Fluka Humic Acid (FHA) and Nordic Humic Acid (NHA).

According to Figure 4.46, the samples displayed different trends in terms of absorbance values at the same wavelength and in terms of the rate of increase in absorbance toward lower wavelengths. In contrast to the DOM_{conc} sample and the DOM sample, increasing rate of absorbance versus decreasing wavelength for the given humic acid samples of AHA, NHA, FHA are almost constant as their spectrum appeared more like linear. When compared with the DOM sample in UV-vis spectra, the DOM_{conc} sample exhibited an exponential increase similar to the DOM sample from 600 to 200 nm with higher absorbance values nearly four-fold of the absorbance values of the DOM sample. In Figure 4.46 while Fluka Humic Acid had the highest absorption above other samples between 250-475 nm, in the wavelength range from 250 to 200 nm, the spectrum of the DOM_{conc} sample increased in a higher rate than FHA and above all other samples reaching a highest value of 1.6555 cm⁻¹ at 200 nm. Humic acids given showed similarity among themselves in their behavior of spectra lines and close absorbance values. In conclusion, UV-vis spectroscopy revealed the differences between given samples depend on the absorbance wavelength and kind of the natural organic matter concerning the comparison given between the DOM_{conc} sample, the DOM sample, and humic acid samples of AHA, FHA, and NHA. Although the DOM_{conc} sample had a very similar absorbance at a wavelength of 254 nm to 20 mg L⁻¹ of AHA (UV₂₅₄ = 0.4373 cm⁻¹), FHA (UV₂₅₄ = 0.5292 cm⁻¹) and NHA (UV₂₅₄ = 0.4690 cm⁻¹), its spectrum behavior between 200-600 nm was in fact different from the given humic acid samples.

Fluorescence measurements of the DOM_{conc} sample, the DOM sample, Aldrich Humic Acid (AHA), Fluka Humic Acid (FHA) and Nordic Humic Acid (NHA) in emission₃₅₀, emission₃₇₀ and synchronous scan modes were presented in Figures 4.47-4.49 to compare the fluorescence characteristics of DOM_{conc} sample with the DOM sample and humic acids which are an important fraction of NOM found in natural waters. Fluorescence spectroscopy is a useful tool to differentiate between the different fractions of NOM in characterization of natural organic matter. Two distinct classes of fluorophores were generally discussed in literature that were called the humiclike fluorophores and the proteinlike fluorophores. Proteinlike fluorophores were reported to be in the emission range of lower wavelengths for e.g., 300-320 nm, 320-350 nm, and humiclike fluorophores were found to be in the emission range of relatively higher wavelengths like 420-480nm,

380-480 nm (Leenheer and Croué, 2003). Humic-type molecules are thought to be largely responsible for the fluorescence observed in natural waters since fluorophores found in NOM are often humic-type molecules (Leenheer and Croué, 2003).

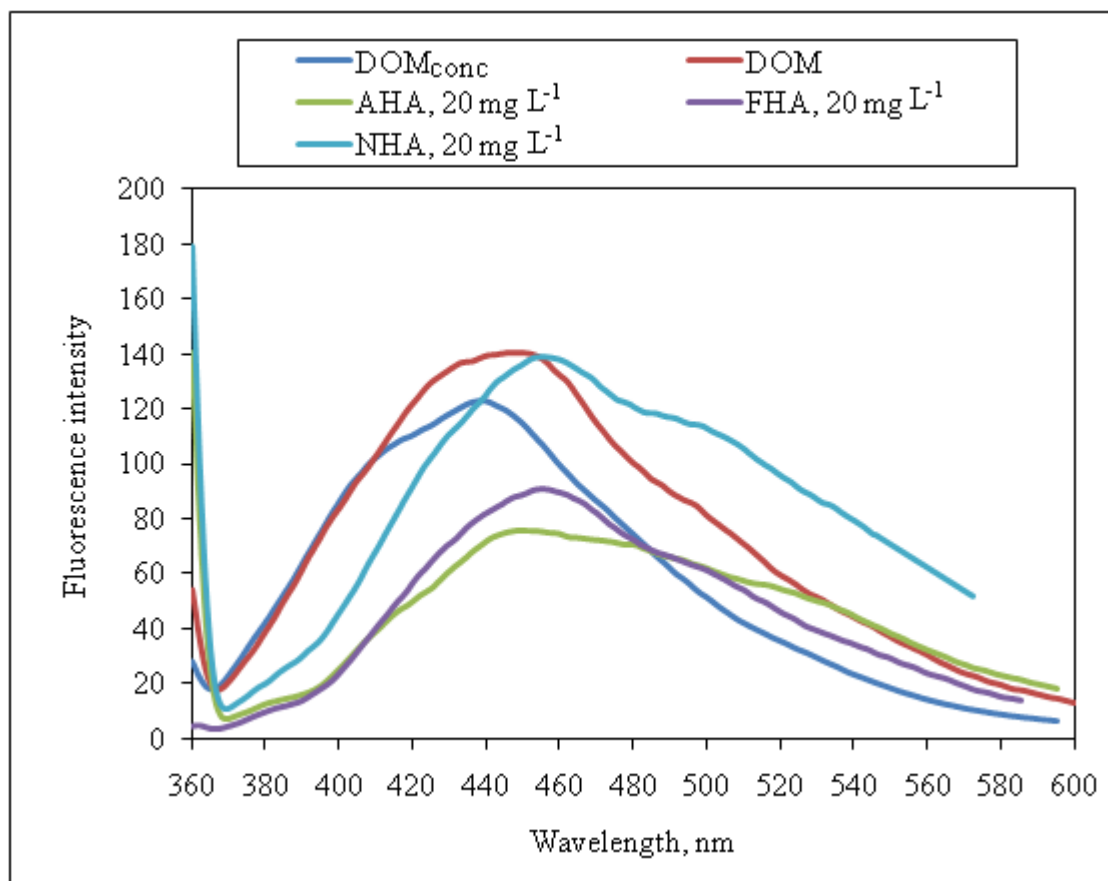


Figure 4.47. Fluorescence emission₃₅₀ spectra of the DOM_{conc} sample, DOM sample, Fluka Humic Acid (FHA) and Nordic Humic Acid (NHA).

Comparison of the dissolved organic matter samples in fluorescence emission₃₅₀ scan mode showed that the DOM_{conc} sample, the DOM sample, AHA, NHA, and FHA all exhibited a spectrum aligning in the wavelength range of 360-600 nm with a peak intensity around 440-460 nm. The DOM_{conc} and the DOM sample displayed similar spectra with a higher fluorescence intensity at a slightly higher wavelength of the latter that might occurred because of the Aldrich Humic Acid component of the DOM sample in a small concentration which did not exist in the DOM_{conc} sample (Figure 4.47).

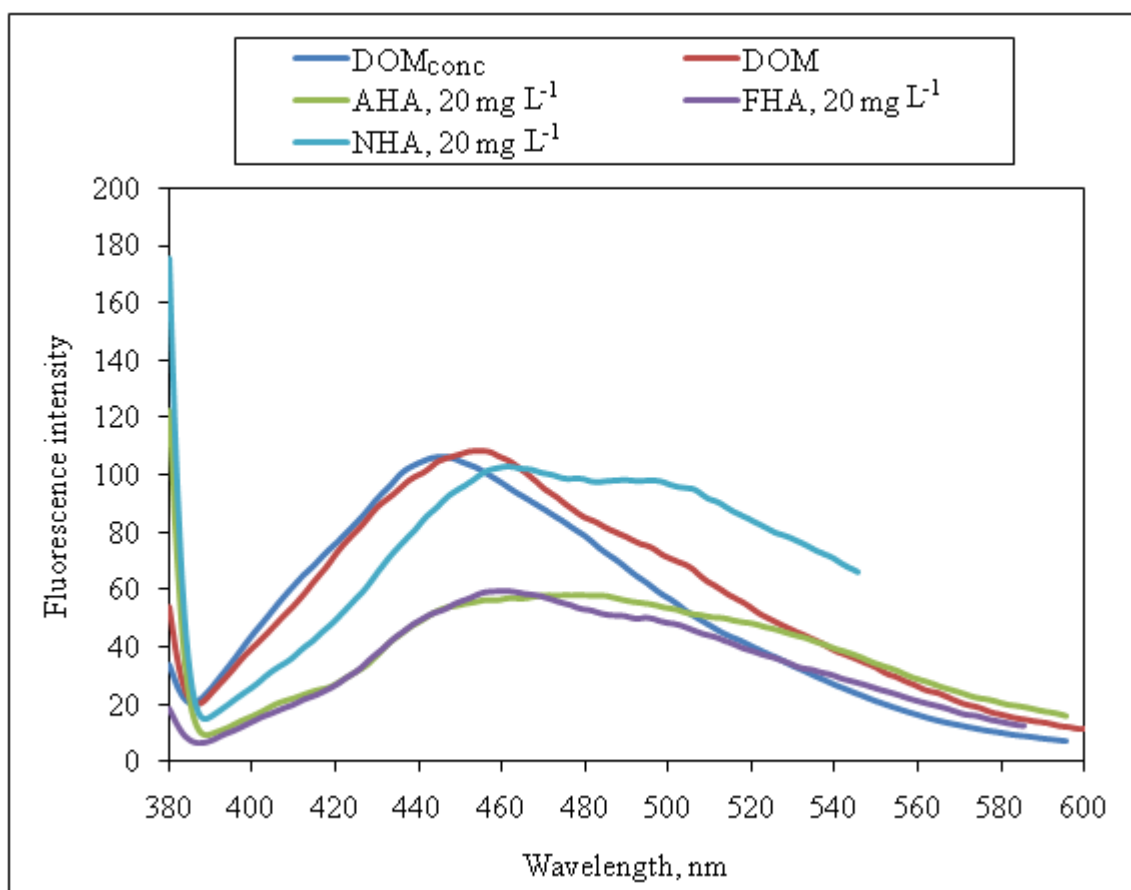


Figure 4.48. Fluorescence emission₃₇₀ spectra of the DOM_{conc} sample, DOM sample, Aldrich Humic Acid (AHA), Fluka Humic Acid (FHA) and Nordic Humic Acid (NHA).

Comparison in emission₃₇₀ ended up with a similar result as in the emission₃₇₀ scan with relatively lower intensities of the compared samples (Figure 4.48). Frimmel and Abbt-Braun, figured out a similar profile to those given in Figure 4.47 and Figure 4.48 while studying with a fulvic acid sample originally isolated from a natural water sample that had a dissolved organic carbon (DOC) amount of 5 mg L⁻¹ at neutral pH showing a peak intensity around 450 nm in fluorescence emission scan (Frimmel and Abbt-Braun, 1999). Boyle and colleagues' findings on fluorescence of natural water samples support the presented results that reported a continuous shift of wavelength where maximum intensity occurred (λ_{max}) to shorter wavelengths with decreasing excitation wavelength over this emission range (Boyle et al., 2009). They further indicated the excitation at wavelengths <375 nm gave rise to a very broad emission that extended well into the red, encompassing

those wavelengths where emission was observed at all longer excitation wavelength ($\lambda_{ex} > 375$ nm) in emission spectra.

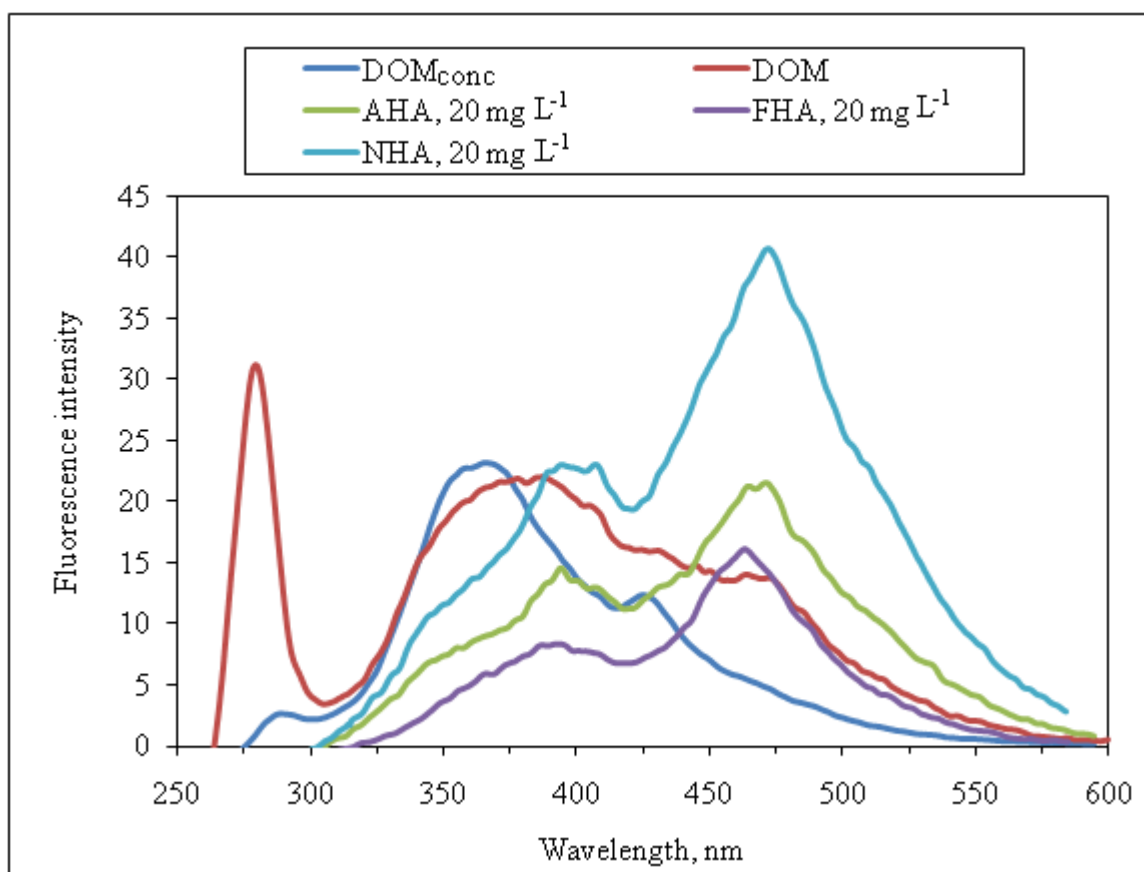


Figure 4.49. Fluorescence synchronous spectra of the DOM_{conc} sample, DOM sample, Aldrich Humic Acid (AHA), Fluka Humic Acid (FHA) and Nordic Humic Acid (NHA).

In synchronous scan mode, the high peak observed at 280 nm in the spectrum of the DOM sample did not appear in the DOM_{conc} sample as in the spectra of the humic acid samples of AHA, NHA and FHA. From 276 to 290 nm, DOM_{conc} sample followed a smooth increased up to an intensity of 2.6095, then after a small decrease to the wavelength of 301 nm the spectrum followed a continuous increase up to 366 nm (Figure 4.49). Between 354-375 nm, the DOM_{conc} sample had a broadened intensity peak in contrast to the humic acid samples of AHA, NHA and FHA that have a very sharp peak at higher wavelengths around 470 nm. In addition, at the wavelength range of 385-400 nm at

the left of the highest peak all the humic samples have a second smaller peak which was called by some researchers as a “shoulder” in the fluorescence spectrum. The small increase-decrease period of the DOM_{conc} sample at 276- 290 nm could be regarded as similar kind of secondary peak in synchronous spectra like those occurred in humic samples. This similarity might reveal the mutual or similar chemical properties such as humiclike fluorophores of the two kind of organic matter samples compared.

Peuravuori and colleagues found out that the fluorescence properties of the bulk of the conventional humic solutes were quite close to those recorded for the original DOM from natural water samples except in the case of the minor and most hydrophobic humic solutes (Peuravuori et al., 2002). Accordingly, characterization of the presented organic matter samples could be compared to evaluate the hydrophilic-hydrophobic structural similarities using fluorescence spectra. In the light of previous findings about the hydrophilic properties of humic substances it could be referred that DOM_{conc} and the DOM samples having more hydrophilic in nature than the AHA, NHA, and FHA humic acid samples.

As indicated previously, regarding to the optimum pH conditions determined as pH=6.0 for alum and pH=5.5 for ferric chloride for coagulation of the DOM sample, coagulation of the DOM_{conc} sample was performed by setting the pH conditions for alum as 6.0 and for ferric chloride as pH 5.5 in this part.

4.3.2. Coagulation of the DOM_{conc} Sample with Alum

Coagulation of the DOM_{conc} sample with alum coagulant for optimum removal of dissolved organic matter was presented in Figure 4.50. Coagulation with alum was performed at pH 6.0 by a series of jar tests in which alum doses were increased between 20 to 100 mg L⁻¹ to find the optimum alum dose for removal of dissolved organic matter in DOM_{conc} sample. According to UV₂₅₄ results in Figure 4.50, using 20 mg L⁻¹ of alum decreased the organic matter by 16 % of UV₂₅₄. Doubling of the coagulant dose to 40 mg L⁻¹ of alum resulted in a further reduction of organic matter with a UV₂₅₄ removal efficiency of 42 %. Using 70 mg L⁻¹ of alum caused a high reduction in UV₂₅₄ by 57 % of removal efficiency. Application of alum doses higher than 70 mg L⁻¹ in the concentrations

of 80 mg L⁻¹, 90 mg L⁻¹ and 100 mg L⁻¹ of alum in coagulation of the DOM_{conc} sample did not improve the organic matter removal rate in terms of the specified UV-vis parameters. According to this profile, optimum dose of alum was determined to be 70 mg L⁻¹ for a highest removal efficiency of dissolved organic matter in DOM_{conc} sample.

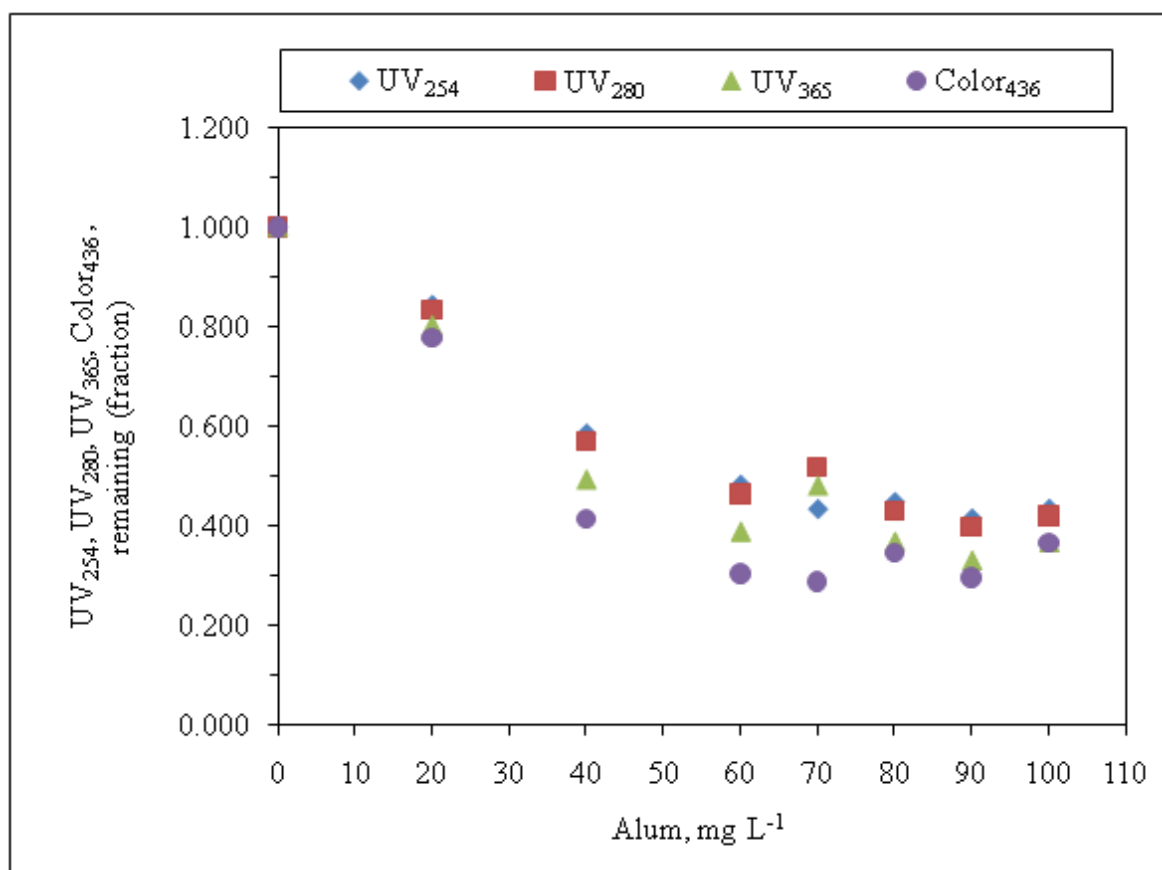


Figure 4.50. DOM_{conc} removal by coagulation with alum at pH 6.0 based on UV-vis parameters.

Removal profiles of UV₂₈₀, UV₃₆₅ and Color₄₃₆ showed a similar behavior to UV₂₅₄ removal in coagulation of the DOM_{conc} sample. In Figure 4.50, it was observed that UV₂₈₀ values matched to UV₂₅₄ values in all points of alum varying in x-axis showing the removal efficiency of coagulation with alum at these applied doses. UV₃₆₅ removal values followed just below those of UV₂₈₀ with a higher removal efficiency. The most efficient removal was gained in terms of Color₄₃₆ in all points. Applying 70 mg L⁻¹ of alum that was

determined to be the optimum dose for alum for the DOM_{conc} sample, 54 % of UV₂₈₀, 62 % of UV₃₆₅ 70 % of Color₄₃₆ removal rates were achieved.

Dissolved organic carbon (DOC) removal rates that were achieved by treatment of the DOM_{conc} sample by coagulation with alum at pH 6.0 by applied doses of alum between 20-100 mg L⁻¹ were presented in Figure 4.51. Applying 20 mg L⁻¹ of alum in coagulation of the DOM_{conc} sample resulted in a DOC removal efficiency of 35 %. Using 40 mg L⁻¹ of alum increased the DOC removal efficiency to 43 %. Using 60 mg L⁻¹ of alum dose resulted in 49 % of DOC removal. Highest removal efficiency of DOC in coagulation of the DOM_{conc} sample was 55 % that was achieved by applying 70 mg L⁻¹ of alum. Application of higher doses of 80 mg L⁻¹, 90 mg L⁻¹ and 100 mg L⁻¹ of alum did not improve DOC removal in the DOM_{conc} sample, and the same removal efficiency rate of 55 % stayed almost constant in applying these doses of alum.

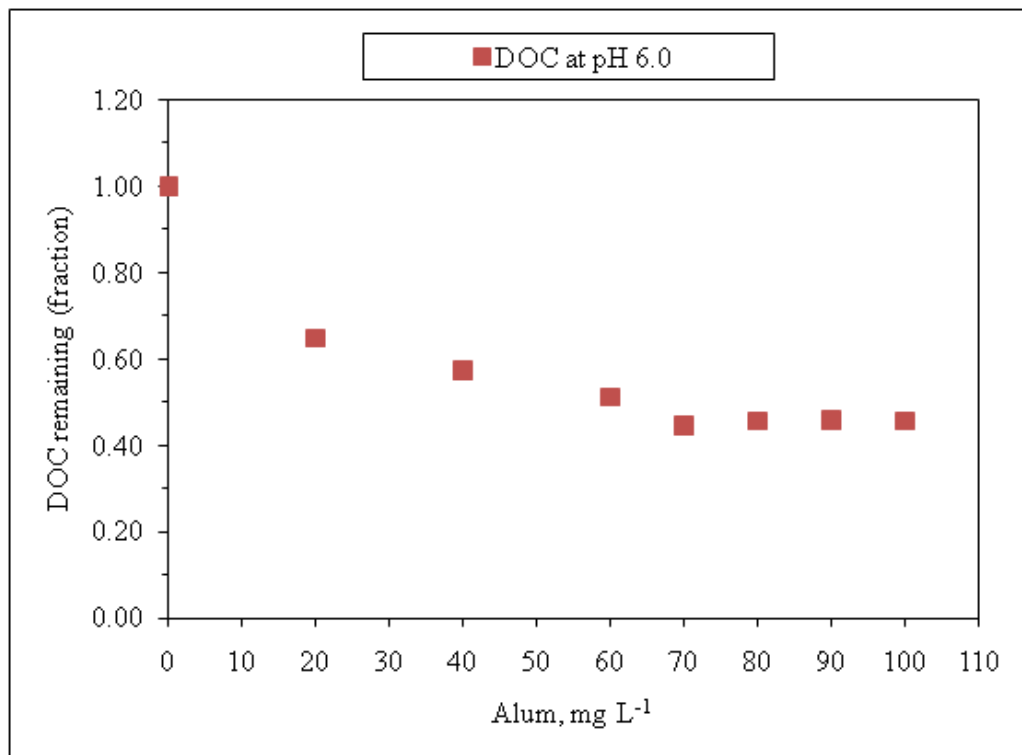


Figure 4.51. DOM_{conc} removal by coagulation with alum at pH 6.0 based on DOC.

When the results of the two parameters that were UV_{254} and DOC showing the organic matter removal efficiency in DOM_{conc} sample, coagulation of the DOM_{conc} sample was more successful with a small difference in decreasing UV_{254} than DOC. Using alum coagulant DOM removal efficiency was 55 % in terms of DOC, while it was 57 % in terms of UV_{254} . The conclusion was not the same for UV_{254} -DOC removal comparison in coagulation of the DOM sample using alum. In coagulation of the DOM sample highest UV_{254} removal efficiency (71 %) was achieved by applying 40 mg L^{-1} was left behind by a more efficient DOC removal with 89 % by applying 50 mg L^{-1} of alum. It can be concluded that coagulation performances in different samples were changed as the characteristics of the two dissolved organic matter samples changed both in terms of components of organic matter such as humic acid found in the DOM sample and in terms of amounts of moieties yielded higher results in the DOM_{conc} sample in UV_{254} and DOC.

In order to provide a more qualified data about changes in the DOM_{conc} sample when DOM removal was achieved by applying various doses of alum, the DOM_{conc} sample after coagulation with alum at pH 6.0 was also presented by UV-vis and fluorescence spectra. UV-vis spectra of the DOM_{conc} sample between 200-600 nm before and after coagulation with alum was given in Figure 4.52.

According to Figure 4.52, at higher wavelengths from 400 nm to 600 nm the absorbance values of all samples approached zero. Between 200-400 nm, absorbance values of the DOM_{conc} sample spectrum were comparable to coagulation spectra at different doses of alum applied to the DOM_{conc} sample. Accordingly, the spectrum of 20 mg L^{-1} of alum treatment came just below the raw DOM_{conc} sample which was followed below with the spectrum of 40 mg L^{-1} of alum treatment. Application of 60 mg L^{-1} and doses higher than that (70 mg L^{-1} , 80 mg L^{-1} , 90 mg L^{-1} , 100 mg L^{-1}) caused an overlapping view of the UV-vis spectra of the DOM_{conc} sample which could be concluded that organic matter removal efficiency did not increase significantly by using higher doses of alum in coagulation treatment of the DOM_{conc} sample.

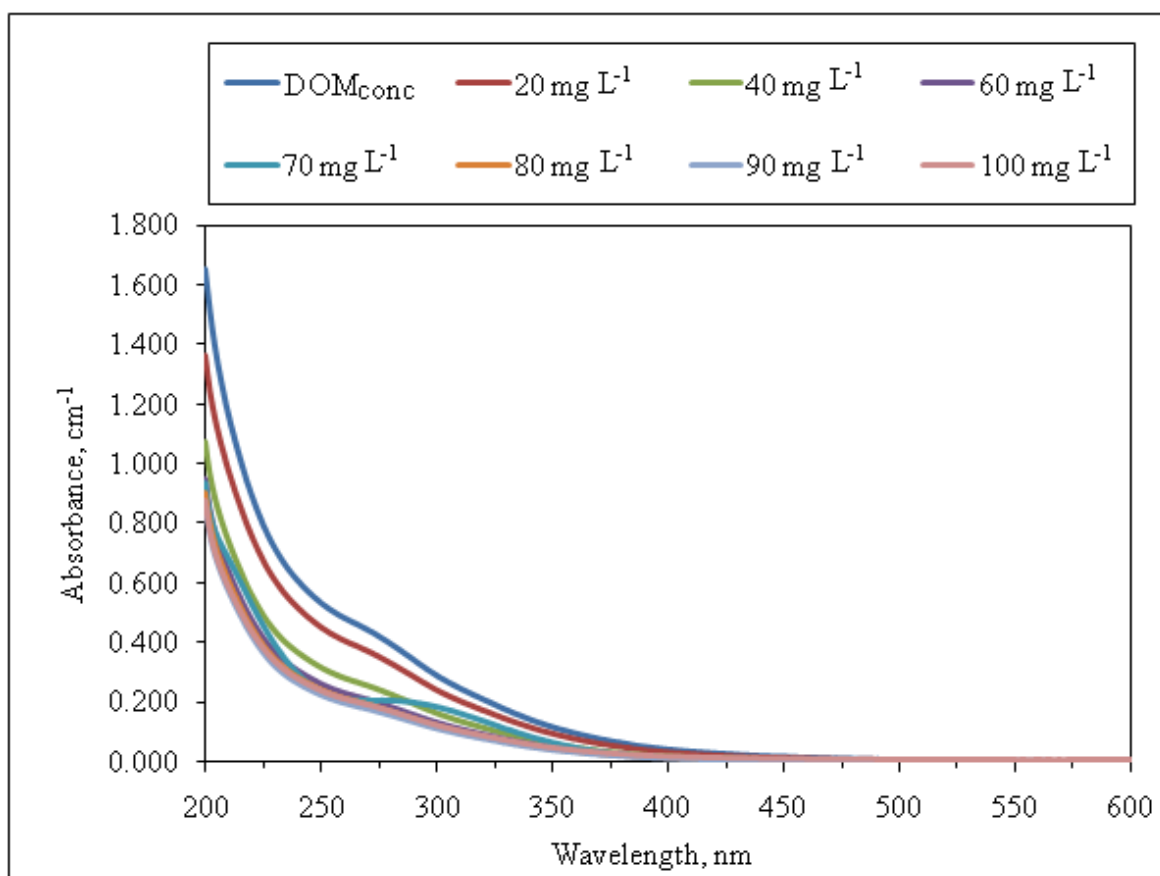


Figure 4.52. UV-vis spectra of the DOM_{conc} sample after coagulation with alum at pH 6.0.

The fluorescence spectra of the untreated and the coagulated DOM_{conc} sample in emission₃₅₀, emission₃₇₀, synchronous scan were presented in Figures 4.53-4.55. Emission₃₅₀, emission₃₇₀, synchronous spectra of untreated and coagulated DOM_{conc} sample at pH 6.0 were different from the presented coagulation results of the DOM sample in previous section. The fluoresce scan in emission and synchronous modes for the DOM_{conc} sample did not show a direct relationship with the applied coagulant concentration of alum versus maximum intensity. The maximum fluorescence intensity of the untreated DOM_{conc} sample occurred below the treated samples with alum in emission₃₅₀, emission₃₇₀, synchronous which was unlike the observed scheme in coagulation of the DOM sample. Treatment with concentrations higher than the optimum dose of 70 mg L^{-1} such as 80 mg L^{-1} , 90 mg L^{-1} , resulted in very close peak intensities except treatment with 100 mg L^{-1} of alum which lied below all the samples in emission and synchronous scans.

Measurement profiles in emission₃₅₀ and emission₃₇₀ were almost the same for coagulation of the DOM_{conc} sample with alum, both with a peak intensity around 440-460 nm.

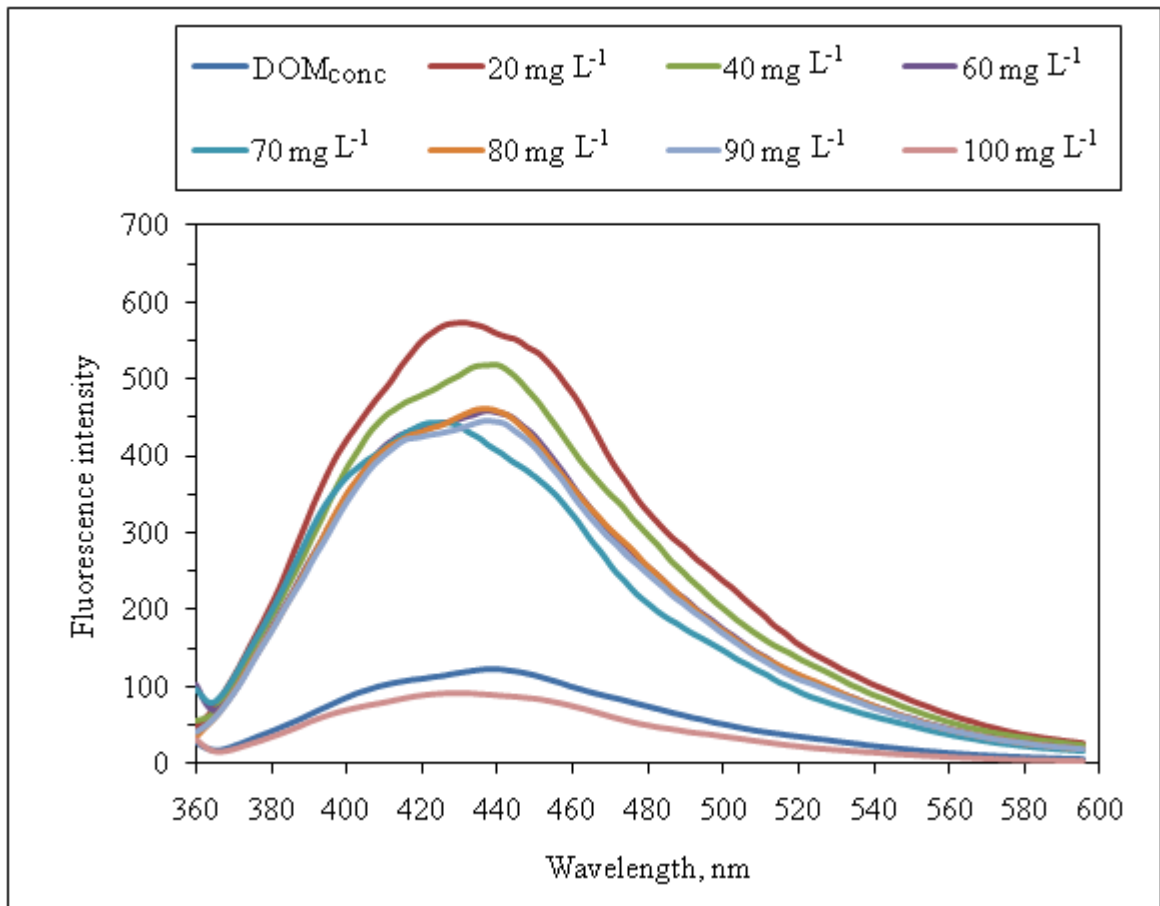


Figure 4.53. Fluorescence emission₃₅₀ spectra of the DOM_{conc} sample after coagulation with alum at pH 6.0.

In synchronous scan mode, two peaks of maximum intensity occurred at the wavelengths of 280 nm and 360 nm with a much higher maximum intensity than the small peak observed at 280 nm as shown in Figure 4.55. When compared with fluorescence results of the DOM sample after coagulation with alum, fluorescence analysis results for the DOM_{conc} sample after treatment with alum gave relatively much more higher fluorescence intensities in emission and synchronous scan measurements than those obtained in fluorescence measurements of the DOM sample after coagulation of with alum.

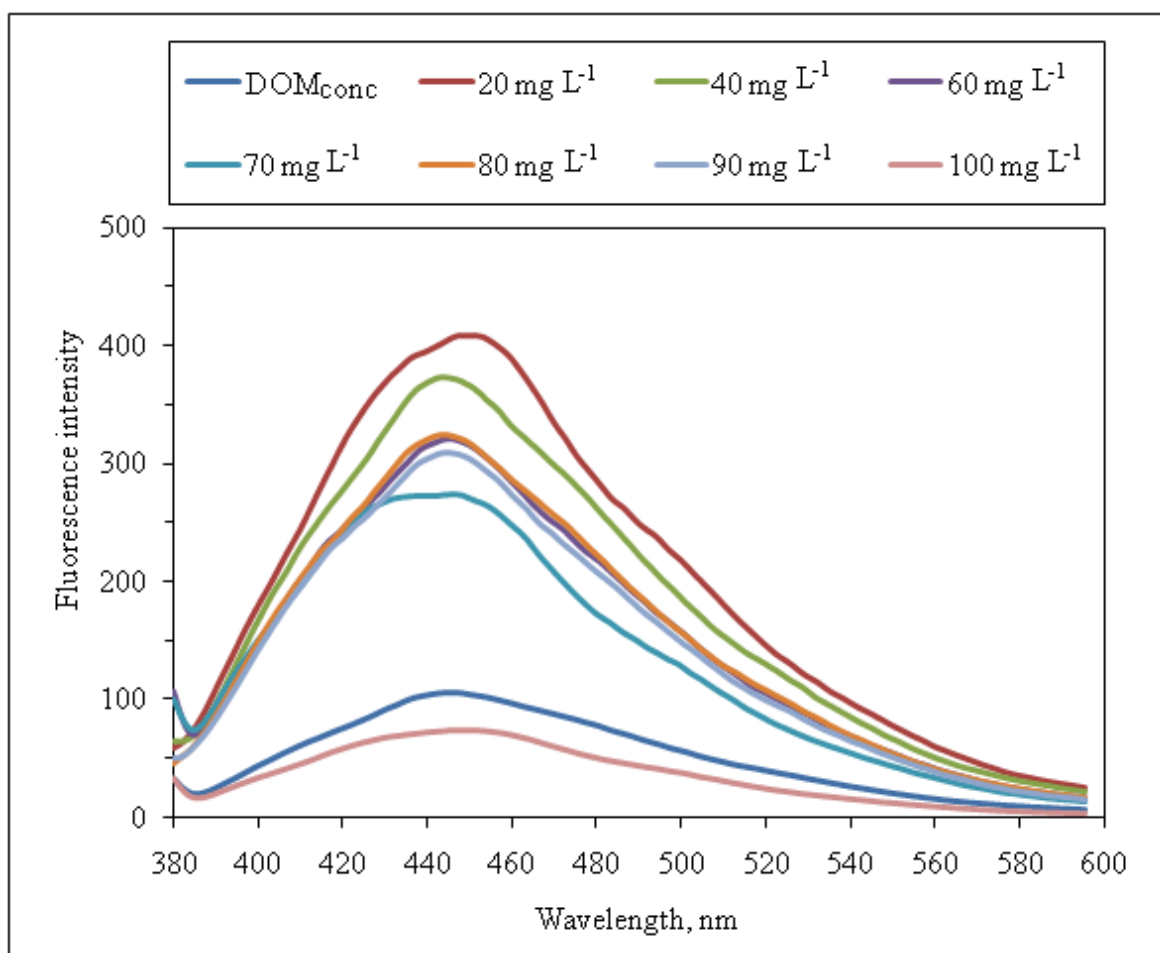


Figure 4.54. Fluorescence emission₃₇₀ spectra of the DOM_{conc} sample after coagulation with alum at pH 6.0.

Based on the fluorescence spectra for coagulation of the DOM_{conc} sample presented in Figures 4.53-4.55 in emission₃₅₀, emission₃₇₀ and synchronous scans it could be concluded that although the DOM sample and DOM_{conc} sample were similar in terms of dissolved organic matter content, differences between the DOM sample and DOM_{conc} sample in terms of dissolved organic matter components i.e. humic acid and algal organic matter in the DOM sample, a very high concentration of DOC in the DOM_{conc} sample, elemental composition of the DOM sample because of synthetic freshwater characteristics, and the coagulant concentration requirements for an optimum removal of organic matter could be the possible sources for the different behaviors of the DOM and DOM_{conc} samples in fluorescence spectroscopy. High alum coagulant demand required for the DOM_{conc} sample

may enhance the emergence of different chemical species of alum complexes resulting in a high fluorescence intensity.

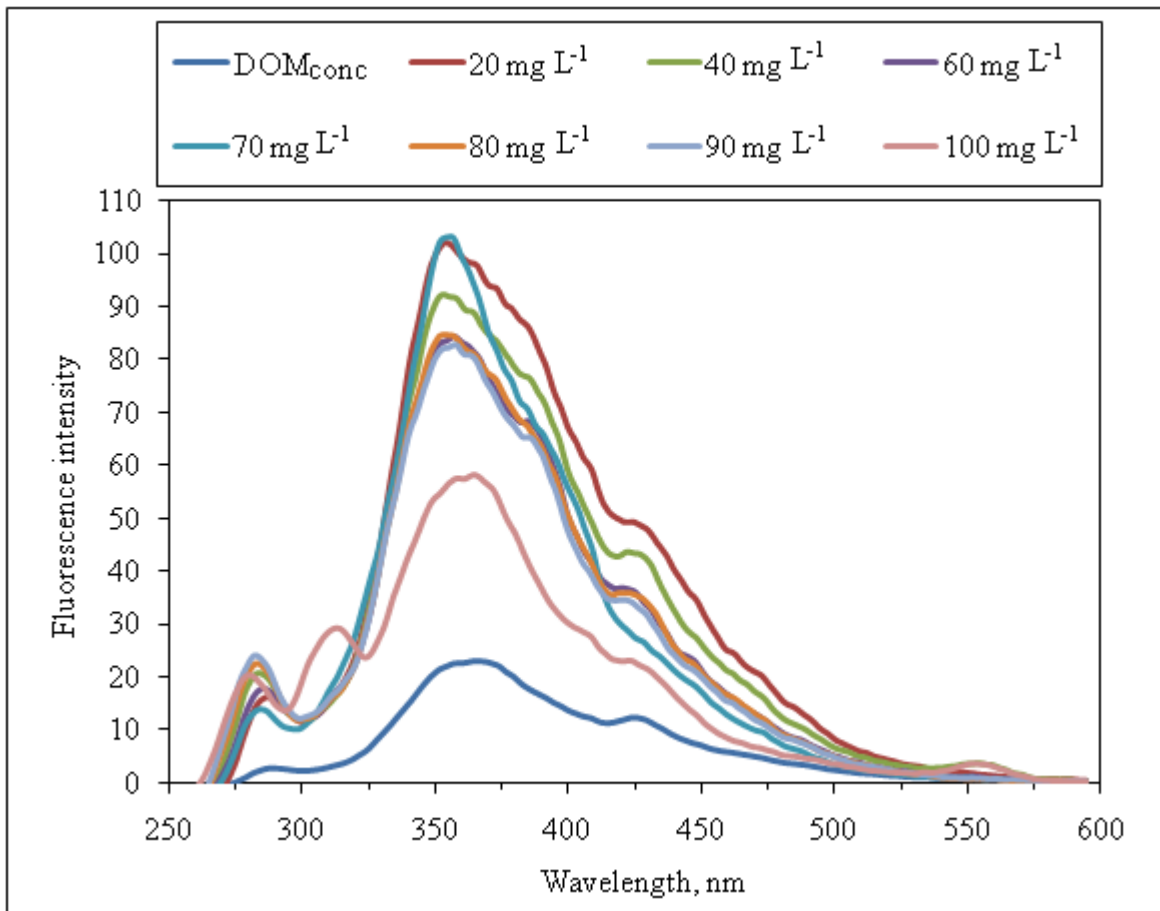


Figure 4.55. Fluorescence synchronous spectra of the DOM_{conc} sample after coagulation with alum at pH 6.0.

When alum dose requirements of the DOM sample and DOM_{conc} sample were compared, the concentration of alum increased to 70 mg L^{-1} alum for the DOM_{conc} sample while it was 40 mg L^{-1} of alum for the DOM sample considering an optimum removal of organics according to UV_{254} and DOC removed. In addition, a small increase in UV_{254} occurred by using high dosages of alum which were higher than the optimum dose the increase in UV_{254} thereby a decrease in organic matter removal efficiency may be because of charge reversal happened in these doses in water sample causing the restabilization of particles to occur. A similar finding was reported by Shin and colleagues indicating a

strong stoichiometric relationships between DOC and coagulant demand in coagulation of NOM with alum at pH 6.0 (Shin et al., 2008). They found a greater removal of NOM at pH 6.0 and a lower dose of alum was required to treat a unit mass of NOM than it was found at pH 7.0. At pH 6, the charge on the aluminum hydrolysis species was reported to be more positive and the charge on the NOM as less negative than at pH 7.0. resulting in a less coagulant requirement at pH 6.0 for the complexation, adsorption, and precipitation of NOM molecules. They further explained in the same context as the role of NOM as coagulation promoter i.e., the presence of NOM, or multivalent anions such as sulfate, promoted floc formation and growth, thereby preventing or suppressing the opportunity for charge reversal. They found the charge reversal occurred but was suppressed at pH 6.0 with the presence of NOM and was prevented entirely by NOM at pH 7, which was consistent with stronger negative charge of NOM at pH 7.0. (Shin et al., 2008).

4.3.3. Coagulation of the DOM_{conc} Sample with Ferric Chloride

Coagulation of the DOM_{conc} sample by using ferric chloride as coagulant at pH 5.5 for the purpose of optimum removal of dissolved organic matter was presented in Figure 4.56. Coagulation application was achieved by a serial of tests in which incremental additions of ferric chloride from 20 to 80 mg L⁻¹ were applied to find the optimum dose of ferric coagulant for removal of dissolved organic matter at pH 5.5 in the concentrated dissolved organic matter sample (Figure 4.56). At first, using 20 mg L⁻¹ ferric chloride reduced the UV₂₅₄ value by a removal efficiency of 44 %. An incremental increase of ferric chloride dose to 40 mg L⁻¹ caused a higher decrease in UV₂₅₄ with a removal efficiency of 88%. Then, by increasing ferric dose to higher than 40 mg L⁻¹ organic matter removal efficiency was this time not improved by using 50 mg L⁻¹ and 60 mg L⁻¹ of ferric. By further increase of ferric dose after 60 mg L⁻¹, a stepwise, high decrease in efficiency in terms of all the UV-vis parameters was observed, probably due to a restabilization occurred at each high dose of ferric application. According to this profile in Figure 4.56 that show organic matter removal performance of ferric coagulant in DOM_{conc} sample in terms of UV₂₅₄ UV₂₈₀, UV₃₆₅ and Color₄₃₆ removal, 40 mg L⁻¹ of ferric chloride was determined to be the optimum dose for an efficient removal of dissolved organic matter in the DOM_{conc} sample at a coagulation pH condition of 5.5.

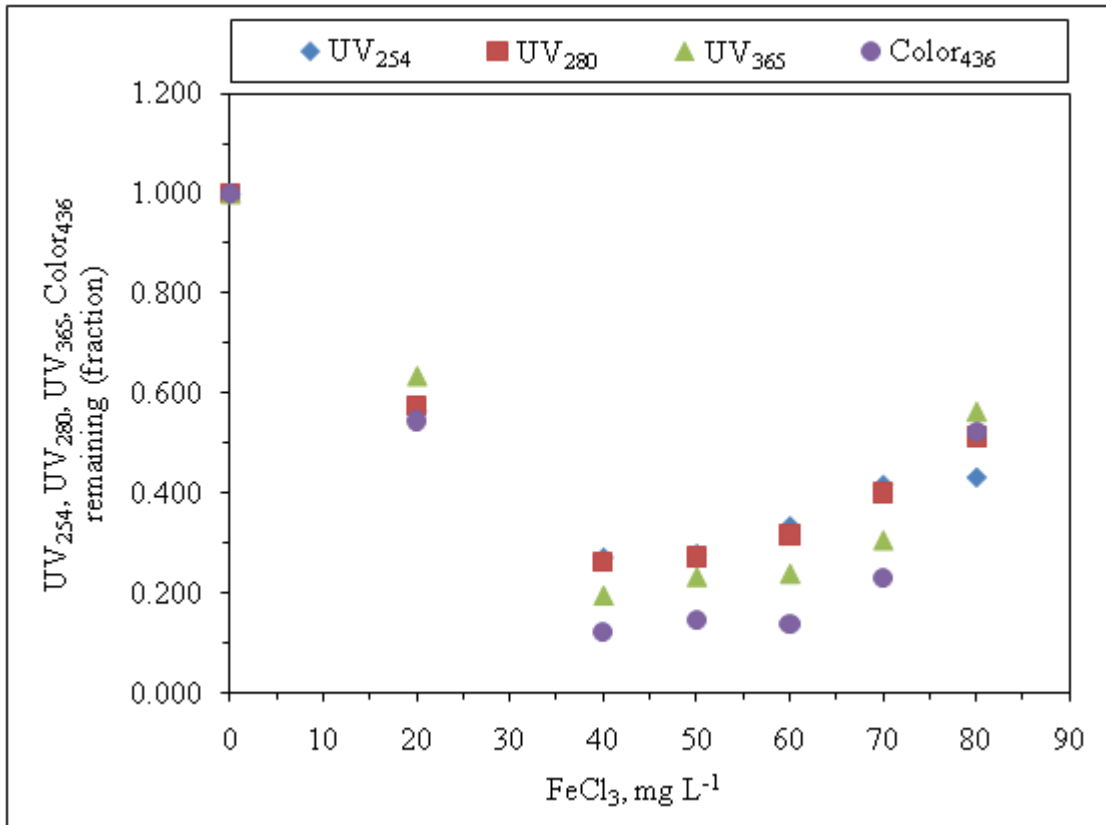


Figure 4.56. DOM_{conc} removal by coagulation with ferric chloride at pH 5.5 based on UV-vis parameters.

Removal profile of UV₂₈₀ displayed a very similar trend to UV₂₅₄ removal in coagulation of the DOM_{conc} sample with ferric chloride such that UV₂₈₀ and UV₂₅₄ values showing the organic matter removal efficiency of coagulation treatment coincided in all points of ferric doses applied varying between 20-80 mg L⁻¹. (Figure 4.56). This was also similar to what was observed in the case of coagulation of the DOM_{conc} sample with alum in terms of comparison of removal efficiencies of UV₂₈₀ and UV₂₅₄ parameters with each other (Figure 4.50). The obtained results of Color₄₃₆ and UV₃₆₅ were different for some of the applied doses of ferric chloride. UV₃₆₅ removal values followed below those of UV₂₈₀ at the applied doses between 40-70 mg L⁻¹ of ferric chloride. However, using 20 mg L⁻¹ and 80 mg L⁻¹ of ferric chloride resulted in higher UV₃₆₅ and Color₄₃₆ values than the other two parameters at these doses which implied that UV₃₆₅ and Color₄₃₆ removal efficiencies were lower than UV₂₅₄ and UV₂₈₀ removal using these concentrations. A reasonable

explanation could be the property of the ferric salt used giving color to the water sample that could not be removed by using a lower dose of ferric chloride such as 20 mg L⁻¹ which was not efficient in removing color in the water sample; and an excess dose of ferric which was 80 mg L⁻¹ in this case probably caused to the restabilization of the interacting iron and colloids to be removed. The most efficient DOM removal was obtained by using 40 mg L⁻¹ of ferric in terms of UV₂₈₀, UV₃₆₅ and Color₄₃₆ in coagulation of the DOM_{conc} sample, with efficiency rates of 74 % for UV₂₈₀, 81 % for UV₃₆₅ and 88 % for Color₄₃₆ removal.

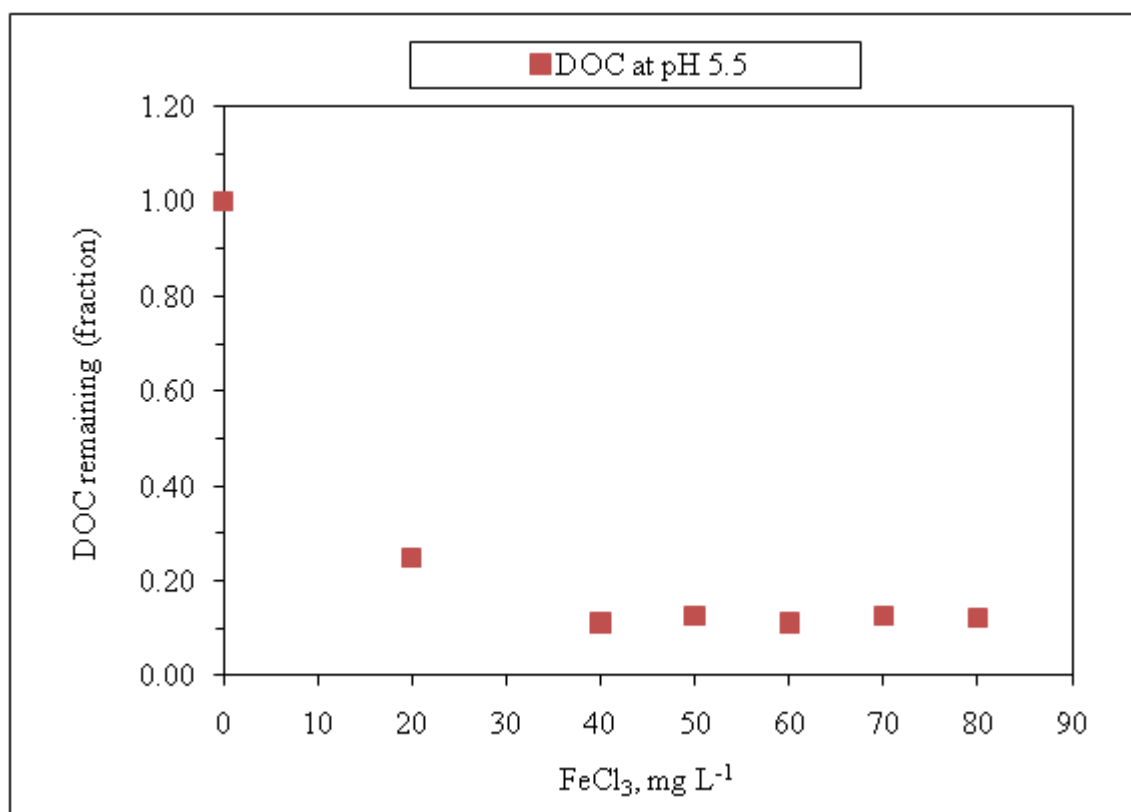


Figure 4.57. DOM removal by coagulation with ferric chloride at pH 5.5 based on DOC.

Dissolved organic carbon (DOC) removal rates in treatment of the DOM_{conc} sample at pH 5.5 by coagulation with ferric chloride in varying doses between 20-80 mg L⁻¹ were presented in Figure 4.57. Applying 20 mg L⁻¹ of ferric salt in coagulation of the DOM_{conc} sample reduced DOC by 75 %. Increasing the ferric dose to 40 mg L⁻¹ provided a further reduction of DOC by 89 %. Application of higher doses of 50 mg L⁻¹, 60 mg L⁻¹ 70 mg L⁻¹ and 80 mg L⁻¹ of ferric resulted in almost same DOC removal efficiency in the DOM_{conc}

sample. The application of higher doses than the optimum dose (40 mg L^{-1}) in coagulation of the DOM_{conc} sample resulted in a decrease in removal efficiency of UV_{254} but it did not happen in removal of DOC by using ferric coagulant higher than 40 mg L^{-1} as it remained almost stable around 88-89 % with only a small variance.

A comparison between the results of UV-vis parameters and DOC measurements (Figures 4.56-4.57) makes it obvious that coagulation of the DOM_{conc} sample with ferric chloride was successful in decreasing both DOC and UV absorbance using determined optimum coagulation conditions of 40 mg L^{-1} of ferric chloride at pH 5.5. Organic matter removal efficiency was 89 % in terms of DOC, when it was 88 % in terms of UV_{254} achieved by using ferric coagulant. In the previous part, coagulation of the DOM sample using ferric chloride as coagulant also resulted in efficient organic matter removal in terms of UV_{254} and DOC removal. Highest UV_{254} removal efficiency was 74 % but lower than DOC removal efficiency of 91 % achieved by applying an optimum dose of ferric chloride 15 mg L^{-1} of alum at pH 5.5 in the DOM sample. Coagulation performances in the DOM sample and the DOM_{conc} sample were both effective but changed according to removal rates which could be as a result of differences between the two dissolved organic matter samples in terms of components of organic matter such as humic acid found in the DOM sample and in terms water sample characteristics.

Studies on natural water samples suggested that seasonal changes in water quality in terms of the variations in organic matter components could affect the coagulation efficiency of DOC removal with metal coagulants (Jarvis et al., 2004). Jarvis and colleagues reported that DOC removal increased with increasing ferric coagulant dose other than in summer when high removal was observed for a low dose. Organic removal rates dropped in autumn and winter at optimum doses suggesting the natural water samples studied were more recalcitrant to treatment. Only small changes in the character of the water were detected throughout most of the year and the hydrophobic components of organic matter such as the humic and fulvic acids were found to be dominant throughout the year accounting for 60–70% of the total DOC. The largest change in the fractional composition was reported to occur in winter when the fulvic acid fraction increased by

20% and with a similar decrease in the humic acid fraction when compared to the other seasons (Jarvis et al., 2004).

The optimum coagulation conditions of the DOM_{conc} sample with ferric chloride determined was also presented by UV-vis spectra between 200-600 nm (Figure 4.58) and fluorescence spectra in emission₃₅₀, emission₃₇₀ and synchronous scans (Figure 4.59-4.61) to analyze the spectral behavior of the treated and untreated DOM_{conc} sample.

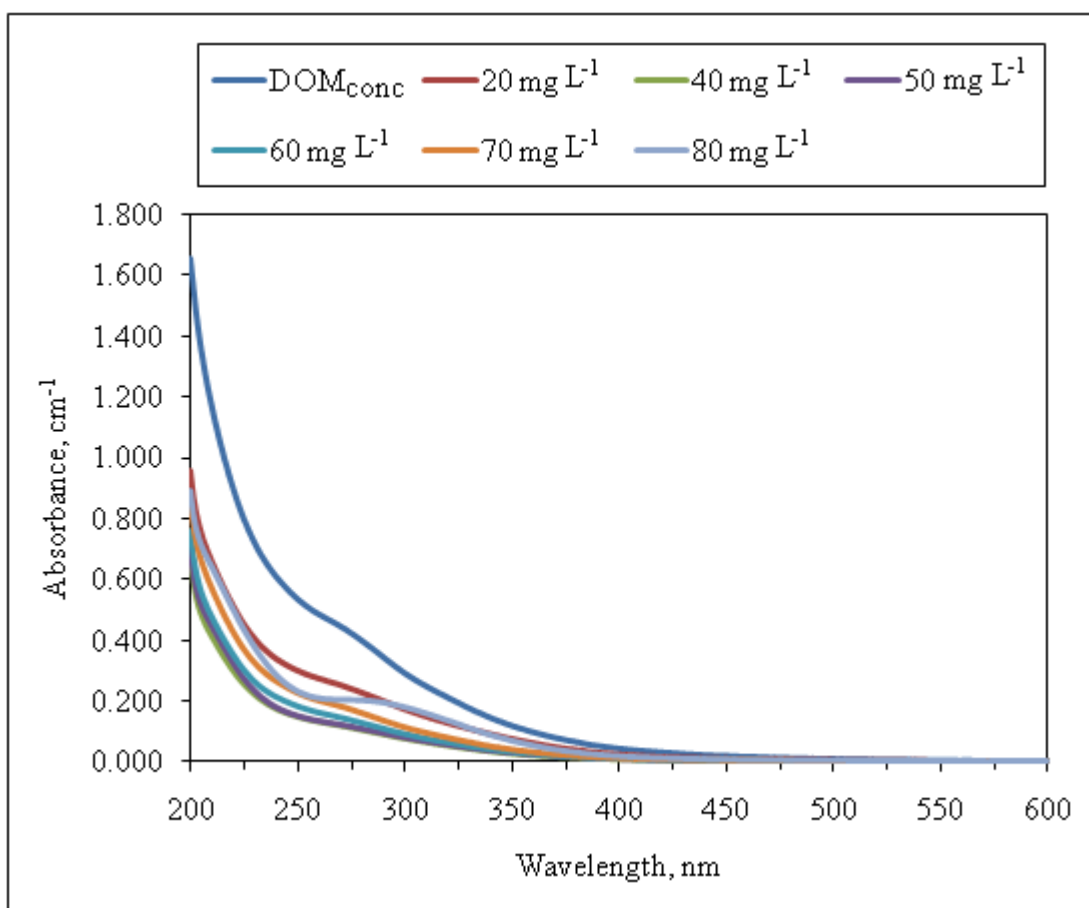


Figure 4.58. UV-vis spectra of the DOM_{conc} sample after coagulation with ferric chloride at pH 5.5.

Coagulation profile of the DOM_{conc} sample with ferric chloride at pH 5.5 was presented by UV-vis spectra between 200-600 nm in Figure 4.58. At higher wavelengths from 400 nm to 600 nm the absorbance values of all samples approached zero. It is possible

to differentiate absorbance values of the DOM_{conc} sample spectra at different doses of alum applied between 200-400 nm of the UV-vis range. Applying a ferric dose of 20 mg L^{-1} in coagulation of the DOM_{conc} sample degraded the initial absorbance values in UV-vis spectra about 30 % between 200-400 nm. With an Increase in the coagulant dose used to 40 mg L^{-1} the most reduction occurred in UV-vis absorbance of the DOM_{conc} sample indicating a well reduction in organic matter matter content. As the ferric concentration increased such as 50 mg L^{-1} 60 mg L^{-1} , 70 mg L^{-1} , 80 mg L^{-1} , UV-vis spectra of the DOM_{conc} sample gradually increased at each dose application. This implies that organic matter removal efficiency reduced which might be related to occurrence of a possible restabilization of the suspension brought by using higher doses of ferric salt than the optimum dose (40 mg L^{-1}) leading a most efficient removal of organic matter.

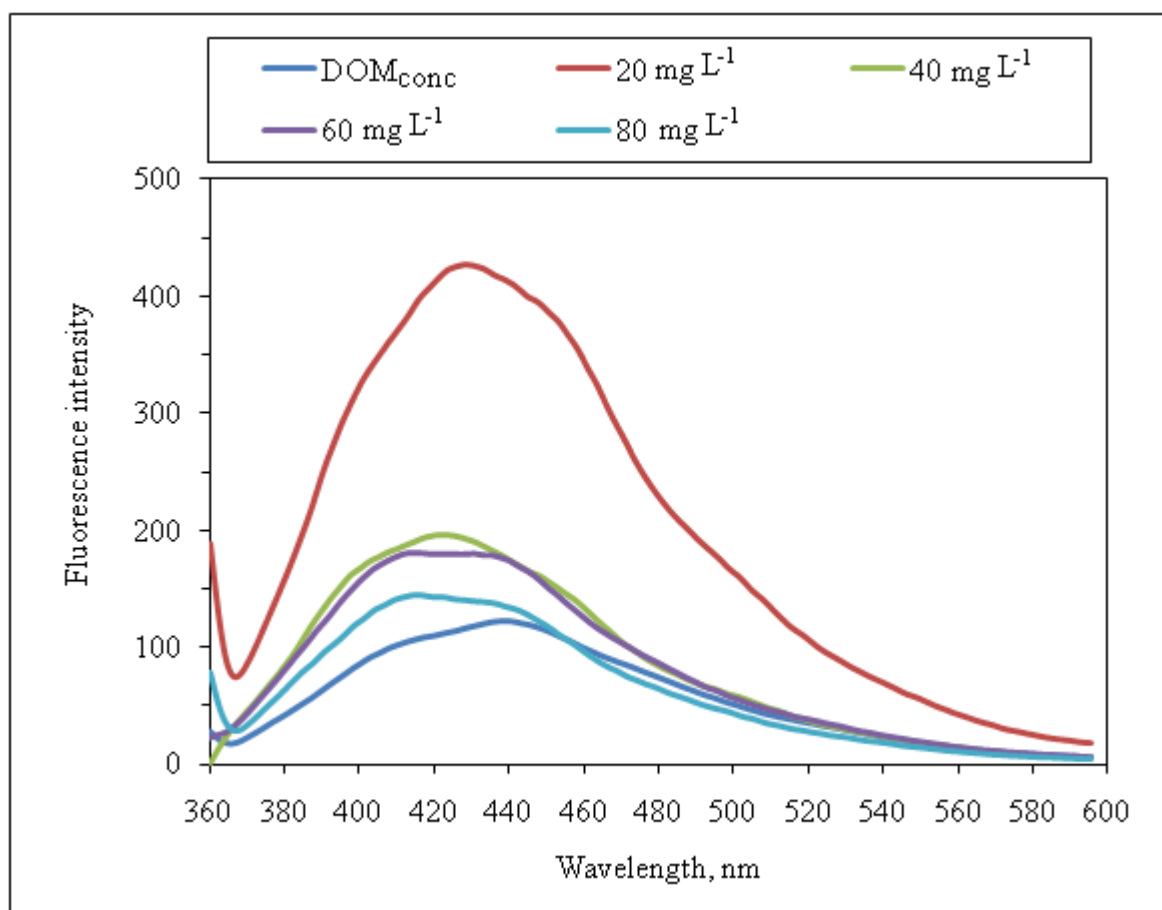


Figure 4.59. Fluorescence emission₃₅₀ spectra of the DOM_{conc} sample after coagulation with ferric chloride at pH 5.5.

Fluorescence spectra of the DOM_{conc} sample in emission₃₅₀ before and after coagulation treatment with ferric chloride presented a peak intensity at 445 nm for each spectrum (Figure 4.59). However, the DOM_{conc} sample did not show a direct relationship with the applied coagulant concentration of ferric chloride versus maximum intensity in emission₃₅₀ fluorescence in contrary to what was previously observed in coagulation of DOM sample (Figure 4.42 and Figure 4.59). The spectra of the untreated DOM_{conc} sample occurred with the lowest intensity below the other spectra of the treated DOM_{conc} sample with varying doses of ferric salt. On the other hand, as the applied coagulant dose was increased in coagulation of the DOM_{conc} sample from 20 mg L⁻¹ to 40 mg L⁻¹, 60 mg L⁻¹ and 80 mg L⁻¹ of ferric chloride, fluorescence spectra of the DOM_{conc} sample followed a decreasing intensity trend in Figure 4.59. Treatment with concentrations higher than the optimum dose of 40 mg L⁻¹ like 60 mg L⁻¹, 80 mg L⁻¹, changes in peak intensity of the DOM_{conc} sample reduced.

Fluorescence spectra of the DOM_{conc} sample in emission₃₇₀ scan before and after coagulation treatment with ferric chloride in Figure 4.60 were very similar to those in emission₃₅₀ with a peak intensity at same wavelength of 445 nm. Fluorescence intensity of the untreated DOM_{conc} sample was lower than the intensities obtained after treatment with various doses of ferric chloride like in the measurement in emission₃₅₀ except the lowest intensity occurred by application of the highest ferric dose of 80 mg L⁻¹. A possible reason could be given as stabilization-restabilization of the DOM-ferric particles in the sample. The two spectra approached together as the sample more restabilized hence reacted like more as the original sample in fluorescence by incremental addition of excess ferric coagulant. As the applied coagulant dose increased by the applications of 20 mg L⁻¹, 40 mg L⁻¹, 50 mg L⁻¹, 60 mg L⁻¹, 70 mg L⁻¹, 80 mg L⁻¹ of ferric chloride, fluorescence intensity decreased by applications of increased dose. Application of 20 mg L⁻¹ caused the highest intensity which was then reduced to half by treatment with 40 mg L⁻¹ of ferric chloride. Using ferric concentrations higher than the optimum dose of 40 mg L⁻¹ caused reduction of the fluorescence intensity of the DOM_{conc} sample in a smaller ratio or matching of the individual spectra at some wavelength ranges such as the collapse of spectrum of 60 mg L⁻¹

with the spectrum of 70 mg L⁻¹. This could be observed in Figure 4.60 by the closeness of the spectra of higher doses than 40 mg L⁻¹.

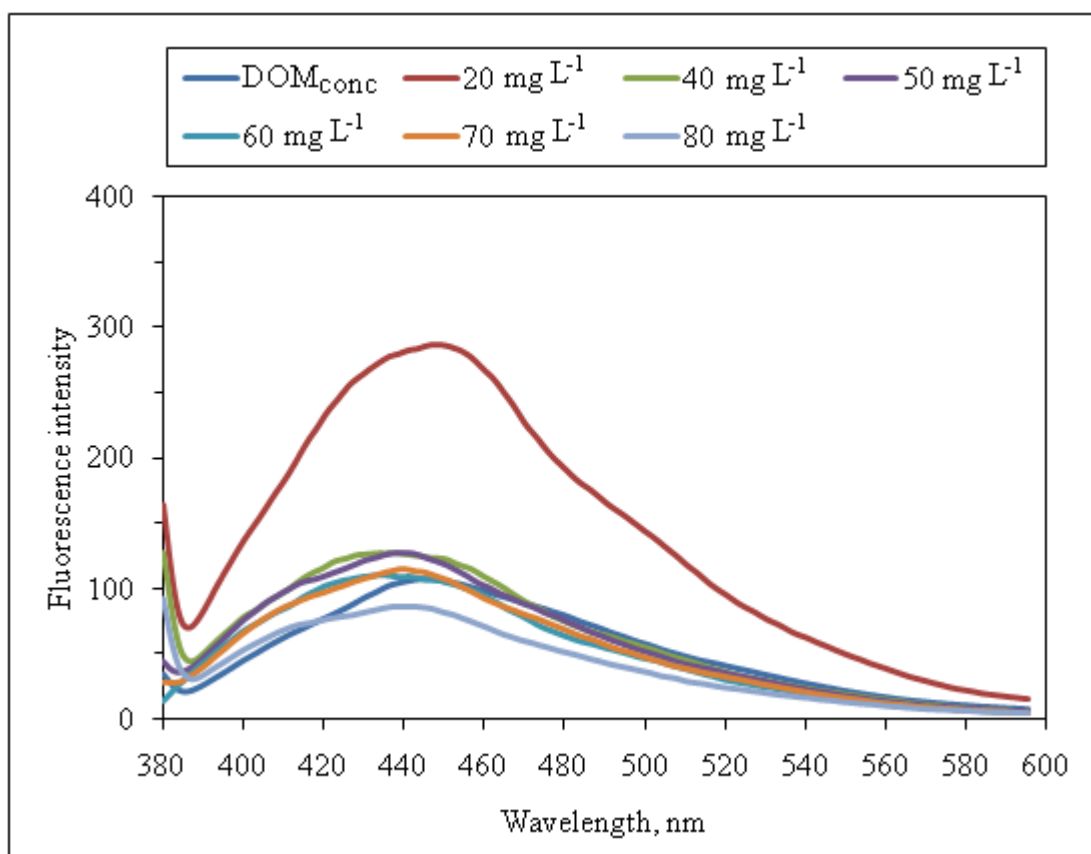


Figure 4.60. Fluorescence emission₃₇₀ spectra of the DOM_{conc} sample after coagulation with ferric chloride at pH 5.5.

Fluorescence synchronous scan results of the DOM_{conc} sample before and after treatment with ferric chloride were presented in Figure 4.61. Fluorescence intensity of the untreated DOM_{conc} sample had the lowest intensity than the intensities obtained after coagulation with ferric chloride. The DOM_{conc} sample has two peaks of intensity that occurred at the wavelengths of 280 nm and 355 nm. The second peak at 355 nm has a much higher intensity than the small peak observed at 280 nm. Fluorescence intensity first was increased by applying 20 mg L⁻¹ of ferric chloride. Application of higher doses decreased the fluorescence intensity in synchronous. As the applied dose of ferric was increased further decrease of fluorescence intensity was observed in each application.

Similar to the trend occurred in emission₃₅₀ and emission₃₇₀ scans, the rate of decrease in fluorescence intensity was reduced after the application of the optimum dose of ferric chloride (40 mg L⁻¹).

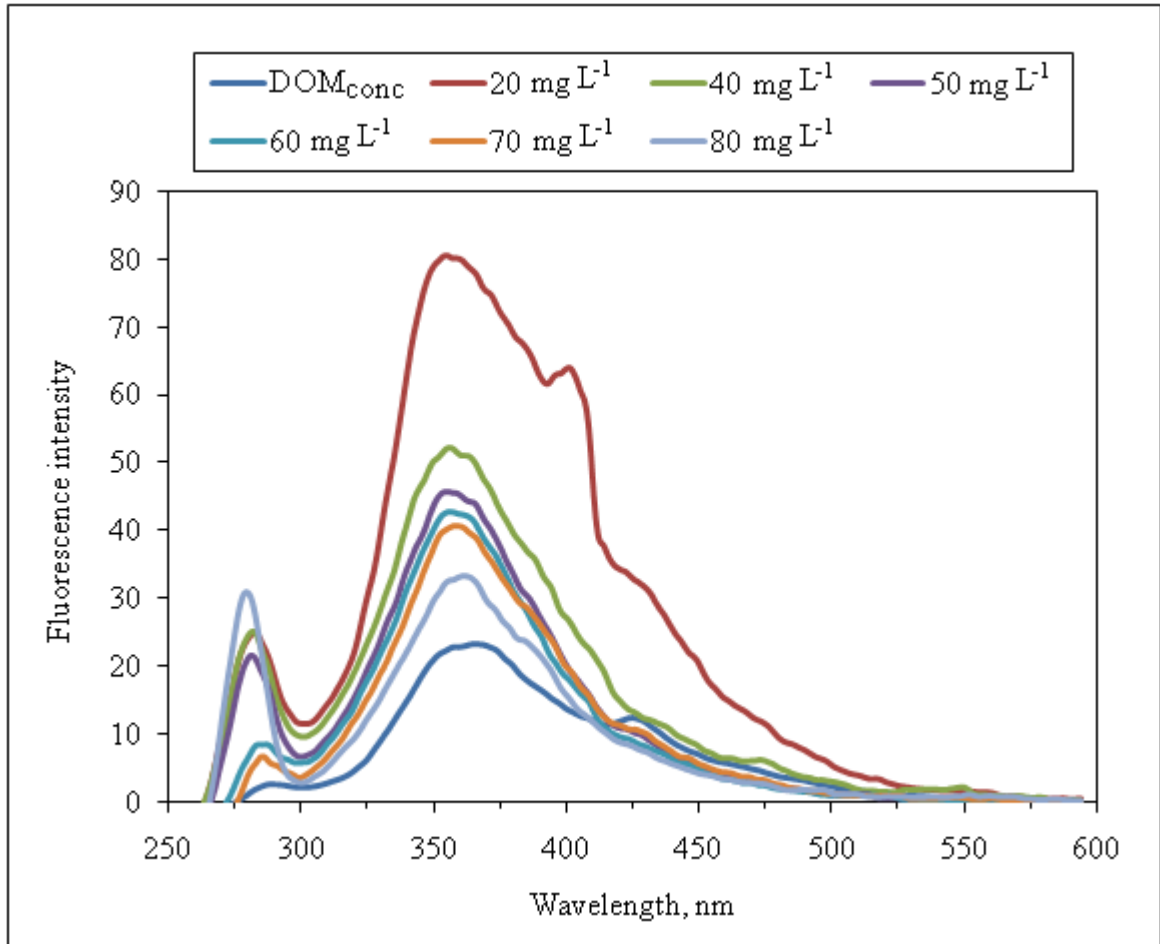


Figure 4.61. Fluorescence synchronous spectra of the DOM_{conc} sample after coagulation with ferric chloride at pH 5.5.

When compared with the fluorescence analysis of the DOM sample after coagulation with ferric chloride, fluorescence analysis results of coagulation of the DOM_{conc} sample with ferric chloride provided much more higher fluorescence intensities especially by using lower doses of ferric such as 20 mg L⁻¹ both in emission and synchronous, than the intensities obtained by the DOM sample after coagulation with ferric as in the case of alum. Ziegmann and co-workers showed in their study on using fluorescence fingerprints

for the estimation of bloom formation that the increase in fluorescence intensities and Microcystins content of a cyanobacterial culture can be explained in first instance by an increase of cell numbers during growth (Ziegmann, 2010). The intensity difference between DOM_{conc} and DOM samples could be explained similarly by the fact that DOM_{conc} sample is an aged algal organic matter sample whose organic matter concentration was higher as could be pronounced with higher DOC and UV-vis absorbance values of the DOM_{conc} sample when compared with DOM sample. It can be concluded that the necessity of using higher coagulant doses, namely alum or ferric chloride in coagulation application in the DOM_{conc} sample for organic matter removal than it was required in the coagulation of DOM sample, together with the differences in the characteristics of the two samples used in coagulation experiments of this study, which were “DOM sample” and “DOM_{conc} sample”, caused different types or amounts of end-product species to occur finally in the coagulated samples leading different behaviors of the two DOM samples in fluorescence spectroscopy.

Uyguner and colleagues reported a similar removal efficiency in organic matter removal by coagulation with alum and ferric chloride in which alum treatment efficiency was 88%, and ferric chloride treatment efficiency was 92 % in terms of UV₂₅₄ removal (Uyguner et al., 2007). In addition their results showed that removal efficiencies were in favor of ferric chloride except for the lower removal efficiency for Color₄₃₆ with ferric chloride than with alum.

Guigui and co-workers reported that the use of ferric chloride allowed high rates of NOM removal about 60% corresponding to a Fe concentration of around $3-4 \times 10^{-4} \text{ mol L}^{-1}$ (Guigui et al., 2002). But they indicated that for this coagulant, an optimal coagulant dose was not found and NOM removal increased with the increase of coagulant dose up to a plateau. The impact of variation of pH was highlighted on the coagulation efficiency so as the concentration of coagulant decreases such that a pH of around 5–6 leading to the highest DOC removal (Guigui et al., 2002). In the present study a similar finding were obtained in using ferric chloride which could be discussed that although high removal efficiency was achieved by using ferric chloride at a low pH of 5.5, there was a difficulty observed by sudden charge reversals occurred with doses higher than the optimum dose

determined causing an increase in UV₂₅₄ absorbance values as well as other followed UV-vis parameters especially in Color₄₃₆ and others of UV₂₈₀ and UV₃₆₅.

4.4. Molecular Size Distribution of Natural Organic Matter by Ultrafiltration

Molecular size distribution (MSD) has many implications in the studies of NOM. MSD strongly effects the design, evaluation, and integration of water treatment processes such as coagulation, membrane filtration, disinfection and adsorption on GAC. Size distribution of dissolved organics has also effects in terrestrial and sedimentary environments such as the fate and transport of synthetic organic chemicals, the complexation of metals, the fertility of soil. In environmental considerations, MSD of dissolved organic matter involves ecological studies of primary productivity, sources of DOM in natural waters and elemental cycling (Tadanier et al., 2000).

The molecular size distribution of natural organic matter is significant in treatment of drinking water by coagulation in several aspects (Randtke, 1988; Amy et al., 1992; Owen et. al, 1995). Size of the natural organic matter has been related with formation of disinfection by-products (DBPs) in terms of the low molecular weight fraction of the organic material. One of the example findings that have been reported in relation to the importance of molecular size distribution of the NOM is the formation of trihalomethanes (THMs) due to low molecular weight portion of humic acid. (Randtke, 1988; Frimmel et al., 2000; Nissinen et al., 2001). Molecular weight and degree of aromaticity of aquatic humic substances have been shown to be important properties that control the amounts of chlorinated disinfection by-products in water treatment (Reckhow et al., 1990).

Ultrafiltration technique (UF) was used to analyze the molecular weight (MW) fractions of water samples depending on the molecular weight cut offs (MWCO) employed. In ultrafiltration of raw water, the colloids and aggregates are mixed with natural organics such as humic acid and both species can play a role. If the natural organics are larger than the membrane pore size, they cause a more significant flux decline. It was found that flux decline was independent of the molecular weight to membrane pore size

ratio, but attributed to the change in colloid size distribution in the presence of organics (Kim et al., 1994; Schäfer, 2000; Schäfer, 2001).

Water treatment processes remove the largest part of natural organic matter such as large to intermediate size of humic fractions in raw waters thus shifting the molecular weight distribution of water with lower molecular weight particles (Nissinen et al., 2001). Natural waters contain humic substances as the main contributors to dissolved organic matter (DOM). Fulvic acids has been reported to have molecular weight greater than 700 Dalton (Da). A water body containing dissolved organic matter with MW range of 5000-10000 Da requires water treatment i.e. chemical coagulation. Medium molecular weight organic substances such as 1000-5000 Da can be removed with adsorption. Low molecular weight substances are reported to be not effectively removed by either coagulation or adsorption. These low molecular weight organics i.e. <1000 Da are important in the formation of THMs and must be removed in water sources (Zhao et al., 2006).

The DOM solution used in this study contained dissolved organic matter released by the algae grown under simulated eutrophication conditions. Considering the physico-chemical properties presented in Table 4.1., the organic carbon content of the DOM sample was 20.5 mg L⁻¹ whereas UV₂₅₄ was 0.1106. Although the amount of organic matter in the DOM sample could be regarded as high, the UV-vis spectroscopic properties were quite low when compared to the properties of the humic acids naturally present in waters. In order to overcome this difficulty thereby to be able to follow the molecular size fractionation of the dissolved organic matter prior to and after coagulation, an aged (3 months) and concentrated solution of algae suspension was taken under investigation. This solution was referred to as the DOM_{conc} sample.

Under these conditions, molecular size fractionation would probably yield lower molecular weight fractions (≤ 3 kDa) resembling fulvic type organic matter. Interestingly, in a study of Iriarté-Velasco and colleagues for the treatment of surface water by coagulation with alum the MWCO < 1 kDa size fraction contributed the largest to THMs precursors of raw water. Its contribution increased after coagulation–flocculation–settling treatment which was concluded that an increase in the portion of small molecules (i.e. due

to eutrophication) can reduce the effectiveness of coagulation (Iriarté-Velasco et al., 2007). Thus characterization of NOM is necessary for enhancing OM removal efficiency in coagulation processes.

4.4.1. Preparation of the DOM_{conc} Sample for Ultrafiltration

After determination of optimum coagulant doses using alum and ferric chloride for dissolved organic matter removal by coagulation in the DOM_{conc} sample, untreated and coagulated DOM_{conc} samples at the optimum coagulation conditions with alum and ferric chloride were subjected to ultrafiltration (UF). In order to be able to apply molecular size distribution to the DOM_{conc} sample after coagulation with alum and ferric chloride a high volume of the DOM_{conc} sample was required. For this purposes two more jar tests were repeated with alum and ferric at their optimum coagulation conditions using higher volume of DOM_{conc} which was 500 mL. UV-vis spectra of the untreated and treated DOM_{conc} water samples using 500 mL of coagulation sample were presented in Figure 4.62.

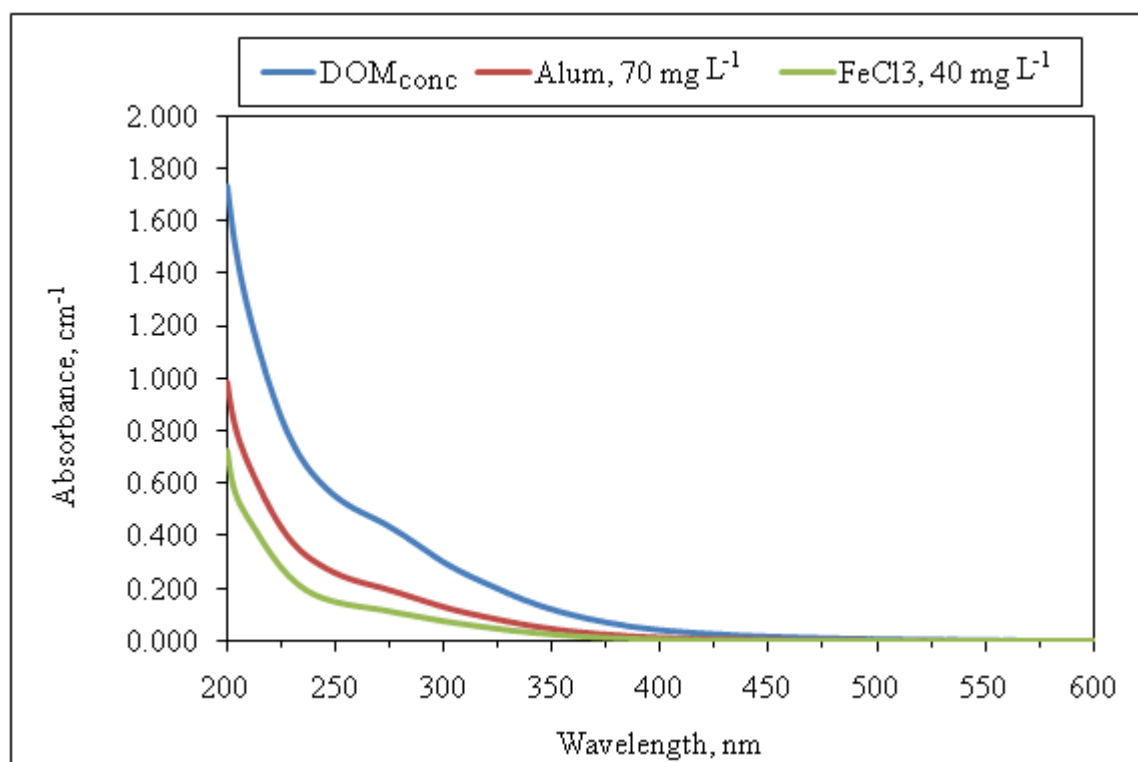


Figure 4.62. DOM_{conc} removal by jar tests using optimum coagulant doses of alum at pH 6.0 and ferric chloride at pH 5.5.

DOM_{conc} sample displayed a very similar decay profile by the UV-vis spectra in Figure 4.62 to the profiles obtained after coagulation of DOM_{conc} sample with optimum doses of alum and ferric chloride that were carried out using 50 mL of coagulation sample size as previously presented in Figure 4.52 and Figure 4.58. An efficient removal of organic matter was achieved with the determined conditions of optimized coagulation in like in previous sections with alum and ferric chloride. UV₂₅₄ removal rates achieved were 64 % by alum and 73 % by ferric coagulation of the DOM_{conc} sample. Similar decay could be observed for natural water samples and humic substances i.e. humic and/or fulvic acids.

4.4.2. Application of Ultrafiltration

Chin and colleagues indicated that given the evidences at 280 nm because $\pi \rightarrow \pi^*$ electron transitions occur in this region of the UV range (i.e., 270-280 nm) for phenolic substances, aniline derivatives, benzoic acids, polyenes, and polycyclic aromatic hydrocarbons, molar absorptivities may yield important clues regarding the degree of aromaticity, source functions, extent of humification, and possibly molecular weight. All these properties may ultimately influence the behavior of humic materials such as interacting with nonpolar organic pollutants, metals, and radionuclides. Hence the degree of aromaticity, MWs and the molar absorptivity of whole-water samples may be used to a first approximation as a spectroscopic predictor of the chemical reactivity of aquatic OM (Chin et al., 1994). Based on this knowledge, MW distribution of the untreated DOM_{conc}, and the changes in its MW distribution brought by coagulation with alum and ferric which could affect the molecular weight and absorptivity of the resulting species were explored based on the measurements of absorbance through UV-vis spectra and DOC.

Untreated DOM_{conc} and the DOM_{conc} samples obtained after treatment by coagulation with alum and ferric were then subjected to molecular size distribution by carrying out a series of ultrafiltration using different molecular size cutoffs. Samples were filtered through 100 kDa, 30 kDa, 10 kDa, 3 kDa and 1 kDa membrane filters in the presented order. According to the ultrafiltration applied, the DOM_{conc} sample was classified into six nominal cutoff ranges of decreasing order such as: “0.45 μm – 100 kDa”, “100kDa – 30

kDa”, “30 kDa – 10 kDa”, “10 kDa – 3 kDa”, “3 kDa – 1 kDa” and lastly “< 1 kDa” which denotes the molecular weight portion of DOM_{conc} that pass through 1 kDa filter size.

UV-vis spectroscopy analysis of the untreated DOM_{conc} sample after ultrafiltration was presented in Figure 4.63. The results showed that the UV-vis spectra for molecular size ranges of “0.45 μm – 100 kDa” and “100 kDa – 30 kDa” of the untreated DOM_{conc} sample were very close to each other. Therefore it could be suggested that the molecular size of the DOM_{conc} sample was indifferent through these ranges according to UV-vis absorbance. In lower cutoffs, sample characteristics revealed that a low molecular weight proportion of the DOM_{conc} sample existed in the nominal ranges of “30 kDa – 10 kDa”, “10 kDa – 3 kDa”, “3 kDa – 1 kDa” and “< 1 kDa” as lower molecular weight components of dissolved organic matter since the differences in UV-vis absorbance occurred while the DOM_{conc} sample passed through filters of 10 kDa, 3 kDa and 1 kDa.

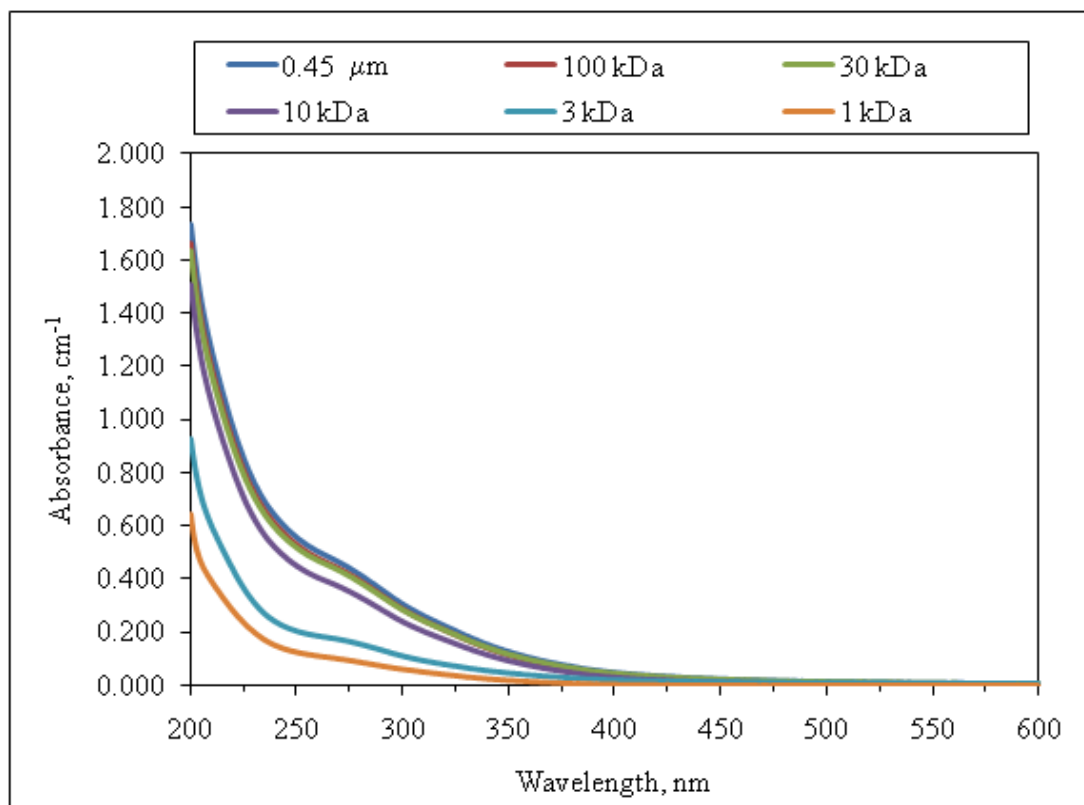


Figure 4.63. Effect of molecular size distribution on UV-vis spectra of the untreated DOM_{conc} sample.

Since DOM_{conc} sample contained dissolved organic matter that was derived from algal organic matter, comparison of its molecular size distribution that was analyzed by UV-vis spectroscopy as shown in Figure 4.63 to the molecular size distribution profiles of other fractions of natural organic matter such as humic/fulvic acids could be relevant for assessing the differences and similarities between the different components of natural organic matter in natural water systems. Ultrafiltration of untreated humic acid samples through the same membrane filters in previous studies exhibited a decreasing trend with the decreasing pore size (Kerç, 2002; Uyguner, 2005). Similar to the decreasing trend of DOM_{conc} sample in Figure 4.63, the reported data for humic acid sample in the study of Kerç displayed greater nominal ranges by the UV-vis spectra in the ranges of “30 kDa – 10 kDa”, “10 kDa – 3 kDa” and “3 kDa – 1”, than the relatively smaller nominal ranges of “450 kDa – 100 kDa”, “100 kDa – 30 kDa”, and “1 kDa – 0.5 kDa” (Kerç, 2002). Although the similarities between these reported humic acid samples and the DOM_{conc} sample, reclining view of 0.45 µm, 100 kDa and 30 kDa cutoff fractions were not observed in humic acid sample as much close as in Figure 4.63 suggesting a difference could exist between humic acids and DOM_{conc} sample as they filtered through these sizes. Thus, it can be concluded that molecular size distribution of DOM_{conc} sample represented similarities in lower molecular sizes to humic acid samples but a distinction in higher molecular sizes which could be attributed to the characteristics of algal organic matter from another sort of natural organic matter component i.e. humic acids.

In Figure 4.63 the molecular weight distribution of untreated DOM_{conc} sample has been put forward by its assesment in terms of UV-vis spectra. As being one of the aims of the present study, to be able to analyze how the DOM_{conc} sample was affected by treatment of coagulation i.e. whether the molecular weight distribution of the DOM_{conc} sample changed after coagulation with metal salts of alum and ferric, DOM_{conc} sample was filtered after the coagulation treatment through ultrafiltration by using the same molecular size cutoffs used for the untreated DOM_{conc} sample as given in Figure 4.63. The molecular size distribution of the DOM_{conc} sample after dissolved organic matter removal was achieved by coagulation with applicaitons of two different coagulants which were alum and ferric chloride were shown in Figure 4.64 and in Figure 4.65 as represented by UV-vis spectra of the filtrated DOM_{conc} samples.

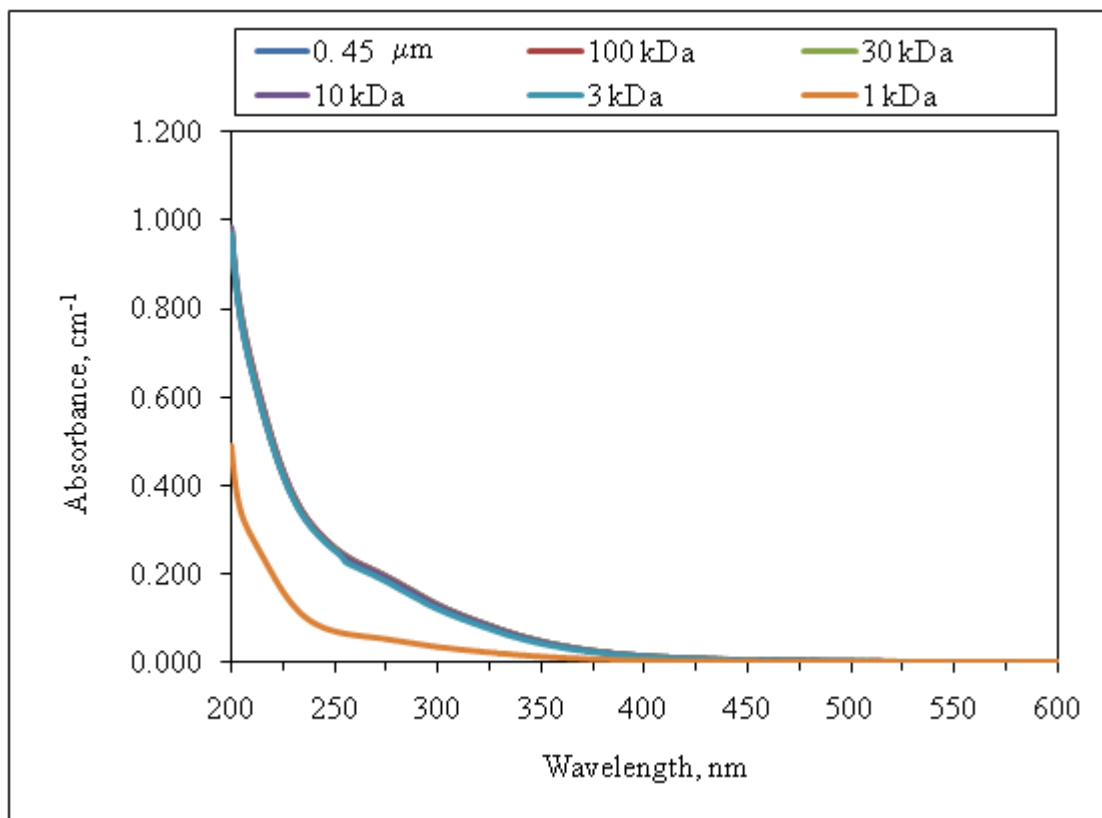


Figure 4.64. Effect of molecular size distribution on UV-vis spectra of the DOM_{conc} sample after coagulation with alum.

UV-vis spectra of the filtrated DOM_{conc} samples after coagulation with alum were presented in Figure 4.64 showing the molecular size distribution profile after treatment with alum. According to the UV-vis spectra in Figure 4.64, molecular size ranges of decreasing order which are “0.45 μm – 100 kDa”, “100kDa – 30 kDa”, “30 kDa – 10 kDa”, “3 kDa – 1 kDa” and “10 kDa – 3 kDa” seem to be identical since the spectra lines obtained by filtering the sample through these cutoffs presented an intermixed view. Only one spectra line that of 1 kDa could be picked and chosen below the other spectra which indicated that molecular size differences were found only in the size ranges of “3 kDa – 1 kDa” and “< 1 kDa”. Obviously this is not the same scheme as observed in untreated DOM_{conc} sample in Figure 4.63. Comparing Figures 4.63 and 4.64, it can be suggested that coagulation with alum infringed the variety in molecular weight distribution of DOM_{conc}

and shifted the molecular weight of DOM_{conc} sample to lower ranges of MW most possibly because the high molecular weight portion of DOM_{conc} were removed by coagulation.

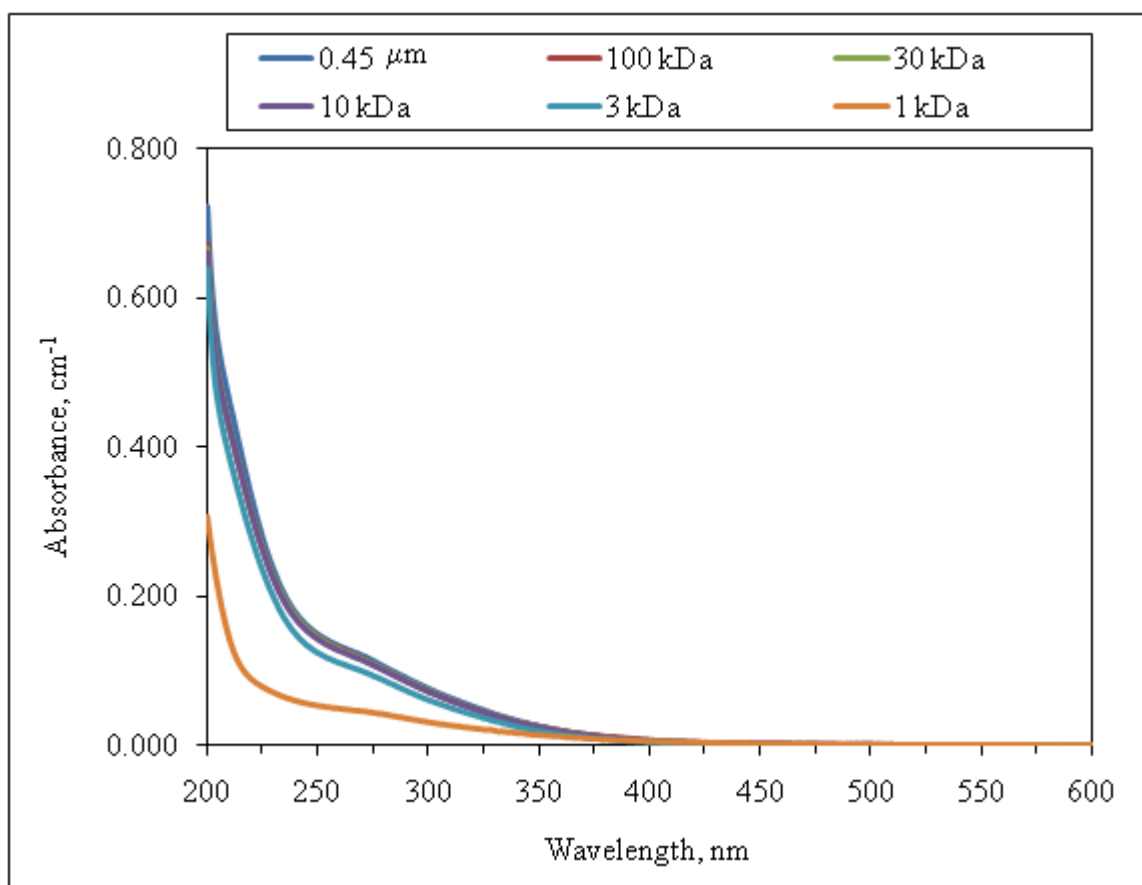


Figure 4.65. Effect of molecular size distribution on UV-vis spectra of the DOM_{conc} sample after coagulation with ferric chloride.

In Figure 4.65, UV-vis spectra of the filtrated DOM_{conc} samples after coagulation with ferric chloride were presented. From the presented spectra only two spectrum lines of 3 kDa and 1 kDa could be selectable among others that show a molecular size decrease in the ranges of “10 kDa – 3 kDa”, “3 kDa – 1 kDa” and “< 1 kDa” in Figure 4.65. The UV-vis absorbance results of ultrafiltration application of treated DOM_{conc} sample suggested that there was a change in the molecular size distribution of DOM_{conc} sample after coagulation with alum and ferric chloride. In the untreated DOM_{conc} sample molecular size decrease seemed to occur in the ranges of “30 kDa – 10 kDa”, “10 kDa – 3 kDa”, “3 kDa – 1 kDa” and “< 1 kDa” while in the case of treatment with ferric chloride the differentiation in

molecular size could appear in a lower size by beginning from the “10 kDa – 3 kDa” down to “< 1 kDa”, and in treatment with alum molecular size decrease was observed in the ranges of “3 kDa – 1 kDa” and “< 1 kDa”.

Molecular size distribution of the DOM_{conc} sample according to UV₂₅₄ (cm⁻¹) and DOC (mg L⁻¹) were presented in Figure 4.66 and in Figure 4.67 respectively.

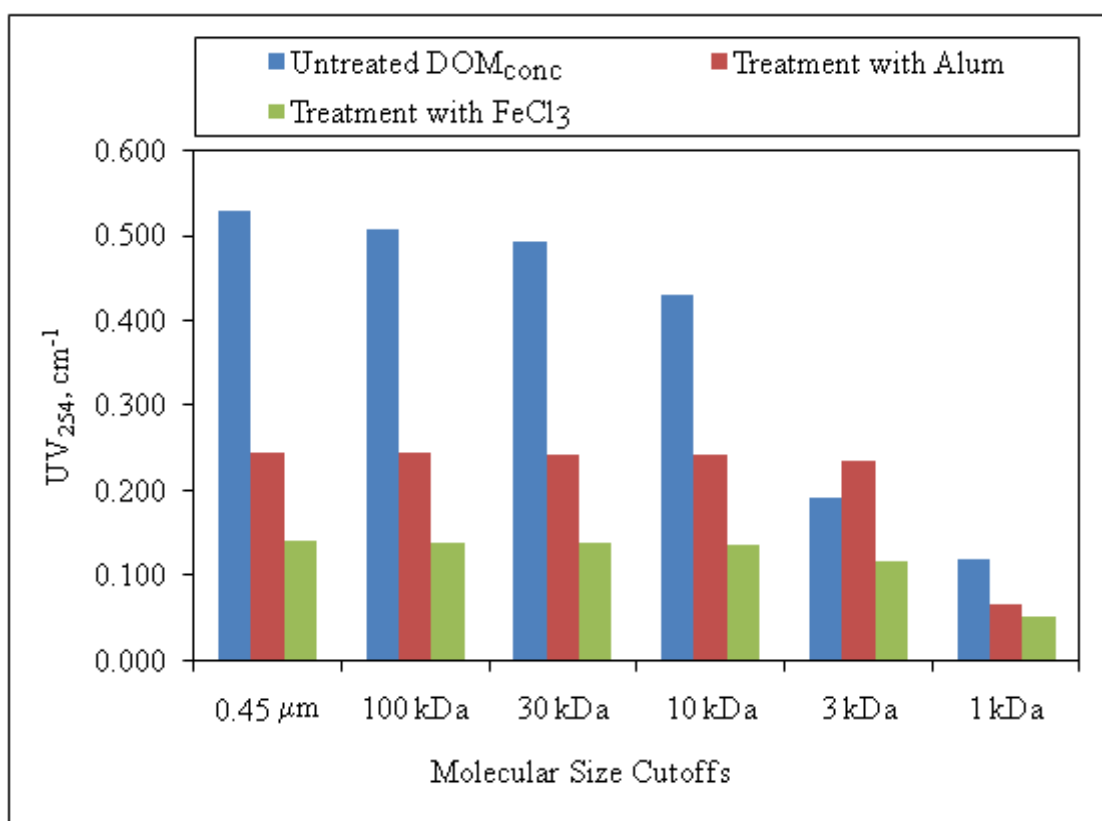


Figure 4.66. Molecular size distribution of the DOM_{conc} sample before and after coagulation based on UV₂₅₄.

The assessment of molecular size distribution of the DOM_{conc} sample before and after coagulation with alum and ferric chloride as discussed based on UV-vis spectra in Figures 4.63-4.65 were similar when the results were compared in terms of UV₂₅₄ and DOC in Figure 4.66 and Figure 4.67. According to Figures 4.66-4.67, it could be suggested that coagulation with alum resulted in a size distribution of identical species except a decrease in the ranges of “3 kDa – 1 kDa” and “< 1 kDa”, while molecular size distribution

decreased in the nominal ranges of “10 kDa – 3 kDa”, “3 kDa – 1 kDa” and “< 1 kDa” after coagulation with ferric chloride.

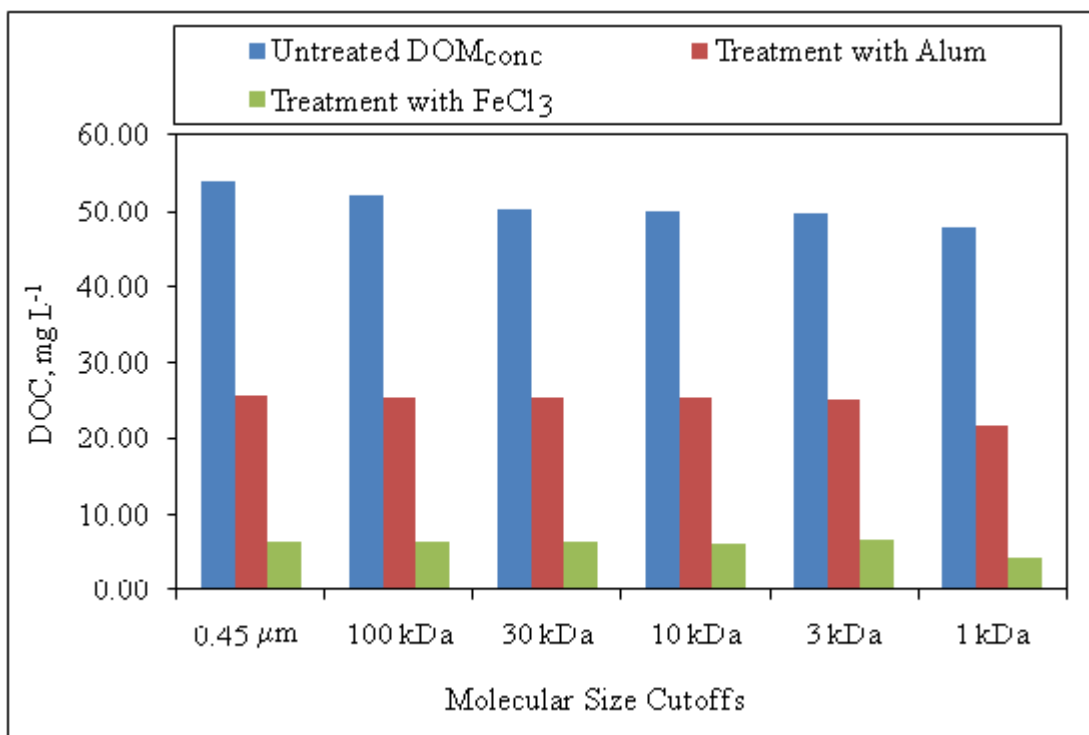


Figure 4.67. Molecular size distribution of the DOM_{conc} sample before and after coagulation based on DOC, mg L⁻¹.

In the present study, “0.45 μm – 100 kDa”, and “100 kDa – 30 kDa” fractions of the DOM_{conc} sample were found to be very similar to each other according to UV-vis spectroscopy. The changes occurred in the DOM_{conc} sample in the nominal molecular size ranges of “30 kDa – 10 kDa”, “10 kDa – 3 kDa” and “3 kDa – 1 kDa”. A similar finding was reported by Assemi and colleagues indicating that the shape of the spectrum for some fractions of a surface water sample containing natural organic matter i.e. “< 0.5 kDa” and “0.5 kDa – 3 kDa”, and “10 kDa – 30 kDa” and “> 30 kDa” were similar in ultrafiltration of the sample (Assemi et al., 2004).

When compared with the coagulated samples, the differences between the size distribution of the raw and coagulated samples are in small amount indicating that the

molecular weight distribution of the water sample changed slightly by coagulation. In addition, the changes occurred in the nominal molecular size ranges of “10 kDa – 3 kDa”, “3 kDa – 1 kDa” and “< 1 kDa” showed consistency with the expected characteristic of DOM_{conc} sample because of its property of being algal organic matter (AOM) which was reported in the previous findings to have a low molecular-sized characteristic (Kerc et al., 2003).

Zhao and colleagues studied on the role of aluminum speciation in the removal of DBP precursors by a coagulation process and the characterization of DBP precursors (Zhao et al., 2008). They suggested that the greatest reduction of HAA precursors with low molecular weights i.e. < 30 kDa occurred through charge neutralization at pH 5.5, and that of HAA precursors in high MW > 30 kDa fractions was through adsorption at pH 7.5. In the different MW fractions, the greatest reduction of THM precursors was through charge neutralization at pH 5.5.

These findings support the findings of the present study that indicated the coagulation with alum and ferric chloride resulted in an efficient removal of dissolved organic matter at low pH conditions such as 5.5 and 6.0. It is interesting to note that the concentrated dissolved organic matter used was only derived from algal organic matter which was reported by previous studies often as having low molecular weight characteristic. This characteristic of AOM differentiates it from other components of NOM such as humic substances that were known to have high molecular weight. The findings on the coagulation performances of aluminum and ferric salts performed in DOM samples in the present case provided insight into the removal mechanisms of a specific component of NOM i.e. algal organic matter, AOM, by coagulation. By displaying molecular weight distribution of the samples before and after coagulation treatment it was demonstrated that the coagulation caused the molecular weight to shift to lower ranges i.e. to 3 kDa and 1 kDa. It could be suggested that removal by coagulation swept away high molecular weight fraction of DOM_{conc} sample and could not remove low molecular weight fraction as to the 3 kDa.

5. CONCLUSIONS

In this study, the effect of eutrophication conditions on the coagulation efficiency of natural organic matter was analyzed using two types of coagulants that were alum and ferric chloride. Algae growth analysis of the simulated freshwater samples were measured to assess the elements of eutrophication. The application of optimized coagulation (OC) method was performed for the assessment of the natural organic matter (NOM) removal efficiency of coagulation in natural waters with a specific focus on algae-laden organic matter (AOM). The characterisation of the natural organic matter was assessed through the molecular size distribution profiles by ultrafiltration (UF) using appropriate filters with certain molecular size cutoffs.

Freshwater algae were cultivated in synthetic freshwater media using different nutrient combinations of nitrate and phosphate, until the optimum growth conditions were reached. The recorded results revealed that the nutrient consumption decreased while the number of algae cells, optical density at 600 nm and chlorophyll a concentration increased in the algae mediums. The kinetics of algae growth in the mediums were assessed by using Michaelis-Menten (Monod) model for growth of microorganisms. The obtained curves showed that algae growth rate reached the highest values in the exponential phase of growth in the mediums. Substrate limitation of algae growth by nitrogen and phosphorus was found to be similar to the assessments of phytoplankton growth in literature implying that the mediums used in this study assimilated the supplied nutrients in a similar way to the consumption behavior during production of algae in natural waters. Different growth media were combined at the end of the following period of two weeks to form a single water sample that included organic matter released by algae and humic acid which was used then in coagulation experiments.

The application of optimized coagulation was managed by finding the optimum coagulant doses at the pH values of 5.5, 6.0, 6.5 and 7.0 by incremental additions of the coagulant used. The applied alum concentration changed between 5 and 100 mg L⁻¹, while ferric chloride concentration was applied in the range of 5-80 mg L⁻¹. Selection of the

optimum conditions were based on the two criteria of optimum coagulant dose and optimum pH for the coagulation-based water purification that were determined according to the removal efficiency based on UV-vis parameter of UV_{254} . Optimum conditions for coagulation with alum was determined as coagulation at pH 6.0 using 40 mg L^{-1} of alum for the DOM sample. Optimum conditions of coagulation with ferric chloride occurred at pH 5.5 using 15 mg L^{-1} of ferric chloride. In the coagulation experiments that were carried out using the concentrated DOM sample (DOM_{conc}), these determined optimum pH values were directly used to find the optimum coagulant doses for the DOM_{conc} sample since the characteristics of both DOM samples used were similar. For coagulation of the DOM_{conc} sample optimum alum dose were determined as 70 mg L^{-1} and optimum ferric chloride dose was found to be 40 mg L^{-1} . The differences between the DOM sample and the DOM_{conc} sample in terms of coagulant demand could represent that the optimum dose necessary for an efficient organic matter removal increased due to the increase in DOC concentration.

In addition to UV_{254} -based assessments, organic matter removal efficiencies were also compared according to measurements of UV_{280} , UV_{365} , $Color_{436}$, DOC and fluorescence intensities in the DOM water samples for the applications of different coagulant doses. The comparisons between these results clarified and supported the arrived conclusions that were based on the evaluations of UV_{254} results.

The percentages of removal efficiencies of the two coagulants were found to be high. Ferric chloride was quite successful in coagulation treatment of the DOM sample reaching a 74% of removal in UV_{254} and 92% in DOC removal. Alum coagulation was also effective yielding in removal levels as high as 71% in UV_{254} and 89 % in DOC removal. Comparing the performances of the two coagulants it can be concluded that using ferric chloride outperformed the alum coagulant in terms of DOM removal efficiency based on UV_{254} and DOC data except the $Color_{436}$ removal efficiencies that were found to be higher for coagulation with alum than with ferric chloride using the determined optimum coagulant doses.

The relationship between removal of DOM by treatment with alum and ferric chloride and the molecular weight distribution of the dissolved organic matter samples before and after removal of organic matter by coagulation were assessed based on UV₂₅₄ and DOC measurements. using a concentrated dissolved organic matter sample which was called as DOM_{conc} that included algal organic matter. The results indicated that an efficient removal of organic matter were achieved with the coagulants used as in the case of coagulation of DOM sample. The observed molecular size distribution of the DOM_{conc} sample indicated that the DOM_{conc} sample consisted of both higher and lower molecular weight fractions as found to be in different molecular weight ranges of 0.45-100 kDa, 100 kDa-30 kDa, 30 kDa-10 kDa, 10 kDa-3 kDa, 3 kDa-1 kDa, and <1 kDa. Measurements of UV-vis and DOC after coagulation of DOM_{conc} sample revealed that the coagulation treatment caused the molecular weight distribution to shift to lower weight ranges i.e. 3k Da - 1 kDa and < 1 kDa by application of both alum and ferric. The difference in the scheme of molecular weight distribution of the DOM_{conc} sample that emerged after coagulation could be linked to the smaller molecular weight characteristic of the organic matter as released by algae which were not removed as much as higher molecular weight fraction of DOM_{conc} sample. It was interesting to note that the whole water sample namely the DOM_{conc} sample contained AOM. It was often reported in literature that humic and fulvic acids shifted the molecular size distribution to a lower weight ranges after the coagulation treatment. Though it can be suggested that the coagulation acted similarly on molecular size distribution of DOM_{conc} sample by leaving lower molecular weight fraction after treatment as in the case of other components of NOM such as humic and fulvic acids that were known to shift the molecular size distribution to a lower range after the coagulation treatment.

REFERENCES

- Aiken, G. R., McKnight, D. M., Wershaw, R.L., MacCarthy, P. (Eds), 1985. Humic Substances in Soil, Sediment and Water: Geochemistry, Isolation, and Characterization, Wiley-Interscience, New York.
- Aktaş-İlgün, S., 2010. Characterization and Reactivity of Natural Organic Matter in Drinking Water Sources, M.S. Thesis, Boğaziçi University.
- Amy, G. L., Sierka, J., Bedessem, D. P., Tan, L., 1992. Molecular size distribution of dissolved organic matter. *Journal of American Water Works Association*, 84, 67–75.
- Andelković, T., Perović, J., Purenović, M., Andelković, D., 2004. Destabilization and aggregation of aqueous humic acids solution by metal ions. *Facta Universitatis Series: Physics, Chemistry and Technology*, 3, 79–85.
- Annadurai, G., Sung, S. S., Lee, D. J., 2003. Floc characteristics and removal of turbidity and humic acid from high-turbidity storm water. *Journal of Environmental Engineering*, 129, 571–575.
- APHA, AWWA, WPCF, 1998. *Standard Methods for the Examination of Water and Wastewater*, 20th Edition, American Public Health Association, Washington D.C.
- Archer, A. D., Singer, P. C., 2006. Effect of SUVA and enhanced coagulation on removal of TOX precursors. *Journal of American Water Works Association*, 98, 97.
- Assemi, S., Newcombe, G., Hepplewhite, C., Beckett, R., 2004. Characterization of natural organic matter fractions separated by ultrafiltration using flow field-flow fractionation. *Water Research*, 38, 1467–1476.

Baker, A., Tipping, E., Thacker, S. A., Gondar, D., 2008. Relating dissolved organic matter fluorescence and functional properties. *Chemosphere*, 73, 1765–1772.

Barrett, S. E., Krasner, S. W., Amy, G. L., 2000. Natural Organic Matter and Disinfection By-Products: Characterization and Control in Drinking Water- An Overview. In Barrett, S. E., Krasner, S. W., Amy, G. L. (Eds.), *Natural Organic Matter and Disinfection By-Products Characterization and Control in Drinking Water*, 2-14, ACS Symposium Series 761, Oxford University Press, U.S.A.

Bergamaschi, B. A., Fram, M. S., Roger, F., Aiken, G. R., Kendall, C., Silva, S. R., 2000. Trihalomethanes Formed from Natural Organic Matter Isolates: Using Isotopic and Compositional Data To Help Understand Sources. In Barrett, S.E., Krasner, S.W., Amy, G.L. (Eds), *Natural Organic Matter and Disinfection By-Products Characterization and Control in Drinking Water*, 206-222, ACS Symposium Series 761, Oxford University Press, U.S.A.

Biber, M. V., Gülaçar, F. O., Buffle, J., 1996. Seasonal variations in principal groups of organic matter in a eutrophic lake using pyrolysis/GC/MS. *Environmental Science and Technology*, 30, 3501-3507.

Black, B. D., Harrington, G. W., Singer, P. C., 1996. Reducing cancer risks by improving organic carbon removal. *Journal of American Water Works Association* 88, ABI/INFORM Trade & Industry, 40–52.

Bose, P., Reckhow, D. A., 1998. Adsorption of natural organic matter on preformed aluminium hydroxide flocs. *Journal of Environmental Engineering*, 124, 803–810.

Boyle, E. S., Guerriero, N., Thiallet, A., Del Vecchio, R., Blough, N. V., 2009. Optical properties of humic substances and CDOM: relation to structure. *Environmental Science and Technology*, 43, 2262–2268.

Bratby, J., 2006. *Coagulation and Flocculation in Water and Wastewater Treatment*, 2nd Edition, IWA Publishing, London.

Brooks, P. D., O'Reilly, C. M., Diamond, S. A., Campbell, D. H., Knapp, R., Bradford, D., Corn, P. S., Hossack, B., Tonnessen, K., 2005. Spatial and temporal variability in the amount and source of dissolved organic carbon: implications for ultraviolet exposure in amphibian habitats. *Ecosystems*, 8, 478–487.

Carpenter, S. R., Caraco, N. F., Correll, D. L., Howarth, R. W., Sharpley, A. N., Smith, V. H., 1998. Nonpoint pollution of surface waters with phosphorus and nitrogen. *Ecological Applications*, 8, 559–568.

Chapra, S. C., 1997. *Surface Water-Quality Modeling*. The McGraw-Hill Companies, Inc., U.S.A.

Chen, H., Burke, J. M., Mosindy, T., Fedorak, P. M., Prepas, E. E., 2009. Cyanobacteria and microcystin-LR in a complex lake system representing a range in trophic status: Lake of the Woods, Ontario, Canada. *Journal of Plankton Research*, 31, 993–1008.

Chen, J., LeBoeuf, E. J., Dai, S., Gu, B., 2003. Fluorescence spectroscopic studies of natural organic matter fractions. *Chemosphere*, 50, 639–647.

Chen, R. F., Zhang, Y., Vlahos, P., Rudnick, S. M., 2002. The fluorescence of dissolved organic matter in the Mid-Atlantic Bight. *Deep-Sea Research*, II, 49, 4439–4459.

Chen, Y. M., Liu, J. C., Ju, Y. H., 1998. Flotation removal of algae from water. *Colloids and Surfaces B: Biointerfaces*, 12, 49–55.

Cheng, W. P., Chi, F. H., 2003. Influence of eutrophication on the coagulation efficiency in reservoir water. *Chemosphere*, 53, 773–778.

Chin Y. P., Aiken, G., O'Loughlin, E., 1994. Molecular weight, polydispersity, and spectroscopic properties of aquatic humic substances. *Environmental Science and Technology*, 28, 1853–1858.

Choppin, G. R., Allard, B., 1985. Cited in Freeman, A. J., Keller, C. (Eds.), *Handbook on the Physics and Chemistry of the Actinides*, 407–442, Elsevier Science Publishers, Amsterdam, the Netherlands.

Chorus, I., Bartram, J., 1999. *Toxic Cyanobacteria in Water: A Guide to Their Public Health Consequences*. World Health Organization, E & FN Spon Press, London.

Chow, C. W. K., van Leeuwen J. A., Fabris, R., Drikas, M., 2009. Optimised coagulation using aluminium sulfate for the removal of dissolved organic carbon. *Desalination*, 245, 120–134.

Collins, M. R., Amy, G. R., Steelink, C., 1986. Molecular weight distribution, carboxylic acidity, and humic substances content of aquatic organic matter: Implications for removal during water treatment. *Environmental Science and Technology*, 20, 1028–1032.

Collins, M. R., Vaughan, C. W., 1996. Characterization of NOM Removal by Biofiltration: Impact of Coagulation, Ozonation, and Sand Media Coating. In Minear, R.A., Amy, G.L. (Eds.), *Disinfection by Products in Water Treatment: The Chemistry of Their Formation and Control*, 449–476, Lewis Publishers, Florida.

Croué, J. P., Debroux, J. F., Amy, G. L., Aiken, G. R., Leenheer, J. A., 1999. Natural Organic Matter: Structural Characteristics and Reactive Properties. In Singer, P. C. (Ed.), *Formation and Control of Disinfection By-Products in Drinking Water*, 65–93, American Water Works Association, Denver, CO.

Croué, J. P., Lefebvre, E., Martin, B., Legube, B., 1993. Removal of dissolved hydrophobic and hydrophilic organic substances during coagulation/flocculation of surface waters. *Water Science and Technology*, 27, 143–152.

Csuros, M., Csuros, C., 1999. *Microbiological Examination of Water and Wastewater*. Lewis Publishers, U.S.

Davies, G., Ghabbour, E. A., 1998. *Humic Substances: Structures, Properties and Uses*. The Royal Society of Chemistry, UK.

Dempsey, B. A., 1989. Reactions between fulvic acids and aluminum. In: Suffet, I.N., MacCarthy, P., (Eds), *Aquatic Humic Substances: Influence on Fate and Treatment of Pollutants*, 409–424, American Chemical Society, Washington, D.C.

Dempsey, B. A., Ganho, R. M., O'Melia, C. R., 1984. The coagulation of humic substances by means of aluminum salts. *Journal of American Water Works Association*, 76, 141–150.

Dickenson, E. R. V., Amy, G. L., 2000. Natural Organic Matter Characterization of Clarified Waters Subjected to Advanced Bench-Scale Treatment Processes. In Barrett, S. E., Krasner, S. W., Amy, G. L. (Eds.), *Natural Organic Matter and Disinfection by-Products Characterization and Control in Drinking Water*, 122–138, ACS Symposium Series 761, Oxford University Press, U.S.A.

Duan, J., Gregory, J., 2003. Coagulation by hydrolysing metal salts. *Advances in Colloid and Interface Science*, 100-102, 475–502.

Edzwald, J. K., Becker, W. C. and Wittier, K. L., 1985. Surrogate parameters for monitoring organic matter and THM precursors, *Journal of American Water Works Association*, 77, 122–132.

U.S. EPA, 1999. *Enhanced Coagulation and Enhanced Precipitative Softening Guidance Manual*. Office of Water (4607). EPA 815-R-99-012. May.

Evangelou, V. P., 1998. *Environmental Soil and Water Chemistry: Principles and Applications*. John Wiley & Sons-Interscience, New York.

Ewald, M., Belin, C., Berger, P., Weber, J. H., 1983. Corrected fluorescence spectra of fulvic acids isolated from soil and water. *Environmental Science and Technology*, 17, 501–504.

Exall, K. N., vanLoon, G. W., 2003. Effects of raw water conditions on solution-state aluminum speciation during coagulant dilution. *Water Research*, 37, 3341–3350.

Frimmel, F. H., Abbt-Braun, G., 1999. Basic characterization of reference NOM from central Europe - similarities and differences. *Environment International*, 25, 191–207.

Frimmel, F. H., 1998a. Impact of light on the properties of aquatic natural organic matter. *Environment International*, 24, 559–571.

Frimmel, F. H., 1998b. Characterization of natural organic matter as major constituents in aquatic systems. *Journal of Contaminant Hydrology*, 35, 201–216.

Frimmel, F. H., Hesse, S., Kleiser, G., 2000. Technology-Related Characterization of Hydrophilic Disinfection By-Products in Aqueous Samples. In Barrett, S.E., Krasner, S.W., Amy, G.L. (Eds), *Natural Organic Matter and Disinfection By-Products Characterization and Control in Drinking Water*, 84–95, ACS Symposium Series 761, Oxford University Press, U.S.A.

Gaffney, S. J., Marley, N. A., Clark, S. B. (Eds.), 1996. *Humic and Fulvic Acids: Isolation, Structure and Environmental Role*, ACS Symposium Series, Washington, D.C.

Gjessing, E. T., Egeberg, P. K., Hakedal, J., 1999. Natural organic matter in drinking water – The “NOM-typing project”, background and basic characteristics of original water samples and NOM isolates. *Environment International*, 25, 145–159.

Gibbs, R. J., 1983. Effect of natural organic coating on the coagulation of particles. *Environmental Science and Technology*, 17, 237–240.

Gregor, J. E., Nokes, C. J., Fenton, E., 1997. Optimising natural organic matter removal from low turbidity waters by controlled Ph adjustment of aluminium coagulation. *Water Research*, 31, 2949–2958.

Guigui, C., Roucha, J. C., Durand-Bourlierb, L., Bonnelyeb, V., Aptel, P., 2002. Impact of coagulation conditions on the in-line coagulation/UFprocess for drinking water production. *Desalination*, 147, 95-100.

Harrington, G. W., Bruchet, A., Rybacki, D., Singer, P.C., 1996. Characterization of Natural Organic Matter and Its Reactivity with Chlorine. In Minear, R. A. and Amy, G. L. (Eds.), *Water Disinfection and Natural Organic Matter: Characterization and Control*, 138–158, ACS Symposium Series 649, American Chemical Society, Washington, D.C.

Henderson-Sellers, B., Markland, H. R., 1987. *Decaying Lakes: The Origins and Control of Cultural Eutrophication*, Wiley, New York.

Hendricks, D., 2006. *Water Treatment Unit Processes Physical and Chemical*, CRC Press, U.S.A.

Her, N., Amy, G., Foss, D., Cho, J., Yoon, Y., Kosenka, P., 2002. Optimization of method for detecting and characterizing NOM by HPLC - size exclusion chromatography with UV and on-line DOC detection. *Environmental Science and Technology*, 36, 1069–1076.

Her, N., Amy, G., Park, H. R., Song, M., 2004. Characterizing algogenic organic matter (AOM) and evaluating associated NF membrane fouling. *Water Research*, 38, 1427–1438.

Hu, C., Liu, H., Qu, J., Wang, D., Ru, J., 2006. Coagulation behavior of aluminum salts in eutrophic water: significance of Al₁₃ species and pH control. *Environmental Science and Technology*, 40, 325–331.

Iriarté-Velasco, U., Alvarez-Uriarte, J. I., Gonzalez-Velasco, J. R., 2007. Enhanced coagulation under changing alkalinity-hardness conditions and its implications on trihalomethane precursors removal and relationship with UV absorbance. *Separation and Purification Technology*, 55, 368–380.

ISKI Istanbul Water and Sewerage Administration Home Page. http://www.iski.gov.tr/Web/UserFiles/File/su_kalite_raporu/swf/WATERQUALITY_FEBRUARY2010.swf . (accessed July 2010) .

Jarvis, P., Jefferson, B., Parsons, S. A., 2004. Characterising natural organic matter flocs. *Water Science and Technology: Water Supply*, 4, 79–87.

Jarvis, P., Jefferson, B., Parsons, S. A., 2005. How the natural organic matter to coagulant ratio impacts on floc structural properties. *Environmental Science and Technology*, 39, 8919–8924.

Jarvis, P., Jefferson, B., Parsons, S. A., 2006. Floc structural characteristics using conventional coagulation for a high doc, low alkalinity surface water source. *Water Research*, 40, 2727–2737.

Jones, M. N., Bryan, N. D., 1998. Colloidal properties of humic substances. *Advances in Colloid and Interface Science*, 78, 1–48.

Jung, A. V., Chanudet, V., Ghanbaja, J., Lartiges, B. S., Bersillon, J. L., 2005. Coagulation of humic substances and dissolved organic matter with a ferric salt: An electron energy loss spectroscopy investigation. *Water Reserch*, 39, 3849–3862.

Karentz, D., Bothwell, M. L., Coffin, R. B., Hanson, A., Herndl, G. J., Kilham, S. S., Lesser, M. P., Lindell, M., Moeller, R. E., Morris, D. P., Neale, P. J., Sanders, R. W., Weiler, C. S., Wetzel, R. G., 1994. Impact of UV-B radiation on pelagic freshwater ecosystems: Report of working group on bacteria and phytoplankton. *Archiv für Hydrobiologie, Beiheft See Ergebnisse der Limnologie*, 43, 31–69.

Kerç, A., 2002. Oxidation of Aqueous Humic Substances by Ozonation, Ph.D. Thesis, Boğaziçi University.

Kerc, A., Bekbolet, M., Saatci, A. M., 2003. Effect of partial oxidation by ozonation on the photo catalytic degradation of humic acids. *International Journal of Photoenergy*, 5, 75–80.

Killops, S., Killops, V., 2005. *Introduction to Organic Geochemistry*, Blackwell Science Ltd., U.S.A.

Kim, C.-H., Hosomi, M., Murakami, A., Okada, M., 1994. Effects of clay on the fouling by organic substances in potable water treatment by ultrafiltration. *Water Science and Technology*, 30, 159–168.

Kim, S. J., Chian, E. S. K., Saunders, F. M., Perdue, E. M., Giabbai, M. F., 1989. Characteristics of Humic Substances and Their Removal Behaviour in Water Treatment. In Suffet, I. H., MacCarthy, P. (Eds), *Aquatic Humic Substances Influence on Fate and Treatment of Pollutants*, 473- 497, American Chemical Society, U.S.A.

Korshin, G. V., Li, C. W., 1996. Monitoring the properties of natural organic matter through UV spectroscopy: a consistent theory. *Water Research*, 31, 1787–1795.

Lagus, A., Suomela, J., Weithoff, G., Heikkilä, K., Helminen, H., Sipura, J., 2004. Species-specific differences in phytoplankton responses to N and P enrichments and the N:P ratio in the Archipelago Sea, northern Baltic Sea. *Journal of Plankton Research*, 26, 779–798.

LeChevallier, M. W., 1990. Coliform regrowth in drinking water: A review. *Journal of American Water Works Association*, 82, 74–86.

LeChevallier, M. W., Schulz, W., Lee, R. G., 1991. Bacterial nutrients in drinking water. *Applied and Environmental Microbiology*, 57, 857–862.

Leenheer, J. A., Croué, J. P., 2003. Characterizing aquatic dissolved organic matter. *Environmental Science and Technology*, 37, 18A–26A.

Lefebvre, E., Legube, B., 1993. *Water Research*, 27, 433–447. Cited in Vilg -Ritter, 1999b.

Lester, J. N., Birkett, J. W., 1999. *Microbiology and Chemistry for Environmental Scientists and Engineers*. E & FN Spon, New York.

Lorentsson, A. V., Chernoberezhskii, Y. M., Dyagileva, A. B., 2002. Determination of the optimal conditions for the coagulation-based water purification using modified coagulation test. *Colloid Journal*, 64, 87–89.

Ma, J., Li, G., 1993. Laboratory and Full Scale Plant Studies of Permanganate Oxidation as An Aid in Coagulation. In Ives, K.J., Bernhardt, H., *Control of Organic Material by Coagulation and Floc-Separation Processes*, Proceedings of the Second Conference of the IAWQ-IWSA Joint Specialist Group on Coagulation, Flocculation, Filtration, Sedimentation and Floatation, Geneva, 1-3 September 1992, *Water Science and Technology*, 27, 47–54.

Ma, J., Liu, W., 2002. Effectiveness and mechanism of potassium ferrate (VI) preoxidation for algae removal by coagulation. *Water Research*, 36, 871–878.

MacCarthy, P., Suffet, I. H., 1989. Aquatic Humic Substances and Their Influence on the Fate and Treatment of Pollutants. In Suffet, I.H., MacCarthy, P. (Eds), Aquatic Humic Substances Influence on Fate and Treatment of Pollutants, American Chemical Society, U.S.A.

McCarthy, J. F., Jimenez, B. D., 1985. Reduced bioavailability to bluegills of polycyclic aromatic hydrocarbons bound to dissolved humic material. *Environ. Toxicol. Chemistry*, 4, 511-521.

Manahan, S. E., 2010. *Environmental Chemistry* (9th Ed.). CRC Press, U.S.A.

Masion, A., Vilg -Ritter, A., Rose, J., Stone, W. E. E., Teppen , B. J., Rybacki , D., Bottero, J., 2000. Coagulation-flocculation of natural organic matter with Al salts: speciation and structure of the aggregates. *Environmental Science and Technology*, 34, 3242–3246.

Miettinen, I. T., Vartiainen, T., Martikainen, P. J., 1997. Phosphorus and bacterial growth in drinking water. *Applied and Environmental Microbiology*, 63, 3242–3245.

Minear, R. A., Amy, G. L. (Eds.), 1996. *Disinfection by Products in Water Treatment: The Chemistry of Their Formation and Control*, 449–476, Lewis Publishers, Florida.

Monod, J., 1949. The growth of bacterial cultures. *Annual Reviews of Microbiology*, 3, 371–394.

Nikolaou, A., Rizzo, L., Selcuk, H. (Eds.), 2007. *Control of Disinfection By-Product in Drinking Water Systems*, Nova Science Publishers, Inc., New York.

Nissinen, T. K., Miettinen, I. T., Martikainen, P. J., Vartiainen T., 2001. Molecular size distribution of natural organic matter in raw and drinking waters. *Chemosphere*, 45, 865–873.

Nollet, L. M., 2000. Handbook of Water Analysis, Marcel Dekker Inc., New York, U.S.A.

O'Melia, C. R., Yao, C., Gray, K., Tobiason, J. E., 1987. 'Raw Water Quality, Coagulant Selection, and Solid-Liquid Separation', AWWA Conference on Influence of Coagulation on the Selection, Operation and Performance of Water Treatment Facilities, AWWA Annual Conference, Kansas City, Missouri. In Srinivasan, P. T., Viraraghavan, T., 2003. Influence of natural organic matter (NOM) on the speciation of aluminum during water treatment. *Water, Air, & Soil Pollution*, 152, 35–54.

Owen, D. M., Amy, G. L., Chowdhury, Z. K., Paode, R., McCoy, G., Viscosil, K., 1995. NOM characterization and treatability. *Journal of American Water Works Association*, 87, 46–63.

Peuravuori, J., Koivikko, R., Pihlaja, K., 2002. Characterization, differentiation and classification of aquatic humic matter separated with different sorbents: synchronous scanning fluorescence spectroscopy. *Water Research*, 36, 4552–4562.

Peuravuori, J., Pihlaja, K., 1997. Isolation and characterization of natural organic matter from lake water: comparison of isolation with solid adsorption and tangential membrane filtration. *Environment International*, 23, 441–451.

Peuravuori, J., Pihlaja, K., 2006. Characterization of Freshwater Humic Matter. In *Handbook of Water Analysis*, Taylor and Francis Group, LLC Press.

Pinheiro, J. P., Mota, A. M., Benedetti, A. M., 2000. Effect of aluminum competition on lead and cadmium binding to humic acids at variable ionic strength. *Environmental Science and Technology*, 34, 5137–5143.

Pivokonsky, M., Kloucek, O., Pivokonska, L., 2006. Evaluation of the production, composition and aluminum and iron complexation of algogenic organic matter. *Water Research*, 40, 3045–3052.

Randtke, S. J., 1988. Organic contaminant removal by coagulation and related process combinations. *Journal of American Water Works Association*, 80, 40–56.

Reckhow, D. A., Singer, P. C., Malcolm, R. L., 1990. Chlorination of humic materials: byproduct formation and chemical interpretations. *Environmental Science and Technology*, 24, 1655–1664.

Schäfer, A. I., Fane, A. G., Waite, T. D., 2001. Cost factors and chemical pretreatment effects in the membrane filtration of waters containing natural organic matter. *Water Research*, 35, 1509–1517.

Schäfer, A. I., Schwicker, U., Fischer, M. M., Fane, A. G., Waite, T. D., 2000. Microfiltration of colloids and natural organic matter. *Journal of Membrane Science*, 171, 151–172.

Schnitzer, M., 1972. Cited in Steinberg, C. E. W., 2003.

Schnitzer, M., Khan, S. U., 1972. *Humic Substances in the Environment*, Marcel Decker, New York.

Schulten, H. R., 1996. A New Approach to the Structural Analysis of Humic Substances in Water and Soils. In Gaffney, S. J., Marley, N. A., Clark, S. B. (Eds.), *Humic and Fulvic Acids: Isolation, Structure and Environmental Role*, 43-56, ACS Symposium Series, Washington, D.C.

Schulten, H. R., Schnitzer, M., 1993. Cited in Jones, M. N., Bryan, N. D., 1998.

Semmens, M. J., Staples, A. B., 1986. The nature of organics removed during treatment of Mississippi river water. *Journal of American Water Works Association*, 78, 76–81.

Şen, S., 2004. Effects of Ozonation, Photocatalytic Oxidation, and Sequential Oxidation on Coagulation of Humic Acids, M.S. Thesis, Boğaziçi University.

Sen-Kavurmaci, S., Bekbolet, M., 2010. The role of oxidative treatment on the trivalent cation complexation properties of natural organic matter. *Journal of Advanced Oxidation Technologies*, 13, 212–220.

Sharp, E. L., Jarvis, P., Parsons, S. A., Jefferson, B., 2006. Impact of fractional character on the coagulation of NOM. *Colloids and Surfaces A: Physicochemical Engineering Aspects*, 286, 104–111.

Shaw, D. J., 1966. Cited in Tchobanoglous, G., Burton, F. L., Stensel, H. D., 2003.

Shi, B. Y. Wei, Q. S., Wang, D. S., Zhu, Z., Tang, H. X., 2007. Coagulation of humic acid: The performance of preformed and non-preformed Al species. *Colloids Surfaces A: Physicochemical Engineering Aspects*, 296, 148–148.

Shin, J. Y., Spinette, R. F., O'Melia, C. R., 2008. Stoichiometry of coagulation revisited. *Environmental Science and Technology*, 42, 2582–2589.

Siéiliéchi, J. M., Lartiges, B. S., Kayem, G. J., Hupont, S., Frochot, C., Thieme, J., Ghanbaja, J., d'Espinose de la Caillerie, J. B., Barres, O., Kamga, R., Levitz, P., Michot, L. J., 2008. Changes in humic acid conformation during coagulation with ferric chloride: Implications for drinking water treatment. *Water Research*, 42, 2111–2123.

Sierra, M. M. D., Giovanela, M., Parlanti, E., Soriano-Sierra, E. J., 2005. Fluorescence fingerprint of fulvic and humic acids from varied origins as viewed by single-scan and excitation/emission matrix techniques. *Chemosphere*, 58, 715–733.

Sigee, D. C., 2005. *Freshwater Microbiology: Biodiversity and Dynamic Interactions of Microorganisms in The Freshwater Environment*, John Wiley & Sons, England.

Smith, V. H., 1983. Low nitrogen to phosphorus ratios favor dominance by blue-green algae in lake phytoplankton. *Science*, 221, 669–671.

Smith, V. H., Tilman, G. D., Nekola, J. C., 1999. Eutrophication: impacts of excess nutrient inputs on freshwater, marine, and terrestrial ecosystems. *Environmental Pollution*, 100, 179–96.

Smith, E. J., Davison, W., Hamilton-Taylor, J., 2002. Methods for preparing synthetic freshwaters. *Water Research*, 36, 1286–1296.

Søndergaard, M., Schierup, H. H., 1982. Dissolved organic carbon during a spring diatom bloom in Lake Moss, Denmark. *Water Research*, 16, 815.

Srinivasan, P. T., Viraraghavan, T., 2003. Influence of natural organic matter (NOM) on the speciation of aluminum during water treatment. *Water, Air, and Soil Pollution*, 152, 35–54.

Steinberg, C. E. W., 2003. *Ecology of Humic Substances in Freshwaters: Determinants from Geochemistry to Ecological Niches*, Springer-Verlag Berlin Heidelberg, Germany.

Steinberg, C. E. W., Kamara, S., Prokhotskaya, V. Y., Manusadzianas, L., Karasyova, T. A., Timofeyev, M. A., Jie, Z., Paul, A., Meinelt, T., Farjalla, V. F., Matsuo, A. Y. O., Burnison, B. K., Menzel, R., 2006. Special Review: Dissolved humic substances – ecological driving forces from the individual to the ecosystem level. *Freshwater Biology*, 51, 1189–1210.

Suffet, I. H., MacCarthy, P. (Eds), 1989. *Aquatic Humic Substances Influence on Fate and Treatment of Pollutants*, American Chemical Society, U.S.A.

Tadanier, C. J., Berry, D. F., Knocke, W. R., 2000. Dissolved organic matter apparent molecular weight distribution and number-average apparent molecular weight by batch ultrafiltration. *Environmental Science and Technology*, 34, 2348–2353.

Tchobanoglous, G., Burton, F. L., Stensel, H. D., 2003. Waste Water Engineering: Treatment and Reuse. Metcalf & Eddy, Inc., 4th Edition, McGraw-Hill Companies, Inc., New York.

Thebault, J. M., Qotbi, A., 1999. A model of phytoplankton development in the Lot River (France): Simulations of scenarios. *Water Research*, 33, 1065-1079.

Thurman, E. M., 1985. *Organic Geochemistry of Natural Waters*. Martinus Nijhoff/Dr W. Junk Publishers, Dordrecht, Germany.

Thurman, E. M., 1986. *Organic Geochemistry of Natural Waters*. Kluwer Academic Publisher., Hingham, MA.

Tulonen, T., 2004. Role of Allochthonous and Autochthonous Dissolved Organic Matter (DOM) as A Carbon Source for Bacterioplankton in Boreal Humic Lakes, Academic Dissertation in Hydrobiology, Ph.D. Thesis, Faculty of Biosciences Department of Biological and Environmental Sciences Aquatic Sciences/Hydrobiology, University of Helsinki.

Uyguner, C. S., 2005. Elucidation of the Photocatalytic Removal Pathways of Humic Substances: Progress Towards Mechanistic Explanations, Ph.D. Thesis, Boğaziçi University.

Uyguner, C. S., Bekbolet, M., 2005a. Implementation of spectroscopic parameters for practical monitoring of natural organic matter. *Desalination*, 176, 47–55.

Uyguner, C. S., Bekbolet, M., 2005b. Evaluation of humic acid photocatalytic degradation by UV-vis and fluorescence spectroscopy. *Catalysis Today*, 101, 267–274.

Uyguner, C. S., Suphandag, S. A., Kerc, A., Bekbolet, M., 2007. Evaluation of adsorption and coagulation characteristics of humic acids preceded by alternative advanced oxidation techniques. *Desalination*, 210, 183–193.

- van Benschoten, J. E., Edzwald, J. K., 1990. Measuring aluminum during water treatment: methodology and application. *Journal of American Water Works Association*, 82, 71.
- van der Kooji, D., 1992. Assimilable organic carbon as an indicator of bacterial regrowth. *Journal of American Water Works Association*, 84, 57–65.
- vanLoon G. W. V., Duffy, S. J., 2005. *Environmental Chemistry: A Global Perspective*, Oxford University Press, New York.
- Vasconcelos, V., 2006. Eutrophication, toxic cyanobacteria and cyanotoxins: When ecosystems cry for help. *Limnetica*, 25, 425–432.
- Del Vecchio, R., Blough, N. V., 2004. On the origin of the optical properties of humic substances. *Environmental Science and Technology*, 38, 3885.
- Vilgé-Ritter, A., Masion, A., Boulang, T., Rybacki, D., Bottero, J.Y., 1999a. Removal of natural organic matter by coagulation-flocculation: A pyrolysis-GC-MS study. *Environmental Science and Technology*, 33, 3027–3032.
- Vilgé-Ritter, A., Rose, J., Masion, A., Bottero, J. Y., Laine, J. M., 1999b. Chemistry and structure of aggregates formed with Fe-salts and natural organic matter. *Colloids and Surfaces A: Physicochemical and Engineering Aspects*, 147, 297–308.
- Vlaski, A., van Breemen, A., Alaerts, G., 1996. Optimisation of coagulation conditions for the removal of cyanobacteria by dissolved air flotation or sedimentation. *Journal of Water Supply: Research and Technology – Aqua*, 45, 253–261.
- Volk, C., Bell, K., Ibrahim, E., Verges, D., Amy, G., Lechevallier, M., 2000. Impact of enhanced and optimized coagulation on removal of organic matter and its biodegradable fraction in drinking water. *Water Research*, 12, 3247–3257.

Volk, C. J., 2001. Biodegradable Organic Matter Measurement and Bacterial Regrowth in Potable Water. In Doyle, R. J. (Ed.), *Methods in Enzymology*, Volume 337, Microbial Growth in Biofilms, Part B: Special Environments and Physicochemical Aspects, 144–170, Academic Press, U.S.A.

Waiser, M. J., Robarts, R. D., 2000. Changes in composition and reactivity of allochthonous dissolved organic matter in a prairie saline lake. *Limnology and Oceanography*, 45, 763–774.

Wall, N. A., Choppin, G. R., 2003. Humic acids coagulation: influence of divalent cations. *Applied Geochemistry*, 18, 1573–1582.

Wang, G., Hsieh, S., 2001. Monitoring natural organic matter in water with scanning spectrophotometer. *Environment International*, 26, 205–212.

Weishaar, J. L., Aiken, G. R., Bergamaschi, B. A., Fram, M. S., Fujii, R., Mopper, K., 2003. Evaluation of specific ultraviolet absorbance as an indicator of the chemical composition and reactivity of dissolved organic carbon. *Environmental Science and Technology*, 7, 4702–4708.

Wershaw, R. L., Leenheer, J. A., Cox, L., 2005. Characterization of dissolved and particulate natural organic matter (NOM) in Neversink Reservoir. U.S. Geological Survey Scientific Investigations Reports, 5108, U.S. Department of the Interior, New York.

Wetzel, R. G., 2001. *Limnology: Lake and River Ecosystem*. Elsevier, USA.

Wilkinson, K. J., Negre, J. C., Buffle, J., 1997. Coagulation of colloid material in surface waters: the role of natural organic matter. *Journal of Contaminant Hydrology*, 26, 229–243.

Xi, W., Rong, W., Fane, A. G., Fook-Sin, W., 2004. Influence of ionic composition on NOM size and removal by ultrafiltration. *Water Science and Technology: Water Supply*, 4, 197–204.

Yu, J., Wang, D., Yan, M., 2007. Optimized coagulation of high alkalinity, low temperature and particle water: pH adjustment and polyelectrolytes as coagulant aids. *Environmental Monitoring and Assessment*, 131, 377–386.

Zajic., J. E., 1971a. *Water Pollution: Disposal and Reuse*, v.1, Marcell Dekker, Inc., New York.

Zajic., J. E., 1971b. *Water Pollution: Disposal and Reuse*, v.2, Marcell Dekker, Inc., New York.

Zhao. H., CHengzhi, H., Huijuan. L., Zhao. X., Jiuhei., Q., 2008. Role of aluminum speciation in the removal of disinfection byproduct precursors by coagulation process. *Environmental Science and Technology*, 42, 5752-5758.

Zhao., Y. Z., Gu, J. D., Fan, X. J., Li, H. B., 2006. Molecular size distribution of dissolved organic matter in water of the Pearl River and trihalomethane formation characteristics with chlorine and chlorine dioxide treatments. *Journal of Hazardous Materials*, B134, 60–66.

Ziegmann, M., Abert, M., Müller, M., Frimmel, F. H., 2010. Use of fluorescence fingerprints for the estimation of bloom formation and toxin production of *Microcystis aeruginosa*. *Water Research*, 44, 195-204.

**APPENDIX A: UV-VIS SPECTRA FOR COAGULATION WITH
ALUM AT PH CONDITIONS OF 5.5, 6.5, 7.0**

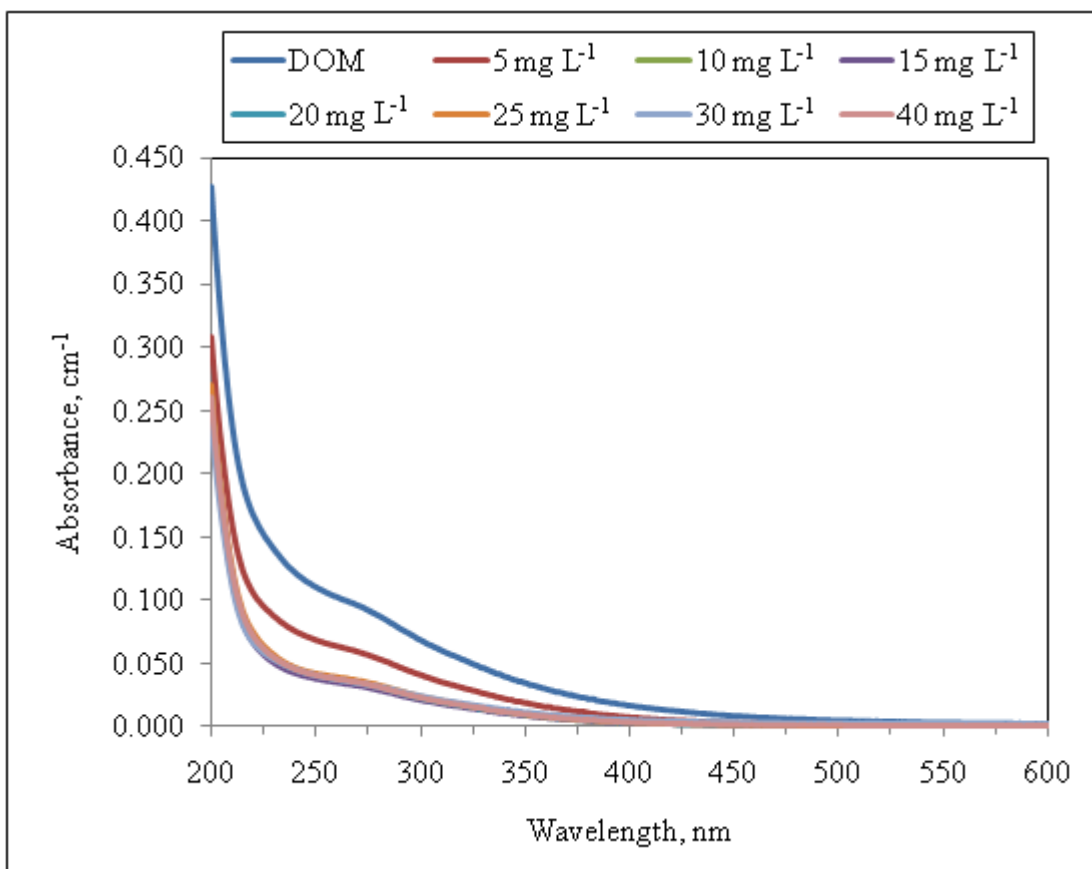


Figure A.1. UV-vis spectra of coagulation with alum at pH 5.5.

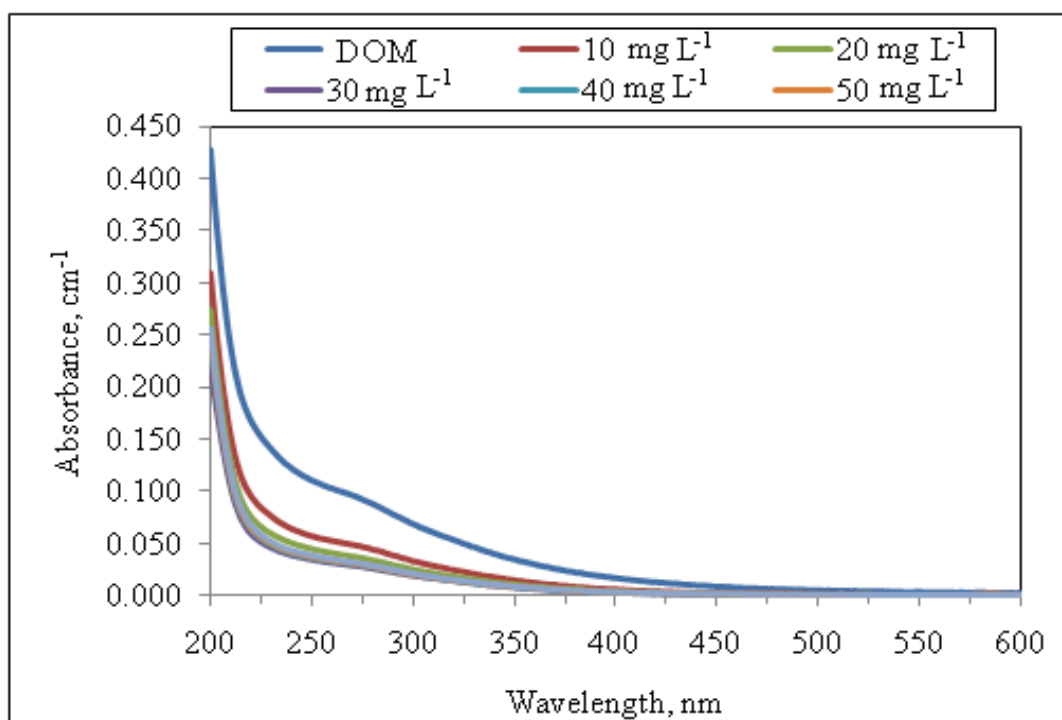


Figure A.2. UV-vis spectra of coagulation with alum at pH 6.5.

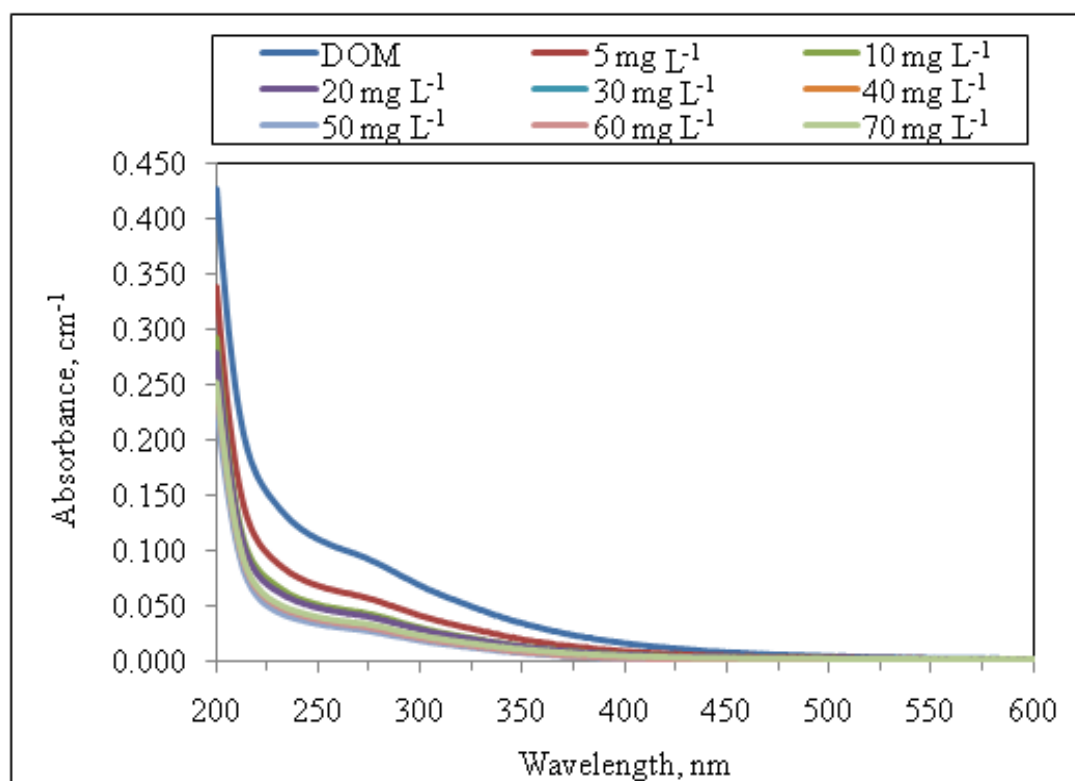


Figure A.3. UV-vis spectra of coagulation with alum at pH 7.0.

**APPENDIX B: FLUORESCENCE SPECTRA FOR COAGULATION
WITH ALUM AT PH CONDITIONS OF 5.5, 6.5, 7.0**

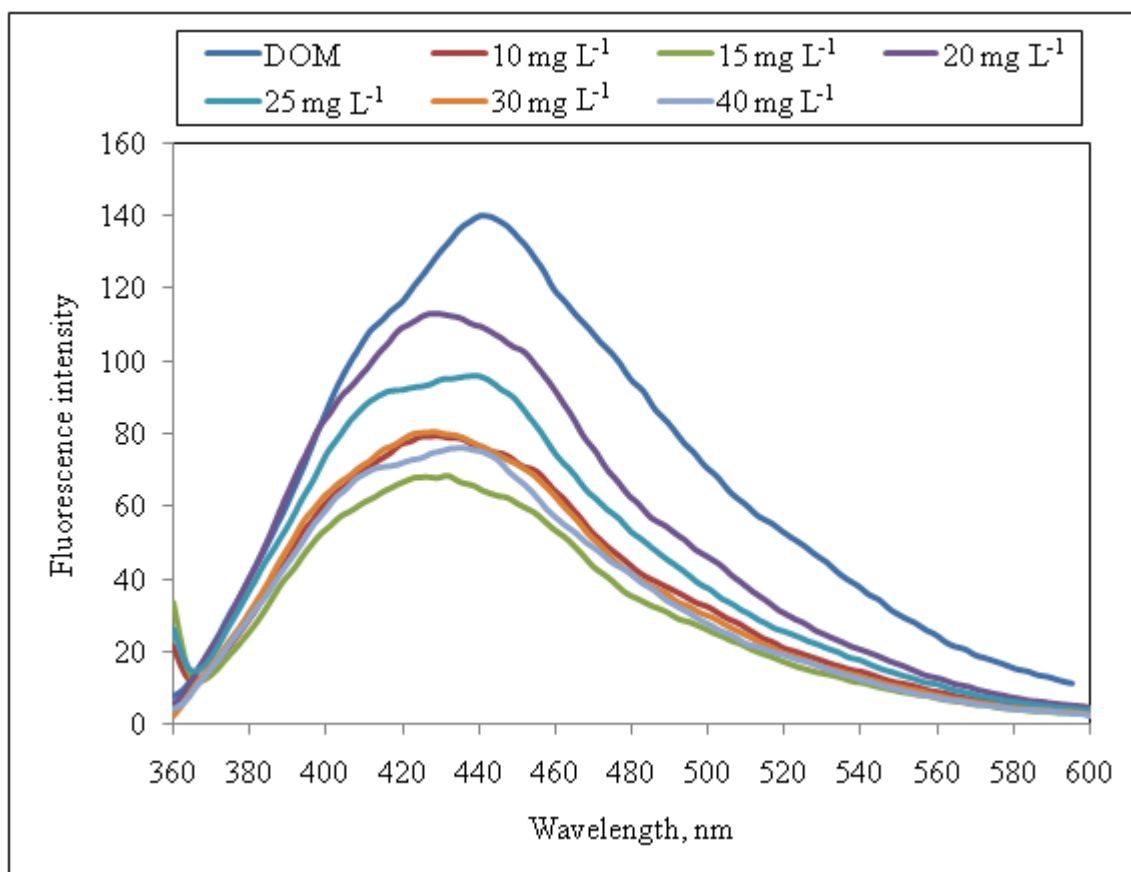


Figure B.1. Fluorescence emission₃₅₀ spectra of the DOM sample after coagulation with alum at pH 5.5.

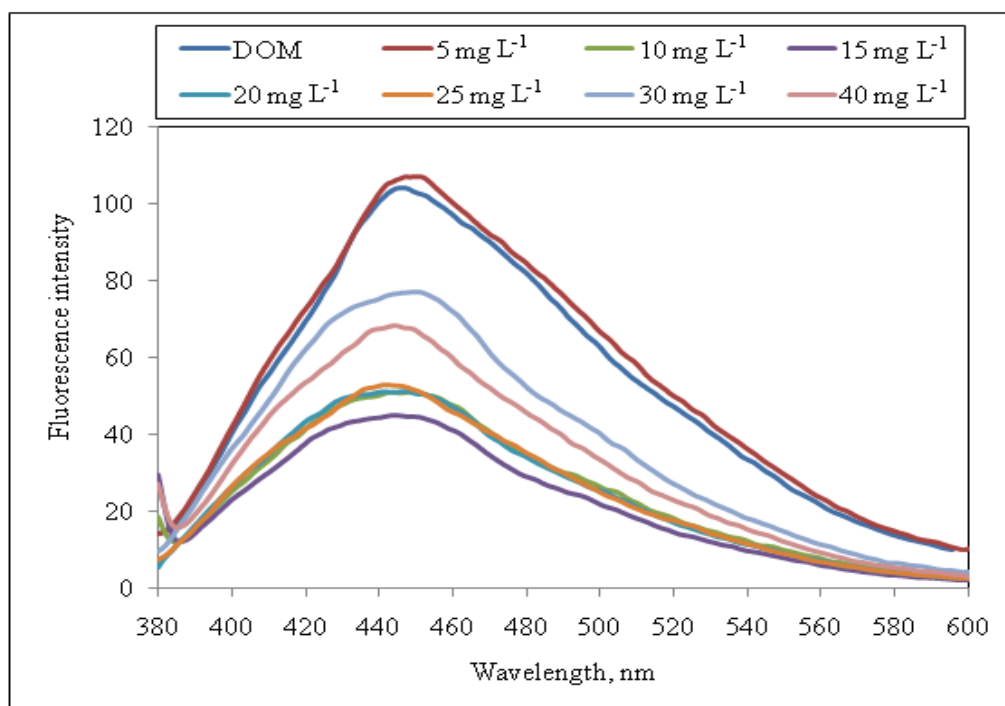


Figure B.2. Fluorescence emission₃₇₀ spectra of the DOM sample after coagulation with alum at pH 5.5.

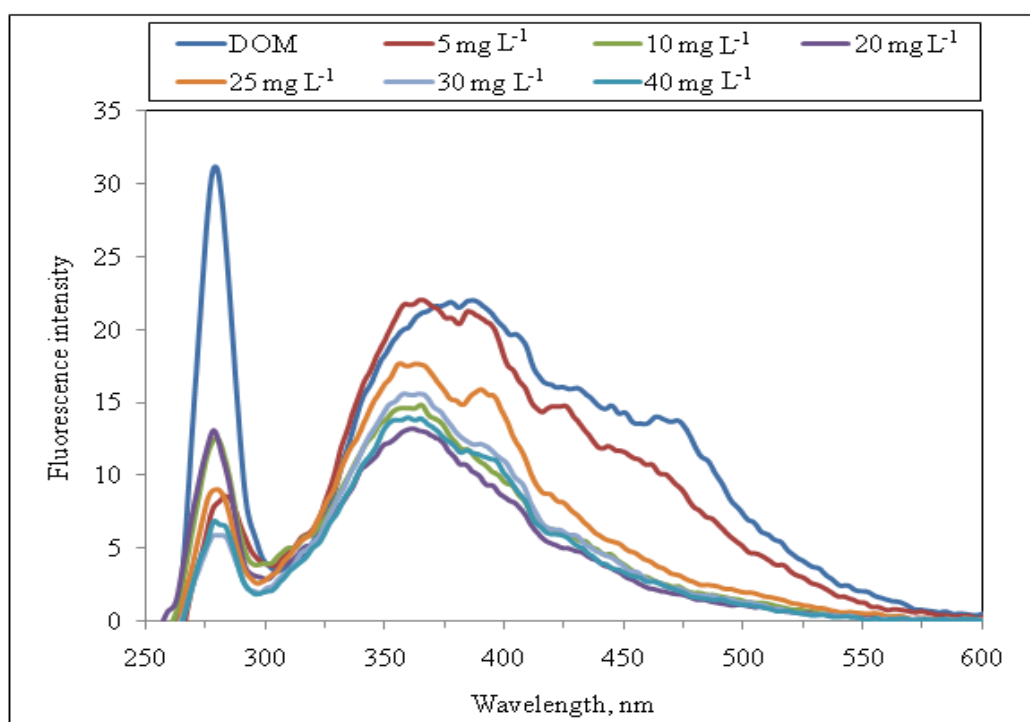


Figure B.3. Fluorescence synchronous spectra of the DOM sample after coagulation with alum at pH 5.5.

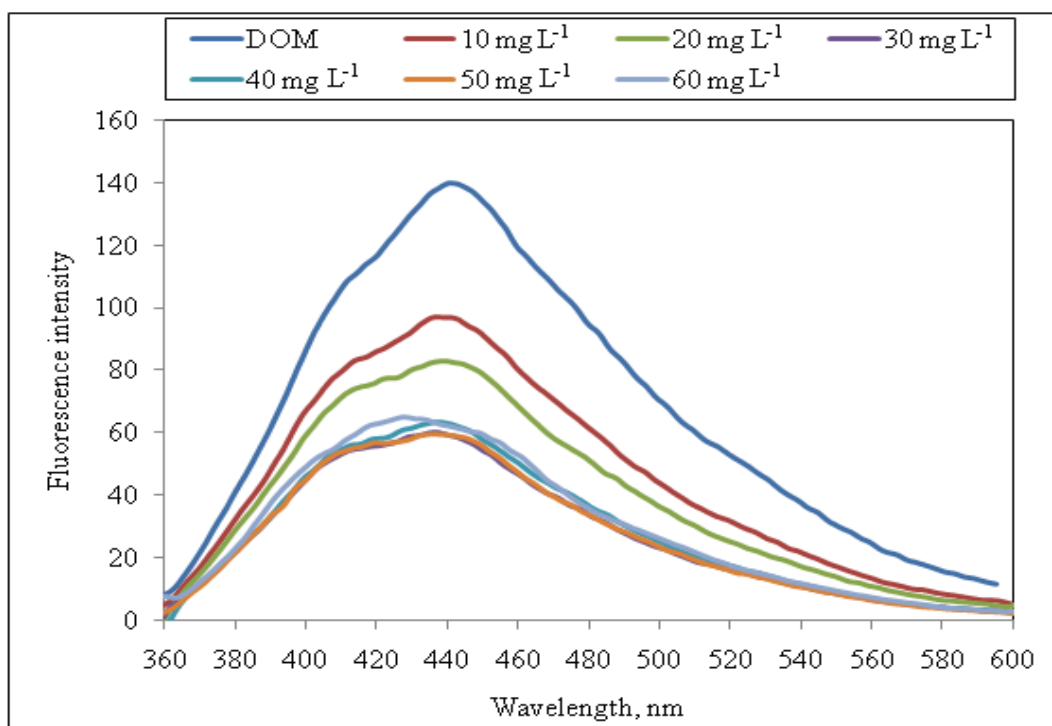


Figure B.4. Fluorescence emission₃₅₀ spectra of the DOM sample after coagulation with alum at pH 6.5

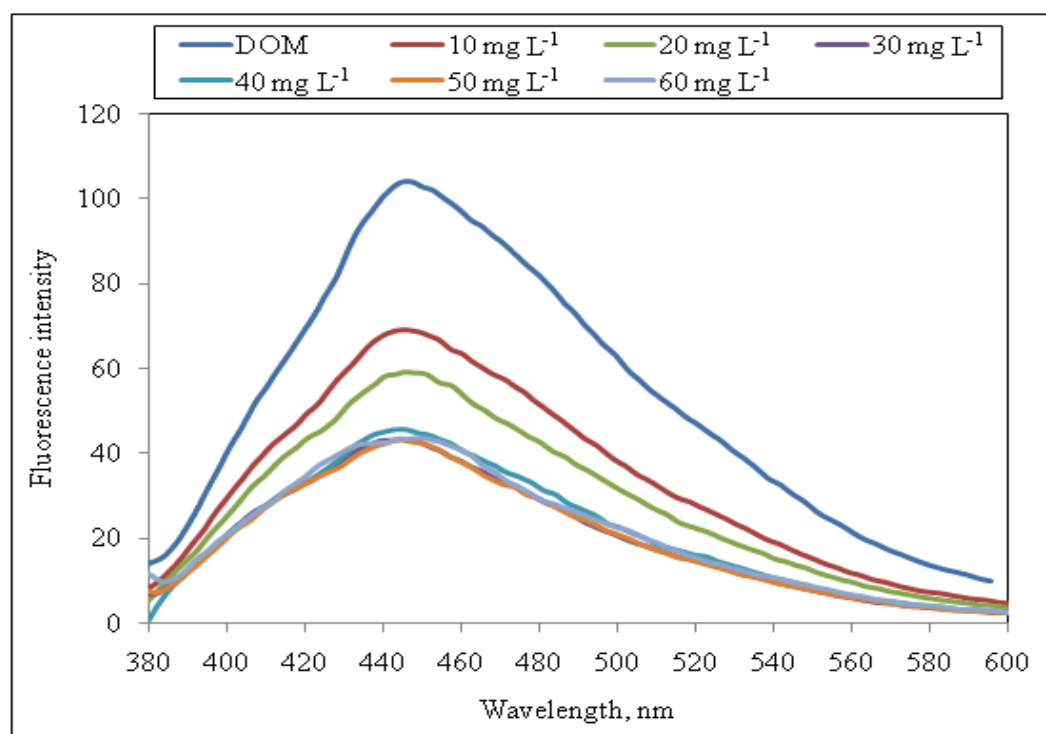


Figure B.5. Fluorescence emission₃₇₀ spectra of the DOM sample after coagulation with alum at pH 6.5.

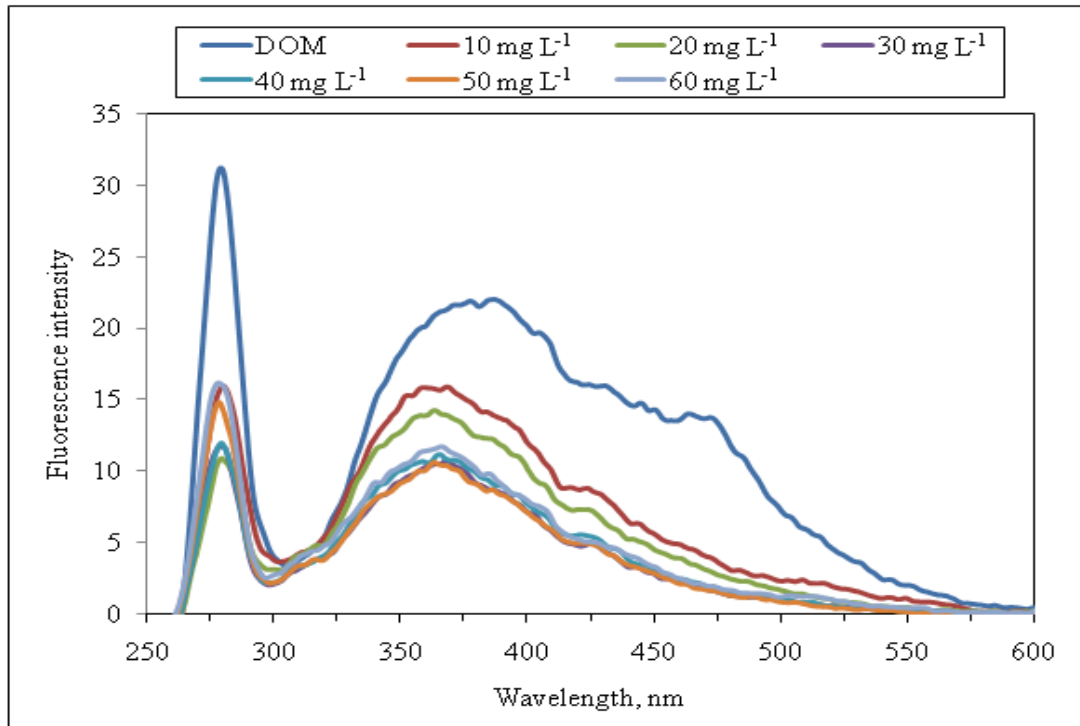


Figure B.6. Fluorescence synchronous spectra of the DOM sample after coagulation with alum at pH 6.5.

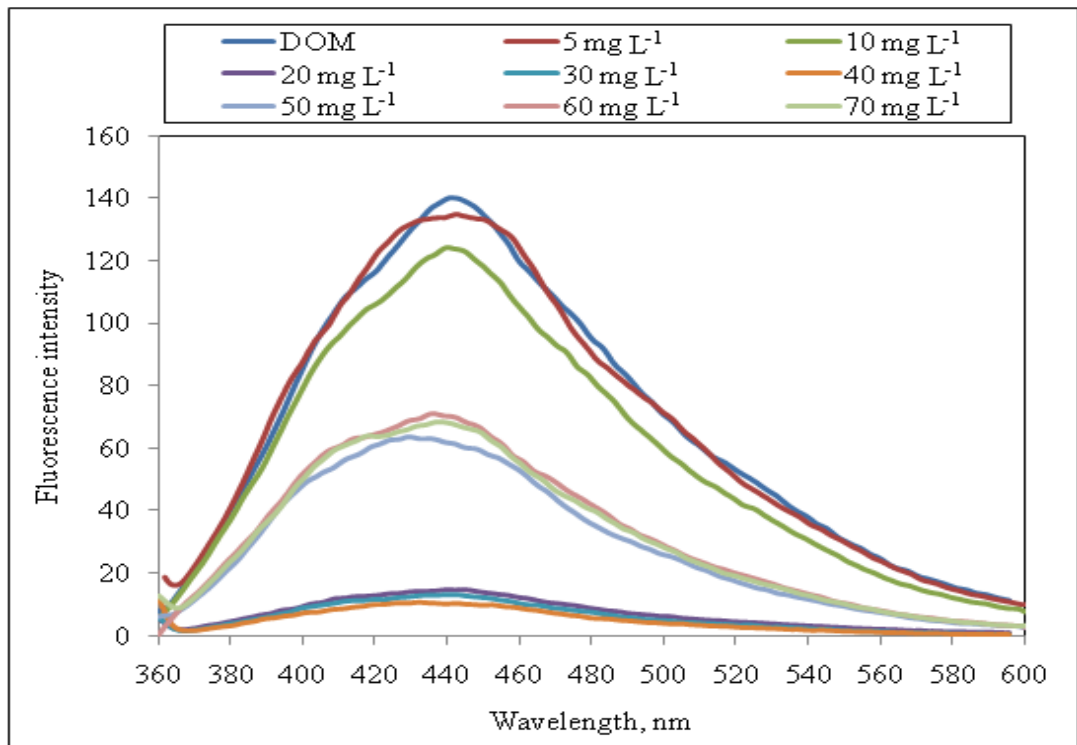


Figure B.7. Fluorescence emission₃₅₀ spectra of the DOM sample after coagulation with alum at pH 7.0.

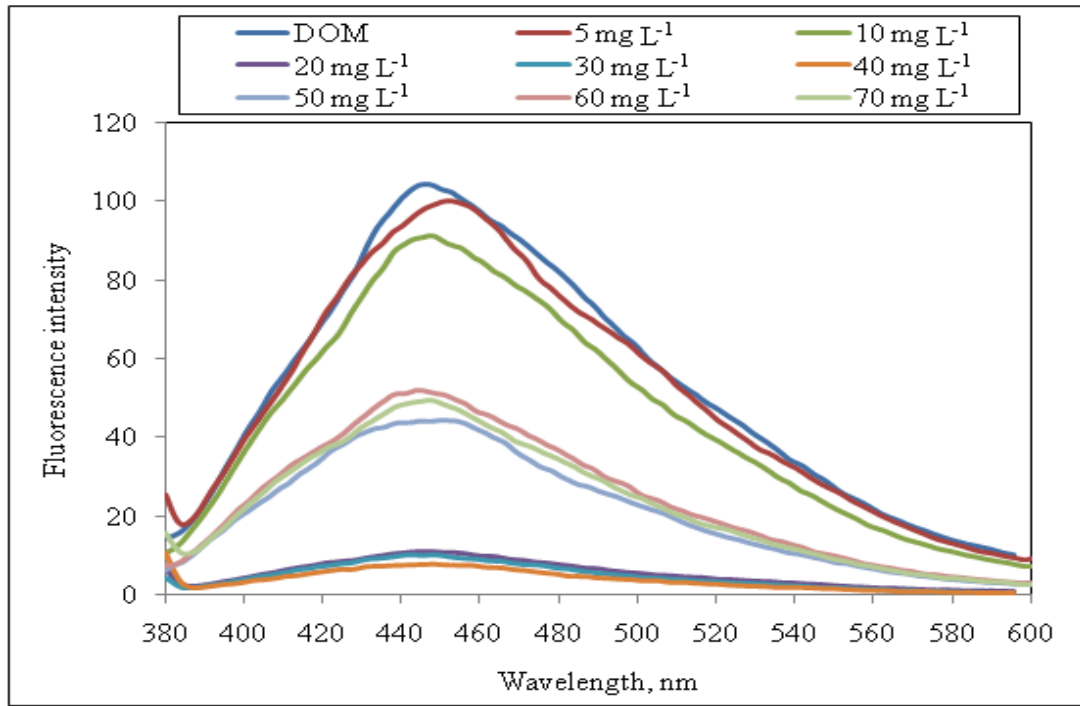


Figure B.8. Fluorescence emission₃₇₀ spectra of the DOM sample after coagulation with alum at pH 7.0.

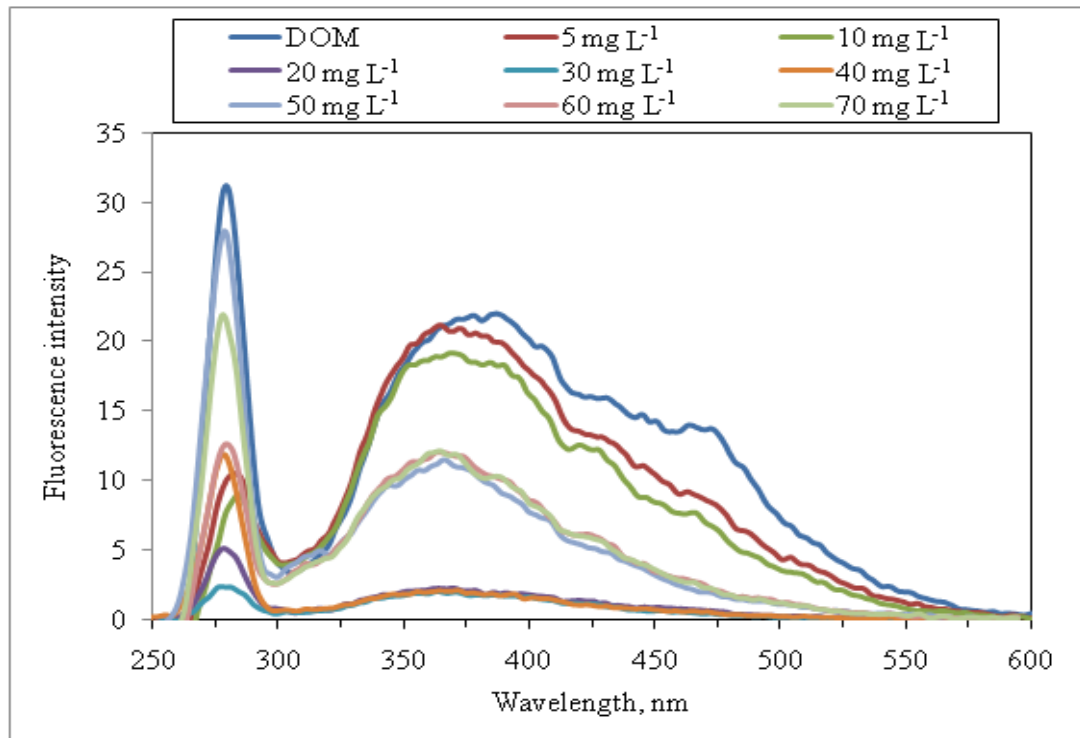


Figure B.9. Fluorescence synchronous spectra of the DOM sample after coagulation with alum at pH 7.0.

**APPENDIX C: UV-VIS SPECTRA FOR COAGULATION WITH
FERRIC CHLORIDE AT PH CONDITIONS OF 6.0, 6.5, 7.0**

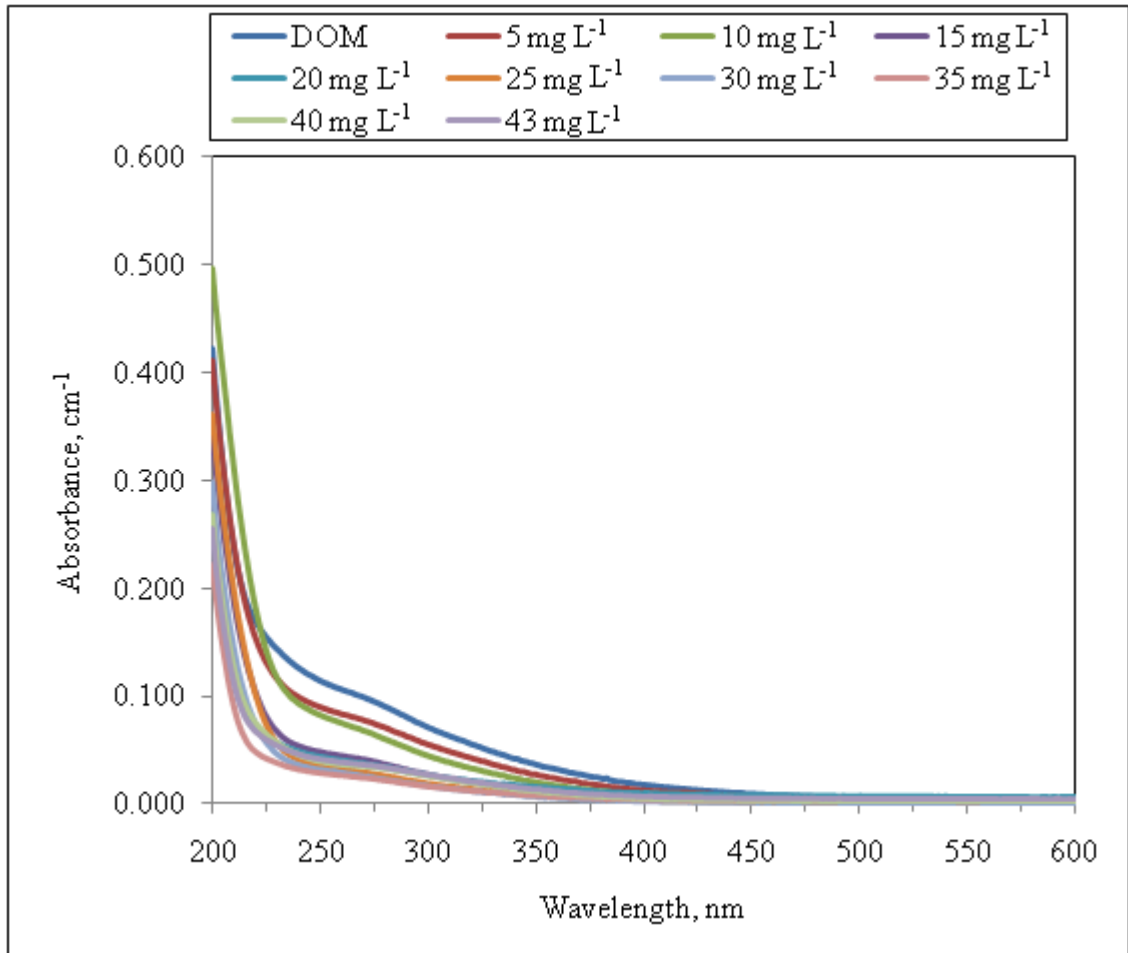


Figure C.1. UV-vis spectra of coagulation with ferric chloride at pH 6.0.

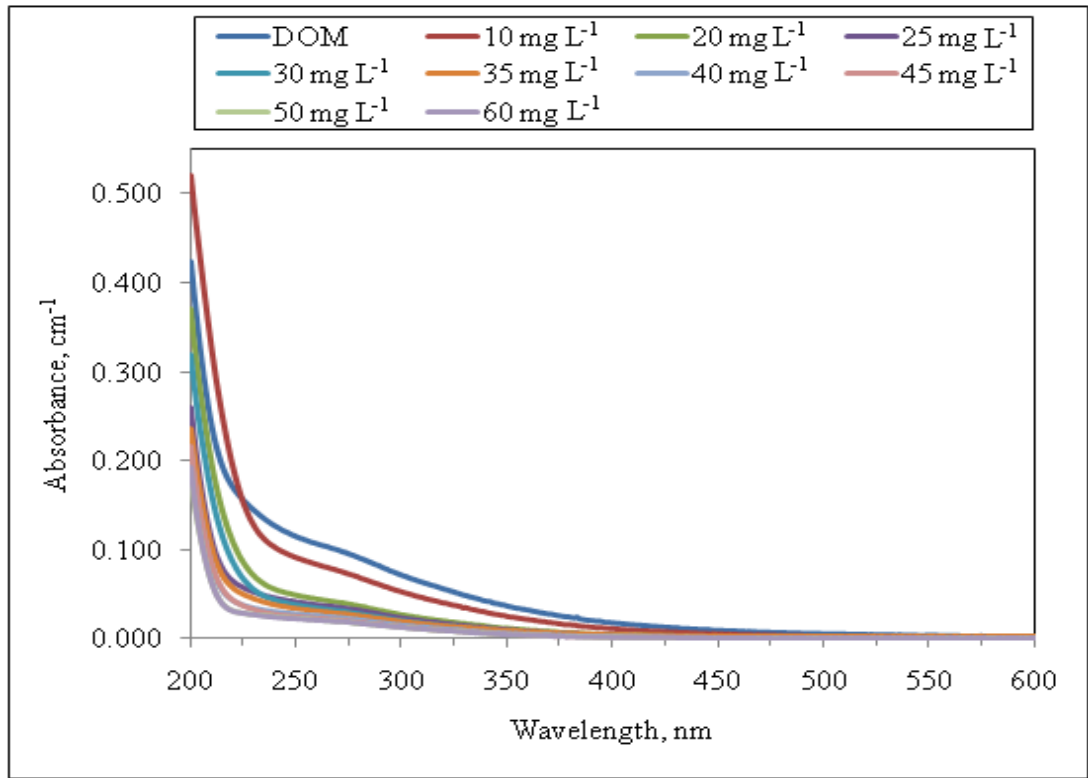


Figure C.2. UV-vis spectra of coagulation with ferric chloride at pH 6.5.

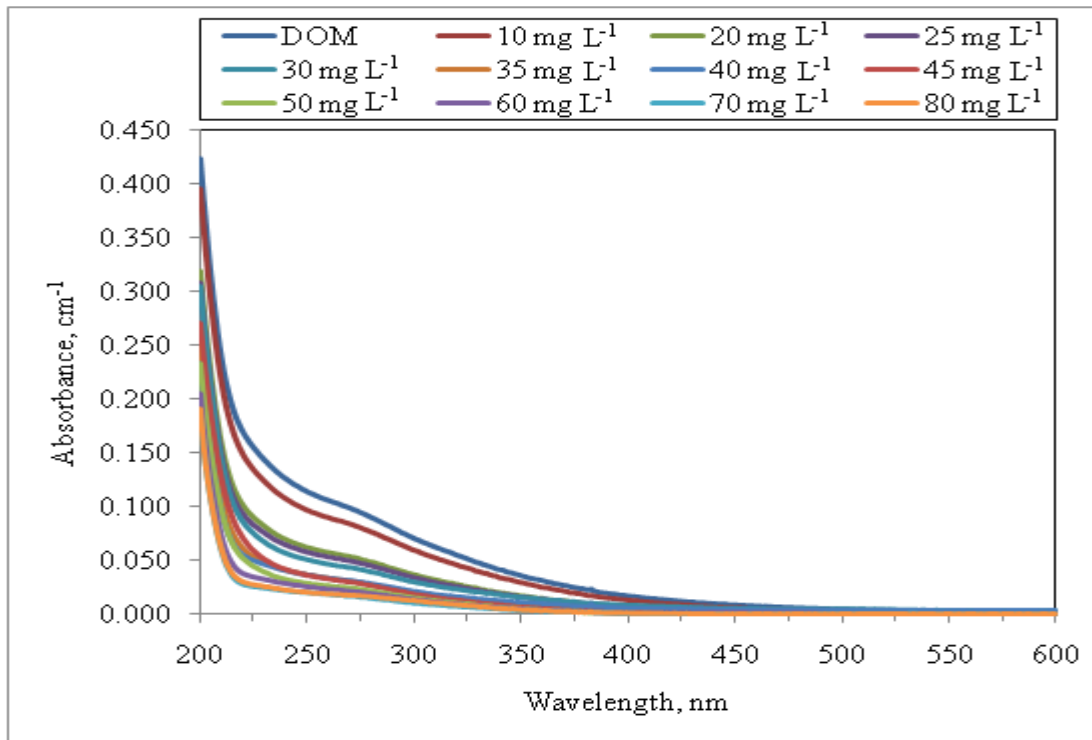


Figure C.3. UV-vis spectra of coagulation with ferric chloride at pH 7.0.

**APPENDIX D: FLUORESCENCE SPECTRA FOR COAGULATION
WITH FERRIC CHLORIDE AT PH CONDITIONS OF 6.0, 6.5, 7.0**

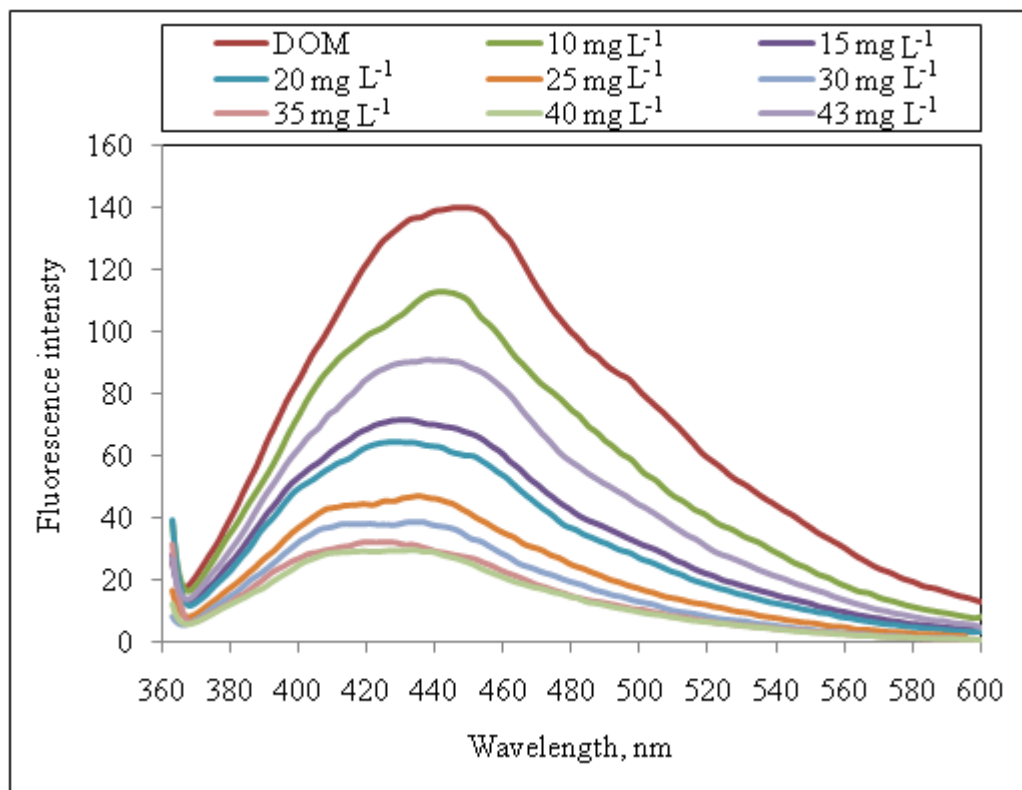


Figure D.1. Fluorescence emission₃₅₀ spectra of the DOM sample after coagulation with ferric chloride at pH 6.0.

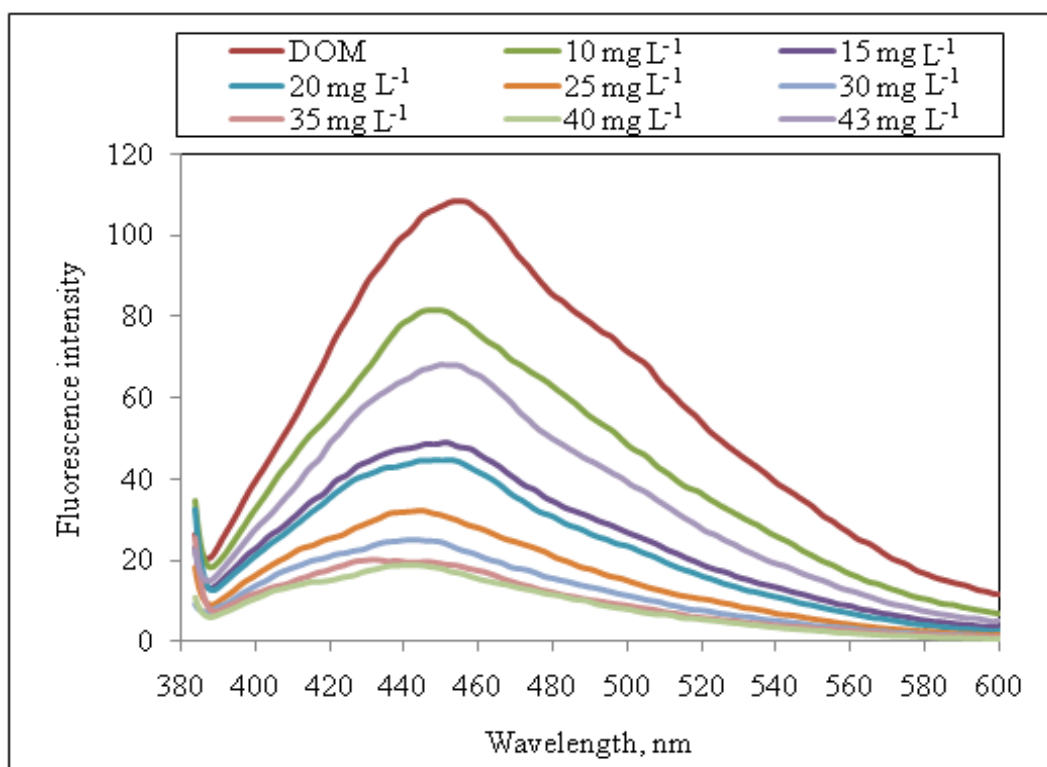


Figure D.2. Fluorescence emission₃₇₀ spectra of the DOM sample after coagulation with ferric chloride at pH 6.0.

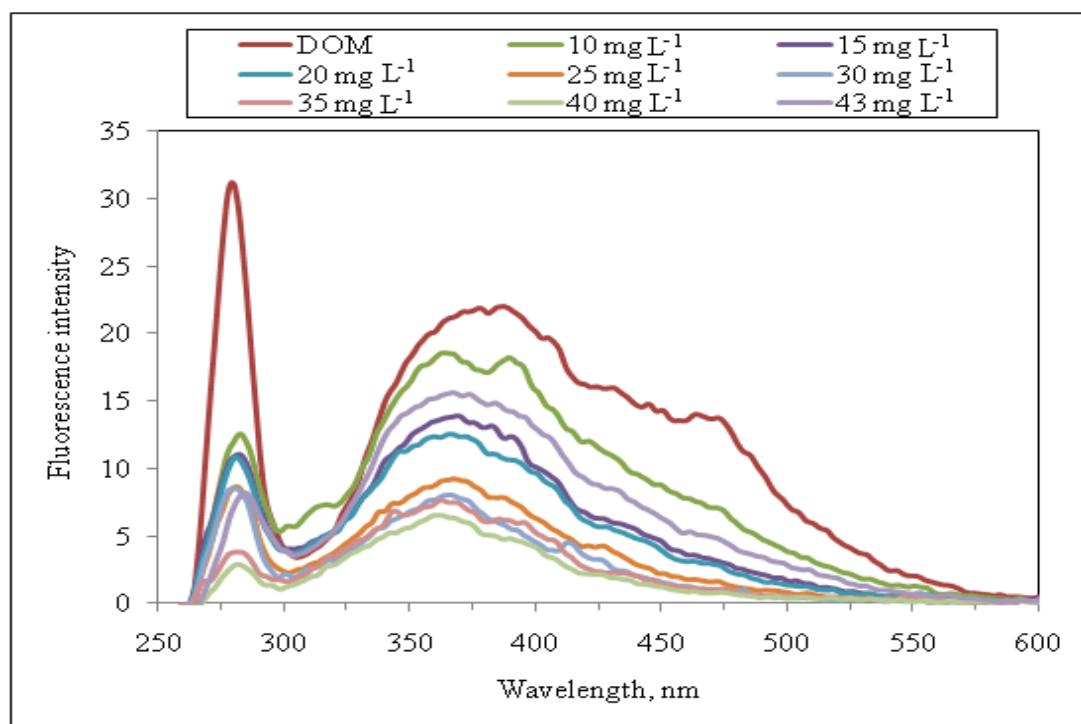


Figure D.3. Fluorescence synchronous spectra of the DOM sample after coagulation with ferric chloride at pH 6.0.

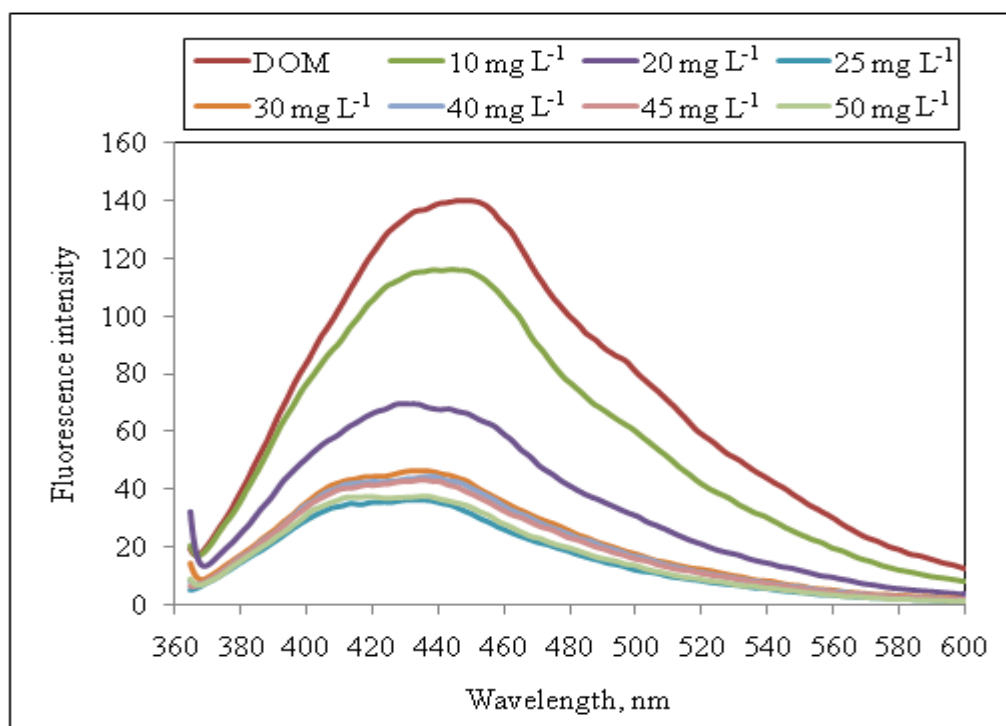


Figure D.4. Fluorescence emission₃₅₀ spectra of the DOM sample after coagulation with ferric chloride at pH 6.5.

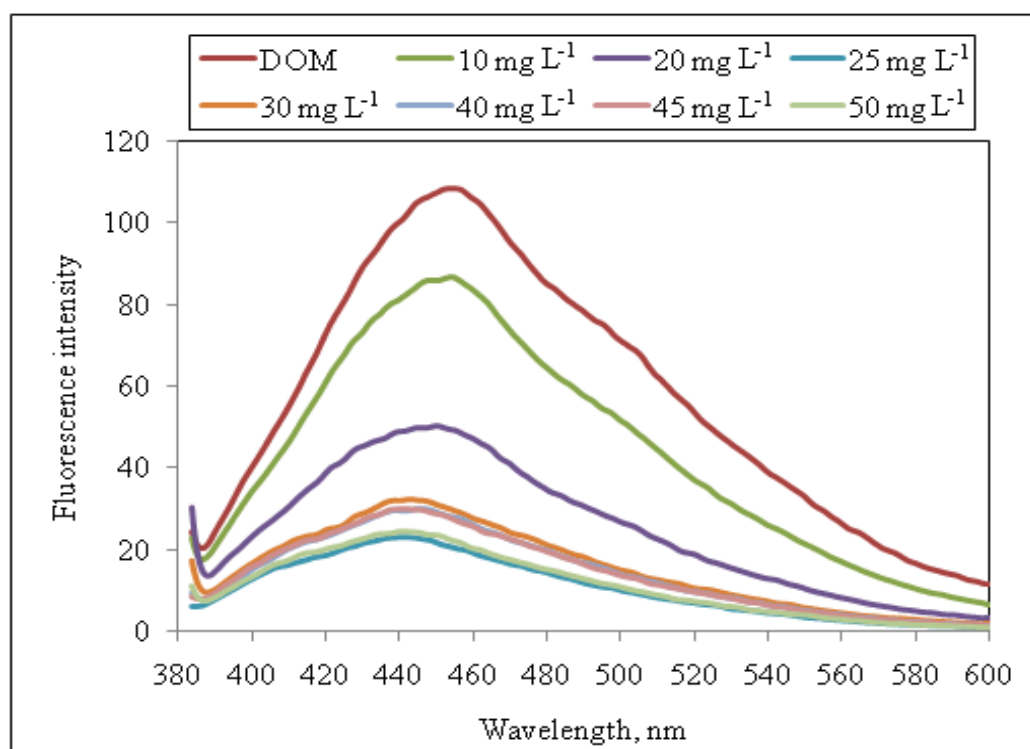


Figure D.5. Fluorescence emission₃₇₀ spectra of the DOM sample after coagulation with ferric chloride at pH 6.5.

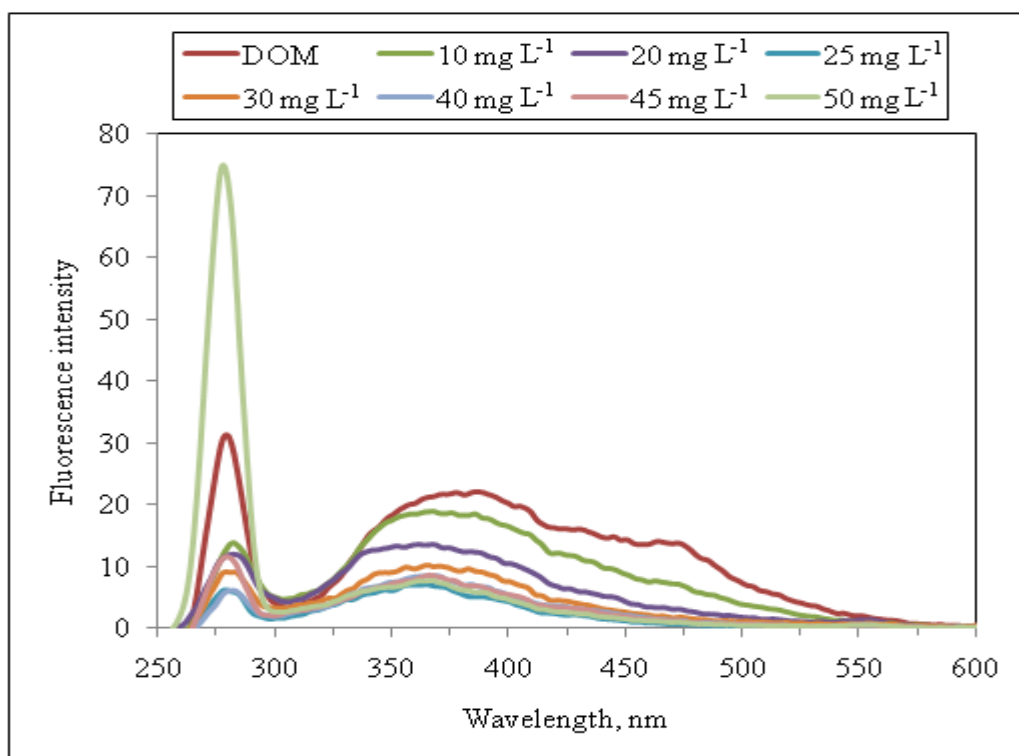


Figure D.6. Fluorescence synchronous spectra of the DOM sample after coagulation with ferric chloride at pH 6.5.

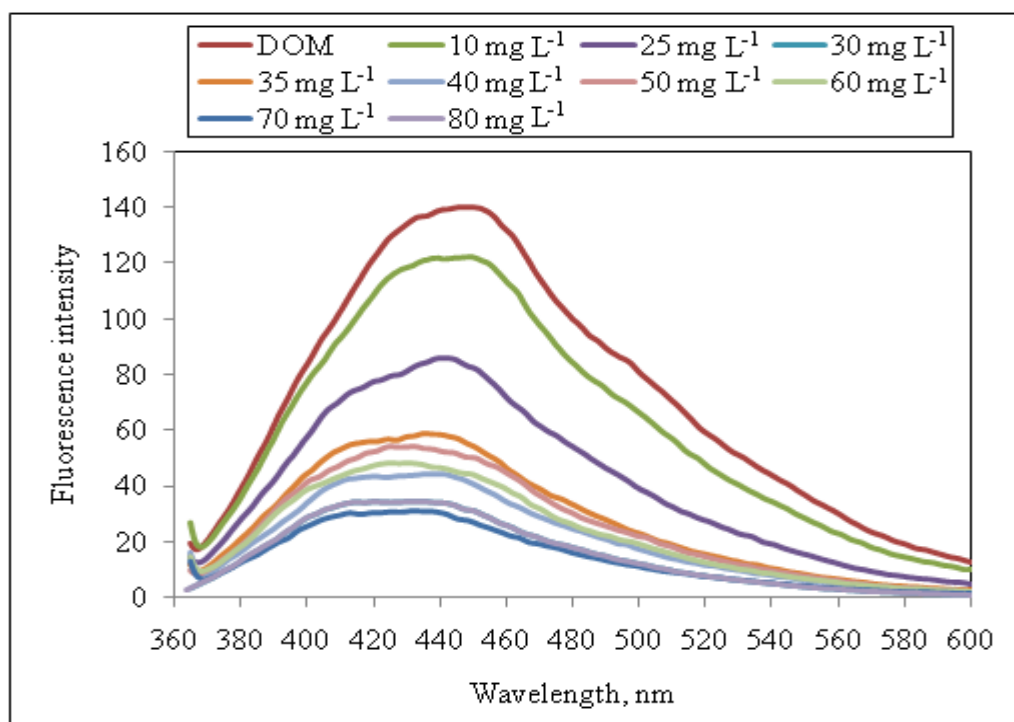


Figure D.7. Fluorescence emission₃₅₀ spectra of the DOM sample after coagulation with ferric chloride at pH 7.0.

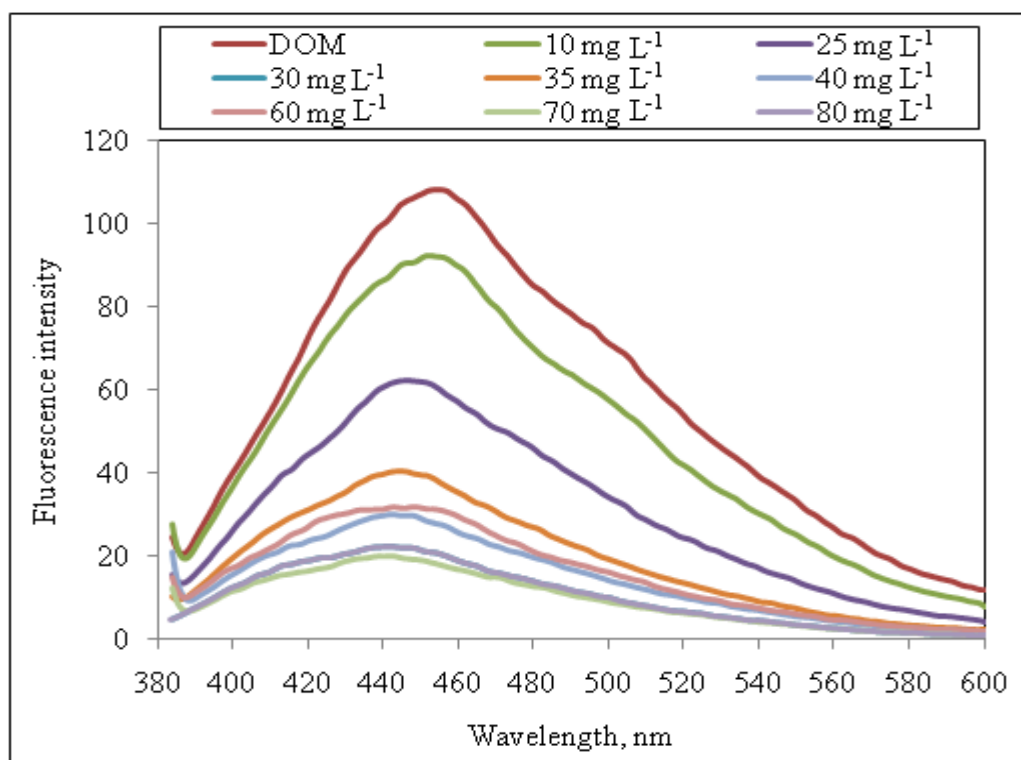


Figure D.8. Fluorescence emission₃₇₀ spectra of the DOM sample after coagulation with ferric chloride at pH 7.0.

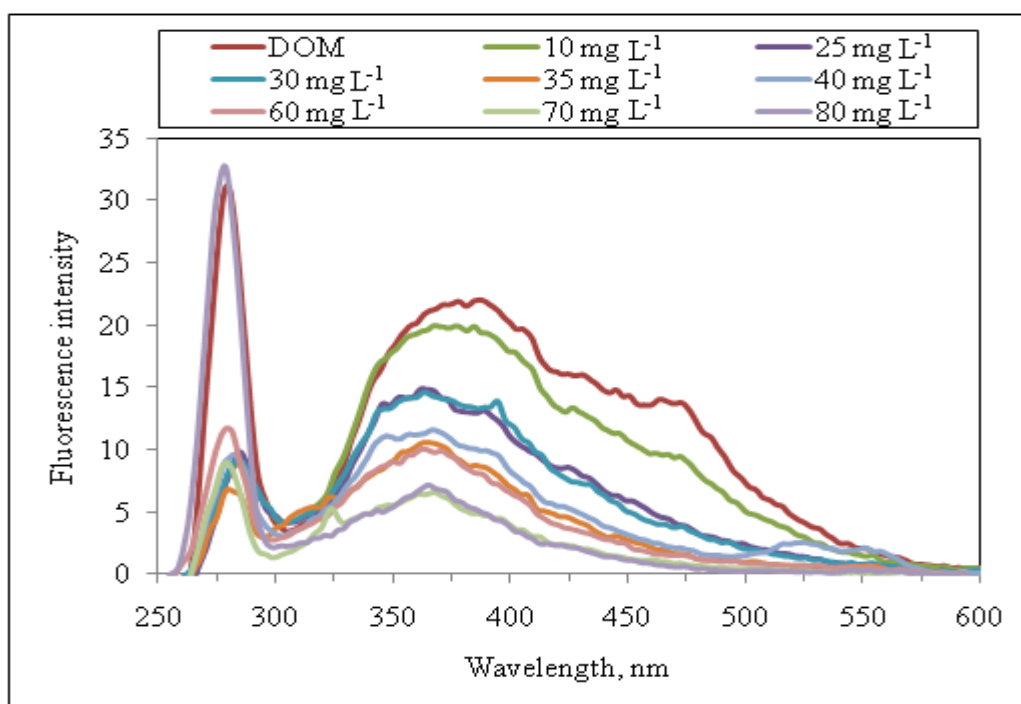


Figure D.9. Fluorescence synchronous spectra of the DOM sample after coagulation with ferric chloride at pH 7.0.